

---

Electronic Thesis and Dissertation Repository

---

9-7-2012 12:00 AM

## Approximate methods for dynamic portfolio allocation under transaction costs

Nabeel Butt  
*The University of Western Ontario*

Supervisor  
Dr Matt Davison  
*The University of Western Ontario* Co-Supervisor  
Dr Greg Reid  
*The University of Western Ontario*

Graduate Program in Applied Mathematics  
A thesis submitted in partial fulfillment of the requirements for the degree in Doctor of Philosophy  
© Nabeel Butt 2012

Follow this and additional works at: <https://ir.lib.uwo.ca/etd>



Part of the [Control Theory Commons](#), [Dynamic Systems Commons](#), [Numerical Analysis and Computation Commons](#), [Portfolio and Security Analysis Commons](#), [Probability Commons](#), and the [Statistical Models Commons](#)

---

### Recommended Citation

Butt, Nabeel, "Approximate methods for dynamic portfolio allocation under transaction costs" (2012). *Electronic Thesis and Dissertation Repository*. 932.  
<https://ir.lib.uwo.ca/etd/932>

This Dissertation/Thesis is brought to you for free and open access by Scholarship@Western. It has been accepted for inclusion in Electronic Thesis and Dissertation Repository by an authorized administrator of Scholarship@Western. For more information, please contact [wlsadmin@uwo.ca](mailto:wlsadmin@uwo.ca).

APPROXIMATE METHODS FOR DYNAMIC PORTFOLIO ALLOCATION  
UNDER TRANSACTION COSTS

(Spine title: Dynamic Portfolio Allocation under transaction costs )

(Thesis format: Monograph)

by

Nabeel Butt

Graduate Program in Applied Mathematics

A thesis submitted in partial fulfillment  
of the requirements for the degree of  
Doctor of Philosophy

The School of Graduate and Postdoctoral Studies  
The University of Western Ontario  
London, Ontario, Canada

© Nabeel Butt 2012

THE UNIVERSITY OF WESTERN ONTARIO  
School of Graduate and Postdoctoral Studies

**CERTIFICATE OF EXAMINATION**

Supervisor:

.....  
Dr. Matt Davison

Joint Supervisor:

.....  
Dr. Greg Reid

Supervisory Committee:

.....  
Dr. Adam Metzler

Examiners:

.....  
Dr. Adam Metzler

.....  
Dr. Ian Mcleod

.....  
Dr. Matt Thompson

.....  
Dr. Mark Reesor

The thesis by

**Nabeel Butt**

entitled:

**APPROXIMATE METHODS FOR DYNAMIC PORTFOLIO ALLOCATION UNDER  
TRANSACTION COSTS**

is accepted in partial fulfillment of the  
requirements for the degree of  
Doctor of Philosophy

.....  
Date

.....  
Chair of the Thesis Examination Board

## Acknowledgments

I would like to start by expressing my deepest gratitude towards God for all His help and support all along. Next I thank my beloved parents for their efforts in helping me get the best education possible. I would also like to thank all my thesis examiners for their insightful comments leading to a much improved version of the thesis.

My PhD years at UWO were some of the best years of my life. My primary Phd supervisor Dr Matt Davison was an ever present support and a great source of guidance. Matt was very helpful in all our meetings and gave me complete freedom to pursue novel ideas. It was Matt who initially directed me towards a MITACS 2008 industrial problem solving workshop. Many of the ideas in the thesis were inspired by different aspects of the hedge fund problem the workshop involved. My co-supervisor Dr Greg Reid was a great source of advice and sparked my interest in Homotopy methods in applied mathematics. Greg also helped me develop an interest in experimental mathematics.

Last but not the least I would like to thank my imaginary friend Mathematica for all its support ! :-)

## Abstract

The thesis provides simple and intuitive lattice based algorithms for solving dynamic portfolio allocation problems under transaction costs. The early part of the thesis concentrates upon developing a toolbox based on discrete probability approximations. The discrete approximations are shown to provide a reasonable approximation for most popular transaction cost models in the academic literature. The tool, once forged, is implemented in the powerful Mathematica based parallel computing environment. In the second part of the thesis we provide applications of our framework to real world problems. We show re-balancing portfolios is more valuable in an investment environment where the growth and volatility of risky assets is non-constant over the time horizon. We also provide a framework for modeling random transaction costs and compute the loss of expected utility of an investor faced with random transaction costs. Approximate methods are provided to solve portfolio constraints such as portfolio insurance and draw-down. Finally, we also highlight a lattice based framework for pairs trading.

**Keywords:** Portfolio Allocation, Transaction costs

# Contents

<b>Certificate of Examination</b>	<b>ii</b>
<b>Acknowledgements</b>	<b>iii</b>
<b>Abstract</b>	<b>iv</b>
<b>List of Figures</b>	<b>x</b>
<b>List of Tables</b>	<b>xxix</b>
<b>List of Appendices</b>	<b>xxxii</b>
<b>1 A quantitative analysis of continuous time portfolio strategies</b>	<b>1</b>
<b>2 Literature review and notations</b>	<b>4</b>
2.1 An overview of dynamic portfolio theory . . . . .	4
2.2 Brief review of transaction cost literature . . . . .	8
2.3 Towards discrete time modeling . . . . .	12
2.4 Notation used in the thesis . . . . .	12
2.5 Lattice framework of the thesis using notations above . . . . .	14
2.5.1 Bermudan put option pricing in the framework . . . . .	14
2.5.2 Growth rate maximization portfolio problem in the framework . . . . .	15
<b>3 Introduction to discrete probability approximation and sketch of modeling approach</b>	<b>19</b>
3.1 Overview . . . . .	19
3.2 Analogy between discrete time and continuous time portfolio theory . . . . .	20
3.3 Bellman principle for discrete time finite horizon problems . . . . .	21
3.4 Utility of terminal wealth . . . . .	21
3.5 An illustrative example: <i>deformation solution</i> for a dynamic investor . . . . .	22
3.6 Transfer of wealth, transaction cost structure and no-transaction region . . . . .	24
3.6.1 Transaction cost models . . . . .	25
Transfer of wealth between risky assets and trading cost proportional to the amount transferred . . . . .	25
Risk-free asset banker for buying/selling risky assets and trading cost proportional to the amount traded . . . . .	28

	Buying/selling risky assets and trading cost proportional to the amount of wealth . . . . .	30
3.7	A synopsis of approximate lattice methods . . . . .	31
3.8	On discrete probability approximations . . . . .	33
3.8.1	The example of a simple model . . . . .	33
3.8.2	Binomial discrete probability approximation . . . . .	36
3.8.3	Overview of basic discrete probability approximation construction procedure . . . . .	38
	Tree in 1-D . . . . .	38
	Tree in 2-D . . . . .	39
	Tree in 3-D . . . . .	40
	General framework for a discrete probability approximation in $\aleph$ -D . . . . .	40
3.9	On the philosophy of probability deformation continuation . . . . .	42
3.10	Towards robust and efficient lattice algorithms . . . . .	46
3.11	Analysis of continuous time dynamic trading strategies . . . . .	51
3.11.1	Risk analysis of strategies . . . . .	51
3.11.2	On the value of re-balancing . . . . .	53
<b>4</b>	<b>Overview of <i>Mathematica</i> Implementations</b>	<b>59</b>
4.1	Tree construction . . . . .	59
4.1.1	Moment/Cross-moment matching . . . . .	60
4.1.2	Trees via more general probability deformation . . . . .	60
4.2	Dynamic programming computations . . . . .	60
4.2.1	Parallel computing in Mathematica . . . . .	60
4.2.2	Recursion via dynamic programming . . . . .	61
4.2.3	Analysis of the optimal control law . . . . .	62
<b>5</b>	<b>Probability deformation continuation schemes</b>	<b>64</b>
5.1	Introduction . . . . .	64
5.2	Probability deformation schemes . . . . .	65
5.3	Deformation schemes for a portfolio model in 1-D . . . . .	66
5.3.1	Model description . . . . .	66
5.3.2	Numerical analysis of probability deformation schemes . . . . .	67
5.4	Deformation schemes for a portfolio model in 2-D . . . . .	70
5.4.1	Model description . . . . .	70
5.4.2	Numerical analysis . . . . .	72
5.5	Some remarks on moment division deformation . . . . .	73
5.6	Applicability to a wide class of stochastic processes for risky growth . . . . .	76
5.7	Towards a distribution-free approach . . . . .	76
5.8	Concluding remarks . . . . .	76
<b>6</b>	<b>Moment based discrete probability approximation of transaction cost models</b>	<b>78</b>
6.1	Tree approximations for fixed transaction cost model . . . . .	78
6.1.1	The model . . . . .	80
6.1.2	Approximation algorithm . . . . .	86

6.1.3	Model output and validation . . . . .	88
	$N = 1$ risky assets . . . . .	88
	Results for $N \geq 2$ risky assets . . . . .	90
6.1.4	Model risk: optimal policies when risky portfolio growth follows an arbitrary distribution . . . . .	93
6.1.5	Analyzing finite horizon boundaries . . . . .	94
6.1.6	Computational complexity and error analysis . . . . .	95
6.2	Approximate dynamic mean-variance portfolio optimization under transaction costs . . . . .	99
6.2.1	Introduction . . . . .	99
6.2.2	The model . . . . .	103
6.2.3	Numerical method . . . . .	109
6.2.4	No-transaction regions with time and efficiency frontiers . . . . .	110
6.2.5	Sharpe ratio time series . . . . .	110
6.2.6	Comparison of solution with model using the exact distribution . . . . .	111
6.2.7	Concluding remarks . . . . .	112
6.3	Tree approximation of proportional transaction cost model . . . . .	113
6.4	Concluding remarks . . . . .	116
<b>7</b>	<b>Value of re-balancing portfolios under transaction costs</b>	<b>117</b>
7.1	Introduction . . . . .	118
7.2	Investment model . . . . .	118
7.3	Numerical analysis of the value of re-balancing . . . . .	120
	7.3.1 Log-utility case . . . . .	121
	7.3.2 CRRA case . . . . .	121
	7.3.3 CARA case . . . . .	124
	7.3.4 Mean-variance case . . . . .	124
7.4	Intuitive explanation of results using the state variable SDE . . . . .	126
7.5	Concluding remarks . . . . .	129
<b>8</b>	<b>Lattice approximation for a dynamic stochastic transaction cost model</b>	<b>140</b>
8.1	Introduction . . . . .	140
8.2	Transaction cost model with stochastic volatility . . . . .	140
8.3	Investment model under transaction costs . . . . .	141
8.4	Formulation as a stochastic transaction cost model . . . . .	142
8.5	Lattice formulation of the model . . . . .	143
8.6	Concluding remarks . . . . .	145
<b>9</b>	<b>Portfolio optimization under transaction costs incorporating realistic constraints</b>	<b>151</b>
9.1	Introduction . . . . .	151
9.2	The model . . . . .	152
9.3	Solution methodology for constraints . . . . .	152
9.4	Numerical results for realistic problems . . . . .	154
9.5	Conclusion . . . . .	155



<b>10</b>	<b>Lattice methods for pairs trading</b>	<b>161</b>
10.1	Dynamic pairs trading based upon discrete time signals . . . . .	161
10.1.1	Model . . . . .	162
10.1.2	Lattice based solution methodology . . . . .	164
10.2	Lattice method for dynamic pairs trading under transaction costs . . . . .	168
10.2.1	Intuition behind dynamic pairs trading . . . . .	168
10.2.2	Dynamic programming formulation of the trading model . . . . .	170
10.2.3	Evolution of portfolio state processes under a pairs trading model . . .	172
	Position 1 - $\mathcal{A}_{1,k}^- > 0$ , $\mathcal{A}_{2,k}^- < 0$ with $\mathcal{A}_{1,k}^- >  \mathcal{A}_{2,k}^- $ : . . . . .	172
10.2.4	A generalized trading model . . . . .	174
	Evolution of state particles without any pre-determined trading rule . .	174
10.2.5	Solution methodology . . . . .	175
10.2.6	Numerical results for control law . . . . .	175
10.2.7	Mean-variance optimality of dynamic pairs trading: . . . . .	176
10.2.8	Concluding remarks . . . . .	177
<b>11</b>	<b>CONCLUSION</b>	<b>179</b>
11.1	Developing methods for improved computational speed . . . . .	182
11.2	Extending our modeling framework to a wider range of asset classes . . . . .	183
11.3	Analyze theoretical economic problems . . . . .	185
11.4	Incorporating parameter uncertainty into our decision making methodology . .	185
11.5	Incorporating macro-economic factors in to our decision making methodology .	187
11.6	A rigorous analysis of different dynamic trading strategies . . . . .	187
	<b>Bibliography</b>	<b>188</b>
<b>A</b>	<b>Mathematica code for chapter 4</b>	<b>194</b>
A.1	Tree construction code: . . . . .	194
A.1.1	Tree construction in 2-D . . . . .	194
A.1.2	Tree construction in 3-D . . . . .	195
A.2	Trees via more general probability deformation code: . . . . .	196
A.2.1	SQID scheme in 1-D . . . . .	196
A.2.2	SQID scheme in 2-D . . . . .	196
A.3	Recursion via dynamic programming code . . . . .	197
A.3.1	Initial recursion . . . . .	197
A.3.2	Subsequent recursion . . . . .	197
A.3.3	Analysis of optimal controls obtained - say constructing the boundaries of no-transaction regions using <b>ConvexHull[]</b> . . . . .	198
A.3.4	Code that uses creation of small ‘Balls’ to create the no-transaction region in chapter 6 . . . . .	198
A.4	Analysis of the optimal control law . . . . .	198
A.4.1	Code snippet showing control storage . . . . .	198
A.4.2	Code snippet showing use of stored controls for further analysis to gen- erate efficient frontier for benchmark problem in section 3.4. . . . .	199

<b>B</b>	<b>Pair Trading Models</b>	<b>200</b>
B.1	Alternate Pair trading models in section 1 of chapter 11 . . . . .	200
B.1.1	Model using $Log(\mathcal{Z}_k) = A_k - \phi_1 - \phi_2 B_k$ signal . . . . .	200
B.2	Dynamic Pair Trading Model in section 2 of chapter 11 . . . . .	201
B.2.1	Position 2: $\mathcal{A}_{1,k}^- > 0, \mathcal{A}_{2,k}^- < 0$ with $\mathcal{A}_{1,k}^- <  \mathcal{A}_{2,k}^- $ : . . . . .	201
B.2.2	Position 3: $\mathcal{A}_{1,k}^- < 0, \mathcal{A}_{2,k}^- > 0$ with $ \mathcal{A}_{1,k}^-  < \mathcal{A}_{2,k}^-$ : . . . . .	203
B.2.3	Position 4: $\mathcal{A}_{1,k}^- < 0, \mathcal{A}_{2,k}^- > 0$ with $ \mathcal{A}_{1,k}^-  > \mathcal{A}_{2,k}^-$ : . . . . .	205
B.3	General trading model . . . . .	208
	<b>Curriculum Vitae</b>	<b>211</b>

# List of Figures

2.1	Static versus Dynamic investor. A static investor re-balances only once while a dynamic investor re-balances at nodes inside. . . . .	5
2.2	<i>Merton</i> line under no-transaction cost with parameters $m = 0.14, \omega = 0.05$ . Where $m$ is the drift for the risky asset and $\omega$ is the risk-free rate. . . . .	7
2.3	Re-balancing to <i>Merton</i> line for CRRA or log-utility. The line is constant with respect to time. . . . .	8
2.4	No-transaction boundaries over a finite horizon for CRRA or log-utility. When the investor moves closer to terminal time the no-transaction region widens. . .	9
2.5	Controlled risky fraction over a finite horizon for CRRA or log-utility under transaction costs. Risky fraction is controlled via transaction so that it never falls outside the buy-side and sell-side boundaries. . . . .	10
2.6	Lattice solution methodology for Bermudan option. . . . .	15
2.7	Lattice solution methodology for dynamic portfolio problem. . . . .	16
3.1	Risk-adjusted value of re-balancing portfolios with parameters $T = 1, \omega = 0.07, \lambda = \mu = 0.005, s = e^{\omega\Delta T}, m = 0.14, \sigma = 0.3$ . Where $T$ is the time horizon for investment, $\omega$ is the continuous time risk-free rate, $(\lambda, \mu)$ are transaction cost factors, $s$ is the risk free growth over the interval, $m$ is the drift for continuous time GBM and $\sigma$ is the volatility for the continuous time GBM. The continuous time GBM implies a risky growth for the risky asset over the interval $\Delta T$ . . . .	24
3.2	Discrete time trading model. The dynamic investor has the option to re-balance or not to re-balance at a time node. The risky asset grows over the re-balancing period and so the fraction of wealth in the risky asset changes. . . . .	25
3.3	A possible piecewise linear function for transaction costs. Transaction costs are a function of the amount traded. . . . .	26
3.4	A possible no-transaction region in state variable space. For Log and CRRA utility if the fraction of wealth in risky asset goes out of the boundaries the risky fraction is brought inside the boundary [28]. . . . .	27
3.5	A no-transaction region for transfer of wealth model between three assets where ♣ denotes no-transaction. Parameters intentionally not supplied. Horizontal axis is the fraction of wealth in first risky asset and vertical axis is the fraction of wealth in second risky asset. . . . .	29
3.6	Approximation with five points. Choosing statistical features of the target probability model for approximation. . . . .	32

3.7	No transaction region boundaries shifting monotonically outwards as investors moves closer to terminal time for last, second and third last stage parameters are: $V = 0.5, T = 0.1, N = 3, \omega = 0.05, s = e^{\omega\Delta T}, m = 0.14, \sigma = 0.8$ . $N$ is number of re-balancing nodes and $s$ is the risky free growth over the interval. $V$ is the co-efficient of risk aversion in the CRRA utility. Also $m$ and $\sigma$ are the parameters of the continuous time GBM and risky growth discrete probability approximation is constructed as we will discuss later in section 3.8.3 and 3.9. Where $T$ is the time horizon for investment, $\omega$ is the continuous time risk-free rate, $(\lambda, \mu)$ are transaction cost factors, $s$ is the risk free growth over the interval, $m$ is the drift for continuous time GBM and $\sigma$ is the volatility for the continuous time GBM. The continuous time GBM implies a risky growth for the risky asset over the interval $\Delta T$ . . . . .	35
3.8	No transaction region in 2-D at time $t=0$ CRRA utility. Parameters not intentionally given. Purpose is to provide a visual depiction. No-transaction region is a parallelogram marked with $\heartsuit$ . . . . .	38
3.9	A discrete probability approximation approximation in 1-D. Here $r_T$ say risky growth over an interval is variable being approximated. . . . .	39
3.10	Illustrating discrete probability approximation construction in 2-D for correlated variables. . . . .	40
3.11	Illustrating discrete probability approximation construction in 3-D for correlated variables. . . . .	41
3.12	Convergence in value for CRRA utility for a discrete probability approximation approximation varying $N = 5, 10, \dots, 30$ and parameters: $T = 1, \omega = 0.1, s = e^{\omega\Delta T}, m = 0.24, \sigma = 1, \lambda = \mu = 0.01, V = 0.5$ . Where $T$ is the time horizon for investment, $N$ is the number of re-balancing nodes. $\omega$ is the continuous time risk-free rate, $(\lambda, \mu)$ are transaction cost factors, $s$ is the risk free growth over the interval, $m$ is the drift for continuous time GBM and $\sigma$ is the volatility for the continuous time GBM. The continuous time GBM implies a risky growth for the risky asset over the interval $\Delta T$ . . . . .	43
3.13	Convergence in value for log-utility for a discrete probability approximation approximation varying $N = 5, 10, \dots, 30$ and parameters: $T = 1, \omega = 0.1, s = e^{\omega\Delta T}, m = 0.14, \sigma = 0.3, \lambda = \mu = 0.01$ . Where $T$ is the time horizon for investment, $N$ is the number of re-balancing nodes. $\omega$ is the continuous time risk-free rate, $(\lambda, \mu)$ are transaction cost factors, $s$ is the risk free growth over the interval, $m$ is the drift for continuous time GBM and $\sigma$ is the volatility for the continuous time GBM. The continuous time GBM implies a risky growth for the risky asset over the interval $\Delta T$ . . . . .	44
3.14	Deformation solution by varying $\gamma_\ell = \frac{1}{5}, \frac{1}{10}, \frac{1}{15}, \frac{1}{20}$ for efficient frontier for a jump diffusion problem with parameters $T = 1, N = 4, \omega = 0.07, s = e^{\omega\Delta T}, m = 0.14, \sigma = 0.3, \theta = 0.1, \delta = 0.05$ . Where $T$ is the time horizon for investment, $N$ is the number of re-balancing nodes. $\omega$ is the continuous time risk-free rate, $(\lambda, \mu)$ are transaction cost factors, $s$ is the risk free growth over the interval, $m$ is the drift for continuous time GBM and $\sigma$ is the volatility for the continuous time GBM. The continuous time GBM implies a risky growth for the risky asset over the interval $\Delta T$ . $\gamma_\ell$ is the deformation parameter. . . . .	46

- 3.15 Deformation solution of value function with log-utility at  $t = 0$  by varying  $\gamma_\ell = \frac{1}{5}, \dots, \frac{1}{30}$  and parameters  $T = 1, N = 4, \omega = 0.1, \lambda = \mu = 0.01, s = e^{\omega\Delta T}, m = 0.14, \sigma = 0.3$ . Where  $T$  is the time horizon for investment,  $N$  is the number of re-balancing nodes.  $\omega$  is the continuous time risk-free rate,  $(\lambda, \mu)$  are transaction cost factors,  $s$  is the risk free growth over the interval,  $m$  is the drift for continuous time GBM and  $\sigma$  is the volatility for the continuous time GBM. The continuous time GBM implies a risky growth for the risky asset over the interval  $\Delta T$ .  $\gamma_\ell$  is the deformation parameter. . . . . 47
- 3.16 Deformation solution of value function with CRRA utility at  $t = 0$  by varying  $\gamma_\ell = \frac{1}{5}, \dots, \frac{1}{30}$  and parameters  $T = 1, N = 4, \omega = 0.1, \lambda = \mu = 0.01, s = e^{\omega\Delta T}, m = 0.14, \sigma = 0.3, V = 0.5$ . Where  $T$  is the time horizon for investment,  $N$  is the number of re-balancing nodes.  $\omega$  is the continuous time risk-free rate,  $(\lambda, \mu)$  are transaction cost factors,  $s$  is the risk free growth over the interval,  $m$  is the drift for continuous time GBM and  $\sigma$  is the volatility for the continuous time GBM. The continuous time GBM implies a risky growth for the risky asset over the interval  $\Delta T$ .  $\gamma_\ell$  is the deformation parameter. . . . . 48
- 3.17 Deformation solution of value function with log-utility and jump diffusion model at  $t = 0$  by varying  $\gamma_\ell = \frac{1}{5}, \dots, \frac{1}{20}$  and parameters:  $T = 1, N = 4, \omega = 0.1, \lambda = \mu = 0.01, s = e^{\omega\Delta T}, m = 0.14, \sigma = 0.6, \theta = 0.1, \delta = 0.05$ . Where  $T$  is the time horizon for investment,  $N$  is the number of re-balancing nodes.  $\omega$  is the continuous time risk-free rate,  $(\lambda, \mu)$  are transaction cost factors,  $s$  is the risk free growth over the interval,  $m$  is the drift for continuous time GBM and  $\sigma$  is the volatility for the continuous time GBM. The continuous time GBM implies a risky growth for the risky asset over the interval  $\Delta T$ .  $\gamma_\ell$  is the deformation parameter. . . . . 49
- 3.18 Deformation solution of value function with CRRA utility and jump diffusion model at  $t = 0$  by varying  $\gamma_\ell = \frac{1}{5}, \dots, \frac{1}{20}$  and parameters:  $T = 1, N = 4, \omega = 0.1, \lambda = \mu = 0.01, s = e^{\omega\Delta T}, m = 0.14, \sigma = 0.3, \theta = 0.1, \delta = 0.05, V = 0.5$ . Where  $T$  is the time horizon for investment,  $N$  is the number of re-balancing nodes.  $\omega$  is the continuous time risk-free rate,  $(\lambda, \mu)$  are transaction cost factors,  $s$  is the risk free growth over the interval,  $m$  is the drift for continuous time GBM and  $\sigma$  is the volatility for the continuous time GBM. The continuous time GBM implies a risky growth for the risky asset over the interval  $\Delta T$ .  $\gamma_\ell$  is the deformation parameter. . . . . 50
- 3.19 Finite time solution to the CARA utility problem:  $T = 5, N = 50, \omega = 0.05, s = e^\omega, m = 0.18, \sigma = 0.4, \lambda = \mu = 0.01, z = 0.01$  using a risky growth discrete probability approximation with 15 branches using a deformation parameter  $= \frac{1}{15}$ . Where  $T$  is the time horizon for investment,  $N$  is the number of re-balancing nodes.  $\omega$  is the continuous time risk-free rate,  $(\lambda, \mu)$  are transaction cost factors,  $s$  is the risk free growth over the interval,  $m$  is the drift for continuous time GBM and  $\sigma$  is the volatility for the continuous time GBM. The continuous time GBM implies a risky growth for the risky asset over the interval  $\Delta T$ .  $\gamma_\ell$  is the deformation parameter. . . . . 52

- 3.20 Terminal wealth distribution for an investor maximizing  $E[Pr(W_N > K)]$  with parameters:  $T = 0.5, N = 5, \omega = 0.05, s = e^{\omega\Delta T}, m = 0.12, \sigma = 0.5, \lambda = \mu = 0.001, K = 0.208$ . Where  $T$  is the time horizon for investment,  $N$  is the number of re-balancing nodes.  $\omega$  is the continuous time risk-free rate,  $(\lambda, \mu)$  are transaction cost factors,  $s$  is the risk free growth over the interval,  $m$  is the drift for continuous time GBM and  $\sigma$  is the volatility for the continuous time GBM. The continuous time GBM implies a risky growth for the risky asset over the interval  $\Delta T$ .  $\gamma_\ell$  is the deformation parameter. . . . . 53
- 3.21 Terminal wealth distribution for an investor minimizing variability of wealth around a target level so that we minimize  $E[(W_N - b)^2]$  with parameters:  $T = 0.5, N = 5, \omega = 0.05, s = e^{\omega\Delta T}, m = 0.12, \sigma = 0.5, \lambda = \mu = 0.001, b = 0.4$ . Where  $T$  is the time horizon for investment,  $N$  is the number of re-balancing nodes. Here  $b$  is the target level,  $\omega$  is the continuous time risk-free rate,  $(\lambda, \mu)$  are transaction cost factors,  $s$  is the risk free growth over the interval,  $m$  is the drift for continuous time GBM and  $\sigma$  is the volatility for the continuous time GBM. The continuous time GBM implies a risky growth for the risky asset over the interval  $\Delta T$ .  $\gamma_\ell$  is the deformation parameter. . . . . 54
- 3.22 Terminal wealth distribution for an investor maximizing  $E[\frac{W_N^V}{V}]$  with parameters:  $T = 0.5, N = 5, \omega = 0.05, s = e^{\omega\Delta T}, m = 0.12, \sigma = 0.5, \lambda = \mu = 0.001, V = 0.5$ . Where  $T$  is the time horizon for investment,  $N$  is the number of re-balancing nodes.  $\omega$  is the continuous time risk-free rate,  $(\lambda, \mu)$  are transaction cost factors,  $s$  is the risk free growth over the interval,  $m$  is the drift for continuous time GBM and  $\sigma$  is the volatility for the continuous time GBM. The continuous time GBM implies a risky growth for the risky asset over the interval  $\Delta T$ .  $\gamma_\ell$  is the deformation parameter. . . . . 55
- 3.23 Terminal wealth distribution for an investor maximizing  $E[\frac{W_N^{V_1}}{V_1} + \frac{W_N^{V_2}}{V_2}]$  with parameters:  $T = 0.5, N = 5, \omega = 0.05, s = e^{\omega\Delta T}, m = 0.12, \sigma = 0.5, \lambda = \mu = 0.001, V_1 = \frac{1}{3}, V_2 = \frac{2}{3}$ . Where  $T$  is the time horizon for investment,  $N$  is the number of re-balancing nodes.  $\omega$  is the continuous time risk-free rate,  $(\lambda, \mu)$  are transaction cost factors,  $s$  is the risk free growth over the interval,  $m$  is the drift for continuous time GBM and  $\sigma$  is the volatility for the continuous time GBM. The continuous time GBM implies a risky growth for the risky asset over the interval  $\Delta T$ .  $\gamma_\ell$  is the deformation parameter. . . . . 55
- 3.24 Variation of value function at time 0 with re-balancing frequency  $N$  for some choice of parameters:  $T = 1, \omega = 0.05, \lambda = \mu = 0.01, s = e^{\omega\Delta T}, m = 0.14, \sigma = 0.7$ . Where  $T$  is the time horizon for investment,  $N$  is the number of re-balancing nodes.  $\omega$  is the continuous time risk-free rate,  $(\lambda, \mu)$  are transaction cost factors,  $s$  is the risk free growth over the interval,  $m$  is the drift for continuous time GBM and  $\sigma$  is the volatility for the continuous time GBM. The continuous time GBM implies a risky growth for the risky asset over the interval  $\Delta T$ .  $\gamma_\ell$  is the deformation parameter. . . . . 56

3.25	Variation of value function at time 0 with re-balancing frequency $N$ with portfolio management fee for some choice of parameters: $T = 1, \omega = 0.07, \lambda = \mu = 0.001, s = e^{\omega\Delta T}, m = 0.182, \sigma = 0.4$ . Where $T$ is the time horizon for investment, $N$ is the number of re-balancing nodes. $\omega$ is the continuous time risk-free rate, $(\lambda, \mu)$ are transaction cost factors, $s$ is the risk free growth over the interval, $m$ is the drift for continuous time GBM and $\sigma$ is the volatility for the continuous time GBM. The continuous time GBM implies a risky growth for the risky asset over the interval $\Delta T$ . $\gamma_\ell$ is the deformation parameter. . . . .	57
3.26	Variation of value function at time 0 with re-balancing frequency $N$ with portfolio management fee when investor <i>always</i> has to re-balance for some choice of parameters: $T = 1, \omega = 0.07, \lambda = \mu = 0.005, s = e^{\omega\Delta T}, m = 0.182, \sigma = 0.4$ . Where $T$ is the time horizon for investment, $N$ is the number of re-balancing nodes. $\omega$ is the continuous time risk-free rate, $(\lambda, \mu)$ are transaction cost factors, $s$ is the risk free growth over the interval, $m$ is the drift for continuous time GBM and $\sigma$ is the volatility for the continuous time GBM. The continuous time GBM implies a risky growth for the risky asset over the interval $\Delta T$ . $\gamma_\ell$ is the deformation parameter. . . . .	58
4.1	Parallel computation on grids. Value function computation at a point in node $k$ only needs to know the value function surface at node $(k + 1)$ . . . . .	61
5.1	Two distributions going as an input to the numerical method. They both give an output to the model using same the numerical method. How close are the two outputs ? . . . . .	65
5.2	Value function in SID scheme with initial wealth=1, initial risky fraction=0.5, varying deformation from $\ell= 15$ to 25 and parameter choice: $\lambda = \mu = 0.01, s = e^{0.1*\Delta T}, m = 0.14, \sigma = 0.3, T = 1, N = 4, \gamma_\ell = \frac{1}{\ell}$ . Where $T$ is the time horizon for investment, $N$ is the number of re-balancing nodes. $\omega$ is the continuous time risk-free rate, $(\lambda, \mu)$ are transaction cost factors, $s$ is the risk free growth over the interval, $m$ is the drift for continuous time GBM and $\sigma$ is the volatility for the continuous time GBM. The continuous time GBM implies a risky growth for the risky asset over the interval $\Delta T$ . $\gamma_\ell$ is the deformation parameter. . . . .	70
5.3	Value function in SQID scheme with initial wealth=1, initial risky fraction=0.5, varying deformation from $\ell= 15$ to 25 and parameter choice: $\lambda = \mu = 0.01, s = e^{0.1*\Delta T}, m = 0.14, \sigma = 0.3, T = 1, N = 4, \gamma_\ell = \frac{1}{\ell}$ . Where $T$ is the time horizon for investment, $N$ is the number of re-balancing nodes. $\omega$ is the continuous time risk-free rate, $(\lambda, \mu)$ are transaction cost factors, $s$ is the risk free growth over the interval, $m$ is the drift for continuous time GBM and $\sigma$ is the volatility for the continuous time GBM. The continuous time GBM implies a risky growth for the risky asset over the interval $\Delta T$ . $\gamma_\ell$ is the deformation parameter. . . . .	71

5.4	Value function in MD scheme with initial wealth=1, initial risky fraction=0.5, varying deformation from $\ell=15$ to 25 and parameter choice: $\lambda = \mu = 0.01, s = e^{0.1*\Delta T}, m = 0.14, \sigma = 0.3, T = 1, N = 4, \gamma_\ell = \frac{1}{\ell}$ . Where $T$ is the time horizon for investment, $N$ is the number of re-balancing nodes. $\omega$ is the continuous time risk-free rate, $(\lambda, \mu)$ are transaction cost factors, $s$ is the risk free growth over the interval, $m$ is the drift for continuous time GBM and $\sigma$ is the volatility for the continuous time GBM. The continuous time GBM implies a risky growth for the risky asset over the interval $\Delta T$ . $\gamma_\ell$ is the deformation parameter. . . . .	71
5.5	Value function in SID scheme with initial wealth=1, initial risky fraction=0.5, varying deformation from $\ell=8$ to 15 and parameter choice: $\lambda = \mu = 0.05, T = 1, N = 4, m_1 = 0.08, \sigma_1 = 0.2, m_2 = 0.14, \sigma_2 = 0.8, \rho = 0.1, \gamma_\ell = \frac{1}{\ell}$ . Where $T$ is the time horizon for investment, $N$ is the number of re-balancing nodes. $\omega$ is the continuous time risk-free rate, $(\lambda, \mu)$ are transaction cost factors, $s$ is the risk free growth over the interval, $m$ is the drift for continuous time GBM and $\sigma$ is the volatility for the continuous time GBM. The continuous time GBM implies a risky growth for the risky asset over the interval $\Delta T$ . $\gamma_\ell$ is the deformation parameter. . . . .	73
5.6	Value function in SQID scheme with initial wealth=1, initial risky fraction=0.5, varying deformation from $\ell=8$ to 15 and parameter choice: $\lambda = \mu = 0.05, T = 1, N = 4, m_1 = 0.08, \sigma_1 = 0.2, m_2 = 0.14, \sigma_2 = 0.8, \rho = 0.1, \gamma_\ell = \frac{1}{\ell}$ . Where $T$ is the time horizon for investment, $N$ is the number of re-balancing nodes. $\omega$ is the continuous time risk-free rate, $(\lambda, \mu)$ are transaction cost factors, $s$ is the risk free growth over the interval, $m$ is the drift for continuous time GBM and $\sigma$ is the volatility for the continuous time GBM. The continuous time GBM implies a risky growth for the risky asset over the interval $\Delta T$ . $\gamma_\ell$ is the deformation parameter. . . . .	74
5.7	A possible deformation stencil in 2-D. . . . .	74
5.8	Tree in 2-D. . . . .	75
6.1	No-transaction region embedded in state variable space at node $k$ . . . . .	83
6.2	Binomial and Trinomial discrete probability approximations for risky growth in one dimension. . . . .	83
6.3	Binomial discrete probability approximation for a pair of risky growth in 2-dimensions. . . . .	84
6.4	A possible approximation in 2-dimensions. . . . .	85
6.5	A multinomial approximation in three dimensions. . . . .	85
6.6	The sell-side and buy-side boundaries for the choice of parameters: $\lambda = 0.001, T = 5, N = 500, \Delta T = \frac{T}{N}, s = e^{0.07\Delta T}, m = 0.182, \sigma = 0.4$ . Where $T$ is the time horizon for investment, $N$ is the number of re-balancing nodes. $\omega$ is the continuous time risk-free rate, $\lambda$ is the transaction cost factor, $s$ is the risk free growth over the interval, $m$ is the drift for continuous time GBM and $\sigma$ is the volatility for the continuous time GBM. The continuous time GBM implies a risky growth for the risky asset over the interval $\Delta T$ . . . . .	89



- 6.7 Width of no-transaction region plotted against iteration depth:  $\lambda = 0.001, T = 5, N = 500, \Delta T = \frac{T}{N}, s = e^{0.07\Delta T}, m = 0.182, \sigma = 0.4$ . The iterations are the same as in the dynamic programming equation. We start from the last stage to go to the initial time. Where  $T$  is the time horizon for investment,  $N$  is the number of re-balancing nodes.  $\omega$  is the continuous time risk-free rate,  $\lambda$  is the transaction cost factor,  $s$  is the risk free growth over the interval,  $m$  is the drift for continuous time GBM and  $\sigma$  is the volatility for the continuous time GBM. The continuous time GBM implies a risky growth for the risky asset over the interval  $\Delta T$ . . . . . 90
- 6.8 Risky fraction boundaries at initial time with respect to transaction cost parameter  $\lambda$ :  $\lambda = 0.001, T = 3, N = 500, \Delta T = \frac{T}{N}, s = e^{0.07\Delta T}, m = 0.182, \sigma = 0.4$ . Where  $T$  is the time horizon for investment,  $N$  is the number of re-balancing nodes.  $\omega$  is the continuous time risk-free rate,  $\lambda$  is the transaction cost factor,  $s$  is the risk free growth over the interval,  $m$  is the drift for continuous time GBM and  $\sigma$  is the volatility for the continuous time GBM. The continuous time GBM implies a risky growth for the risky asset over the interval  $\Delta T$ . . . . . 91
- 6.9 Variation of the width of risky fraction boundaries in the last stage with respect to transaction cost parameter and parameters:  $T = 3, N = 100, \Delta T = \frac{T}{N}, s = e^{0.07\Delta T}, m = 0.182, \sigma = 0.4$ . Mathematica's **FindFit[]** command used to directly do non-linear least squares optimization. Where  $T$  is the time horizon for investment,  $N$  is the number of re-balancing nodes.  $\omega$  is the continuous time risk-free rate,  $\lambda$  is the transaction cost factor,  $s$  is the risk free growth over the interval,  $m$  is the drift for continuous time GBM and  $\sigma$  is the volatility for the continuous time GBM. The continuous time GBM implies a risky growth for the risky asset over the interval  $\Delta T$ . . . . . 92
- 6.10 Risky boundary approximation: Comparing trinomial approximation for approximate normal with binomial approximation for exact log-normal with  $\lambda = 0.001, T = 5, N = 500, \Delta T = \frac{T}{N}, s = e^{0.07\Delta T}, m = 0.182, \sigma = 0.4$ . Where  $T$  is the time horizon for investment,  $N$  is the number of re-balancing nodes.  $\omega$  is the continuous time risk-free rate,  $\lambda$  is the transaction cost factor,  $s$  is the risk free growth over the interval,  $m$  is the drift for continuous time GBM and  $\sigma$  is the volatility for the continuous time GBM. The continuous time GBM implies a risky growth for the risky asset over the interval  $\Delta T$ . . . . . 93
- 6.11 Risky boundary approximation: Varying time step divisions in Binomial approximation for exact log-normal with  $\lambda = 0.001, T = 5, N = 500, \Delta T = \frac{T}{N}, s = e^{0.07\Delta T}, m = 0.182, \sigma = 0.4$ . Where  $T$  is the time horizon for investment,  $N$  is the number of re-balancing nodes.  $\omega$  is the continuous time risk-free rate,  $\lambda$  is the transaction cost factor,  $s$  is the risk free growth over the interval,  $m$  is the drift for continuous time GBM and  $\sigma$  is the volatility for the continuous time GBM. The continuous time GBM implies a risky growth for the risky asset over the interval  $\Delta T$ . . . . . 94

- 6.12 Risky boundary approximation: Varying time step divisions in Trinomial approximation for approximate normal with  $\lambda = 0.001, T = 5, N = 500, \Delta T = \frac{T}{N}, s = e^{0.07\Delta T}, m = 0.182, \sigma = 0.4$ . Where  $T$  is the time horizon for investment,  $N$  is the number of re-balancing nodes.  $\omega$  is the continuous time risk-free rate,  $\lambda$  is the transaction cost factor,  $s$  is the risk free growth over the interval,  $m$  is the drift for continuous time GBM and  $\sigma$  is the volatility for the continuous time GBM. The continuous time GBM implies a risky growth for the risky asset over the interval  $\Delta T$ . . . . . 95
- 6.13 Independent stocks in 2-D. Horizontal axis is fraction of wealth in risky asset 1 and vertical axis is fraction of wealth in risky asset 2. Variation of the region of inaction with time:  $\lambda = 0.01, T = 5, N = 100, \Delta T = \frac{T}{N}, s = e^{0.10\Delta T}, m_1 = 0.13, \sigma_1 = 0.40, m_2 = 0.15, \sigma_2 = 0.44$ . Where  $T$  is the time horizon for investment,  $N$  is the number of re-balancing nodes.  $\omega$  is the continuous time risk-free rate,  $\lambda$  is the transaction cost factor,  $s$  is the risk free growth over the interval,  $m$  is the drift for continuous time GBM and  $\sigma$  is the volatility for the continuous time GBM. The continuous time GBM implies a risky growth for the risky asset over the interval  $\Delta T$ . . . . . 96
- 6.14 Horizontal axis is fraction of wealth in risky asset 1 and vertical axis is fraction of wealth in risky asset 2. Wealth fractions for two assets in a triangular simplex and correlated stocks in 2-D with:  $\lambda = 0.001, T = 2, N = 100, \Delta T = \frac{T}{N}, s = e^{0.07\Delta T}, m_1 = 0.13, \sigma_1 = \sqrt{0.1}, m_2 = 0.15, \sigma_2 = \sqrt{0.17}, \rho = \frac{0.07}{\sigma_1\sigma_2}$ . Here  $T$  is the time horizon for investment,  $N$  is the number of re-balancing nodes.  $\omega$  is the continuous time risk-free rate,  $\lambda$  is the transaction cost factor,  $s$  is the risk free growth over the interval,  $m$  is the drift for continuous time GBM and  $\sigma$  is the volatility for the continuous time GBM. The continuous time GBM implies a risky growth for the risky asset over the interval  $\Delta T$ . . . . . 97
- 6.15 Horizontal axis is fraction of wealth in risky asset 1 and vertical axis is fraction of wealth in risky asset 2. Square simplex and correlated stocks in 2-D with:  $\lambda = 0.001, T = 2, N = 100, \Delta T = \frac{T}{N}, s = e^{0.07\Delta T}, m_1 = 0.13, \sigma_1 = \sqrt{0.1}, m_2 = 0.15, \sigma_2 = \sqrt{0.17}, \rho = \frac{0.07}{\sigma_1\sigma_2}$ . Where  $T$  is the time horizon for investment,  $N$  is the number of re-balancing nodes.  $\omega$  is the continuous time risk-free rate,  $\lambda$  is the transaction cost factor,  $s$  is the risk free growth over the interval,  $m$  is the drift for continuous time GBM and  $\sigma$  is the volatility for the continuous time GBM. The continuous time GBM implies a risky growth for the risky asset over the interval  $\Delta T$ . . . . . 98
- 6.16 Triangle simplex and comparing discrete probability approximation solution to CASE I in [69]:  $\lambda = 0.001, T = 2, N = 100, \Delta T = \frac{T}{N}, s = e^{0.07\Delta T}, m_1 = 0.13, \sigma_1 = \sqrt{0.1}, m_2 = 0.15, \sigma_2 = \sqrt{0.17}, \rho = \frac{0.07}{\sigma_1\sigma_2}$ . Where  $T$  is the time horizon for investment,  $N$  is the number of re-balancing nodes.  $\omega$  is the continuous time risk-free rate,  $\lambda$  is the transaction cost factor,  $s$  is the risk free growth over the interval,  $m$  is the drift for continuous time GBM and  $\sigma$  is the volatility for the continuous time GBM. The continuous time GBM implies a risky growth for the risky asset over the interval  $\Delta T$ . . . . . 99

6.17 Triangle simplex and high correlation: $\lambda = 0.001, T = 2, N = 100, \Delta T = \frac{T}{N}, s = e^{0.07\Delta T}, m_1 = 0.13, \sigma_1 = \sqrt{0.1}, m_2 = 0.15, \sigma_2 = \sqrt{0.17}, \rho = 0.9$ . Where $T$ is the time horizon for investment, $N$ is the number of re-balancing nodes. $\omega$ is the continuous time risk-free rate, $\lambda$ is the transaction cost factor, $s$ is the risk free growth over the interval, $m$ is the drift for continuous time GBM and $\sigma$ is the volatility for the continuous time GBM. The continuous time GBM implies a risky growth for the risky asset over the interval $\Delta T$ . . . . .	102
6.18 For some parameter choice boundaries could be rapidly changing. Triangle simplex and high correlation: $\lambda = 0.001, T = 2, N = 100, \Delta T = \frac{T}{N}, s = e^{0.07\Delta T}, m_1 = 0.13, \sigma_1 = \sqrt{0.1}, m_2 = 0.15, \sigma_2 = \sqrt{0.17}, \rho = 0.96$ . Where $T$ is the time horizon for investment, $N$ is the number of re-balancing nodes. $\omega$ is the continuous time risk-free rate, $\lambda$ is the transaction cost factor, $s$ is the risk free growth over the interval, $m$ is the drift for continuous time GBM and $\sigma$ is the volatility for the continuous time GBM. The continuous time GBM implies a risky growth for the risky asset over the interval $\Delta T$ . . . . .	103
6.19 Finite horizon no-transaction boundary obtained at $T = 1$ with parameters: $\lambda = 0.01, T = 1, N = 100, \Delta T = \frac{T}{N}, s = e^{0.07\Delta T}, m = 0.182, \sigma = 0.4$ . Where $T$ is the time horizon for investment, $N$ is the number of re-balancing nodes. $\omega$ is the continuous time risk-free rate, $\lambda$ is the transaction cost factor, $s$ is the risk free growth over the interval, $m$ is the drift for continuous time GBM and $\sigma$ is the volatility for the continuous time GBM. The continuous time GBM implies a risky growth for the risky asset over the interval $\Delta T$ . . . . .	104
6.20 Value function approximation for one stage problem with different moment matching. Parameters: $\lambda = 0.001, T = 0.04, N = 1, \Delta T = \frac{T}{N}, s = e^{0.07\Delta T}, m = 0.182, \sigma = 0.4$ . Where $T$ is the time horizon for investment, $N$ is the number of re-balancing nodes. $\omega$ is the continuous time risk-free rate, $\lambda$ is the transaction cost factor, $s$ is the risk free growth over the interval, $m$ is the drift for continuous time GBM and $\sigma$ is the volatility for the continuous time GBM. The continuous time GBM implies a risky growth for the risky asset over the interval $\Delta T$ . . . . .	105
6.21 Analytic curve $\mathbf{C}(\lambda, x, y; \mathcal{H})$ and Sharpe-ratio maximization . . . . .	108
6.22 No-transaction region $\mathcal{R}$ at a time slice . . . . .	109
6.23 Grid of lattice approximation at a time snapshot. . . . .	110
6.24 Time variation of risky fraction boundaries with parameters $\lambda = \mu = 0.05, T = 0.5, N = 10, s = e^{0.05\Delta T}, m_1 = 0.08, \sigma_1 = 0.42, m_2 = 0.14, \sigma_2 = 0.8, \rho = 0.05$ . Where $T$ is the time horizon for investment, $N$ is the number of re-balancing nodes. $\omega$ is the continuous time risk-free rate, $(\lambda, \mu)$ are transaction cost factors, $s$ is the risk free growth over the interval, $m_i$ is the drift for continuous time GBM and $\sigma_i$ is the volatility for the continuous time GBM. The continuous time GBM implies a risky growth for the risky asset over the interval $\Delta T$ . . . .	111

- 6.25 Impact of transaction cost on dynamic efficiency frontier with parameters  $T = 0.3, N = 6, s = e^{0.05\Delta T}, m_1 = 0.08, \sigma_1 = 0.42, m_2 = 0.14, \sigma_2 = 0.8, \rho = 0.05$ . Where  $T$  is the time horizon for investment,  $N$  is the number of re-balancing nodes.  $\omega$  is the continuous time risk-free rate,  $(\lambda, \mu)$  are transaction cost factors,  $s$  is the risk free growth over the interval,  $m_i$  is the drift for continuous time GBM and  $\sigma_i$  is the volatility for the continuous time GBM. The continuous time GBM implies a risky growth for the risky asset over the interval  $\Delta T$ . . . . 112
- 6.26 Sharpe ratio time series evaluated at  $t = 0$ , initial fraction in asset one =0.5, initial wealth =0.2, for different times with parameters  $\lambda = \mu = 0.005, T = 1, N = 10, s = e^{0.05\Delta T}, m_1 = 0.08, \sigma_1 = 0.42, m_2 = 0.14, \sigma_2 = 0.8, \rho = 0.05$ . Where  $T$  is the time horizon for investment,  $N$  is the number of re-balancing nodes.  $\omega$  is the continuous time risk-free rate,  $(\lambda, \mu)$  are transaction cost factors,  $s$  is the risk free growth over the interval,  $m_i$  is the drift for continuous time GBM and  $\sigma_i$  is the volatility for the continuous time GBM. The continuous time GBM implies a risky growth for the risky asset over the interval  $\Delta T$ . . . . 113
- 6.27 Sharpe ratio series with myopic investment in individual assets evaluated at  $t=0$  for different times with parameters  $\lambda = \mu = 0.005, T = 1, N = 10, s = e^{0.05\Delta T}, m_1 = 0.08, \sigma_1 = 0.42, m_2 = 0.14, \sigma_2 = 0.8, \rho = 0.05$ . Where  $T$  is the time horizon for investment,  $N$  is the number of re-balancing nodes.  $\omega$  is the continuous time risk-free rate,  $(\lambda, \mu)$  are transaction cost factors,  $s$  is the risk free growth over the interval,  $m_i$  is the drift for continuous time GBM and  $\sigma_i$  is the volatility for the continuous time GBM. The continuous time GBM implies a risky growth for the risky asset over the interval  $\Delta T$ . . . . . 114
- 6.28 Obtaining infinite horizon solution using boundary update numerical methods with parameters  $m = 0.14, \sigma = 0.3, \lambda = \mu = 0.05, \omega = 0.1, s = e^{\omega\Delta T}$ . Where  $T$  is the time horizon for investment,  $N$  is the number of re-balancing nodes.  $\omega$  is the continuous time risk-free rate,  $(\lambda, \mu)$  are transaction cost factors,  $s$  is the risk free growth over the interval,  $m$  is the drift for continuous time GBM and  $\sigma$  is the volatility for the continuous time GBM. The continuous time GBM implies a risky growth for the risky asset over the interval  $\Delta T$ . . . . . 115
- 6.29 Obtaining finite horizon no-transaction boundaries with parameters  $T = 1, N = 10, m = 0.08, \sigma = 0.42, \lambda = \mu = 0.01, \omega = 0.05, s = e^{\omega\Delta T}$ . Here iteration corresponds to the iteration in dynamic programming. Where  $T$  is the time horizon for investment,  $N$  is the number of re-balancing nodes.  $\omega$  is the continuous time risk-free rate,  $(\lambda, \mu)$  are transaction cost factors,  $s$  is the risk free growth over the interval,  $m$  is the drift for continuous time GBM and  $\sigma$  is the volatility for the continuous time GBM. The continuous time GBM implies a risky growth for the risky asset over the interval  $\Delta T$ . . . . . 116
- 7.1 Parameters switching over the investment horizon. The three regimes have different drift and volatility for GBM of the risky asset. . . . . 120

- 7.2 Value of re-balancing for log-utility with initial risky fraction=0.5 and wealth =1 the parameters  $\lambda = \mu = 0.05$ ,  $s = e^{0.05\Delta T}$ ,  $amin = 0.001$ ,  $amax = 0.999$ ,  $da = 0.01$ ,  $T = 1$ ,  $m = 0.14$ ,  $\sigma = 0.6$ . Where  $T$  is the time horizon for investment,  $N$  is the number of re-balancing nodes.  $\omega$  is the continuous time risk-free rate,  $(\lambda, \mu)$  are transaction cost factors,  $s$  is the risk free growth over the interval,  $m$  is the drift for continuous time GBM and  $\sigma$  is the volatility for the continuous time GBM. The continuous time GBM implies a risky growth for the risky asset over the interval  $\Delta T$ . ( $amin, amax$ ) are the bounds for risky fraction state space. . . . . 122
- 7.3 Value of re-balancing for log-utility with initial risky fraction=0.5 and wealth =1 the parameters  $\lambda = \mu = 0.05$ ,  $s = e^{0.05\Delta T}$ ,  $amin = 0.001$ ,  $amax = 0.999$ ,  $da = 0.01$ ,  $T = 5$ ,  $m = 0.14$ ,  $\sigma = 0.6$ . Where  $T$  is the time horizon for investment,  $N$  is the number of re-balancing nodes.  $\omega$  is the continuous time risk-free rate,  $(\lambda, \mu)$  are transaction cost factors,  $s$  is the risk free growth over the interval,  $m$  is the drift for continuous time GBM and  $\sigma$  is the volatility for the continuous time GBM. The continuous time GBM implies a risky growth for the risky asset over the interval  $\Delta T$ . ( $amin, amax$ ) are the bounds for risky fraction state space. . . . . 122
- 7.4 Value of re-balancing for log-utility with initial risky fraction=0.5 and wealth =1 the parameters  $\lambda = \mu = 0.05$ ,  $s = e^{0.05\Delta T}$ ,  $amin = 0.001$ ,  $amax = 0.999$ ,  $da = 0.01$ ,  $T = 1$ ,  $m = 0.14$ ,  $\sigma = 1.0$ . Where  $T$  is the time horizon for investment,  $N$  is the number of re-balancing nodes.  $\omega$  is the continuous time risk-free rate,  $(\lambda, \mu)$  are transaction cost factors,  $s$  is the risk free growth over the interval,  $m$  is the drift for continuous time GBM and  $\sigma$  is the volatility for the continuous time GBM. The continuous time GBM implies a risky growth for the risky asset over the interval  $\Delta T$ . ( $amin, amax$ ) are the bounds for risky fraction state space. . . . . 123
- 7.5 Value of re-balancing for log-utility with initial risky fraction=0.5 and wealth =1 the parameters  $\lambda = \mu = 0.05$ ,  $s = e^{0.05\Delta T}$ ,  $amin = 0.001$ ,  $amax = 0.999$ ,  $da = 0.01$ ,  $T = 5$ ,  $m = 0.14$ ,  $\sigma = 0.6$ . Where  $T$  is the time horizon for investment,  $N$  is the number of re-balancing nodes.  $\omega$  is the continuous time risk-free rate,  $(\lambda, \mu)$  are transaction cost factors,  $s$  is the risk free growth over the interval,  $m$  is the drift for continuous time GBM and  $\sigma$  is the volatility for the continuous time GBM. The continuous time GBM implies a risky growth for the risky asset over the interval  $\Delta T$ . ( $amin, amax$ ) are the bounds for risky fraction state space. . . . . 123
- 7.6 Value of re-balancing when objective function is decomposed over small time horizons to yield controls which are then applied to long-term value function with parameters  $\lambda = \mu = 0.05$ ,  $s = e^{0.05\Delta T}$ ,  $amin = 0.001$ ,  $amax = 0.999$ ,  $da = 0.1$ ,  $T = 1$ ,  $m = 0.14$ ,  $\sigma = 0.6$ . Where  $T$  is the time horizon for investment,  $N$  is the number of re-balancing nodes.  $\omega$  is the continuous time risk-free rate,  $(\lambda, \mu)$  are transaction cost factors,  $s$  is the risk free growth over the interval,  $m$  is the drift for continuous time GBM and  $\sigma$  is the volatility for the continuous time GBM. The continuous time GBM implies a risky growth for the risky asset over the interval  $\Delta T$ . ( $amin, amax$ ) are the bounds for risky fraction state space. 124

- 7.7 Value of re-balancing with parameters that switch over the horizon -investor has perfect foresight. Each regime is of length  $5/3$  years. Parameters for first  $m = 0.4, \sigma = 0.8$ ; for second  $m = 0.3, \sigma = 0.7$ ; and for third  $m = 0.14, \sigma = 0.6$ . Also  $T = 5, \lambda = \mu = 0.05, s = e^{0.05\Delta T}, amin = 0.001, amax = 0.999$ . Where  $T$  is the time horizon for investment,  $N$  is the number of re-balancing nodes.  $\omega$  is the continuous time risk-free rate,  $(\lambda, \mu)$  are transaction cost factors,  $s$  is the risk free growth over the interval,  $m$  is the drift for continuous time GBM and  $\sigma$  is the volatility for the continuous time GBM. The continuous time GBM implies a risky growth for the risky asset over the interval  $\Delta T$ . ( $amin, amax$ ) are the bounds for risky fraction state space. . . . . 125
- 7.8 Value of re-balancing for CRRA utility with initial risky fraction=0.5 and wealth =1 the parameters  $V = 0.5, \lambda = \mu = 0.05, s = e^{0.05\Delta T}, amin = 0.001, amax = 0.999, da = 0.01, T = 1, m = 0.14, \sigma = 1.0$ . Where  $T$  is the time horizon for investment,  $N$  is the number of re-balancing nodes.  $\omega$  is the continuous time risk-free rate,  $(\lambda, \mu)$  are transaction cost factors,  $s$  is the risk free growth over the interval,  $m$  is the drift for continuous time GBM and  $\sigma$  is the volatility for the continuous time GBM. The continuous time GBM implies a risky growth for the risky asset over the interval  $\Delta T$ . ( $amin, amax$ ) are the bounds for risky fraction state space. . . . . 126
- 7.9 Value of re-balancing for CRRA utility with initial risky fraction=0.5 and wealth =1 the parameters  $V = 0.5, \lambda = \mu = 0.05, s = e^{0.05\Delta T}, amin = 0.001, amax = 0.999, da = 0.01, T = 5, m = 0.14, \sigma = 1.0$ . Where  $T$  is the time horizon for investment,  $N$  is the number of re-balancing nodes.  $\omega$  is the continuous time risk-free rate,  $(\lambda, \mu)$  are transaction cost factors,  $s$  is the risk free growth over the interval,  $m$  is the drift for continuous time GBM and  $\sigma$  is the volatility for the continuous time GBM. The continuous time GBM implies a risky growth for the risky asset over the interval  $\Delta T$ . ( $amin, amax$ ) are the bounds for risky fraction state space. . . . . 127
- 7.10 Value of re-balancing for CRRA utility with initial risky fraction=0.5 and wealth =1 the parameters  $V = 0.5, \lambda = \mu = 0.05, s = e^{0.05\Delta T}, amin = 0.001, amax = 0.999, da = 0.01, T = 1, m = 0.4, \sigma = 1.5$ . Where  $T$  is the time horizon for investment,  $N$  is the number of re-balancing nodes.  $\omega$  is the continuous time risk-free rate,  $(\lambda, \mu)$  are transaction cost factors,  $s$  is the risk free growth over the interval,  $m$  is the drift for continuous time GBM and  $\sigma$  is the volatility for the continuous time GBM. The continuous time GBM implies a risky growth for the risky asset over the interval  $\Delta T$ . ( $amin, amax$ ) are the bounds for risky fraction state space. . . . . 128

- 7.11 Value of re-balancing for CRRA utility with initial risky fraction=0.5 and wealth =1 the parameters  $V = 0.5, \lambda = \mu = 0.05, s = e^{0.05\Delta T}, amin = 0.001, amax = 0.999, a = 0.01, T = 5, m = 0.4, \sigma = 1.5$ . Where  $T$  is the time horizon for investment,  $N$  is the number of re-balancing nodes.  $\omega$  is the continuous time risk-free rate,  $(\lambda, \mu)$  are transaction cost factors,  $s$  is the risk free growth over the interval,  $m$  is the drift for continuous time GBM and  $\sigma$  is the volatility for the continuous time GBM. The continuous time GBM implies a risky growth for the risky asset over the interval  $\Delta T$ .  $(amin, amax)$  are the bounds for risky fraction state space. . . . . 129
- 7.12 Value of re-balancing for CRRA utility with initial risky fraction=0.5 and wealth =1 the parameters  $V = 0.5, \lambda = \mu = 0.05, s = e^{0.05\Delta T}, amin = 0.001, amax = 0.999, da = 0.01, T = 1, m = 0.4, \sigma = 2.0$ . Where  $T$  is the time horizon for investment,  $N$  is the number of re-balancing nodes.  $\omega$  is the continuous time risk-free rate,  $(\lambda, \mu)$  are transaction cost factors,  $s$  is the risk free growth over the interval,  $m$  is the drift for continuous time GBM and  $\sigma$  is the volatility for the continuous time GBM. The continuous time GBM implies a risky growth for the risky asset over the interval  $\Delta T$ .  $(amin, amax)$  are the bounds for risky fraction state space. . . . . 130
- 7.13 Value of re-balancing for CRRA utility with initial risky fraction=0.5 and wealth =1 the parameters  $V = 0.5, \lambda = \mu = 0.05, s = e^{0.05\Delta T}, amin = 0.001, namax = 0.999, da = 0.01, T = 5, m = 0.4, \sigma = 2$ . Where  $T$  is the time horizon for investment,  $N$  is the number of re-balancing nodes.  $\omega$  is the continuous time risk-free rate,  $(\lambda, \mu)$  are transaction cost factors,  $s$  is the risk free growth over the interval,  $m$  is the drift for continuous time GBM and  $\sigma$  is the volatility for the continuous time GBM. The continuous time GBM implies a risky growth for the risky asset over the interval  $\Delta T$ .  $(amin, amax)$  are the bounds for risky fraction state space. . . . . 130
- 7.14 Value of re-balancing with parameters that switch over the horizon -investor has perfect foresight. Each regime is of length 5/3 years. Parameters for first  $m = 0.4, \sigma = 1.2$ ; for second  $m = 0.3, \sigma = 1.1$ ; and for third  $m = 0.14, \sigma = 1.0$ . Also  $V = 0.5, T = 5, \lambda = \mu = 0.05, s = e^{0.05\Delta T}, amin = 0.001, amax = 0.999$ . Where  $T$  is the time horizon for investment,  $N$  is the number of re-balancing nodes.  $\omega$  is the continuous time risk-free rate,  $(\lambda, \mu)$  are transaction cost factors,  $s$  is the risk free growth over the interval,  $m$  is the drift for continuous time GBM and  $\sigma$  is the volatility for the continuous time GBM. The continuous time GBM implies a risky growth for the risky asset over the interval  $\Delta T$ .  $(amin, amax)$  are the bounds for risky fraction state space. . . . . 131

- 7.15 Scaled value of re-balancing for CARA utility with initial wealth in risky asset =100 the parameters  $\lambda = \mu = 0.05, s = e^{0.05\Delta T}, amin = 0.001, amax = 0.999, da = 0.01, T = 1, m = 0.14, \sigma = 0.6$ . Where  $T$  is the time horizon for investment,  $N$  is the number of re-balancing nodes.  $\omega$  is the continuous time risk-free rate,  $(\lambda, \mu)$  are transaction cost factors,  $s$  is the risk free growth over the interval,  $m$  is the drift for continuous time GBM and  $\sigma$  is the volatility for the continuous time GBM. The continuous time GBM implies a risky growth for the risky asset over the interval  $\Delta T$ . ( $amin, amax$ ) are the bounds for risky fraction state space. . . . . 132
- 7.16 Scaled value of re-balancing for CARA utility with initial wealth in risky asset =100 the parameters  $\lambda = \mu = 0.05, s = e^{0.05\Delta T}, amin = 0.001, amax = 0.999, da = 0.01, T = 5, m = 0.14, \sigma = 0.6$ . Where  $T$  is the time horizon for investment,  $N$  is the number of re-balancing nodes.  $\omega$  is the continuous time risk-free rate,  $(\lambda, \mu)$  are transaction cost factors,  $s$  is the risk free growth over the interval,  $m$  is the drift for continuous time GBM and  $\sigma$  is the volatility for the continuous time GBM. The continuous time GBM implies a risky growth for the risky asset over the interval  $\Delta T$ . ( $amin, amax$ ) are the bounds for risky fraction state space. . . . . 132
- 7.17 Value of re-balancing depicted by a shift in the efficiency frontier calculated for the initial wealth =0.2 and initial risky fraction =0.5. Parameters are chosen as:  $T = 0.3, \lambda = \mu = 0.005, s = e^{0.05\Delta T}, m_1 = 0.08, \sigma_1 = 0.42, m_2 = 0.14, \sigma_2 = 0.8, \rho = 0.05, amin = 0.001, amax = 0.999$ . . . . . 133
- 7.18 Mean variance CASE for AMAZON stock by forming a portfolio with risk free asset and AMAZON stock with parameters  $\lambda = \mu = 0.01, s = e^{0.05\Delta T}, T = 0.5, m = 0.18, \sigma = 0.4, \lambda = \mu = 0.01$ . Where  $T$  is the time horizon for investment,  $N$  is the number of re-balancing nodes.  $\omega$  is the continuous time risk-free rate,  $(\lambda, \mu)$  are transaction cost factors,  $s$  is the risk free growth over the interval,  $m$  is the drift for continuous time GBM and  $\sigma$  is the volatility for the continuous time GBM. The continuous time GBM implies a risky growth for the risky asset over the interval  $\Delta T$ . . . . . 133
- 7.19 Log utility CASE for AMAZON stock by forming a portfolio with risk free asset and AMAZON stock with parameters  $\lambda = \mu = 0.01, s = e^{0.05\Delta T}, T = 1, m = 0.18, \sigma = 0.4, \lambda = \mu = 0.01$ . Where  $T$  is the time horizon for investment,  $N$  is the number of re-balancing nodes.  $\omega$  is the continuous time risk-free rate,  $(\lambda, \mu)$  are transaction cost factors,  $s$  is the risk free growth over the interval,  $m$  is the drift for continuous time GBM and  $\sigma$  is the volatility for the continuous time GBM. The continuous time GBM implies a risky growth for the risky asset over the interval  $\Delta T$ . . . . . 134



7.20	CRRA utility CASE for AMAZON stock by forming a portfolio with risk free asset and AMAZON stock with parameters $\lambda = \mu = 0.01, s = e^{0.05\Delta T}, T = 1, m = 0.18, \sigma = 0.4, \lambda = \mu = 0.01$ . Where $T$ is the time horizon for investment, $N$ is the number of re-balancing nodes. $\omega$ is the continuous time risk-free rate, $(\lambda, \mu)$ are transaction cost factors, $s$ is the risk free growth over the interval, $m$ is the drift for continuous time GBM and $\sigma$ is the volatility for the continuous time GBM. The continuous time GBM implies a risky growth for the risky asset over the interval $\Delta T$ . . . . .	135
7.21	CARA utility CASE for AMAZON stock by forming a portfolio with risk free asset and AMAZON stock with parameters $\lambda = \mu = 0.01, s = e^{0.05\Delta T}, T = 1, m = 0.18, \sigma = 0.4, \lambda = \mu = 0.01, z = 0.01$ . Value function is scaled and evaluated with initial wealth in risky asset =100. Where $T$ is the time horizon for investment, $N$ is the number of re-balancing nodes. $\omega$ is the continuous time risk-free rate, $(\lambda, \mu)$ are transaction cost factors, $s$ is the risk free growth over the interval, $m$ is the drift for continuous time GBM and $\sigma$ is the volatility for the continuous time GBM. The continuous time GBM implies a risky growth for the risky asset over the interval $\Delta T$ . . . . .	136
7.22	Log-utility CASE: Phase geometry of no-transaction region with respect to <i>Merton</i> point and mean-reversion of risky fraction with parameters $\lambda = \mu = 0.05, s = e^{0.1\Delta T}, T = 6, N = 80, amin = 0.001, amax = 0.999, da = 0.001, m = 0.14, \sigma = 0.3$ . . . . .	136
7.23	CRRA utility CASE: Phase geometry of no-transaction region with respect to <i>Merton</i> point and mean-reversion of risky fraction with parameters $V = 0.5, \lambda = \mu = 0.005, s = e^{0.05\Delta T}, T = 1, N = 10, amin = 0.001, amax = 0.999, da = 0.001, m = 0.08, \sigma = 0.42$ . . . . .	137
7.24	CARA-utility CASE: Phase geometry of no-transaction region with respect to <i>Merton</i> line with parameters $\lambda = \mu = 0.01, s = e^{0.05\Delta T}, T = 1, N = 10, xmin = 5, xmax = 600, dx = 1, \eta = 0.01, m = 0.18, \sigma = 0.4, z = 0.01$ . Here $[xmin, xmax]$ denotes the bounds for amount of wealth in risky asset state space. Using the same parameters as estimated for AMAZON stock in this chapter. . . . .	137
7.25	CARA utility CASE: Phase geometry of no-transaction region with respect to time varying <i>Merton</i> line $\eta = 0.01, \lambda = \mu = 0.01, s = e^{0.05\Delta T}, T = 1, N = 10, xmin = 5, xmax = 600, dx = 1, m = 0.18, \sigma = 0.4, z = 0.01$ . Here $[xmin, xmax]$ denotes the bounds for amount of wealth in risky asset state space	138
7.26	Mean-variance ( <i>pre-committed</i> controls -also called 'benchmark' objective ) CASE: Phase stencil of no-transaction topology with respect to mean-reversion of risky fraction. Parameters are chosen as: $T = 0.3, N = 6, \lambda = \mu = 0.05, s = e^{0.05\Delta T}, m_1 = 0.08, \sigma_1 = 0.42, m_2 = 0.14, \sigma_2 = 0.8, \rho = 0.05, amin = 0.001, amax = 0.999$ . . . . .	138
7.27	Reflection of the 'risky fraction' process about the no-transaction boundaries and the value of re-balancing. . . . .	139
8.1	Joint evolution discrete probability approximation for (risky growth, change in volatility. ) . . . . .	143

8.2	Evolution of risky growth. . . . .	146
8.3	Evolution of change in volatility. . . . .	146
8.4	Dynamic programming on a grid and truncation on volatility axis to avoid extrapolation errors. . . . .	147
8.5	Transaction cost processes. . . . .	148
8.6	No-transaction topology at time $t=0.45$ and parameters $m = 0.14, \theta = 0.1, \Lambda = 0.8, \xi = 0.02, T = 0.5, \rho = 0.1, \sigma_{min} = 0.5, \sigma_{max} = 1.1, \lambda = \mu = 0.01 + 0.01\sigma, \gamma = 2, L = 10N^\gamma, s = e^{0.05\Delta T}, N = 10, da = \frac{amax-amin}{L}, \Delta T = \frac{T}{N}, amin = 0.001, amax = 0.999$ . Volatility axis horizontal and risky fraction axis vertical. We have $\theta, \Lambda, \xi$ and $\rho$ as the parameters for the joint evolution tree. Also $da$ represents the risky fraction space discretization with $[amin, amax]$ being the bounds. Where $T$ is the time horizon for investment, $N$ is the number of re-balancing nodes. $\omega$ is the continuous time risk-free rate, $(\lambda, \mu)$ are transaction cost factors, $s$ is the risk free growth over the interval, $m$ is the drift for continuous time GBM and $\sigma$ is the volatility for the continuous time GBM. The continuous time GBM implies a risky growth for the risky asset over the interval $\Delta T$ . . . . .	149
8.7	No transaction geometry at time $t=0.1$ and parameters $m = 0.14, \theta = 0.1, \Lambda = 0.8, \xi = 0.02, T = 0.5, \rho = 0.1, \sigma_{min} = 0.5, \sigma_{max} = 1.1, \lambda = \mu = 0.01 + 0.01\sigma, \gamma = 2, L = 10N^\gamma, s = e^{0.05\Delta T}, N = 10, da = \frac{amax-amin}{L}, \Delta T = \frac{T}{N}, amin = 0.001, amax = 0.999$ . Volatility axis horizontal and risky fraction axis vertical. We have $\theta, \Lambda, \xi$ and $\rho$ as the parameters for the joint evolution tree. Also $da$ represents the risky fraction space discretization with $[amin, amax]$ being the bounds. Where $T$ is the time horizon for investment, $N$ is the number of re-balancing nodes. $\omega$ is the continuous time risk-free rate, $(\lambda, \mu)$ are transaction cost factors, $s$ is the risk free growth over the interval, $m$ is the drift for continuous time GBM and $\sigma$ is the volatility for the continuous time GBM. The continuous time GBM implies a risky growth for the risky asset over the interval $\Delta T$ . . . . .	150
9.1	CRRA utility and no-transaction region for portfolio insurance constraint problem at time $t=0.75$ yrs with parameters: $\gamma_N = \frac{1}{10}, T = 1, N = 4, \lambda = \mu = 0.01, s = e^{0.1\Delta T}, m = 0.14, \sigma = 0.3, K = 0.2, V = 0.5$ . We denote $K$ as the portfolio insurance level. Where $T$ is the time horizon for investment, $N$ is the number of re-balancing nodes. $\omega$ is the continuous time risk-free rate, $(\lambda, \mu)$ are transaction cost factors, $s$ is the risk free growth over the interval, $m$ is the drift for continuous time GBM and $\sigma$ is the volatility for the continuous time GBM. The continuous time GBM implies a risky growth for the risky asset over the interval $\Delta T$ . $\gamma_\ell$ is the deformation parameter. Also $V$ is the risk aversion co-efficient for CRRA utility. . . . .	156

9.2	CRRA utility and no-transaction region for portfolio insurance constraint problem at time =0 yrs with parameters: $\gamma_N = \frac{1}{10}, T = 1, N = 4, \lambda = \mu = 0.01, s = e^{0.1\Delta T}, m = 0.14, \sigma = 0.3, K = 0.2, V = 0.5$ . We denote $K$ as the portfolio insurance level. Where $T$ is the time horizon for investment, $N$ is the number of re-balancing nodes. $\omega$ is the continuous time risk-free rate, $(\lambda, \mu)$ are transaction cost factors, $s$ is the risk free growth over the interval, $m$ is the drift for continuous time GBM and $\sigma$ is the volatility for the continuous time GBM. The continuous time GBM implies a risky growth for the risky asset over the interval $\Delta T$ . $\gamma_\ell$ is the deformation parameter. Also $V$ is the risk aversion co-efficient for CRRA utility. . . . .	157
9.3	Here $\star$ =BUY, $\blacklozenge$ =DO-NOTHING and $\bullet$ = SELL for no-transaction region geometry with CRRA utility for draw-down constraint problem at time =0.75 yrs and wealth =0.07 with parameters: $\gamma_N = \frac{1}{10}, T = 1, N = 4, \lambda = \mu = 0.01, s = e^{0.1\Delta T}, m = 0.14, \sigma = 0.3, \alpha = 0.25, V = 0.5$ . We denote $\alpha$ as important number in the draw-down constraint. Where $T$ is the time horizon for investment, $N$ is the number of re-balancing nodes. $\omega$ is the continuous time risk-free rate, $(\lambda, \mu)$ are transaction cost factors, $s$ is the risk free growth over the interval, $m$ is the drift for continuous time GBM and $\sigma$ is the volatility for the continuous time GBM. The continuous time GBM implies a risky growth for the risky asset over the interval $\Delta T$ . $\gamma_\ell$ is the deformation parameter. Also $V$ is the risk aversion co-efficient for CRRA utility. . . . .	158
9.4	Here $\star$ =BUY, $\blacklozenge$ =DO-NOTHING and $\bullet$ = SELL for no-transaction region geometry with CRRA utility for draw-down constraint problem at time =0 yrs and wealth =0.07 with parameters: $\gamma_N = \frac{1}{10}, T = 1, N = 4, \lambda = \mu = 0.01, s = e^{0.1\Delta T}, m = 0.14, \sigma = 0.3, \alpha = 0.25, V = 0.5$ . We denote $\alpha$ as important number in the draw-down constraint. Where $T$ is the time horizon for investment, $N$ is the number of re-balancing nodes. $\omega$ is the continuous time risk-free rate, $(\lambda, \mu)$ are transaction cost factors, $s$ is the risk free growth over the interval, $m$ is the drift for continuous time GBM and $\sigma$ is the volatility for the continuous time GBM. The continuous time GBM implies a risky growth for the risky asset over the interval $\Delta T$ . $\gamma_\ell$ is the deformation parameter. Also $V$ is the risk aversion co-efficient for CRRA utility. . . . .	159
9.5	Initial wealth=0.5 and initial risky fraction=0.5. CRRA utility and terminal wealth distribution for portfolio insurance constraint problem with parameters: $\gamma_N = \frac{1}{15}, T = 1, N = 4, \lambda = \mu = 0.01, s = e^{0.1\Delta T}, m = 0.14, \sigma = 0.3, K = 0.2, V = 0.5$ . Also $V$ is the risk aversion co-efficient for CRRA utility. . . . .	160
10.1	Trading Rule with entry and exit signals. . . . .	162
10.2	Transition diagram for the state $S_k \in \{\mathbf{N}, \mathbf{S}, \mathbf{L}\}$ . . . . .	163
10.3	Value function at time $t = 0$ for spread process calibrated to “LOW” and “HD” stock pair. At $t = 0$ investor is short the spread with $\mathcal{Z}_0 = 1.0$ . The time horizon for trading is 0.5 years with 10 observation points and data calibrated to history from May 2011 to May 2012. . . . .	165

10.4	Simulation of gross realized profit (not including transaction costs) with trading starting at (2007,3,1) and look back of 500 days. The time horizon for trading is 0.5 years with 10 observation points and data calibrated with historical look back. . . . .	165
10.5	Simulation of gross realized profit (not including transaction costs) with trading starting at (2007,3,1) and look back of 100 days. The time horizon for trading is 0.5 years with 10 observation points and data calibrated with the historical look back. . . . .	166
10.6	Histogram of realized profits for trading starting points chosen equally spaced in 2005-2011. Stock pair is ( <b>LOW,HD</b> ). Look back of 180 days and trading horizon of 180 days. . . . .	167
10.7	Approximate dependence expected return of the <b>MS</b> stock on the ( <b>MS,GS</b> ) stock pair spread using the daily closing stock prices from July 2005 to July 2006. . . . .	169
10.8	Approximate dependence expected return of the <b>GS</b> stock on the ( <b>MS,GS</b> ) spread using the daily closing stock prices from July 2005 to July 2006. . . . .	169
10.9	Pair trading signals - shorting when the spread falls below a barrier and longing when the spread goes above. . . . .	169
10.10	Dynamic pairs trading - pair trading quadrants with different controls illustrated. . . . .	171
10.11	Optimal control law at time $t = 0$ and spread =0.25 under dynamic trading for the following choice of parameter which are already defined earlier : $\lambda = \mu = 0.005, T = 0.2, N = 2, s = e^{0.05\Delta T}, a = 0.16, b = 0.1, \sigma_1 = 0.1, c = 0.1, d = 0.9, \sigma_2 = 0.2, \rho = 0.05$ . Also $\diamond \mapsto$ SS, $\bullet \mapsto$ SL, $\star \mapsto$ LS, $+$ $\mapsto$ LL and $\# \mapsto$ NN. . . . .	176
10.12	Optimal control law at time $t = 0$ and spread =0.5 under dynamic trading for the following choice of parameter which are already defined earlier: $\lambda = \mu = 0.005, T = 0.2, N = 2, s = e^{0.05\Delta T}, a = 0.16, b = 0.1, \sigma_1 = 0.1, c = 0.1, d = 0.9, \sigma_2 = 0.2, \rho = 0.05$ . Also $\diamond \mapsto$ SS, $\bullet \mapsto$ SL, $\star \mapsto$ LS, $+$ $\mapsto$ LL and $\# \mapsto$ NN. . . . .	177
10.13	Probability distribution of terminal wealth. . . . .	178
11.1	No-transaction geometries for growth rate maximization when parameters change over the horizon and investor has perfect foresight. Parameters: $m_1 = 0.14, \sigma_1 = 0.6, m_2 = 0.2, \sigma_2 = 0.5, m_3 = 0.15, \sigma_3 = 0.45$ . Here $(m_i, \sigma_i)$ is the drift and volatility for regime $i$ . . . . .	180
11.2	First passage time distribution using lattice compared to exact result. SQID scheme used to create 25 branches for Standard Brownian motion. Parameters: $a = 0.25, N = 90, T = 0.2, wmin = -1, wmax = +1, mmin = -1, mmax = +1, dw = 0.05, dm = 0.05$ . Here $a$ is the barrier, $N$ is the number of time steps, $T$ is the time period, $(wmin, wmax)$ are the bounds for actual value of Standard Brownian motion, $(mmin, mmax)$ are the bounds for attained maximum value of Standard Brownian motion, $dw$ is the size of state step in $W_k$ -space and $dm$ is the size of state step in $M_k$ space. . . . .	181

11.3	First passage time distribution using lattice compared to exact result. Moment matching of first 19 moments for Standard Brownian motion. Parameters: $a = 0.25, N = 90, T = 0.2, wmin = -1, wmax = +1, mmin = -1, mmax = +1, dw = 0.05, dm = 0.05$ . Here $a$ is the barrier, $N$ is the number of time steps, $T$ is the time period, $(wmin, wmax)$ are the bounds for actual value of Standard Brownian motion, $(mmin, mmax)$ are the bounds for attained maximum value of Standard Brownian motion, $dw$ is the size of state step in $W_k$ -space and $dm$ is the size of state step in $M_k$ space. . . . .	182
11.4	Lattice framework for spread evolution. . . . .	183
11.5	No-transaction region variation with time for exchange rate model under a simple jump diffusion model with growth rate maximization for exchange rate portfolio. In the discrete time re-balancing we have no-transaction strips at $t = 0, 0.25, 0.5, 0.75$ . Parameter choice is : $T = 1, N = 4, \lambda = \mu = 0.01, r_1 = e^{0.05\Delta T}, r_2 = e^{0.07\Delta T}, m = 0.14, \sigma = 0.6, \theta = 0.1, \delta = 0.05$ . . . . .	185
11.6	Realization of wealth for an investor trying to maximize Sharpe ratio by investing in SP500 and GS starting (2010,1,1) for one year with initial wealth =0.5 and initial fraction in SP500=0.5. Also Lookback =40 days. Paramater choice $T = 1, N = 5, \lambda = 0.005, r = 0.05$ . . . . .	186

# List of Tables

2.1	Summary of Notations Used. . . . .	18
3.1	Transfer of wealth configurations between 3 risky assets where $(i, j)$ is equal to 0 if he transfers from $i$ to $j$ and 1 if he transfers from $j$ to $i$ . This table includes all the possibilities for transferring wealth under the control constraints. . . . .	28
3.2	A nice discrete probability approximation structure with correlated standard normals in 3-D . . . . .	42
5.1	Relative percentage error in value function with initial wealth=1, initial risky fraction=0.2, varying deformation from $\ell = 15$ to 25 and parameter choice: $\lambda = \mu = 0.01, s = e^{0.1*\Delta T}, m = 0.14, \sigma = 0.3, \gamma_\ell = \frac{1}{\ell}$ . Where $T$ is the time horizon for investment, $N$ is the number of re-balancing nodes. $\omega$ is the continuous time risk-free rate, $(\lambda, \mu)$ are transaction cost factors, $s$ is the risk free growth over the interval, $m$ is the drift for continuous time GBM and $\sigma$ is the volatility for the continuous time GBM. The continuous time GBM implies a risky growth for the risky asset over the interval $\Delta T$ . $\gamma_\ell$ is the deformation parameter. . . . .	69
5.2	Relative percentage error in value function with initial wealth=1, initial risky fraction=0.5, varying deformation from $\ell = 15$ to 25 and parameter choice: $\lambda = \mu = 0.01, s = e^{0.1*\Delta T}, m = 0.14, \sigma = 0.3, \gamma_\ell = \frac{1}{\ell}$ . Where $T$ is the time horizon for investment, $N$ is the number of re-balancing nodes. $\omega$ is the continuous time risk-free rate, $(\lambda, \mu)$ are transaction cost factors, $s$ is the risk free growth over the interval, $m$ is the drift for continuous time GBM and $\sigma$ is the volatility for the continuous time GBM. The continuous time GBM implies a risky growth for the risky asset over the interval $\Delta T$ . $\gamma_\ell$ is the deformation parameter. . . . .	69
5.3	Relative percentage error in value function with initial wealth=1, initial risky fraction=0.9, varying deformation from $\ell = 15$ to 25 and parameter choice: $\lambda = \mu = 0.01, s = e^{0.1*\Delta T}, m = 0.14, \sigma = 0.3, \gamma_\ell = \frac{1}{\ell}$ . Where $T$ is the time horizon for investment, $N$ is the number of re-balancing nodes. $\omega$ is the continuous time risk-free rate, $(\lambda, \mu)$ are transaction cost factors, $s$ is the risk free growth over the interval, $m$ is the drift for continuous time GBM and $\sigma$ is the volatility for the continuous time GBM. The continuous time GBM implies a risky growth for the risky asset over the interval $\Delta T$ . $\gamma_\ell$ is the deformation parameter. . . . .	69

5.4	relative percentage error in value function with initial wealth=1, initial risky fraction=0.5, varying deformation from $\ell=8$ to 15 and parameter choice: $\lambda = \mu = 0.05, T = 1, N = 4, \mu_1 = 0.08, \sigma_1 = 0.2, \mu_2 = 0.14, \sigma_2 = 0.8, \rho = 0.1, \gamma_\ell = \frac{1}{\ell}$ . Where $T$ is the time horizon for investment, $N$ is the number of re-balancing nodes. $\omega$ is the continuous time risk-free rate, $(\lambda, \mu)$ are transaction cost factors, $s$ is the risk free growth over the interval, $m$ is the drift for continuous time GBM and $\sigma$ is the volatility for the continuous time GBM. The continuous time GBM implies a risky growth for the risky asset over the interval $\Delta T$ . $\gamma_\ell$ is the deformation parameter. . . . .	72
5.5	Lexicographic ordering of a monomial set in 2-D . . . . .	75
5.6	Lexicographic ordering of a monomial set in 3-D . . . . .	75
6.1	same first and second moments as an equivalent log-normal with: $\lambda = 0.001, T = 0.04, N = 1, \Delta T = \frac{T}{N}, s = e^{0.07\Delta T}, m = 0.182, \sigma = 0.4$ . . . . .	93
6.2	same first and second moments as an equivalent log-normal with: $\lambda = 0.001, T = 0.04, N = 1, \Delta T = \frac{T}{N}, s = e^{0.07\Delta T}, m = 0.182, \sigma = 0.4$ . . . . .	94
6.3	Comparison of finite horizon no-transaction boundary obtained at $T = 1$ with parameters: $\lambda = 0.01, T = 1, N = 100, \Delta T = \frac{T}{N}, s = e^{0.07\Delta T}, m = 0.182, \sigma = 0.4$ . . . . .	95
6.4	Scaling of time taken for some range of parameters with $10 \leq l \leq 50$ and $200 \leq n \leq 1000$ . Parameters: $\lambda = 0.001, T = 1, \Delta T = \frac{T}{N}, s = e^{0.07\Delta T}$ . . . . .	100
6.5	Scaling of absolute error for some range of parameters. For $\gamma_1$ we vary $l$ and $n$ kept to some large value. Similarly, for $\gamma_2$ we vary $n$ and $l$ kept to some large value. Parameters chosen: $\lambda = 0.001, T = 1, \Delta T = \frac{T}{N}, s = e^{0.07\Delta T}$ . . . . .	100
6.6	Time taken vs time division. $\lambda = 0.001, T = 5, da = 0.001, \Delta T = \frac{T}{N}, s = e^{0.07\Delta T}, m = 0.182, \sigma = 0.4$ . . . . .	100
6.7	Time taken vs state space division. $\lambda = 0.001, T = 5, m = 500, \Delta T = \frac{T}{N}, s = e^{0.07\Delta T}, m = 0.182, \sigma = 0.4$ . . . . .	100
6.8	relative percentage error vs time step division. $\lambda = 0.001, T = 1, da = 0.001, \Delta T = \frac{T}{N}, s = e^{0.07\Delta T}, m = 0.182, \sigma = 0.4$ . . . . .	100
6.9	Error vs state space division. $\lambda = 0.001, T = 1, N = 100, \Delta T = \frac{T}{N}, s = e^{0.07\Delta T}, m = 0.182, \sigma = 0.4$ . . . . .	101
6.10	relative absolute percentage error at different nodal points in 2-D with 2nd order moment matching with: $\lambda = 0.001, T = 0.05, N = 1, \Delta T = \frac{T}{N}, s = e^{0.07\Delta T}, m_1 = 0.13, \sigma_1 = \sqrt{0.1}, m_2 = 0.15, \sigma_2 = \sqrt{0.17}, \rho = \frac{0.07}{\sigma_1\sigma_2}$ . . . . .	101
6.11	relative absolute percentage error at different nodal points in 2-D with 3rd order moment matching with: $\lambda = 0.001, T = 0.05, N = 1, \Delta T = \frac{T}{N}, s = e^{0.07\Delta T}, m_1 = 0.13, \sigma_1 = \sqrt{0.1}, m_2 = 0.15, \sigma_2 = \sqrt{0.17}, \rho = \frac{0.07}{\sigma_1\sigma_2}$ . . . . .	101
6.12	Accuracy dependent on order of moment matching with $\lambda = 0.001, T = 0.04, N = 1, \Delta T = \frac{T}{N}, s = e^{0.07\Delta T}, m = 0.182, \sigma = 0.4$ . . . . .	101
6.13	Relative absolute percentage error in the value function at time $t = 0$ different nodal points in 2-D with parameters $\lambda = \mu = 0.005, T = 0.25, N = 5, s = e^{0.05\Delta T}, m_1 = 0.08, \sigma_1 = 0.42, m_2 = 0.14, \sigma_2 = 0.8, \rho = 0.05$ . . . . .	112

6.14	Infinite horizon upper and lower boundaries computed using discrete probability approximation with parameters $m = 0.14, \sigma = 0.3, \lambda = \mu = 0.05, \omega = 0.1, s = e^{\omega\Delta T}$ . . . . .	115
8.1	Expected utility measured at $t = 0$ as a result of uncertain transaction costs with parameters: $m = 0.14, \theta = 0.1, \Lambda = 0.4, \xi = 0.5, T = 0.4, \rho = 0.1$ . We have $\theta, \Lambda, \xi$ and $\rho$ as the parameters for the joint evolution tree. . . . .	144
8.2	Relative absolute percentage error in the value function at time for different nodal points in 2-D with parameters $m = 0.14, \theta = 0.1, \xi = 0.8, \xi = 0.02, T = 0.04, \rho = 0.1, \sigma_{min} = 0.7, \sigma_{max} = 0.9, \lambda = \mu = 0.01 + 0.01\sigma, \gamma = 2, L = 100N^\gamma, s = e^{0.05\Delta T}, N = 6, da = \frac{amax-amin}{L}, \Delta T = \frac{T}{N}, amin = 0.001, amax = 0.999$ . We have $\theta, \Lambda, \xi$ and $\rho$ as the parameters for the joint evolution tree. Also $da$ represents the risky fraction space discretization with $[amin, amax]$ being the bounds. Where $T$ is the time horizon for investment, $N$ is the number of re-balancing nodes. $\omega$ is the continuous time risk-free rate, $(\lambda, \mu)$ are transaction cost factors, $s$ is the risk free growth over the interval, $m$ is the drift for continuous time GBM and $\sigma$ is the volatility for the continuous time GBM. The continuous time GBM implies a risky growth for the risky asset over the interval $\Delta T$ . . . . .	145
10.1	Terminal wealth distribution statistics initial risky fraction 1=0.2, initial risky fraction 2 =-0.2, stochastic spread=0.7, with parameter: $\lambda = \mu = 0.005, T = 0.5, N = 5, s = e^{0.05\Delta T}, a = 0.16, b = 0.1, \sigma_1 = 0.1, c = 0.1, d = 0.9, \sigma_2 = 0.1, \rho = 0.2$ . . . . .	177
10.2	Terminal wealth distribution statistics initial risky fraction 1=0.2, initial risky fraction 2 =-0.2, stochastic spread=0.55, with parameter: $\lambda = \mu = 0.005, T = 0.5, N = 5, s = e^{0.05\Delta T}, a = 0.16, b = 0.1, \sigma_1 = 0.1, c = 0.1, d = 0.9, \sigma_2 = 0.2, \rho = 0.2$ . . . . .	177
10.3	Terminal wealth distribution statistics initial risky fraction 1=0.2, initial risky fraction 2 =-0.2, stochastic spread=0.5, with parameter: $\lambda = \mu = 0.005, T = 0.5, N = 5, s = e^{0.05\Delta T}, a = 0.16, b = 0.1, \sigma_1 = 0.1, c = 0.1, d = 0.9, \sigma_2 = 0.1, \rho = 0.2$ . . . . .	178



# List of Appendices

Appendix A Mathematica code for chapter 4 . . . . .	194
Appendix B Pair Trading Models . . . . .	200

# Chapter 1

## A quantitative analysis of continuous time portfolio strategies

In quantitative portfolio analysis investment portfolios are assembled from underlying assets so that the resulting portfolio taken as a whole performs in a way that is deemed optimal. So the idea is not simply to pick the best stocks, but to pick the best team of stocks. The idea goes back to Markowitz [61], who looked at the portfolio with the lowest standard deviation of returns for a given expected level of returns: the so-called *efficient frontier*. This work has been very influential in the 50 years that followed, both in practice and in theory. However, it is highly limited by being a single period model in which all investment decisions are made at some initial time and the value of the portfolio is considered at a single, later, time.

Of course portfolios may be rebalanced. So in 1969 Merton developed a continuous time framework in [64] which allowed for portfolios to be rebalanced and consumed from over time. The investor chose consumption and allocation decision rules so as to maximize the expected utility of future consumption plus the expected utility of future bequest, all suitably time discounted. This framework is modeled by some very nice nonlinear Partial Differential equations (PDEs) which can, for a wide class of utility functions, be solved analytically. However, this model is limited by its assumption of transaction cost free trading: an assumption which dramatically simplifies the resulting equations and their solutions.

Since 1970 a variety of models which incorporate transaction costs have been proposed. These models are computationally challenging and each has their advantages and disadvantages. All have the goal of either understanding how actual investors make decisions (descriptive studies) or in helping actual investors make better decisions (normative models).

The current thesis aims to contribute to the literature on normative portfolio theory models. Mathematical and computational techniques are developed to handle the challenging quantitative problems emerging from this subject. The tool used is that of *discrete multinomial trees* optimized using topological ideas and implemented using a powerful parallel computing *Mathematica* environment. The tool, once forged, is used to better understand a number of problems in portfolio optimization distinguished from existing work by their improved realism.

This thesis is about optimizing the re-balancing of investment portfolios when trading between assets attracts transaction costs. This financial problem may be cast as the mathematical problem of determining a value function that depends on the price of each of the  $n$  assets comprising the portfolio and time. At each time there is a best portfolio, defined by an  $n$ -vector

which gives the wealth allocation to each of the  $n$  assets. However, stochastic asset price fluctuations result in the actual asset allocations moving away from this optimal point. The presence of transaction costs makes continuous re-balancing of the portfolio to their optimal level. So, as the introduction to this thesis will show, this problem's solution involves a small "no trade" region surrounding the optimal asset point.

The problem of determining the boundaries of this region is very complicated. It may be cast as a partial differential equation, in which case a linear partial differential operator applies inside the region, with moving boundaries determined using the transaction cost structure in a way reminiscent of the determination of the American options early exercise boundary. Since the number of assets comprising realistic portfolios is very large – 20, 30, or even 100 assets are not unheard of, numerical partial differential techniques are simply impractical for this problem.

Monte Carlo approaches might be better suited to this, but their inherent noisiness suffer from difficulties in accurate determining boundaries. To be sure, these problems may be overcome using the stochastic tree and mesh proposed by Broadie Glasserman in [17] or using Longstaffe and Schwartz's Least Squares Monte Carlo method in [57]. But those techniques are difficult to code and require substantial computational power.

In this thesis we take a different approach. We follow the Monte Carlo route insofar as we model the problem of re-balancing at one of a finite number of re-balance times, using the dynamic programming principle to solve the problem from the final time horizon backwards in time to the beginning. But we replace the simulation approach to computing the expectations required in this stochastic dynamic program by a deterministic approach using trees designed to well approximate the high dimensional probability transition functions from re-balance time to re-balance time. Although our method is also destined to fail for large numbers of dimensions, we show that it works remarkably well for problems involving two, three, or four assets. The method proposed here is easy to code and easy to understand.

Careful study of realistic portfolio problems with a small number of risky assets is very useful in building financial intuition, as existing literature provides little guidance for the transaction cost problem with more than two risky assets. This thesis models and solves a number of portfolio and trading strategy problems using the tree formalism and draws financial conclusions.

The outline of the thesis is as follows. The first section of the thesis is devoted to foundational materials. In Chapter 2 a brief review of the key papers in the field is provided; this chapter also serves the purpose of setting the notation used in the remainder of the thesis. In Chapter three our basic numerical approach, that of discrete multinomial trees, is introduced. Results providing evidence that these trees converge, in the appropriate limit, to the continuous problem are also provided in Chapter 3. The *Mathematica* implementation of these models on our small custom built computer cluster is described in Chapter 4. Chapter 5 situates some of the tree building results in the context of homotopy theory. In Chapter 5 we discuss discretization schemes for the continuous time probability model so that our problems could be solved over a larger time interval  $\Delta T$ . This methodology could significantly reduce the interpolation errors which arise as a consequence of the fact that we represent our value function numerically at each stage of dynamic programming.

With the above results in hand we have forged a tool which allows us to present some analysis in context of continuous time portfolio theory. In first section of Chapter 6 the tool

is used in a fairly simple setting in which risky assets follow Geometric Brownian motion (GBM) and trading has linear transaction costs, but with multiple underlying risky assets. Links are drawn with existing approximations in the literature. The second section of Chapter 6 extends the first section results to a practical situation in which the risk free asset no longer acts as a banker for the trades. This means the trades in section 2 of Chapter are financed by transfer of wealth between risky assets. In the third section we consider a model in which transaction cost is proportional to the amount traded. Chapter 7 is devoted to looking at the cost of inattention: how much utility is lost by re-balancing portfolios less frequently. We also consider this problem in a more realistic situation in which the parameters of the random process change with time and find that, for an investor able to accurately assess the changes, the value of re-balancing is greatly enhanced. At the same time Chapter 7 may be considered to be a validation of the discrete time/state approach to its continuous limit. Chapter 7 initially examines the value of re-balancing a portfolio for a dynamic investor when the parameters of risky asset are constant over the investment horizon. It subsequently provides a framework for the value of re-balancing when the parameters shift over the investment horizon but the investor knows in advance all the possible future changes. It shows the value of accurate financial analyst recommendations regarding stock growth and volatility for an investor dynamically allocating portfolios under transaction costs.

In the final part of the thesis we move farther afield from the theoretical roots of the field and add realism by making better models for transaction costs, portfolio optimization constraints and the class of trading strategies. In Chapter 8 we consider a model in which the bid-ask component of transaction costs depend, in a deterministic way, on the market volatility, itself modeled as changing via a Heston style formulation. We compare the portfolio utility lost as a result of uncertainty in transaction costs. Chapter 9 examines the way in which realistic constraints on solvency and draw-downs may be added to the formalism developed here and some conclusions drawn. We show the optimal investment allocation rules in the form of no-transaction geometries at a snapshot. An application of the thesis techniques to the hedge fund strategy of pairs trading is displayed in Chapter 10. This chapter examines a simple pair trading strategy in which an optimal trading rule is constructed both in the absence and presence of transaction costs. The thesis concludes in the Chapter 11, with some suggestions for future research.

If the reader is mostly interested in the financial implications of the ideas we suggest they read Chapters 2 and 3 to get a flavor of the methods then Chapters 7, 8, 9 and 10. Modeling and numerical aspects of the thesis are covered in Chapters 3, 4, 5 and 6.

It is clearly impossible to make much headway on the problems described in Chapters 7, 8, 9 and 10 analytically. The thesis provides simple, intuitive and robust numerical algorithms. The numerical solution of the problems is very challenging and motivated us to develop (see especially Chapters 3, 4, 5 and 6 ) sophisticated discrete probability approximation algorithms in the thesis and implement them in a powerful Mathematica based parallel computing environment.

# Chapter 2

## Literature review and notations

Chapter 2 provides the main underlying ideas behind dynamic portfolio theory. We provide a brief overview of the transaction cost literature and set the notation for the rest of the thesis.

### 2.1 An overview of dynamic portfolio theory

The models of the thesis are *dynamic* in contrast to being *static*. The word *dynamic* corresponds to active portfolio management and the word *static* to *passive* portfolio management. The classical one-period portfolio theory of *Markowitz* is the canonical example of a static model as it considers the decision of a myopic investor who over a time horizon selects his portfolio composition only at the initial time to optimize his terminal objective. In contrast, this thesis addresses dynamic portfolio models. This means that we have a multi-period portfolio theory in which a dynamic investor could re-balance at a fixed number of observation points before the terminal time. See Figure 2.1 which compares dynamic with a static investor.

Let the number of possible re-balancing points be  $N$  for an investment horizon of length  $T$  years. By letting  $N \rightarrow \infty$  we go from a discrete-time to a continuous-time world. However, the continuous world is slightly unrealistic because trading is could be done discretely. The continuous world also offers an interesting set of numerical challenges.

Merton's 1969 paper [64] is the seminal paper on continuous time portfolio theory. Using a PDE formalism for a particular type of investment objective the optimal control policy is to buy/sell the risky asset so as to maintain a constant fraction of wealth in the risky asset at the *Merton* point for logarithmic or 'CRRA' utility and a constant amount of wealth for 'CARA' utility. The *Merton* point will be a term used for the optimal re-balancing point and is utility structure dependent. The optimal re-balancing point is a point which would help the dynamic investor achieve his investment objective over the horizon. The optimal control law is a classic example of a *time consistent* strategy in sense that the law, once determined at the initial time, does not change through time. The optimal control law holds true even for the multi-dimensional case. A brief review of the work is provided below ; the interested reader may wish to consult [64] for a detailed description of calculations. A brief review of utility theory of what CRRA and CARA utilities mean will be given in Section 3.4 of the thesis.

Let  $W(t)$  be the wealth and  $\nu(t)$  be the volatility at time  $t$  for the risky asset price  $x_t$  which follows

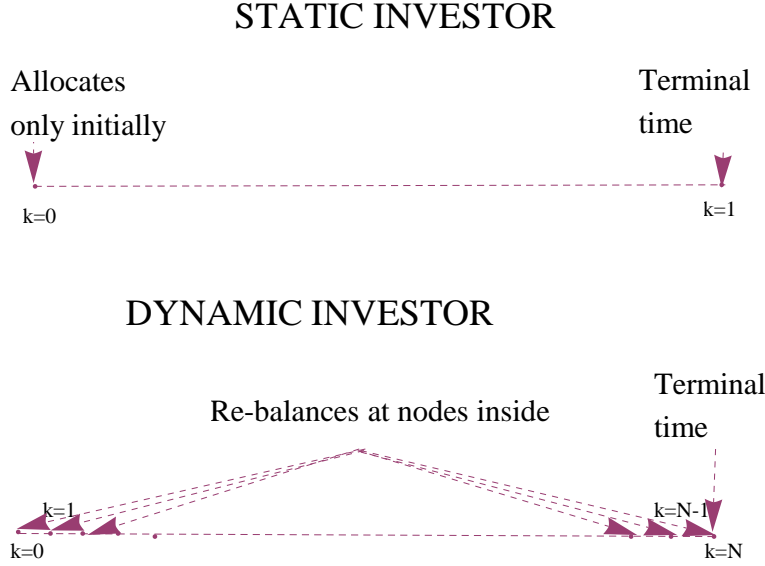


Figure 2.1: Static versus Dynamic investor. A static investor re-balances only once while a dynamic investor re-balances at nodes inside.

$$dx_t = x_t(mdt + \sqrt{v}dZ_t^1) \quad (2.1)$$

for a Brownian motion  $Z_t^1$  and drift rate  $m$ .

The volatility process is also general and assumed to be

$$dv = a(v, t)dt + b(v, t)dZ_t^2 \quad (2.2)$$

for a Brownian motion  $Z_t^2$ . Also  $a(v, t)$  and  $b(v, t)$  are functions of volatility and time.

For simplicity of exposition we also assume independence of Brownian motions via

$$E[dZ_t^1 dZ_t^2] = 0. \quad (2.3)$$

Let the value function be denoted by  $J$  :

$$J(W, v, t) = \max E[\phi(W(T)) | \mathcal{F}_t] \quad (2.4)$$

where  $\mathcal{F}_t$  is the filtration generated by Brownian motions and  $\phi$  is a utility function of terminal wealth. Utility function is mathematical means for describing satisfaction from wealth. They will be described in detail in chapter 3. There is no need to introduce discount factor in our framework as we are merely interested in a functional of terminal wealth.

Further, let  $\alpha_t$  be the fraction of wealth invested in the risky asset and  $\omega$  be the risk-free rate. Then the wealth evolves according to :

$$\frac{dW}{W} = \alpha_t(mdt + \sqrt{v}dZ_t^1) + (1 - \alpha_t)\omega dt. \quad (2.5)$$

Using the dynamic programming principle [64] we have :

$$\max_{(\alpha_t)} \mathbf{E} \left[ (J_t dt + J_W dW + \frac{1}{2} J_{WW} dW^2 + J_v dv + \frac{1}{2} J_{vv} dv^2) | \mathcal{F}_t \right] = 0 \quad (2.6)$$

Substituting and using Ito's lemma gives :

$$\max_{(\alpha_t)} \mathbf{E} \left[ (J_t dt + J_W (W(\alpha_t(m - \omega)dt + \omega)dt) + \frac{1}{2} J_{WW} W^2 \alpha^2 v dt + J_v (a(v, t)dt) + \frac{1}{2} J_{vv} (b(v, t)^2 dt)) | \mathcal{F}_t \right] = 0 \quad (2.7)$$

It follows from above by optimizing with respect to the risky fraction that the optimal risky fraction is :

$$\alpha_t^* = \frac{-(m - \omega)J_W}{v_t W_t J_{WW}} \quad (2.8)$$

Now assume log-utility. Using the *ansatz*<sup>1</sup>  $J = \text{Log}(W) + f(v, t)$  in Equation 2.7 yields :

$$\alpha_t^* = \frac{(m - \omega)}{v_t} \quad (2.9)$$

Especially of note is the fact that, for a log utility decision maker, the most optimal risky fraction in the absence of transaction costs is independent of the level of wealth and depends upon the level of volatility. Figure 2.2 shows the variation of the *Merton* line with volatility. Figure 2.3 depicts a *Merton* line that is unchanged with time for constant volatility.

However, Geometric Brownian Motion (GBM) is not a process of bounded variation so unless trading is frictionless, bringing portfolios to the most optimal *Merton* point would incur substantial transaction costs [28]. Thus, when subject to transaction costs the investor would re-balance only if his position is sufficiently away from the optimal point. These ideas are illustrated in Figure 2.4. Simply speaking, introducing transaction costs would introduce buy and sell side boundaries. Figure 2.5 shows the controlled risky fraction process evolving inside the no-transaction region. One might argue about the optimality of no-transaction boundaries. It turns out that the risky fraction process is mean-reverting about the *Merton* point for logarithmic utility and so from a cost-benefit analysis perspective the investor would re-balance to a point that is *sufficiently* close to the optimal point e.g. points B,D in Figure 2.4. Inside the no-transaction region the cost of re-balancing outweighs the benefit of re-balancing due to mean-reverting nature of risky fraction process.

The optimal control law depends on the structure of transaction costs. Assume for now that transaction costs are proportional to amount traded. In this case it may be shown that the optimal control law is simple. If the risky fraction goes above the sell side boundary the investor sells enough of risky asset so that the risky fraction is brought to the boundary once again. If the risky fraction goes below the buy side boundary the investor buys enough to bring the risky fraction back to the boundary. It may be shown that if the transaction cost depends upon the amount of wealth then the optimal control law is to an optimal point inside the no-transaction region [69].

---

<sup>1</sup>We will later show in chapter 8 that discrete time modeling provides some level of support for the brute force *ansatz* we resorted to here.

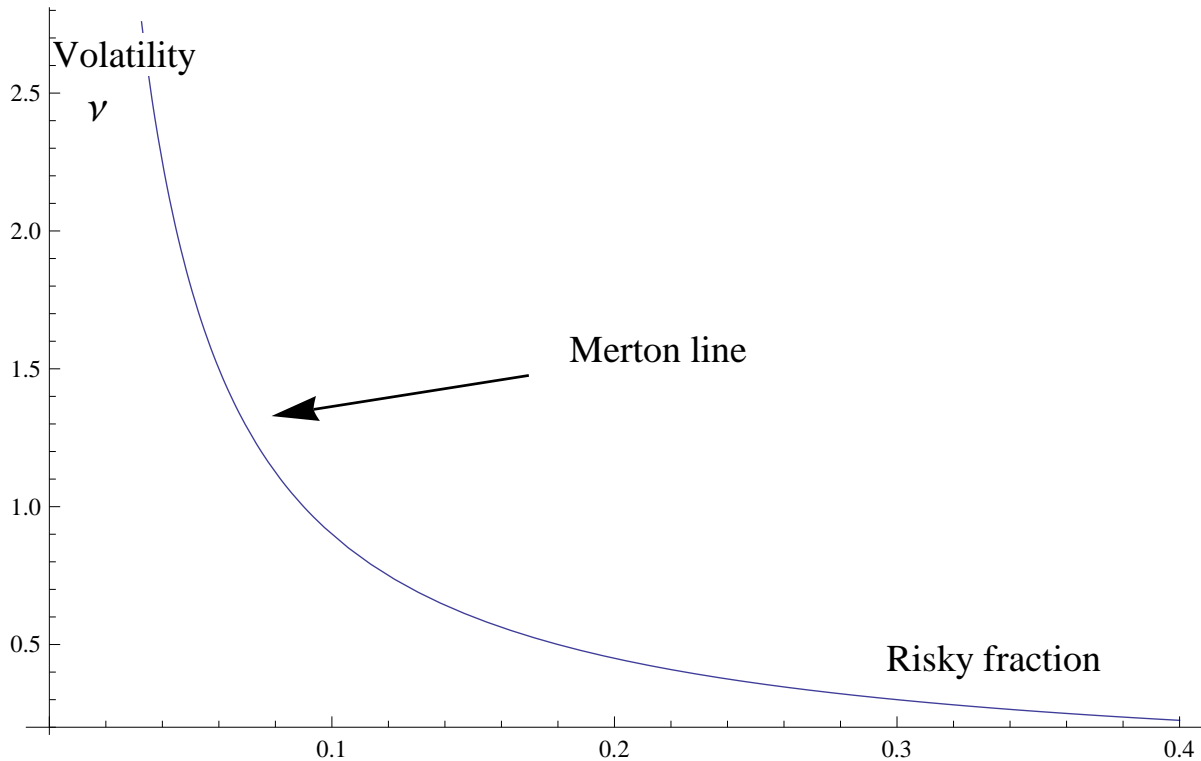


Figure 2.2: *Merton line* under no-transaction cost with parameters  $m = 0.14$ ,  $\omega = 0.05$ . Where  $m$  is the drift for the risky asset and  $\omega$  is the risk-free rate.

We must mention, however, the exact nature of the no-transaction region is dependent upon the investment objective. For CARA and log-utility the no-transaction region was expressed in terms of the risky fraction co-ordinate. This tends to change with utility function structure. Liu in [55] works with the CARA utility function and shows we need “*the amount of wealth in the risky asset*” instead of “*the fraction of wealth in the risky asset*” to express the no-transaction region. This point will be discussed again at the end of Section 3.10.

The most representative transaction cost models in the continuous time literature are Davis and Norman in [28] and Pliska et al. in [69]. In [28] transaction cost are proportional to amount traded while in [69] transaction cost is proportional to the amount of wealth.

In a nutshell the basic structure of dynamic portfolio selection models could be broken down to the ingredients I, II and III below.

### **I- Trading cost model**

These models answer the questions :

- a) Are the transaction costs proportional to the amount traded or to the amount of wealth under management ?
- b) Are there fixed costs per trade ?
- c) Is there *non-linear* dependence on transaction costs in the model ?

### **II- Model for risky asset growth**

It is usually assumed that the risky assets follow a diffusion process of which the simplest is multi-dimensional GBM. One may, therefore, think of portfolio optimization as finding optimal



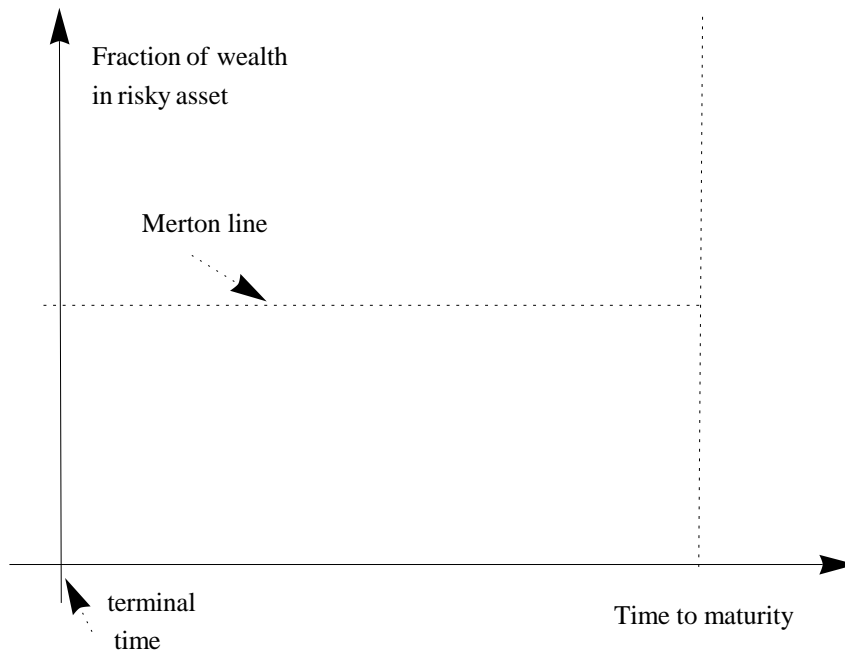


Figure 2.3: Re-balancing to *Merton* line for CRRA or log-utility. The line is constant with respect to time.

wealth control involving stochastic processes.

### III- Investment objective

The investment objective over a horizon could be finite horizon or infinite horizon. If it is infinite horizon then the problem becomes time independent and the optimal control law is independent of time. If it is finite horizon then the problem is time dependent and the optimal control law is in general dependent on time. Many popular investment objectives include intermediate consumption as part of the objective. This thesis focuses only on objectives which are a pure function of terminal wealth expressed via utility functions.

## 2.2 Brief review of transaction cost literature

Most academic literature for portfolio theory under transaction costs is in the continuous-time domain. Such *dynamic portfolio optimization problems* with transaction costs can usually be formulated as *Stochastic Control* problems with so called *singular controls*. These *singular controls* (e.g. transactions) can bring about an instantaneous change in the state variable ( e.g. fraction invested in the asset) rather than just a change in the rate of change of state. Solutions to such singular control problems are sought by first arguing that the problem is equivalent to solving a related partial differential equation known as the Hamilton-Jacobi-Bellman (HJB) equation. The arising *magical* HJB equation<sup>2</sup> (which varies under different model formulations) is of the free boundary type, that is, the boundary of the region in which the HJB

<sup>2</sup>No boundaries in the no-transaction cost case.

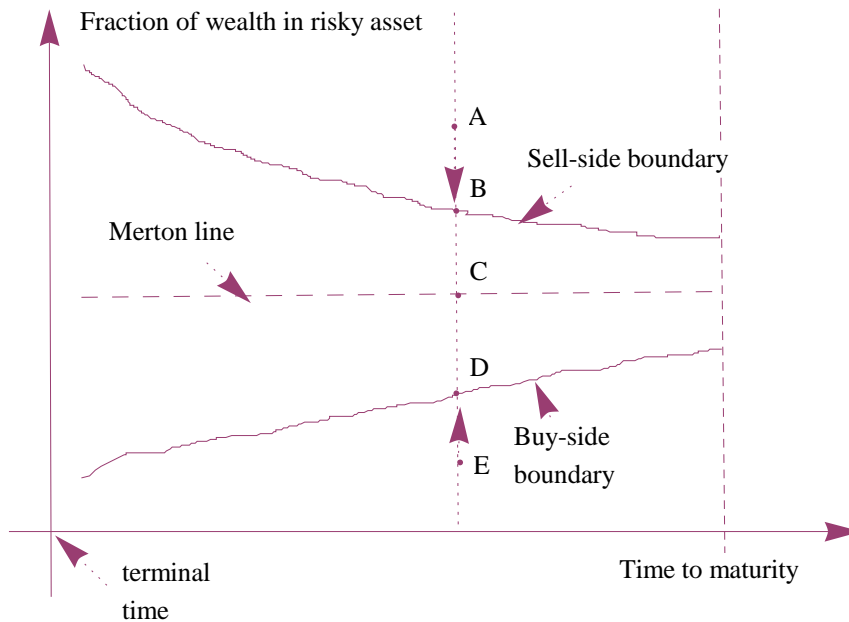


Figure 2.4: No-transaction boundaries over a finite horizon for CRRA or log-utility. When the investor moves closer to terminal time the no-transaction region widens.

PDE is to be solved is not specified and is obtained as a part of the solution itself. Solving a portfolio optimization problem with a large number of stocks essentially reduces to solving a free-boundary problem in high dimensions. Run-times of existing solution methods grow super-exponentially with dimension - making them unsuitable for problems with more than even three stocks [71].

Much of modern financial theory neglects *market imperfections* such as transaction costs. Perhaps its most successful implementations - continuous time portfolio choice and Black-Scholes option pricing - are theoretically inconsistent with the existence of any transaction costs at all. For instance, the hedging strategy proposed by [13] to value derivative assets is not rationally feasible when the portfolio adjustment is not costless. Similarly, other arguments adopted to justify alternative pricing methods do not seem to be immediately applicable when the transaction costs impinge upon the investment returns. When they are applied, straightforward continuous adjustment of the portfolio consumption would lead to an infinite transaction in a finite time.

One popular investment objective in literature has been of maximizing the long-term growth rate of the portfolio in a market that contains one risk-free asset (bank) and multiple risky assets (stocks). The maximization of expected growth rate under proportional transaction costs was first studied by Taksar et al. in [81]. Taksar et al. were the first to apply the theory of stochastic singular control to a consumption-investment problem with transaction costs. Denoting the portfolio's total wealth over time as a stochastic process  $W(t)$ , the objective is to maximize the long-term growth rate  $\lim_{t \rightarrow \infty} \inf E[\frac{\text{Log}(W(t))}{t}]$ . Other objective functions draw their inspiration from modern microeconomic theory and their aim is to maximize expected lifetime utility

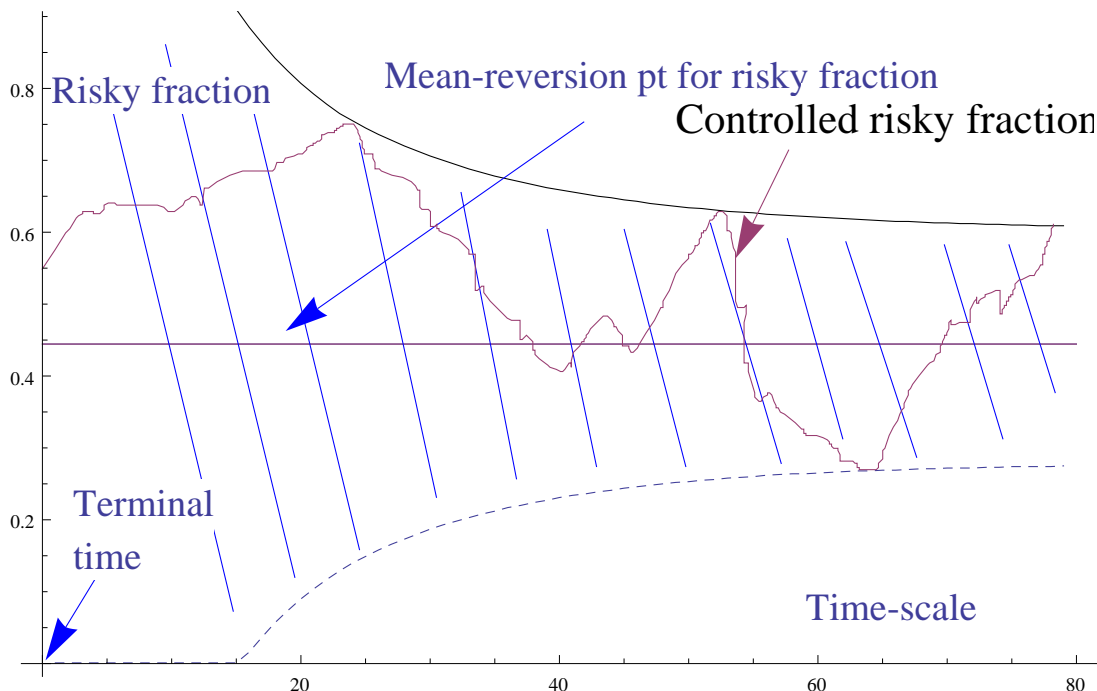


Figure 2.5: Controlled risky fraction over a finite horizon for CRRA or log-utility under transaction costs. Risky fraction is controlled via transaction so that it never falls outside the buy-side and sell-side boundaries.

of consumption or the expected utility of terminal consumption if there is no intermediate consumption.

For the optimization problem stated above, it can be argued that the optimal policy is specified by a no-transaction region. When the proportions of the investor's wealth invested in stocks lie within this region, the investor makes no transactions. When fluctuations in the price processes drive the proportion of wealth invested in stock out of the boundary of the no-transaction region, the investor transacts minimal amount required to keep the proportions in the region. The key difficulty is that the domain over which HJB PDE is to be solved is not pre-specified and must be computed as part of the solution.

Continuous time portfolio optimization problems can be broadly classified into two classes based on the objectives that are considered. The first set of models consider another decision variable, consumption, and maximize a function (usually discounted utility) of consumption. The second set of models do not consider consumption and maximize a function of wealth in the portfolio directly. This thesis is concerned with the second set of problems.

Magill and Constantinides in [60] first considered one-stock and one risk free asset portfolio optimization problem with proportional transaction cost and conjectured that the optimal policy would be characterized by a no-transaction region, such that optimal policy would not transact when the fraction of wealth in the stock lies in this interval. When the fraction lies outside the interval, the optimal policy would be to buy and sell just enough to bring the fraction into the interval. Davis and Norman in [28] considered proportional costs in Merton's setting again restricting their analysis to the one-stock case. They provided a detailed characterization of the optimal policy and conditions under which the HJB equation has a smooth solution. A

representative list of other papers which consider the one stock case include [20], [78], [84], [49], and [71]. The paper [20] consider the problems from an economic perspective while [78] provides a rigorous stochastic analysis. Iterative schemes are provided in [84] and [49] while [71] provides a boundary update procedure for solving such problems.

The number of papers that treat the multiple stock case with transaction costs is much lower. Kumar and Mutharaman in [71] consider the multi-dimensional problem in Merton's setting with transaction costs and maximize the discounted utility of consumption. They transform the resulting free-boundary problem into a sequence of fixed boundary problems that can be solved with the finite element numerical method. Other papers that consider the multi-stock portfolio optimization under various other model settings include [1], [6], [10], [54], [55] and [59]. A numerical procedure for multiple asset problem under growth rate maximization is provided in [1] and analysis for fixed transaction cost problems in [6]. Reference [59] considers a fairly simple setting with proportional transaction costs under a dynamic programming formulation. Capital gains taxes are considered in [54] while [55] considers the CARA (or exponential) utility function. In its most general formulation, portfolio optimization is a continuous-time dynamic optimization problem and like many other such mathematical problems it suffers from the *curse of dimensionality* in which the computational complexity of the standard techniques grows exponentially with the number of independent variables. Hence no amount of computer power could ever hope to solve such crucial problems when the number of independent variables is sufficiently large. Interestingly, paper [83] proposes a radial basis function based PDE technique that hopes to tame dimensionality in dynamic portfolio choice with transaction cost.

In [10], Pliska and Bielecki develop a continuous time risk-sensitive portfolio optimization model with a general transaction cost structure in which the individual securities and asset categories are explicitly affected by underlying economic factors. The security prices and factors follow diffusion processes with the drift and diffusion coefficients for the securities being functions of factor levels. The authors develop methods of risk sensitive impulsive control theory in order to maximize an infinite horizon objective that is natural and features the long-run expected growth rate, the asymptotic variance, and a single risk aversion parameter. The optimal trading strategy has a simple characterization in terms of the security prices and the factor levels. Moreover, it can be computed by solving a risk sensitive quasi-variational inequality.

In [49], Korn applied the theories of optimal stopping and quasi-variational inequalities to two portfolio management problems both involving two assets ( a bank account with interest rate of zero and a geometric brownian motion stock) and transaction costs of the form  $K + \kappa\Delta S$ , where  $\Delta S$  is the amount of funds added to the stock position when a transaction occurs. One problem is to maximize the expected utility of wealth at a fixed finite time horizon: the other is to maximize the expected discounted utility of consumption over an infinite planning horizon, where consumption occurs in discrete lumps at discrete amounts of times. Korn in [49] also characterized the optimal solutions and showed how these may be computed with iterative schemes. His asset and transaction cost problems are similar to [10] but his portfolio management problems do not overlap with the infinite horizon risk objective.

The Davis and Norman [28] model for portfolio selection under transaction costs serves as a representative model for maximizing expected utility. For such problems Tourin in [84] has characterized a unique viscosity solution to the variational inequality. This reference provided monotone, stable and consistent numerical schemes to compute the unique viscosity solution to the variational inequality. Mokkhaveva et al. in [66] have applied perturbation methods sim-

ilar to those of Wilmott et al. in [6] to problems involving life-time utility maximization for a general class of utility functions. They show that, in the presence of small transaction costs, the optimal boundaries separating the transaction and no-transaction regions of an investor with any utility preference can be found rapidly once the corresponding optimal allocation for that utility has been determined numerically or analytically. A no-transaction region is determined in which the investor holds the portfolio and transacts when the asset moves up the boundary. Kumar and Mutharaman in [73] successfully applied the boundary update procedure to give a computational scheme for optimal investment-consumption with proportional transaction costs. The computational scheme transforms the arising free-boundary problem to a sequence of fixed boundary problems.

## 2.3 Towards discrete time modeling

The first section of this chapter contained a short review of current abundant literature in continuous time transaction cost models. In contrast to continuous time models relatively little work has been done in discrete time. For more details see [18]. The very first paper to model transaction costs was [60] which was quickly followed by rigorous analytics in [31]. The spark in interest for discrete time models in this area has been fairly recent. Most discrete-time work (See [16], [35], [27]) has been in a no-transaction cost setting. A simulation based approach to such problems is provided in [16] while the fairly recent work [35] emphasizes numerical techniques to reduce dimensionality in portfolio problems. Discrete time portfolio selection under transaction cost for CRRA and exponential utility using asymptotic approximations is studied in [5] and [4]. Veins and Kim in [48] analyzes portfolio re-balancing in discrete time under a fairly restrictive setting for stochastic volatility. Luenberger and Kuhn in [50] study the value of re-balancing under growth rate maximization criterion for an investor who always re-balances at a critical point. The contribution of the thesis is to improve upon the current discrete time literature by providing robust algorithms for solving both existing portfolio problems and newly modeled problems. The methods proposed here are simple both to implement and to understand

## 2.4 Notation used in the thesis

To keep a balance with the relevant literature cited, the notations unavoidably change somewhat from one chapter to another. We will try our best to minimize notational disruption. The models are somewhat similar so we highlight the important notations used by considering a dynamic investor.

The risky assets follow a geometric Brownian motion (GBM) described by

$$\frac{dS_i}{S_i} = m_i dt + \sigma_i dZ_t^i \quad (2.10)$$

where the vector  $(dZ_t)$  represents Brownian motion vector,  $S_i$  represents the asset price,  $m_i$  represents the drift and  $\sigma_i$  the volatility.

The processes  $Z_t^i; t > 0$  are standard Brownian motions on a filtered probability space  $(\mathcal{S}, \mathcal{F}, \mathcal{F}_t, \mathcal{P})$  with  $Z_0^i = 0$  almost surely and constant co-efficients of correlation  $\rho_{ij}$  namely

$E^{\mathbf{P}}[dZ_t^i dZ_t^j] = \rho_{ij} dt$ . We also assume that the filtration  $\mathcal{F}_t$  is right-continuous and each  $\mathcal{F}_t$  contains all  $\mathcal{P}$ -null sets of  $\mathcal{F}_\infty$ . The correlation co-efficients imply a correlation structure for multi-dimensional GBM.

We could also represent the above via a *Cholesky* decomposition as

$$\frac{dS_i}{S_i} = m_i dt + \sum_{l=1}^M q_{il} dB_t^l \quad (2.11)$$

where  $(dB_t)$  represent an independent Brownian motion vector and  $q_{il}$  are extracted as entries of the variance-covariance matrix of the vector  $(dZ_t)$ .

We will follow the notation given below. By ‘time node’ we mean the node value as shown in Figure 2.1. ‘Time node’ is different from the actual value of time.

$E^{\mathbf{P}}$  : represents the expectation under the natural probability measure<sup>3</sup>

$W_k^-$  : total wealth of the investor at time node  $k$  immediately before re-balancing<sup>4</sup>

$\mathcal{A}_{i,k}^-$  : fraction of wealth in the risky asset  $i$  at time node  $k$  immediately before re-balancing

If there is only one risky asset in our model we would suppress one subscript and use  $\mathcal{A}_k^-$  as the fraction of wealth in the risky asset.

$X_{i,k}^-$  : amount of wealth in the risky asset  $i$  at time node  $k$  immediately before re-balancing

If there is only one risky asset in our model we would suppress one subscript and use  $X_k^-$  for the amount of wealth in the risky asset.

$Y_k^-$  : amount of wealth in the risk-free asset at time node  $k$  immediately before re-balancing  
Analogous variables for the above exist for immediately after re-balancing.

$T$  : length of the time horizon

$N$  : number of observation points available for re-balancing

$\Delta_k$  : transfer of wealth under a control strategy at time node  $k$

$r_{i,k}$  : risky growth for asset  $i$  over a period  $\Delta T_k$  defined as the ratio  $\frac{S_{i,k+1}}{S_{i,k}}$

$s_k$  : risk-free interest rate over period  $\Delta T_k$

$\gamma_\ell$  : the deformation parameter where  $\gamma_\ell \rightarrow 0$  for convergence (discussed in chapter 5)

$V$  : is the co-efficient of risk aversion in CRRA utility.

$z$  : is the co-efficient in CARA utility.

The structure of transaction cost in chapter six<sup>5</sup> is different but in most of the chapters we will have :

$\lambda_k$  : transaction cost factor in buy-side direction

$\mu_k$  : transaction cost factor in sell-side direction

If the state space vector at time  $k$  is denoted by  $\vec{\phi}_k$  and control vector by  $\vec{\zeta}_k$  then value function under utility function  $U(W_N)$  is :

$$\mathcal{J}(\vec{\phi}_k) = \max_{\vec{\zeta}} E_{\vec{\zeta}}^{\mathbf{P}}(U(W_N)|\mathcal{F}_k) \quad (2.12)$$

$\varpi$  : probability density of risky growth over an interval.

$\eta_k^{i,j,+}$  : fraction of wealth transferred from asset  $i$  to asset  $j$ .

<sup>3</sup>We will not invoke the *numeraire* concept anywhere in the thesis so as to use martingale methods with respect to a risk-neutral probability measure, as portfolio optimization is intrinsically a real world measure topic.

<sup>4</sup>Wealth is measured in monetary terms invested in total in individual assets. It is not measured as a result of liquidation in risk-free asset or by using one asset as a numeraire.

<sup>5</sup>In Chapter six we assess transaction costs proportional to the amount of wealth traded.

$\mathcal{M}_k$  : maximum wealth attained at a time node  $k$ .

$\mathcal{Z}_k$  : denotes spread value at time node  $k$ .

$\pi_k$  : cumulative profits at time node  $k$ .

$\delta_k$  : profit in period  $k$ .

We must emphasize some notational confusion that might occur. By  $W(t)$  we would mean the wealth at time  $t$  and this is usually the case for continuous time exposition of problems. In discretized form by  $W_k$  we would mean the wealth at node  $k$  where there are say  $N$  nodes over the time horizon. Such notational differences are applicable to all relevant dynamic portfolio variables.

Note: The labeling of axes might have fonts not perfectly aligned because this was done manually in the Mathematica generated graphics.

In the next chapter we will present the basic modeling framework of the thesis.

## 2.5 Lattice framework of the thesis using notations above

To give the reader a broad feel of the thesis we will highlight some simple models using the notations above. We will also in simple terms highlight the discrete probability approximation solution methodology.

### 2.5.1 Bermudan put option pricing in the framework

Consider a Bermudan put option with a strike  $K$  written over a time horizon  $T$ . The recursive formulation for the valuation of a Bermudan put would read as:

$$V(S_k, k) = \max(K - S_k, e^{-s\Delta T} E^Q[V(S_k(1 + g_k), k + 1)]) \quad (2.13)$$

where  $k = 0, 1, 2, \dots, N - 1$  and  $V(S_N, N) = (K - S_N)^+$  represents the terminal condition.

Here  $V$  denotes the option price as a function of stock price  $S_k$ . Here  $Q$  is the risk-neutral probability measure. Also  $(1 + g_k)$  is the factor by which the stock price grows over the interval  $\Delta T$ . Also  $K$  is the strike price and  $s$  is the risk free rate.

The essential feature of the thesis is to create a discrete probability approximation of the random variable  $g_k$  over which the expectation is taken. We create an  $\ell$  point approximation for the continuous risky growth implied by the GBM. The limit  $\ell \rightarrow \infty$  will be used to approximate the solution for GBM based model. The state space is a grid of stock price values bounded by a minimum and maximum. Starting from the terminal node  $k = N$  we move backwards using Equation 2.13 to determine the value function at earlier stages. Using the recursive formulation we will determine the value function at each point in state space for a time node. Numerical interpolation will be used to numerically represent the value function values for a particular time node.

We highlight our lattice solution methodology in Figure 2.6. The Figure shows a point at time node  $N - 1$  with a stock price value of  $S_{N-1}$ . Under a three point discrete probability approximation the risky growth can take three possible values at the start of the next node. The dynamic programming problem involves constructing a lattice of stock price space which in this case is  $[S_{min}, S_{max}]$ . Going recursively backwards at each point in state space we determine

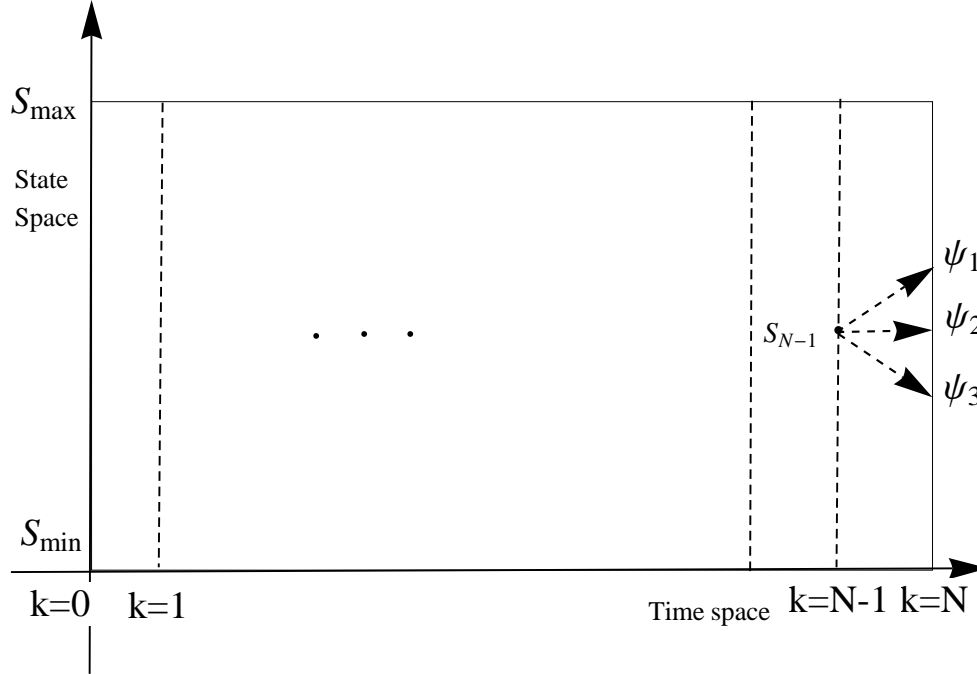


Figure 2.6: Lattice solution methodology for Bermudan option.

the value function by optimizing over an expectation operator for the next value function as in Equation 2.13.

### 2.5.2 Growth rate maximization portfolio problem in the framework

Consider an investor who invests in one risky and one risk-free asset. The investment horizon is  $T$  years. The investor takes only long position in the risky and risk-free asset. The amount of wealth in risky asset immediately before re-balancing is  $X_k^-$ . The amount of wealth in risk-free immediately before re-balancing is  $Y_k^-$ . Also the fraction of wealth held in the risky asset is adjusted so that he is able to achieve his terminal investment objective. However, he incurs transaction costs in the process. The transaction costs are assumed to be proportional to the amount of wealth and a certain fraction  $\lambda_k$  of wealth gets lost in the transaction process. There are  $N$  re-balancing periods and  $k = 0, 1, \dots, N - 1$  denotes a time node i.e. the start of a re-balancing period. Let  $W_k^-$  be the total amount of wealth immediately before re-balancing. Also let  $\mathcal{A}_k^-$  be the fraction of wealth in the risky asset immediately before re-balancing and  $\mathcal{A}_k^+$  denote the fraction immediately after re-balancing.

The stochastic system re-presenting the transaction process can be described by a system of equations.

At the beginning of each period, if re-balancing is selected then the following system of equation hold:

$$X_{k+1}^- = (1 - \lambda_k)W_k^- \mathcal{A}_k^+ r_k \quad (2.14)$$

$$Y_{k+1}^- = (1 - \lambda_k)W_k^- (1 - \mathcal{A}_k^+) s_k \quad (2.15)$$



$$\mathcal{A}_{k+1}^- = \frac{\mathcal{A}_k^+ r_k}{\mathcal{A}_k^+ r_k + (1 - \mathcal{A}_k^+) s_k} \quad (2.16)$$

If re-balancing is not selected then the following system holds :

$$X_{k+1}^- = W_k^- \mathcal{A}_k^- r_k \quad (2.17)$$

$$Y_{k+1}^- = W_k^- (1 - \mathcal{A}_k^-) s_k \quad (2.18)$$

$$\mathcal{A}_{k+1}^- = \frac{\mathcal{A}_k^- r_k}{\mathcal{A}_k^- r_k + (1 - \mathcal{A}_k^-) s_k} \quad (2.19)$$

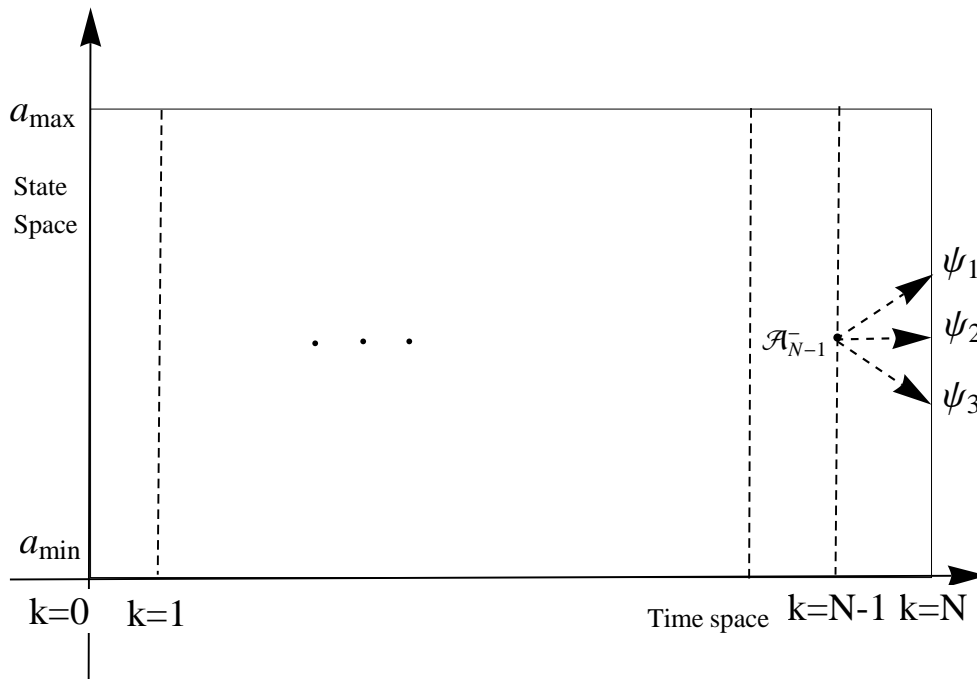


Figure 2.7: Lattice solution methodology for dynamic portfolio problem.

The dynamic investor will have an investment objective that will be a function of his terminal wealth  $W_N^-$ . Dynamic programming provides the necessary toolkit to solve such problems recursively.

Let  $\mathcal{J}_k(W_k^-, \mathcal{A}_k^-) = E^{\mathbb{P}}[\log[W_N^-] | \mathcal{F}_k]$  be the value function under the CRRA utility. Then under the control set  $\{\zeta\}$  we have:

$$\mathcal{J}_k(W_k^-, \mathcal{A}_k^-) = \max_{\{\zeta\}} E^{\mathbb{P}}[\mathcal{J}_{k+1}(W_{k+1}^-, \mathcal{A}_{k+1}^-) | \mathcal{F}_k]. \quad (2.20)$$

Where  $k = 0, 1, 2, \dots, N - 1$ .

Also, for the terminal condition we have :

$$\mathcal{J}_N(W_N^-, \mathcal{A}_N^-) = \text{Log}[W_N^-] \quad (2.21)$$

The solution of the above portfolio model involves solving the equations recursively. We start from the terminal node  $k = N$  and move backwards using equation (2.20) to determine the value function at earlier stages. The control set at a point in time determines whether the investor buys, sells or does nothing. It is determined as a function of the state variables which in our case is wealth  $W_k^-$  and fraction of wealth in the risky asset  $\mathcal{A}_k^-$ . But to solve recursively we need to figure out a clever way to determine the expectation operator approximately. The idea of the thesis is to approximate the risky growth of the risky asset over the interval  $\Delta T$  as a discrete probability mass function. In simple terms we would create an  $\ell$  point approximation for the continuous risky growth implied by the GBM. The limit  $\ell \rightarrow \infty$  will be used to approximate the solution for GBM based model. Note the discrete probability approximation is only over the interval  $\Delta T$ . This is quite different from the tree methods you see in context of option pricing in which you have a re-combining tree that branches out.

Our lattice methodology solves our problem over a lattice of state variables. We will later show in Chapter 6 that this problem is separable in wealth for certain utility functions and the only relevant state variable is the risky fraction  $\mathcal{A}_k^-$ .

We highlight our lattice solution methodology in Figure 2.7. The Figure shows a point at time node  $N - 1$  with a risky fraction value of  $\mathcal{A}_{N-1}^-$ . Under a three point approximation for risky growth and investor decision to buy, sell or do-nothing the risky fraction can take three possible values at the start of the next node. The dynamic programming problem involves constructing a lattice of risky fraction space which in this case is  $[0, 1]$ . Going recursively backwards at each point in state space we use determine the value function by optimizing over an expectation operator for the next value function as in Equation 2.20.

In summary, the framework of the thesis is lattice based. The state variables are represented on a lattice. The state variables are bounded and for, instance in the portfolio model above are bounds were  $[amin, amax]$ . Relevant probability models are approximated as discrete probability mass functions. Dynamic programming provides the essential toolkit for determining the optimal control law recursively. In the next chapter we provide more detail for our modeling framework for solution methods.

Symbol	Notations
$E^P$	Expectation under natural probability measure.
$W_k^-$	Wealth at node $k$ immediately before re-balancing.
$\mathcal{A}_{i,k}^-$	Fraction of wealth in risky asset $i$ at node $k$ immediately before re-balancing.
$X_{i,k}^-$	Wealth in risky asset $i$ at node $k$ immediately before re-balancing.
$Y_k^-$	Wealth in risk free asset at node $k$ immediately before re-balancing.
$T$	Investment horizon length.
$N$	Number of point available for re-balancing.
$r_{i,k}$	Risky growth vector of risky asset $i$ .
$s_k$	Risk free growth rate.
$\omega$	Continuous risk-free rate.
$\gamma_\ell$	Deformation parameter introduced in Chapter 3 and discussed more in Chapter 5.
$\lambda_k$	Transaction cost factor in buy side but in Section 6.1 no direction.
$\mu_k$	Transaction cost factor in sell side direction.
$\vec{\phi}_k$	State space vector.
$\vec{\zeta}_k$	Control vector.
$U(W_N)$	Utility of terminal wealth.
$\mathcal{J}(\vec{\phi}_k)$	Value function.
$\varpi$	Probability density of risky growth.
$\eta_k^{i,j,+}$	Fraction of wealth transferred from asset $i$ to asset $j$ .
$\mathcal{M}_k$	Maximum wealth attained at time node $k$ .
$\mathcal{Z}_k$	Spread value at time node $k$ in Chapter 10.
$\pi_k$	Cumulative profits to date in Chapter 10.
$\delta_k$	Profits in period $k$ in Chapter 10.
$V$	Co-efficient of risk aversion in CRRA utility.
$z$	Co-efficient in CARA utility.

Table 2.1: Summary of Notations Used.

# Chapter 3

## Introduction to discrete probability approximation and sketch of modeling approach

### 3.1 Overview

This thesis presents robust, simple and easily implementable *approximate* numerical algorithms to solve problems in dynamic portfolio theory under *transaction costs*. Such algorithms are important because in most cases the solution of portfolio problems under transaction costs involve complex numerical procedures which can become numerically intractable. Such problems are also computationally very demanding. Instead of working in continuous domain we chose to work in a discrete domain<sup>1</sup>. The reason for this modeling choice is two-fold:

1- *Discrete phenomena* are realistic. Trading in real life is discrete time. Moreover, continuous time trading is rationally not feasible because of market frictions like transaction costs, liquidity etc. Infinite transaction costs would be incurred if trading were done continuously.

2- Discrete models may be deformed to a continuous domain. This means that the solution obtained using discrete domain can be used to obtain solution to continuous domain. We will later show a discrete domain is highly amenable to simple easily implementable numerical algorithms via stochastic dynamic programming.

The thesis has two main contributions:

1- Mathematical and computational techniques. These involve constructing simple, intuitive and easily implementable lattice based approaches to solve problems.

2- Financial applications.

We cover a broad spectrum of *realistic* dynamic portfolio and trading problems under several constraints. These include:

- Bankruptcy prohibition / solvency constraints.
- Leverage / liquidity constraints.
- Draw-down constraints.
- Portfolio insurance constraints.

---

<sup>1</sup>Discreteness in time as well as space.

The problems considered above can still be solved in continuous time but with greater numerical challenges depending upon the nature of the problem. For instance by introducing transaction costs we have free boundary PDE formulation [28] the solution of which is complex.

One of the central themes of the thesis is to study inter-connectivity between financial variables for a dynamic investor like the relationship between transaction costs and market volatility. This will be explored in detail in the chapter on *stochastic transaction costs*.

In line with the above theme, this thesis studies the behavior of the portfolio for a dynamic investor i.e. the value of re-balancing portfolios under different investment objectives, ranking risk / return of dynamic trading strategies etc. We provide a simple and intuitive framework for a rigorous analysis of dynamic portfolio problems.

A major goal is to incorporate parameter estimation error in the dynamic programming methodology (so making the problem *time inconsistent*<sup>2</sup>) and obtain heuristics for problems like these in our Chapter 7 and Chapter 11.

*Lattices* will be the basic mathematical structure for encapsulating our financial models. Our approach is to determine the laws of a system using mathematical experiments. The framework of the thesis will be the beginning of a journey that will help us mimic the complex behavior in financial systems via lattices. We believe the complexity can be discovered and embedded into lattices. Like Stephen Wolfram [37] we feel that present day mathematical structures are not sufficiently rich to depict the complexity displayed in real life.

Finally, we conclude by presenting some interesting real life problems solvable under our lattice framework. These include algorithmic trading, hedge fund maximum draw-down and portfolio insurance.

## 3.2 Analogy between discrete time and continuous time portfolio theory

Our discrete time framework is related to continuous time portfolio theory in a similar way that a Bermudan option is related to a American option. The solution of a perpetual American option can easily be obtained by solving a differential equation whereas for a perpetual Bermudan option, different mathematical formulations could be obtained by relying on the principle of stochastic dynamic programming.

The recursive formulation for the valuation of a perpetual Bermudan would read as:

$$V(S_k) = \max(K - S_k, e^{-s\Delta T} E^Q[V(S_k(1 + g_k))]) \quad (3.1)$$

where  $V$  denotes the option price as a function of stock price  $S_k$ . Here  $Q$  is the risk-neutral probability measure. Also  $(1 + g_k)$  is the factor by which the stock price grows over the interval  $\Delta T$ . Also  $K$  is the strike price and  $s$  is the risk free rate.

Something similar is happening here. In continuous portfolio theory we have free boundary PDEs that could most often be solved only numerically. In discrete time a nice *analytical* structure is not currently known and we have to resort to stochastic dynamic programming.

---

<sup>2</sup>As described in more detail in section 3.5.

### 3.3 Bellman principle for discrete time finite horizon problems

This thesis is *primarily* devoted to discrete time finite horizon portfolio problems. The perpetual limits could be used to obtain infinite horizon solutions. Let  $\vec{\Phi}_k$  be the state space vector<sup>3</sup> defining the portfolio problem at time  $k$ .

Define the value function for the problem as:

$$\mathcal{J}_k(\vec{\Phi}_k) = \max_{\zeta} E(U(\vec{\Phi}_N) | \mathcal{F}_k) \quad (3.2)$$

where  $\zeta$  is the control law to be determined as part of optimization at each stage of dynamic programming.

Using the principle of optimality, Markov property of the underlying asset price process and law of iterated expectations the Bellman principle (or dynamic programming principle) can be stated as<sup>4</sup>:

$$\mathcal{J}_k(\vec{\Phi}_k) = \max_{\zeta} E(\mathcal{J}_{k+1}(\vec{\Phi}_{k+1}) | \mathcal{F}_k) \quad (3.3)$$

### 3.4 Utility of terminal wealth

In economics, the utility  $U(x)$  is a measure of relative satisfaction from wealth. The utility function approach as a means of making economic decisions was developed by John von Neumann and Oskar Morgenstern in [67]. The von Neumann-Morgenstern utility  $U(x)$  is a concave function  $U'(x) > 0$ ,  $U''(x) < 0$  that is defined up to an *affine transformation*.

The dynamic investor in this thesis has no intermediate consumption. Utility functions are a mathematical way of describing the level of satisfaction the dynamic investor receives from his terminal wealth. Commonly used utility functions are:

- 1- Quadratic utility function:  $U(W_N) = W_N - aW_N^2$ .
- 2- CRRA utility:  $U(W_N) = \frac{W_N^V}{V}$  for risk-aversion co-efficient  $V \in (-\infty, 1) \setminus 0$ .
- 3- Log-utility of Kelly Criterion:  $U(W_N) = \text{Log}(W_N)$ .
- 4- CARA or exponential utility:  $U(W_N) = -e^{-zW_N}$  for  $z \in \mathfrak{R}^+$ .

While not being a utility function in the strict sense, it is also possible to have utility metrics like the *level reaching indicator*:  $U(W_N) = 1_{(W_N \geq W^*)}$ .

The above utility functions can be shown to be equivalent to other possible utility functions and investment criteria. For instance, as in [10], the exponential utility could be used to model risk-sensitized asset allocation.

Consider a dynamic investor trying to maximize the probability that log-returns are above a certain target level. It can be shown that the investor has a level reaching utility *metric* as follows:

---

<sup>3</sup>Depending upon the problem could include fraction of wealth in risky assets, amount of wealth in risk assets and many other variables as we will see later.

<sup>4</sup>Provided we have no intermediate costs.

$$\max P(R_N > R^*) = \max P(W_N > W^*) \quad (3.4)$$

$$= \max E^{\mathbf{P}}(1_{(W_N \geq W^*)}) \quad (3.5)$$

### 3.5 An illustrative example: *deformation solution* for a dynamic investor

Let us try to highlight the solution mechanism in terms of the dynamic programming methodology briefly highlighted in Section 3.3. The two main ingredients of dynamic programming are defining the value function and the recursion equation. The purpose of this example is to present our problem solution methodology in broad brush. Consider a dynamic investor trying to maximize his return subject to a given level of volatility. The investor invests in a risky asset and a risk-free asset.

The investment has a finite time horizon of  $T$  divided into  $N$  periods so that each period is of length  $\Delta T = \frac{T}{N}$  and  $k = 0, 1, 2, \dots, N$ .

Without going in more mathematical detail for now, mean-variance problems in *pre-committed* form are really benchmark problems in which the investor tries to minimize the variability of wealth around a target level  $b$  which depends upon the initial wealth and risky fraction. Standard dynamic programming could not be applied to our objective in this form as it manifests itself as a time inconsistent control problem. This is because if the investor wants to minimize the variance of terminal wealth subject to an expected terminal value constraint, then this implies a particular  $b(t)$  at time node  $k = 0$  (for the mean-variance problem cast in deviation from the target form). However, when an investor moves to the next time node  $k = 1$  the risky fraction and wealth both change which requires changing  $b(t)$  to meet the mean-variance objectives over the investment horizon. See the papers [7] and [58] for a review of mean-variance problems in pre-committed form. The changing value of  $b(t)$  over the investment horizon implies that the control strategy is clearly time inconsistent. Similarly, a time consistent problem is one in which controls initially determined do not change through time. Merton's portfolio allocation problem for CRRA or log-utility in Section 2.2 of Chapter 2 is time consistent because the optimal policy of holding a constant fraction of wealth at each point in time does not change with time. The slight difference between time consistency and time inconsistency is discussed in [7] and [58].

One of the best examples to illustrate time inconsistency in control problems is when parameter uncertainty comes in. Suppose an investor is trying to maximize a certain objective at terminal time that is a function of terminal wealth. Assume the utility function is general. Under parameter uncertainty the controls estimated at  $t = 0$  may not be optimal if the parameters change. In other words, in this case a straightforward application of the dynamic programming principle is not possible<sup>5</sup>.

In [7], the strategy of maximizing the mean-variance objective at time node  $k = 0$  is termed the pre-commitment control, i.e. once the initial control is found at the initial time, the trader

---

<sup>5</sup>Note, however, it is still possible under parameter uncertainty to have time consistent controls i.e. with logarithmic or CARA utility and no-transaction costs primarily due to the fact that these problems allow separability in wealth.

commits to this optimal control, even if the optimal mean variance control computed at a later date differs from the pre-commitment control. This contrasts with time-consistent controls, whereby the dynamic investor optimizes the mean-variance trade-off at each instant in time, assuming optimal mean-variance strategies at each later instant. The advantages and disadvantages of these two different approaches are discussed in [7]. See also [26] for a similar discussion on pre-committed controls.

The dynamic problem is:

$$\min_{(\zeta)} E^{\mathbb{P}}[(W_N - b)^2] \quad (3.6)$$

where  $\mathbb{P}$  is a risk-neutral probability measure.

Clearly the investor is minimizing the variability of his wealth around a target level. By choosing a  $b$  we are choosing a point on the efficient frontier (as discussed in section 6.2). Let  $W_k^-$  be the total wealth and  $\mathcal{A}_{i,k}^-$  be the fraction of wealth in the risky asset immediately before re-balancing.

Using the dynamic programming principle for the pre-committed control problem (now the problem has been made time consistent because the controls are pre-committed):

$$\mathcal{J}(W_{k-1}^-, \mathcal{A}_{i,k-1}^-) = \min_{(\zeta)} E^{\mathbb{P}}[\mathcal{J}(W_k^-, \mathcal{A}_{i,k}^-) | \mathcal{F}_{k-1}] \quad (3.7)$$

Then for  $k = N$  with  $W_N^- = W_{N-1}^- \phi_{N-1}(\mathcal{A}_{i,N-1}^-)$  we have:

$$\mathcal{J}(W_{N-1}^-, \mathcal{A}_{i,N-1}^-) = \min_{(\zeta)} E^{\mathbb{P}}[(W_N^- - b)^2 | \mathcal{F}_{N-1}] \quad (3.8)$$

$$= \min_{(\zeta)} E^{\mathbb{P}}[(W_{N-1}^- \phi_{N-1}(\mathcal{A}_{i,N-1}^-) - b)^2 | \mathcal{F}_{N-1}] \quad (3.9)$$

In a similar vein we could recursively go backwards and determine values for  $k = N - 2, N - 3, \dots, 2, 1$ . Figure 3.1 shows the efficient frontier generated by varying  $b$  in the above equations 3.8-3.9 for a particular choice of parameters.

Over the interval  $\Delta T$  the risky growth of risky asset is log-normally distributed since the continuous domain model is Geometric Brownian motion (GBM). Working with exact distributions is computationally intensive. In most cases an exact analytical solution is not possible and the *curse of dimensionality* could be a greater problem in the continuous domain. This motivates us to deform our probability model in to a discrete model with  $M$  risky evolution branches<sup>6</sup>. Techniques that focus on how to create such deformations are the subject of Chapter 5 for a theoretical discussion and Chapter 4 for Mathematica based implementation.

We will later show the dynamic portfolio problems show nice decomposability with respect to the probability model of risky asset growth. That problem is a more complex version of numerical quadrature: evaluating the integral

$$\int f(x) * g(x) dx \quad (3.10)$$

<sup>6</sup>A discrete approximation of a continuous distribution of risky growth over the interval  $\Delta T$



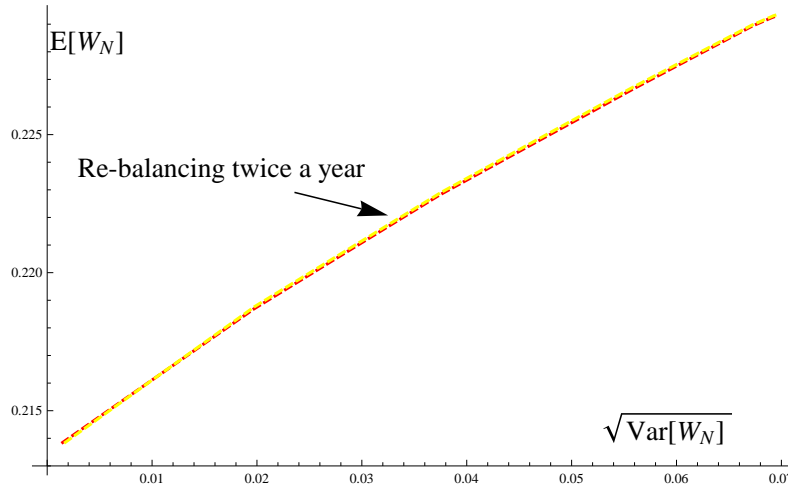


Figure 3.1: Risk-adjusted value of re-balancing portfolios with parameters  $T = 1$ ,  $\omega = 0.07$ ,  $\lambda = \mu = 0.005$ ,  $s = e^{\omega\Delta T}$ ,  $m = 0.14$ ,  $\sigma = 0.3$ . Where  $T$  is the time horizon for investment,  $\omega$  is the continuous time risk-free rate,  $(\lambda, \mu)$  are transaction cost factors,  $s$  is the risk free growth over the interval,  $m$  is the drift for continuous time GBM and  $\sigma$  is the volatility for the continuous time GBM. The continuous time GBM implies a risky growth for the risky asset over the interval  $\Delta T$ .

Instead of applying numerical methods on the integral itself we will apply methods on the approximation with respect to a function so that:

$$\int f(x) * g(x)dx = \sum a_i f^*(x_i)g(x_i) \quad (3.11)$$

where  $f^*$  is an approximation to the function  $f$ , where  $a_i$  denote the weights assigned to the nodes  $x_i$ .

In Figure 3.1 the exact solution for efficient frontier matches closely with a probability deformation scheme. Yet the computational cost of the deformation based solution is only a fraction of the exact solution. This is because the exact solution requires numerical evaluation of integrals which can be computationally challenging to attain a desired level of accuracy<sup>7</sup>.

### 3.6 Transfer of wealth, transaction cost structure and no-transaction region

Throughout we will consider an investor who distributes his wealth between risky and non-risky assets. It is of some value to the dynamic investor to re-balance his wealth to the most optimal risky fractions given the state variable values<sup>8</sup>. Under transaction costs most often he would trade to the boundary of the no-transaction region. The optimal re-balancing point in the absence of transaction costs is situated inside the no-transaction region. These ideas

<sup>7</sup>There is a trade-off between speed and accuracy but we are going for speed with reasonable accuracy.

<sup>8</sup>For a general utility function the most optimal risky fractions could become wealth dependent.

have already been discussed in context of continuous time portfolio theory in Chapter 2. Re-balancing is equivalent to transfer of wealth between assets. A system of equations holds for an investor shifting his wealth between assets<sup>9</sup>.

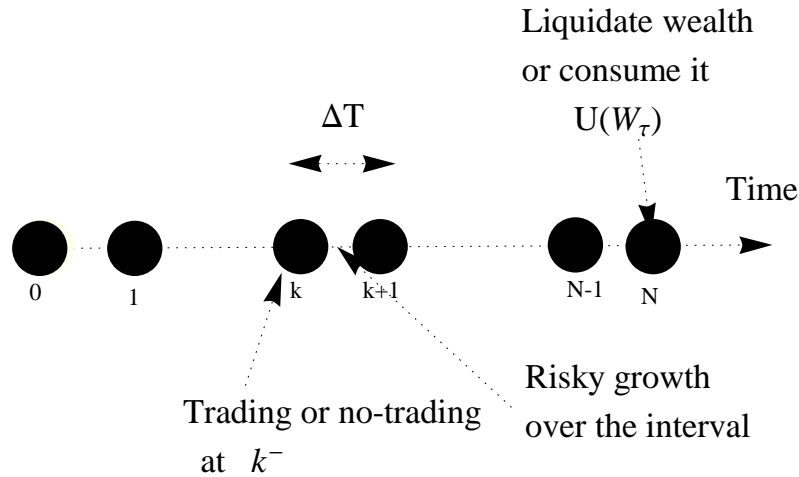


Figure 3.2: Discrete time trading model. The dynamic investor has the option to re-balance or not to re-balance at a time node. The risky asset grows over the re-balancing period and so the fraction of wealth in the risky asset changes.

### 3.6.1 Transaction cost models

Transaction costs are often modeled as proportional to the amount traded. Transaction costs have a *non-linear* structure which varies with the amount traded. For modeling purposes if  $\Delta$  is the amount traded then one possible model is to express the transaction cost in terms of a polynomial basis as  $\sum_{i=0}^I a_i \Delta^i$ . Another possible model would be to express transaction cost as being a piecewise linear function of  $\Delta$  as shown in Figure 3.3. The level of transaction costs change over time making a random model attractive and the actual dependence of such models on market volatility is explored in Chapter 8.

#### Transfer of wealth between risky assets and trading cost proportional to the amount transferred

Let  $W_k^-$  be the total amount of wealth and  $\mathcal{A}_{i,k}^-$  be the fraction of wealth in the risky asset  $i$  at the beginning of period  $k$  immediately before re-balancing. So  $\mathcal{A}_{i,k}^+$  is the fraction immediately after re-balancing. Also  $\eta_k^{j,i,+} W_k^-$  is a fraction,  $\eta_k^{j,i,+}$ , of the current wealth level immediately before re-balancing. Here  $\eta_k^{j,i,+} W_k^-$  denotes the net wealth added at the beginning of the period

<sup>9</sup>This section illustrates the system of equations that should hold under different transaction cost models.

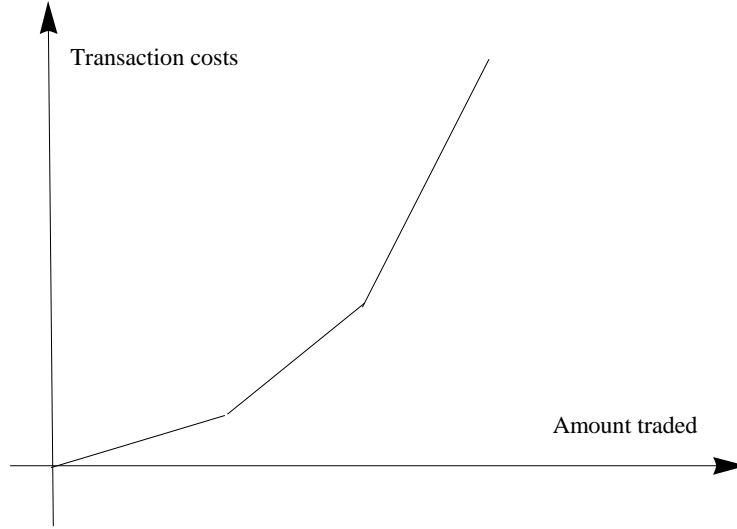


Figure 3.3: A possible piecewise linear function for transaction costs. Transaction costs are a function of the amount traded.

that comes from transferring wealth from risky asset  $j$  to risky asset  $i$ . Re-balancing is only done at the beginning of the period. The transaction costs are proportional to the amount transferred so a trading cost of  $\lambda_k \eta_k^{j,i,+} W_k^-$  is incurred. Immediately after re-balancing there is no growth in risky asset as growth only occurs over an interval. Denote by  $s_{i,k}$  the risky growth of asset  $i$  over the period  $k$ . We define *risky growth* as new price levels divided by the previous price levels. If  $S_{i,k}$  is the asset price at the beginning of period  $k$  and  $S_{i,k+1}$  at the beginning of period  $k+1$  then the risky growth is  $s_{i,k} = \frac{S_{i,k+1}}{S_{i,k}}$ . No simultaneous transfer of wealth between risky assets is allowed. This means if the investor transfers wealth from asset  $j$  to asset  $i$  then he is not allowed to transfer wealth from asset  $i$  to asset  $j$ .

At the beginning of each period if the investor decides to transfer wealth from asset  $j$  to asset  $i$ , the following system of equation holds:

$$X_{i,k}^+ = \mathcal{A}_{i,k}^- W_k^- + \eta_k^{j,i,+} W_k^- \quad (3.12)$$

$$X_{j,k}^+ = \mathcal{A}_{j,k}^- W_k^- - (1 + \lambda_k) \eta_k^{j,i,+} W_k^- \quad (3.13)$$

$$\mathcal{A}_{i,k+1}^- = \frac{\mathcal{A}_{i,k}^+ s_{i,k}}{\mathcal{A}_{i,k}^+ s_{i,k} + (1 - \mathcal{A}_{i,k}^+) s_{j,k}} \quad (3.14)$$

In an analogous fashion we could write the system of equations that should hold for wealth transferred from asset  $i$  to asset  $j$ .

$$X_{j,k}^+ = \mathcal{A}_{j,k}^- W_k^- + \eta_k^{i,j,+} W_k^- \quad (3.15)$$

$$X_{i,k}^+ = \mathcal{A}_{i,k}^- W_k^- - (1 + \lambda_k) \eta_k^{i,j,+} W_k^- \quad (3.16)$$

$$\mathcal{A}_{i,k+1}^- = \frac{\mathcal{A}_{i,k}^+ s_{i,k}}{\mathcal{A}_{i,k}^+ s_{i,k} + (1 - \mathcal{A}_{i,k}^+) s_{j,k}} \quad (3.17)$$

If the investor decides to do nothing:

$$X_{j,k}^+ = \mathcal{A}_{j,k}^- W_k^- \quad (3.18)$$

$$X_{i,k}^+ = \mathcal{A}_{i,k}^- W_k^- \quad (3.19)$$

$$\mathcal{A}_{i,k+1}^- = \frac{\mathcal{A}_{i,k}^- s_{i,k}}{\mathcal{A}_{i,k}^- s_{i,k} + (1 - \mathcal{A}_{i,k}^-) s_{j,k}} \quad (3.20)$$

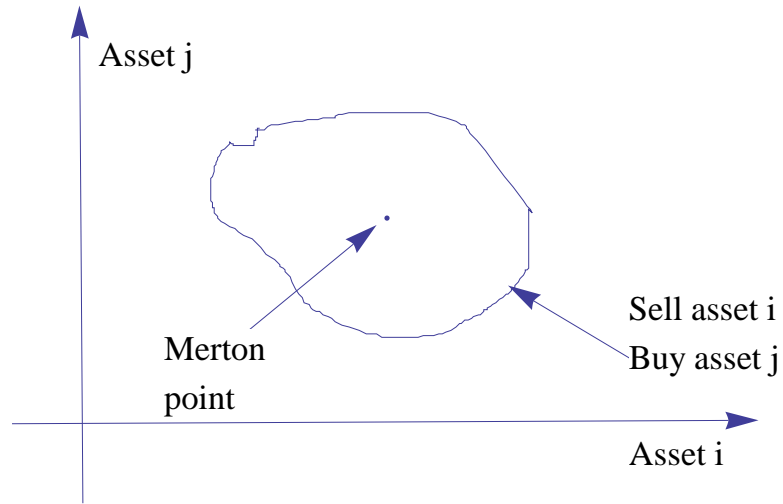


Figure 3.4: A possible no-transaction region in state variable space. For Log and CRRA utility if the fraction of wealth in risky asset goes out of the boundaries the risky fraction is brought inside the boundary [28].

For most well-behaved utility functions like CARA and CRRA the no-transaction region seems to be a closed curve (see Figure 3.4) with respect to the relevant state variables [51]. If the transaction is proportional to the amount traded the investor would try to bring it to the boundary of the region. If transaction cost is independent of the amount traded then he would try to bring it to some point inside (see [69]). Also the state variable in which the region is expressed is of some importance. It turns out that for CRRA and log-utility we have separability in wealth and the no-transaction region can be expressed through the fraction of

(1,2)	(1,3)	(2,3)
0	0	0
0	0	1
0	1	0
0	1	1
1	0	0
1	0	1
1	1	0
1	1	1

Table 3.1: Transfer of wealth configurations between 3 risky assets where  $(i, j)$  is equal to 0 if he transfers from  $i$  to  $j$  and 1 if he transfers from  $j$  to  $i$ . This table includes all the possibilities for transferring wealth under the control constraints.

wealth in the individual risky assets(see [28]). For exponential or CARA utility it can be expressed through the amount of wealth in the individual risky assets ( see [55]).

Keeping in view the above modeling framework, consider a three risky asset model with no risk-free asset. At a given time the investor has nine possible alternative choices. The simplest of these options is to do nothing at all. There are  $2^3 = 8$  possible configurations for transferring wealth between the 3 risky assets (See Table 3.1). In general, for a transfer of wealth model and  $l$  risky assets we have  $2^l + 1$  available strategies at any point in time.

Now consider an investment that has a finite time horizon of  $T$ . There are  $N$  periods so that each period is of length  $\Delta T = \frac{T}{N}$  and  $k = 1, 2, \dots, N$ . The investor objective is to maximize the logarithm of terminal wealth over a finite horizon. At a particular time snapshot (say the initial time,  $k = 0$ ) a no-transaction *geometry* could look like as in Figure 3.5. Parameters are not supplied for are computed solution in 3.5 because we have not discussed the model yet. We just wish to give a visual depiction of no-transaction geometries.

A no-transaction *geometry* is essentially the optimal control law at a point in time visually depicted in the risky fraction state space. Whenever the relevant state space vector is inside the no-transaction region the investor does not transact. We later demonstrate in Chapter 6 that logarithmic and CRRA utility posses decomposability with respect to wealth so that the optimal control law only depends upon the fraction of wealth held in the risky assets.

### **Risk-free asset banker for buying/selling risky assets and trading cost proportional to the amount traded**

Consider a simple model where our portfolio consists of a risky and non-risky asset. The investor shifts his wealth between assets subject to a control strategy given his terminal investment objective. There are  $N$  periods and an investment horizon of length  $T$  years.

Let us illustrate a transaction process involving two assets. Let  $X_k^+$  be the wealth in the risky asset immediately after re-balancing and  $Y_k^+$  for the wealth in the risk-free asset. Also  $\mathcal{A}_k^-$  is the fraction of wealth in the risky asset immediately before re-balancing. Let  $\Delta_k$  be the

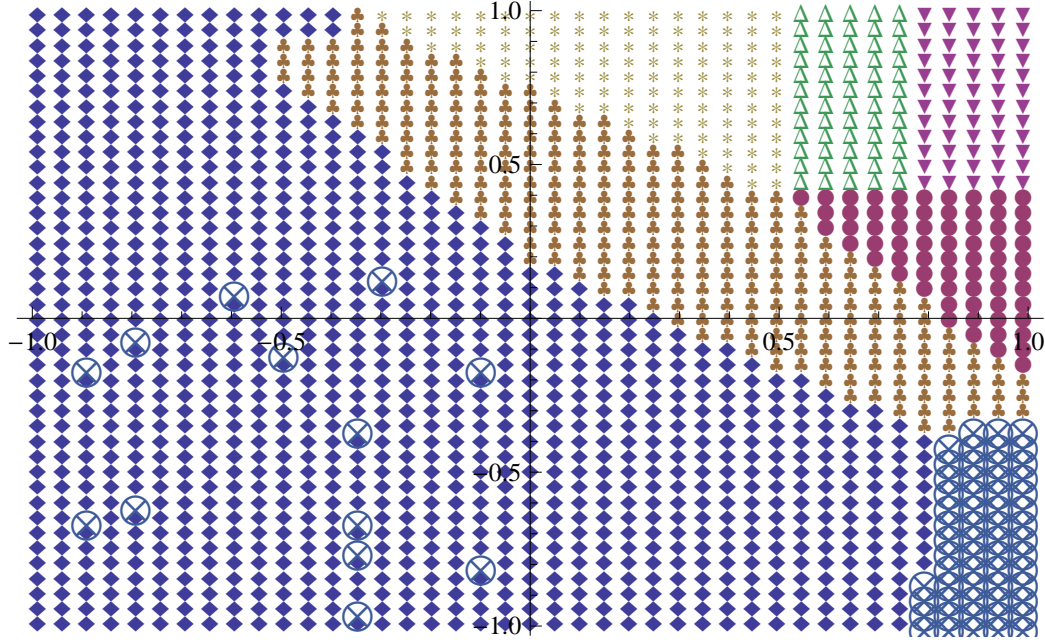


Figure 3.5: A no-transaction region for transfer of wealth model between three assets where ♣ denotes no-transaction. Parameters intentionally not supplied. Horizontal axis is the fraction of wealth in first risky asset and vertical axis is the fraction of wealth in second risky asset.

amount of wealth transferred and transaction cost is incurred which is illustrated by the system of equations below. Denote by  $r_k$  by the growth rate of the risky asset and  $s_k$  by the growth rate of risk-free asset.

If asset 1 is bought:

$$X_k^+ = \mathcal{A}_k^- W_k^- + \Delta_k = \epsilon_k^+ W_k^- \quad (3.21)$$

$$Y_k^+ = (1 - \mathcal{A}_k^-) W_k^- - (1 + \lambda_k) \Delta_k \quad (3.22)$$

$$\mathcal{A}_{k+1}^- = \frac{\epsilon_k^+ r_k}{\epsilon_k^+ r_k + ((1 - \mathcal{A}_k^-) - (1 + \lambda_k)(-\mathcal{A}_k^- + \epsilon_k^+)) s_k} \quad (3.23)$$

If asset 1 is sold:

$$X_k^+ = \mathcal{A}_k^- W_k^- - \Delta_k = \epsilon_k^+ W_k^- \quad (3.24)$$

$$Y_k^+ = (1 - \mathcal{A}_k^-) W_k^- + (1 - \mu_k) \Delta_k \quad (3.25)$$

$$\mathcal{A}_{k+1}^- = \frac{\epsilon_k^+ r_k}{\epsilon_k^+ r_k + ((1 - \mathcal{A}_k^-) + (1 - \mu_k)(\mathcal{A}_k^- - \epsilon_k^+)) s_k} \quad (3.26)$$

If re-balancing is not selected:

$$X_k^+ = \mathcal{A}_k^- W_k^- \quad (3.27)$$

$$Y_k^+ = (1 - \mathcal{A}_k^- W_k^-) \quad (3.28)$$

$$A_{k+1}^- = \frac{\mathcal{A}_k^- r_k}{\mathcal{A}_k^- r_k + (1 - \mathcal{A}_k^-) s_k} \quad (3.29)$$

It is easy to incorporate constraints on the state variable under control. For example, if we desire  $\mathcal{A}_k^+ \leq 1$ . This could be easily be put in to action by letting:

$$\frac{\epsilon_k^+}{\epsilon_k^+ + ((1 - \mathcal{A}_k^-) - (1 + \lambda_k)(-\mathcal{A}_k^- + \epsilon_k^+))} \leq 1 \quad (3.30)$$

$$\Rightarrow \epsilon_k^+ \leq \frac{1 + \lambda_k \mathcal{A}_k^-}{1 + \lambda_k} \quad (3.31)$$

### Buying/selling risky assets and trading cost proportional to the amount of wealth

Lets consider a different transaction cost structure in which cost depends upon the total amount of wealth<sup>10</sup>. At the beginning of period  $k$  we have  $W_k^- = \sum Y_{i,k}^- + X_k^-$ . Denote  $Y_k^-$  as the amount of wealth in risk free asset and  $X_{i,k}$  as the amount in the risky asset  $i$  immediately before re-balancing. Denote  $r_{i,k}$  as the growth rate of the risky asset  $i$  and  $s_k$  as the growth rate of risk-free asset. A transaction proportional to the amount of wealth is incurred. At the beginning of each period if he decides to re-balance then the following system of equation holds:

$$X_{i,k+1}^- = (1 - \lambda_k) W_k^- \mathcal{A}_{i,k}^+ r_{i,k} \quad (3.32)$$

$$Y_{k+1}^- = (1 - \lambda_k) W_k^- \left(1 - \sum \mathcal{A}_{i,k}^+\right) s_k \quad (3.33)$$

$$\mathcal{A}_{i,k+1}^+ = \frac{\mathcal{A}_{i,k}^+ r_{i,k}}{\sum \mathcal{A}_{i,k}^+ r_{i,k} + (1 - \sum \mathcal{A}_{i,k}^+) s_k} \quad (3.34)$$

If he decides not to re-balance then the following system holds :

$$X_{i,k+1}^- = W_k^- \mathcal{A}_{i,k}^- r_{i,k} \quad (3.35)$$

$$Y_{k+1}^- = W_k^- \left(1 - \sum \mathcal{A}_{i,k}^-\right) s_k \quad (3.36)$$

$$\mathcal{A}_{i,k+1}^- = \frac{\mathcal{A}_{i,k}^- r_{i,k}}{\sum \mathcal{A}_{i,k}^- r_{i,k} + (1 - \sum \mathcal{A}_{i,k}^-) s_k} \quad (3.37)$$

<sup>10</sup>Also dubbed management fee.

### 3.7 A synopsis of approximate lattice methods

One of the main goals of this thesis is to formulate efficient methods for solving dynamic investment problems under transaction costs. In this section we provide a brief overview of our solution methodology. The problems considered in the thesis with a proper terminal objective are cast in a dynamic programming framework. We will consider the time consistent version of the mean-variance example considered in Section 3.5 for the purpose of illustration.

Our aim is to work with as much generality as possible. In particular we do not assume  $\Delta T$  to be small to make our framework as general as possible.

To begin with the dynamic programming formulation as in Section 3.5 reads as:

$$\mathcal{J}(W_{k-1}^-, \mathcal{A}_{i,k-1}^-) = \min_{(\zeta)} E^{\mathbb{P}}[\mathcal{J}(W_k^-, \mathcal{A}_{i,k}^-) | \mathcal{F}_{k-1}] \quad (3.38)$$

Here  $(W_{k-1}^-, \mathcal{A}_{i,k-1}^-)$  is the state variable space for our problem. Starting with the terminal utility we will recursively go backwards to determine the optimal control law as a function of state variables.

To do such a recursion we will work with a discrete domain and divide our state space in to equidistant intervals. There are two important issues we must address:

- 1- Interpolation errors.
- 2- Extrapolation errors.

If we use a fine enough discretization we could manage *interpolation errors*. In particular, the fineness of state space discretization is dependent on the fineness in time space discretization. If we have  $n$  divisions in time space then the state space division would obey the power law form  $n^\gamma$  for convergence to occur where  $\gamma$  represents the order of the law. This conjecture is inspired from the classic work done by [34] in context of Asian option pricing using lattice based methods. The exact nature of the law is problem structure dependent. The nature of this law has been discussed in detail in [34].

To take care of extrapolation errors we must truncate the domain at the previous time-step so that in the discrete approximation for risky growths, our state space variables do not overflow outside the domain. In the above example the risky fraction space is always confined to  $[0, 1]$ . However, the wealth variable might go outside our working domain (because of recursive nature of dynamic programming) introducing extrapolation errors<sup>11</sup>. Given a discrete approximation for risky growth this could easily be handled. If  $(1 + g)$  is the maximum factor by which a risky asset can grow we could simply truncate our domain by a factor of  $\frac{1}{(1+g)}$  in the wealth space.

Instead of solving equation (3.38) using an exact probability model we will approximate it with a discrete distribution. Tree approximations as used in option pricing theory rely on a moment based approximation for the probability model. In portfolio problems we could have log-normal distribution for risky growth in 1-dimension and multi-variate log-normal in higher dimensions. Consider the following:

---

<sup>11</sup>Almost always the state space variable would obey some sort of constraints. In the above example, bankruptcy becomes an interesting constraint if the investor is allowed to short risky assets. This could easily be dealt with by penalizing the constraint violation in the value function - thus the investor always chooses controls which do not violate the constraints.



$$E[f(x, r)] = E \left[ f(x, r_0) + (r - r_0)f'(x, r_0) + \frac{(r - r_0)^2}{2}f''(x, r_0)\dots \right] \quad (3.39)$$

where  $x$  denotes the set of state variables and  $r$  is a random variable.

It appears that discrete probability approximation methods can work well only if the time interval for risky growth  $\Delta T$  is very small. This is because moments of order  $n$  for a relevant random variable which in our case is mostly risky growth scales as  $(\Delta T)^n$  so when the  $\Delta T$  gets smaller the higher order moments are relatively less likely to hurt the *distributional* approximation. Of course this also depend upon the form of the utility function and values of state variables.

The thesis proposes *deformation methods* for approximating the probability for solving portfolio problems in greater generality. With these methods we do not require  $\Delta T$  to be small. Our solutions are found to be reasonably accurate by benchmarking them against the solutions obtained using exact distributions. This is discussed in detail in Chapter 5.

The basic idea in deformation schemes is to sample a discrete approximation of the distribution based upon its essential statistical characteristics. These characteristics need not necessarily be moments. Figure 3.6 shows an approximation using five points. We successively deform the probability<sup>12</sup> and see the continuation behavior to project the solution under the exact probability model. A brief description of schemes is provided in Section 3.9 and the thesis will discuss in the detail the solution schemes in Chapter 5.

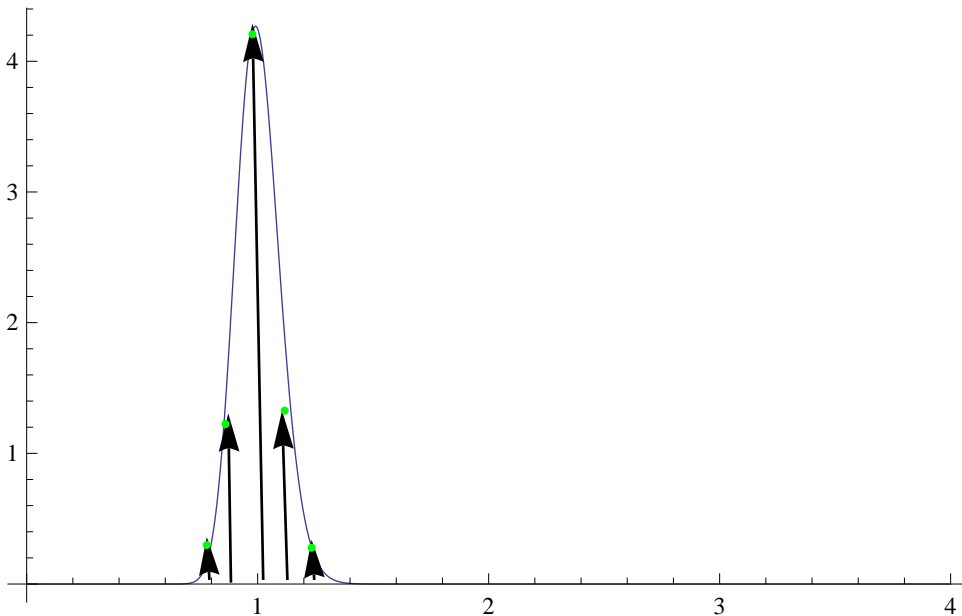


Figure 3.6: Approximation with five points. Choosing statistical features of the target probability model for approximation.

The dimensionality<sup>13</sup> in our models is controlled by primarily:

<sup>12</sup>So that the next probability structure is closer to the target probability model.

<sup>13</sup>In terms of the computational effort needed to solve them.

- 1- State space dimensionality.
- 2- Probability space dimensionality.
- 3- Control space dimensionality.

In the absence of transaction costs the optimal control law is independent of the risky fraction vector and model dimensionality is controlled primarily by the probability and control spaces. The state space dimensionality includes only wealth and time.

The *curse of dimensionality* will continue to live. We can merely *tame* it in our discrete domain by using:

- 1- *Deformation schemes* as discussed earlier. We are significantly reducing the dimensionality of the probability model.
- 2- Using continuation schemes on the pattern of *Richardson extrapolation* in the state space and time-space domain.

## 3.8 On discrete probability approximations

### 3.8.1 The example of a simple model

Consider a portfolio consisting of one risky and one risk-free asset. The time line is divided into discrete nodes so that  $k = 1, \dots, N$  denotes the point in time when the re-balancing decision can be taken. The fraction in the risky asset changes with time. Let  $X_{k-1}^+$  be the amount of risky asset at the beginning of the period immediately after the re-balancing has been done. Let  $W_{k-1}^-$  be the amount of wealth before re-balancing at a time node  $k - 1$ . Also  $s_k$  and  $r_k$  denote the risky and risk-free growth over a particular period respectively. No simultaneous buying or selling of risky asset is allowed.

We will assume the optimal trading rule specified via the existence of buy side and sell boundaries. What we mean is that if the fraction of wealth in the risky asset falls below the buy side boundary then the investor buys enough of the risky asset so that the risky fraction moves to the buy-side boundary. Similarly, if the fraction of wealth in the risky asset falls above the sell-side boundary then the investor sells enough of the risky asset so that the risky fraction moves to the sell-side boundary. Using dynamic programming we are thereupon finding the optimal buy and sell side boundaries. However, there is no reason for us to believe that such a trading rule exists if  $\Delta T$  is large because we don't have analytic in discrete time to support such a conjecture. When  $\Delta T$  is small, standard portfolio theory under transaction cost postulates the existence of risky fraction boundaries encapsulating the optimal trading rule. If there were no transaction costs the following equation holds:

$$W_k^- = (W_{k-1}^- - \eta_{k-1})s_k + X_{k-1}^+ r_k \quad (3.40)$$

To build a transaction cost model let  $\mathcal{A}_{k-1}$  be the fraction of wealth invested in risky asset at the beginning of the period.  $L_{k-1}$  and  $R_{k-1}$  be the fraction of risky asset bought or sold. Then if  $\lambda_{k-1}$  and  $\mu_{k-1}$  denote the buying and selling proportional transaction costs then the following equations hold:

$$W_k^- = W_{k-1}^- F_{k-1} \quad (3.41)$$

$$F_{k-1} = (1 - \mathcal{A}_{k-1}) - (1 + \lambda_{k-1})L_{k-1} + (1 - \mu_{k-1})R_{k-1}s_k + (\mathcal{A}_{k-1} + L_{k-1} - R_{k-1})r_k \quad (3.42)$$

We assume that under the optimal trading rule  $F_{k-1}$  takes the following functional form:

$$\begin{aligned} F_{k-1}(\mathcal{A}_{k-1}) &= 1_{(\mathcal{A}_{k-1} < \phi_{k-1}^-)}(s_k + \phi_{k-1}^-(r_k - s_k) - \lambda_{k-1}(\phi_{k-1}^- - \mathcal{A}_{k-1})s_k) \\ &\quad + 1_{(\phi_{k-1}^- < \mathcal{A}_{k-1} < \phi_{k-1}^+)}(s_k + \mathcal{A}_{k-1}(r_k - s_k) + 1_{(\mathcal{A}_{k-1} > \phi_{k-1}^+)}) \\ &\quad + (s_k + \phi_{k-1}^+(r_k - s_k) + \mu_{k-1}(\phi_{k-1}^+ - \mathcal{A}_{k-1})s_k) \end{aligned} \quad (3.43)$$

where  $k = 1, 2, \dots, N-1, N$ . Here  $(\phi_{k-1}^-, \phi_{k-1}^+)$  denotes the risky fraction boundaries which need to be determined as part of dynamic programming. The assumption is reasonable from an intuitive standpoint because if we have too much or too less of risky asset we would need to re-adjust our portfolio. The exact nature of the formulation is inspired by the continuous time results in [28].

The stage is now set to highlight the dynamic programming technique for the optimal portfolio problem. Define the value function by:

$$\mathcal{J}(W_k, \mathcal{A}_k, k) = E^P[W_N^V | \mathcal{F}_k] \quad (3.44)$$

where  $V \in [0, 1]$

Consequently, for a given boundary specification we can write:

$$\mathcal{J}(W_k, \mathcal{A}_k, k) = \max(E^P[\mathcal{J}(W_{k+1}, \mathcal{A}_{k+1}, k+1) | \mathcal{F}_k]) \quad (3.45)$$

Furthermore,

$$\mathcal{J}(W_{N-1}, \mathcal{A}_{N-1}, N-1) = \max(E^P[W_{N-1}^V F_{N-1}^V | \mathcal{F}_{N-1}]) \quad (3.46)$$

$$= W_{N-1}^V \max(E^P[F_{N-1}^V | \mathcal{F}_{N-1}]) \quad (3.47)$$

$$= W_{N-1}^V \mathcal{J}^{(1)}(\mathcal{A}_{N-1}) \quad (3.48)$$

represents the value function for the last stage. Using recursion we could successively determine value function for earlier stages.

In the second last stage of the recursion we have:

$$\begin{aligned} \mathcal{A}_{N-1} &= 1_{(\mathcal{A}_{N-2} < \phi_{N-2}^-)} \left( \frac{\phi_{N-2}^- r_{N-1}}{(s_{N-1} + \phi_{N-2}^-(r_{N-1} - s_{N-1}) - \lambda_{N-2}(\phi_{N-2}^- - \mathcal{A}_{N-2})s_{N-1})} \right) \\ &\quad + 1_{(\mathcal{A}_{N-2} > \phi_{N-2}^+)} \left( \frac{\phi_{N-2}^+ r_{N-1}}{(s_{N-1} + \phi_{N-2}^+(r_{N-1} - s_{N-1}) + \mu_{N-2}(\phi_{N-2}^+ - \mathcal{A}_{N-2})s_{N-1})} \right) \\ &\quad + 1_{(\phi_{N-2}^- < \mathcal{A}_{N-2} < \phi_{N-2}^+)} \left( \frac{\mathcal{A}_{N-2} r_{N-1}}{(1 - \mathcal{A}_{N-2})s_{N-1} + \mathcal{A}_{N-2} r_{N-1}} \right) \end{aligned} \quad (3.49)$$

It is therefore easy to see that:

$$\mathcal{J}(W_{N-2}, \mathcal{A}_{N-2}, N-2) := \max(E^P[\mathcal{J}(W_{N-1}, \mathcal{A}_{N-1}, N-1)]) = W_{N-2}^V \mathcal{J}^{(2)}(\mathcal{A}_{N-2}) \quad (3.50)$$

In fact, to determine  $\mathcal{J}^{(2)}$  is basically to determine the risky fraction boundaries in the second last stage of recursion. In this way we can go back to the initial time  $t = 0$  and determine the value function at that point.

For a suitable choice of parameters we show the variation of risky fraction boundaries with the transaction cost parameter in Figure 3.7. It can be seen that no-transaction boundaries widen with the transaction cost parameter. Also we plot in Figure 3.7 the boundaries for the last three stages. It is observed that as the investor moves closer to terminal time the boundaries widen. Our goal will be to find  $\mathcal{J}^{(N)}(A_0)$  so that we could examine the optimal re-balancing of our portfolio at initial time i.e.  $t = 0$ .

Here  $\mathcal{J}^{(N)}$  denotes the separable portion of the value function after wealth is taken out.

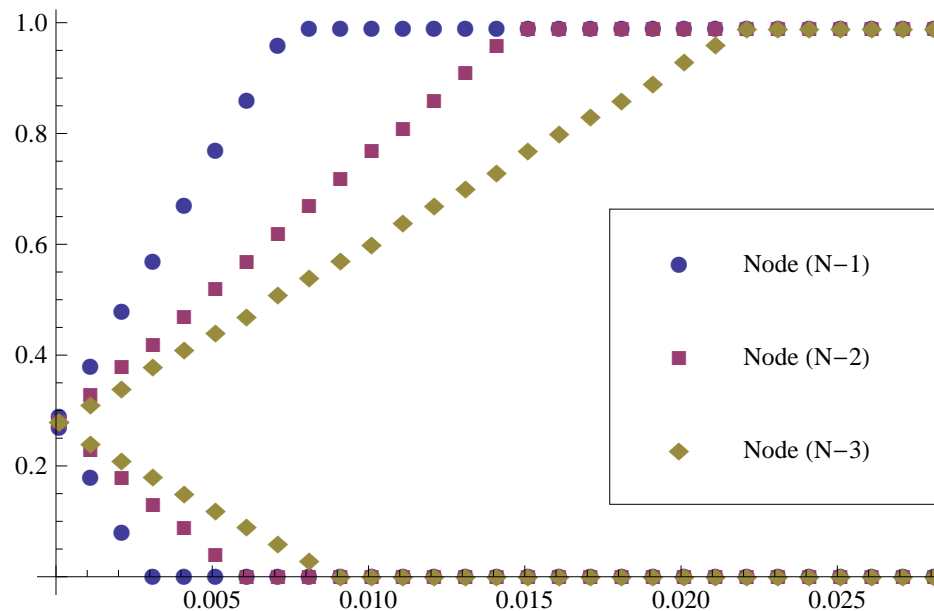


Figure 3.7: No transaction region boundaries shifting monotonically outwards as investors moves closer to terminal time for last, second and third last stage parameters are:  $V = 0.5$ ,  $T = 0.1$ ,  $N = 3$ ,  $\omega = 0.05$ ,  $s = e^{\omega\Delta T}$ ,  $m = 0.14$ ,  $\sigma = 0.8$ .  $N$  is number of re-balancing nodes and  $s$  is the risky free growth over the interval.  $V$  is the co-efficient of risk aversion in the CRAA utility. Also  $m$  and  $\sigma$  are the parameters of the continuous time GBM and risky growth discrete probability approximation is constructed as we will discuss later in section 3.8.3 and 3.9. Where  $T$  is the time horizon for investment,  $\omega$  is the continuous time risk-free rate,  $(\lambda, \mu)$  are transaction cost factors,  $s$  is the risk free growth over the interval,  $m$  is the drift for continuous time GBM and  $\sigma$  is the volatility for the continuous time GBM. The continuous time GBM implies a risky growth for the risky asset over the interval  $\Delta T$ .

### 3.8.2 Binomial discrete probability approximation

In this section we consider a simple binomial model for risky growth evolution. To obtain some analytic insights for the model in section 3.8.1, let us define the risky growth  $G^*$  as the ratio of future time step stock price and to the previous time step stock price i.e.  $G^* = \frac{S_{k+1}}{S_k}$ . In this section we consider a simple binomial model for risky growth evolution. To obtain some analytic insights for the model in section 3.8.1, let us define the risky growth  $G^*$  as the ratio of future time step stock price and to the previous time step stock price i.e.  $G^* = \frac{S_{k+1}}{S_k}$ . To obtain some analytic intuition assume that the risky growth  $G^*$  evolves binomially. It is  $(1 + g)$  with a probability of  $p$  and  $(1 - g)$  with a probability of  $(1 - p)$ . The dynamic programming problem discussed in the previous section still holds and so each stage involves a non-linear optimization problem. To find the risky boundaries at the previous stage we set  $\mathcal{A}_k = 0$  or  $\mathcal{A}_k = 1$  in the beginning of the period to force the buy or selling of the risky asset and hence determine the buy and sell-side boundaries. To get exact analytic formulas, however, we linearize with respect to  $\lambda$ ,  $\mu$  and  $V$ . This approximately holds valid for some range of values for the transaction cost and risk aversion parameters. This helps us determine  $(\phi^-, \phi^+)$  so that we could get some analytic insights into the risky boundaries.

Let us see how the approximation works for the last stage of the portfolio problem. In the analysis we will assume  $V \in [0, 1]$

Start with the buy-side boundary approximation. If  $A > 0$  denotes the buy-side boundary then it satisfies the following non-linear equation as a result of optimization on control in the dynamic programming equation given in Section (3.8.1) :

$$p(s + \lambda sA - sA + A(1 + g))^V + (1 - p)(s - \lambda sA - sA + A(1 - g))^V = 0 \quad (3.51)$$

where  $s$  is the growth rate over the interval for risk-free asset.

However, in the above observe the co-efficients of  $A$ . If we assume  $\| \frac{1+g}{s} - (1 + \lambda) \|$  and  $\| \frac{1-g}{s} - (1 + \lambda) \|$  are small<sup>14</sup> for some small transaction costs then we can linearize to get the *buy-side* boundary:

$$\phi^- = \inf(\sup(a + b\lambda, 0), 1) \quad (3.52)$$

where

$$a = \frac{s(-2gp + g + s - 1)}{(V - 1)(g^2 - 2g(2p - 1)(s - 1) + (s - 1)^2)} \quad (3.53)$$

$$b = \frac{s^2(g^2(8p^2 - 8p + 1) - 2g(2p - 1)(s - 1) + (s - 1)^2)}{(V - 1)(g^2 - 2g(2p - 1)(s - 1) + (s - 1)^2)} \quad (3.54)$$

Similarly consider with the sell-side approximation. If  $A < 1$  denotes the sell-side boundary then it satisfies the following non-linear equation as a result of optimization on control in the dynamic programming equation given in Section (3.8.1) :

<sup>14</sup>  $\frac{1+g}{1+s} - (1 + \lambda) = \frac{g-s}{1+s} - \lambda$  which is small if  $g$  is close to  $s$  and transaction costs are small!!

$$p(s + A(1 + g - s) + \mu(A - 1)s)^V + (1 - p)(s + A(1 - g - s) + \mu(A - 1)s)^V = 0 \quad (3.55)$$

where  $s$  is the growth rate over the interval for risk-free asset.

However, in the above observe the co-efficients of  $A$ . If we assume  $\| \frac{1+g}{s} - (1 - \mu) \|$  and  $\| \frac{1-g}{s} - (1 - \mu) \|$  are small for some small transaction costs then we can linearize to get the *sell-side* boundary:

$$\phi^+ = \sup(\inf(a + d\lambda, 1), 0) \quad (3.56)$$

where  $a$  is defined earlier and

$$d = \frac{s(g^3(2p - 1) + g^2(8p^2 - 8p - 2s + 3) + g(2p - 1)(s^2 - 4s + 3) + (s - 1)^2)}{(V - 1)(g^2 - 2g(2p - 1)(s - 1) + (s - 1)^2)} \quad (3.57)$$

Provided  $E[G^*] > s - 1$  we will show  $a > 0$  and  $b < 0$  for some range of parameters which agrees with our intuition.

Holding all else constant increasing  $V$  increases  $a, b$  and  $d$  while decreasing  $V$  decreases the same parameters.

Assuming  $E[G^*] > s - 1$  results in  $g(2p - 1) > s - 1$ . Further we assume  $0 < p < 1, 1 < s < 2$  and  $0 < g < 1$ .

**Proposition 3.8.1** *In the portfolio model (3.43)-(3.49)  $a = c > 0$ :*

**Proof** *Examine a.* To prove  $a > 0$  we need to find the signs of terms in the numerator and denominator. Now  $-(2p - 1) > -1$  implies  $-2g(2p - 1)(s - 1) > -2g(s - 1)$  implies  $g^2 - 2g(2p - 1)(s - 1) + (s - 1)^2 > (g - (s - 1))^2 > 0$ .

Since  $g(-2p + 1) + (s - 1) < 0$  as described earlier we can state:  
 $a = c > 0$

■

**Proposition 3.8.2** *In the portfolio model (3.43)-(3.49)  $b < 0$  if  $p \in [p^*, 1 - p^*]$ :*

**Proof** *Let us examine b.* To prove  $b < 0$  we need to find the signs of terms in the numerator and denominator. Now  $g(2p - 1) > s - 1$  implies  $-2g(2p - 1)(s - 1) < -2(s - 1)^2$  which implies  $-2g(2p - 1)(s - 1) + (s - 1)^2 < -(s - 1)^2 < 0$ . So if  $8p^2 - 8p + 1 < 0$  then  $b < 0$ .

*In short:  $b < 0$  if  $p^* < p < 1 - p^*, E[G^*] > s - 1$  where  $p^*$  is obtained by solving the quadratic equation  $8p^2 - 8p + 1 < 0$ .*

■

The signs of  $a, c$  match the financial intuition behind the structure of no-transaction boundaries and thus provides support to our analytics. Note that it isn't always true that  $d < 0$  as this statement holds only for a particular set of parameters. We will illustrate numerically the dependence of no-transaction boundaries on transaction cost at different stages of dynamic problem for some choice of parameters in Figure 3.7.

This was a short introduction to discrete probability approximations which are really moment and cross-moment based approximations for risky growth. But what are the best moments to match? Are these the moments of risky growths or moments for some function of risky growth? The nature of the value function provides the key to answer these. Most often if the risky growth appears linearly in the value function the best way is to choose moment based approximation for the risky growth itself. The thesis will discuss in detail the methodology and provide some applications.

### 3.8.3 Overview of basic discrete probability approximation construction procedure

Creating discrete probability-based approximations for probability models is well known in the context of option pricing. Cox, Ross and Rubinstein (CRR) [21] pioneered the lattice approach. They developed a discrete time binomial approach to price options. Boyle [15] took the CRR methodology a step further and proposed a trinomial option pricing model. In [44] the discrete probability-approximated values are shown to converge to the true option values as number of time step divisions goes to infinity. Creating multinomial discrete probability approximation with positive probabilities for an arbitrary correlation structure is a hot topic of research. Reference [45] provides a fairly generalized methodology to model  $k$  sources of uncertainty in the form of a *numerical* discrete probability approximation.

The most basic discrete probability approximation construction procedure revolves around the idea of moment matching. The thesis however, aims to construct fairly general discrete probability approximation which could use any possible statistical feature as in Chapter 5. It is very similar to how we construct lattices to price options.

Let  $\Upsilon$  represent a discrete probability approximation<sup>15</sup> for a probability space in  $\aleph$  dimensions. Then for any  $\oplus \in \Upsilon$  we have  $\oplus = (\oplus_1, \oplus_2)$  where  $|\oplus_1| = \aleph$  and  $\oplus_2 \in [0, 1]$ . Especially, a pair in a discrete probability approximation is a joint evolution of risky growth vector coupled together with a probability where the individual probabilities sum to one.

#### Tree in 1-D

If  $\aleph = 1$  the possible example of  $\Upsilon$  are  $((u, p), (d, 1 - p)), ((u, p), (m, q), (l, 1 - p - q))$  etc: many distinct discrete probability approximation are possible in one dimension.

The discrete probability approximation is constructed so that moments are matched. Consider  $((u, p), (m, q), (l, 1 - p - q))$  for example. This group has five unknowns and so we will need typically five equations to specify these unknowns<sup>16</sup>. In general, for a  $\Upsilon$  with  $g$  unknowns (probability of branches and stochastic evolution of random variable ) requires  $g$  equations and hence the first  $g$  moments must be matched.

<sup>15</sup>The thesis is interested in discrete probability approximation for risky growth vector over an interval  $\Delta T$ .

<sup>16</sup>Generally for  $z$  unknowns we require  $z$  non-linear equations to have a finite dimensional solution set which is not necessarily unique but the solutions are often permuted versions of each other.

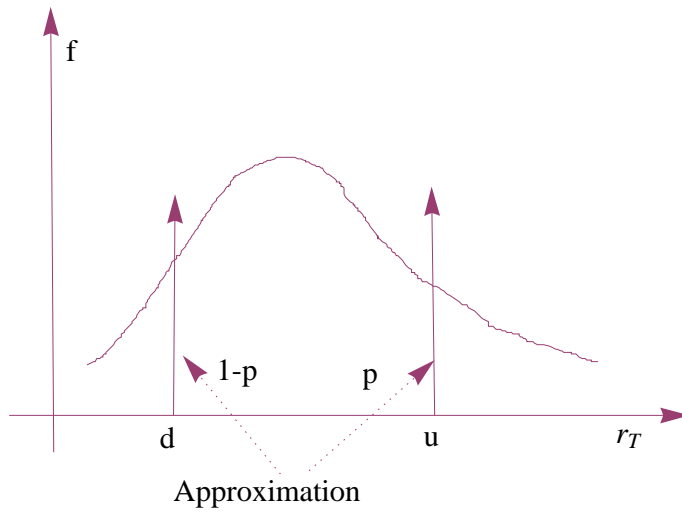


Figure 3.9: A discrete probability approximation approximation in 1-D. Here  $r_T$  say risky growth over an interval is variable being approximated.

Figure 3.9 shows a continuous probability model of risky growth approximated by a discrete probability approximation. The discrete probability approximation is  $((u, p), (d, 1 - p))$ . As such three parameters must be found. These could be found by matching the first three moments as below:

$$up + d(1 - p) = E(r_T) \quad (3.58)$$

$$u^2p + d^2(1 - p) = E(r_T^2) \quad (3.59)$$

$$u^3p + d^3(1 - p) = E(r_T^3) \quad (3.60)$$

### Tree in 2-D

If  $\aleph = 2$  a possible example of  $\Upsilon$  is  $((u_1, u_2), p), ((u_1, d_2), q), ((d_1, u_2), r), ((d_1, d_2), 1 - p - q - r)$ . Note that the  $\Upsilon$  is a discrete probability approximation for joint evolution of risky growths and it implies discrete probability approximation of one dimension lower for the respective risky growths. The idea is illustrated in Figure 3.10 where a parent discrete probability approximation branches off into two sub-trees. The discrete probability approximation for risky growth of asset one would be  $((u_1, p + q), (d_1, 1 - p - q))$ . The discrete probability approximation for risky growth of asset two would be  $((u_2, p + r), (d_2, 1 - p - r))$ .

The discrete probability approximation  $\Upsilon$  has seven unknowns in the above example. To fill in the values we will need seven equations. It is simple to get seven equations by matching first 3 moments of discrete probability approximation of lower dimension and then using  $\Upsilon$  to match the cross-moment. Figure 3.10 illustrates the ideas discussed.



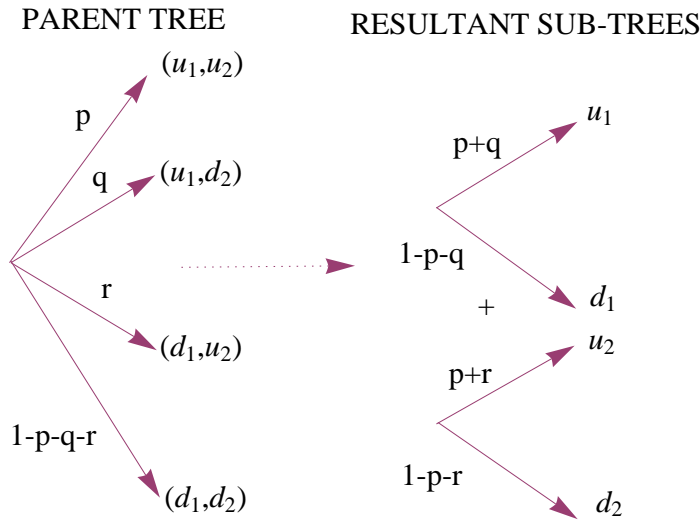


Figure 3.10: Illustrating discrete probability approximation construction in 2-D for correlated variables.

### Tree in 3-D

If  $\aleph = 3$  it is obvious that discrete probability approximation at the highest level has eight branches for up/down branching for a lowest level discrete probability approximation, implying three trees with four branches at a lower level. This further implies three trees with two branches at the lowest level. If our original tree had say thirteen unknowns then we need thirteen equations. Since  $13=9+3+1$  we could get all the equation by matching first three moments for the three trees at the lowest level, cross moments for three trees at a higher level and cross moment for one discrete probability approximation at the highest level. Figure 3.11 illustrates the ideas discussed with a parent tree implying sub-trees. There are many possible ways to construct trees in 3-D if lower level trees are allowed to have more arbitrary number of states. For instance, instead of just up/down we might have up/middle/down. If the dynamics of the asset prices are dependent on state variables we could easily accommodate this by having trees dependent on state variables.

### General framework for a discrete probability approximation in $\aleph$ -D

#### Binomial lowest level discrete probability approximation

The most general form for  $\Upsilon$  at the highest level would have  $2^\aleph$  branches if only up/down movements are allowed for lowest level discrete probability approximation. With  $\binom{\aleph}{2}$  discrete probability approximation at a lower level with four branches to match cross moments. At the lowest level we have  $\aleph$  discrete probability approximations with just 2 branches.

To fill out  $\Upsilon$  we need  $2^\aleph - 1 + 2\aleph$  equations which could be obtained by matching moments from trees at different levels. This is because  $2^\aleph - 1$  parameters for probabilities and  $2\aleph$  for states.

Also for  $\aleph$  dimensions we have  $\aleph$  first moments,  $\aleph + \frac{\aleph(\aleph-1)}{2} = \frac{\aleph(1+\aleph)}{2}$  second moments and

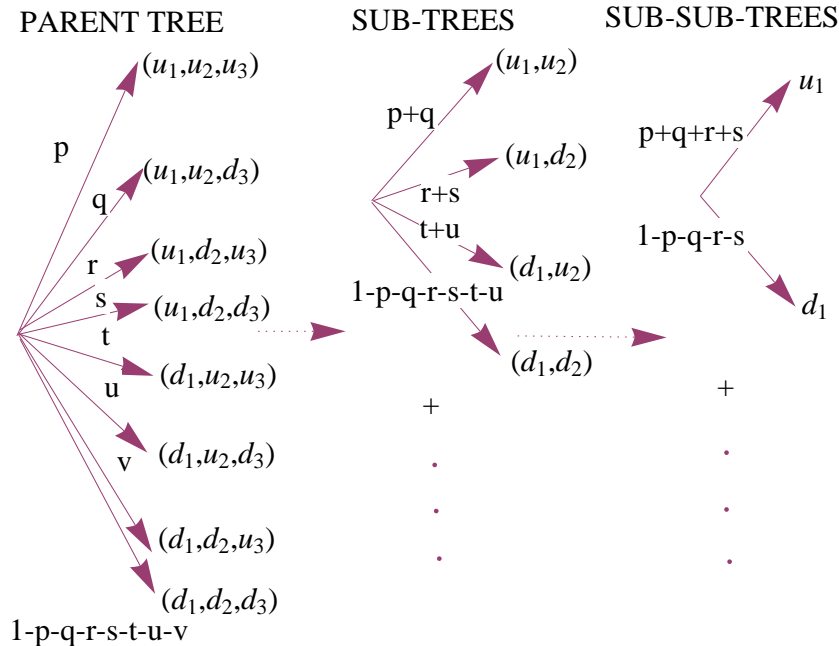


Figure 3.11: Illustrating discrete probability approximation construction in 3-D for correlated variables.

$\aleph + \aleph(\aleph - 1) = \aleph^2$  third moments. As  $\aleph$  increases at first three moments are exactly enough, then more than enough, but eventually not nearly enough to capture all the probability outcomes. If we are aiming for five or fewer dimensions then three moments are enough.

If more than up/down movements are allowed for lowest level trees we will have many more equations!

**Trinomial lowest level trees**

This analysis follows a discussion similar to that given for the binomial case. To fill out  $\Upsilon$  we need  $3^\aleph - 1 + 3\aleph$  equations which could be obtained by matching moments from trees at different levels. This is because  $3^\aleph - 1$  parameters for probabilities and  $3\aleph$  for states.

The above discussion provided a general framework. Note it is possible to create trees with nice structure at a cost of low moment matching. We could do this by *pre-filling* the probabilities. Lets give an example using a correlated set of standard normal random variables  $Z_i$  in 3-D. Suppose the standard normals could either take a value of -1 or +1. Also lets denote  $\rho_{ij}$  as the correlation between a pair of standard normals  $i$  and  $j$ . A very simple discrete probability approximation structure is given in Table 3.2.

As we see there is a lot of innovation in which we could match cross moments. Are we just interested in matching the entries of a covariance matrix? or are interesting in matching some creative cross-moments? All just depends upon the degree of accuracy we seek to achieve. For some problems, for instance, second order moment matching might suffice. Consider a single period Markovitz objective. It explicitly contains just the mean and variance, so any discrepancies in the higher moments is not relevant. In a more formal notation consider two risky assets who have the same expected return over a period that is:

Outcome	Probability
<b>uuu</b>	$\frac{1+\rho_{12}+\rho_{23}+\rho_{31}}{8}$
<b>uud</b>	$\frac{1+\rho_{12}-\rho_{23}-\rho_{31}}{8}$
<b>udu</b>	$\frac{1-\rho_{12}-\rho_{23}+\rho_{31}}{8}$
<b>udd</b>	$\frac{1-\rho_{12}+\rho_{23}-\rho_{31}}{8}$
<b>duu</b>	$\frac{1-\rho_{12}+\rho_{23}-\rho_{31}}{8}$
<b>dud</b>	$\frac{1-\rho_{12}-\rho_{23}+\rho_{31}}{8}$
<b>ddu</b>	$\frac{1+\rho_{12}-\rho_{23}-\rho_{31}}{8}$
<b>ddd</b>	$\frac{1+\rho_{12}+\rho_{23}+\rho_{31}}{8}$

Table 3.2: A nice discrete probability approximation structure with correlated standard normals in 3-D

$$E[r_{1,T}] = R, E[r_{2,T}] = R \quad (3.61)$$

The investor allocates a fraction  $\alpha$  so as to minimize the variability in total returns that is:

$$\min_{\alpha} \text{Var}[r_T] = \min_{\alpha} \text{Var}[\alpha r_{1,T} + (1 - \alpha)r_{2,T}] \quad (3.62)$$

$$\begin{aligned} &= \min_{\alpha} (\alpha^2(E[r_{1,T}^2] - E[r_{1,T}]^2) + (1 - \alpha)^2(E[r_{2,T}^2] - E[r_{2,T}]^2) \\ &\quad + 2\alpha(1 - \alpha)(E[r_{1,T}r_{2,T}] - E[r_{1,T}]E[r_{2,T}])) \end{aligned} \quad (3.63)$$

The above example could be generalized to an  $N$  dimensional single *Markowitz* portfolio problem and it can easily be seen that it is distribution independent and all what we require is that moments/cross moments up to order two must be matched. As we see for most practical purposes trees do provide a reasonable approximation.

If we let the time step division  $\Delta T \rightarrow 0$  we approach a continuous time behavior under a suitable moment matching scheme. For *well-behaved* utility functions we could approach the continuous time solution implied by using exact distributions. We will use a binomial discrete probability approximation with moment matching of order two to illustrate such a behavior in Figure 3.12 and 3.13. The transaction cost structure is the standard Davis and Norman model (see [28]). We use CRRA and log-utilities. Convergence behavior is illustrated in Figures 3.12 and 3.13 for a suitable choice of parameters and utility functions.

### 3.9 On the philosophy of probability deformation continuation

In this thesis, moment based discrete probability approximation approximations are only used for getting numerical results. Our goal is to construct efficient lattice methods that don't rely on  $\Delta T$  to be small for appropriate convergence to occur. Our aim is to be able to solve exact models for an arbitrary  $\Delta T$ . This is the goal of *probability deformation schemes*.

The central philosophy revolves around creating an  $\ell$  point formula that expresses the statistical feature of risky growth over an interval  $\Delta T$ . This expression is not unique: there might

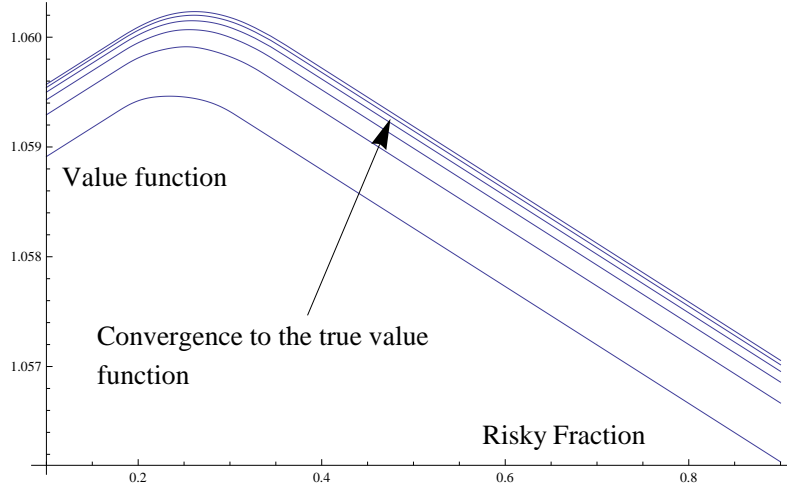


Figure 3.12: Convergence in value for CRRA utility for a discrete probability approximation varying  $N = 5, 10, \dots, 30$  and parameters:  $T = 1, \omega = 0.1, s = e^{\omega\Delta T}, m = 0.24, \sigma = 1, \lambda = \mu = 0.01, V = 0.5$ . Where  $T$  is the time horizon for investment,  $N$  is the number of re-balancing nodes.  $\omega$  is the continuous time risk-free rate,  $(\lambda, \mu)$  are transaction cost factors,  $s$  is the risk free growth over the interval,  $m$  is the drift for continuous time GBM and  $\sigma$  is the volatility for the continuous time GBM. The continuous time GBM implies a risky growth for the risky asset over the interval  $\Delta T$ .

be any number of such approximations. Let  $\mathcal{Q}$  represent a multi-period portfolio problem with  $\mathcal{J}_k$  being the value function and  $\zeta_k$  being the control law under the exact probability density function  $p$  over an interval  $\Delta T$ . Suppose we have  $p_\ell$  as an  $\ell$ -point approximation for  $p$  such that  $p_\ell \mapsto p$  in some probabilistic sense<sup>17</sup>. In Chapter 5 we present evidence that weak convergence (convergence in distribution) might be enough. Then without proving we speculate  $\mathcal{J}_k^\ell \mapsto \mathcal{J}_k$  and  $\zeta_k^\ell \mapsto \zeta_k$  as  $\ell \mapsto \infty$ . Our speculation is supported by some numerical experiments we provide in Chapter 5. It is numerically very convenient to express the continuation behavior of the value function (or control law) in terms of the deformation parameter  $\gamma_\ell = 1/\ell$  to get the desired solution with respect to the original problem. A deformation parameter of  $\gamma_\ell = 1/\ell$  would mean  $\ell$  point discrete probability approximation for a corresponding continuous time probability model. We will later show that the *power law* and *polynomials* provide a good *basis set* to express the continuation behavior.

In the thesis three schemes are highlighted namely:

**1- Simple interval division (SID):** This will involve dividing the domain of the random variable in to  $\ell$  equidistant chunks to form  $\ell$  intervals and finding the mid-point of the variable in the interval.

**2- Simple quantile interval division (SQID):** This will involve dividing the domain of random variable by using  $\ell$  quantiles using the quantile function and finding the mean of variable in the interval. A probability of  $\frac{1}{\ell}$  is assigned to each mean to get a discrete probability approximation.

**3- Moment division (MD):**

<sup>17</sup>i.e. Convergence in probability, almost sure or in distribution.

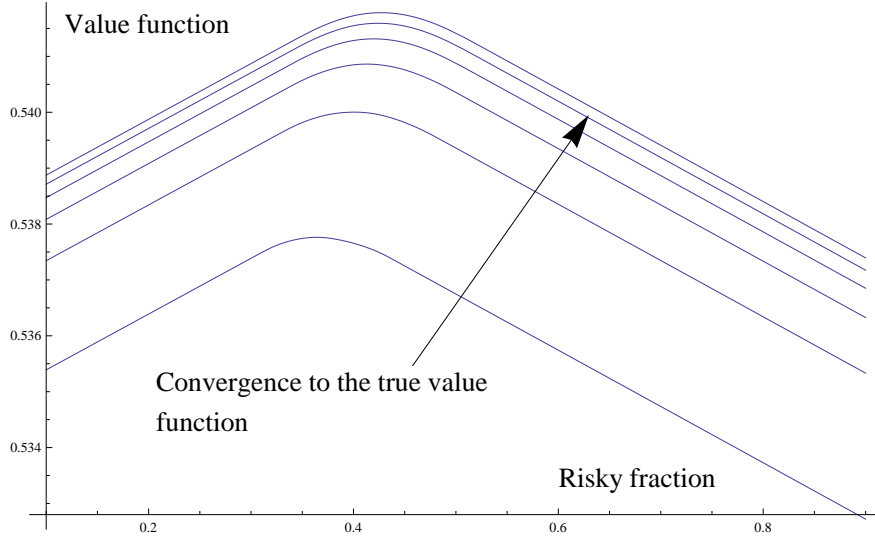


Figure 3.13: Convergence in value for log-utility for a discrete probability approximation approximation varying  $N = 5, 10, \dots, 30$  and parameters:  $T = 1, \omega = 0.1, s = e^{\omega\Delta T}, m = 0.14, \sigma = 0.3, \lambda = \mu = 0.01$ . Where  $T$  is the time horizon for investment,  $N$  is the number of re-balancing nodes.  $\omega$  is the continuous time risk-free rate,  $(\lambda, \mu)$  are transaction cost factors,  $s$  is the risk free growth over the interval,  $m$  is the drift for continuous time GBM and  $\sigma$  is the volatility for the continuous time GBM. The continuous time GBM implies a risky growth for the risky asset over the interval  $\Delta T$ .

I-Using an approximate moment matching algorithm using *Gaussian quadrature* as in [65] so that if  $\ell$  the number of points for *Gaussian quadrature* the accuracy of the distribution matching increases.

II- Or instead of *Gaussian quadrature* we could match moments using standard discrete probability approximation construction as in Section 3.7.3.

The above approach could have many possible variations. For example, in SID or SQID we could chose to take the median instead of the mean.

The fact that the approximation probability distribution converges to the exact probability distribution of the model along the continuation path means the problem constraints also converge in some probabilistic sense.

Let us illustrate the methodology by considering the same problem set-up as in Section 2. We have a dynamic investor trying to minimize the variability of his wealth about a target level  $b^*$ . We replace the standard **GBM** for risky assets by a *jump diffusion process*.

$$\frac{dS_t^{(i)}}{S_t^{(i)}} = m^{(i)} dt + \sigma^{(i)} dZ_t + dq_t \quad (3.64)$$

in which the Poisson process  $dq_t$ , is characterized by jump intensity  $C$  as well as jump size  $Y$  which is assumed independently log-normally distributed i.e.  $\text{Log}(Y) \sim N(\theta, \delta^2)$ .

The logarithm of the risky growth over an interval  $\Delta T$  follows:

$$\log\left(\frac{S_{t+\Delta T}^{(i)}}{S_t^{(i)}}\right) = (\alpha^{(i)} - \frac{(\sigma^{(i)})^2}{2})\Delta T + \sigma^{(i)}\sqrt{\Delta T}Z_t + \sum_{t=1}^{n_t} \log(Y_t) \quad (3.65)$$

where  $n_t$  is the number of jumps in the interval  $\Delta T$ .

Further, let  $f(x)$  denote the density of  $\log\left(\frac{S_{t+\Delta T}^{(i)}}{S_t^{(i)}}\right)$

$$f(x) = \sum_{n=0}^{\infty} \frac{e^{-C\Delta T}(\Delta T)^n}{n!} N\left(x; (\alpha^{(i)} - \frac{(\sigma^{(i)})^2}{2})\Delta T + n\theta, (\sigma^{(i)})^2\Delta T + n(\delta)^2\right) \quad (3.66)$$

We now have an analytic representation for the distribution of  $\log(1+g)$  which does not rely on  $\Delta T$  being small<sup>18</sup>. The desired  $(1+g)$  is obviously a monotonic transformation (apart from the fact the *quantiles* get monotonically transformed) and we could easily work numerically with our deformation schemes as mentioned.

See Figure 3.14. Letting  $\gamma_\ell \rightarrow 0$  we see convergence behavior in the efficient frontier at terminal time using SQID scheme. This quite essentially is the essence of the deformation philosophy in action<sup>19</sup>.

Without going into modeling details we will illustrate some graphs of the SQID scheme in action in Figure 3.14-3.18. In all these graphs convergence was seen to the solution implied by exact probability. Different utility functions were used.

From a dynamic programming perspective we will want to construct an approximation such that as  $X_n \mapsto X$  then  $E[f(X_n)] \mapsto E[f(X)]$ . Fortunately when weak convergence occurs we have the following result:

**Theorem 3.9.1** *Let  $(X_n : 1 \leq n \leq \infty)$  be a sequence of finite real-valued random variables. Then the following are equivalent:*

- i)  $X_n \xrightarrow{D} X$
- ii) For each bounded and continuous  $f : \mathfrak{X} \mapsto \mathfrak{R}$  we have  $E[f(X_n)] \mapsto E[f(X)]$

The *Continuous mapping* theorem also provides some important convergence results:

**Theorem 3.9.2** *Let  $(X_n : 1 \leq n \leq \infty)$  be a sequence of finite real-valued random variables with  $f : \mathfrak{X} \mapsto \mathfrak{R}$  a continuous function. Then the following are equivalent:*

- i) If  $X_n \xrightarrow{a.s} X$  then we have  $f(X_n) \xrightarrow{a.s} f(X)$
- ii) If  $X_n \xrightarrow{p} X$  then we have  $f(X_n) \xrightarrow{p} f(X)$
- iii) If  $X_n \xrightarrow{D} X$  then we have  $f(X_n) \xrightarrow{D} f(X)$

It will be obvious that for algorithms to work from a dynamic programming perspective all we require is *weak convergence*. Under a moment matching scheme for instance increasing the order of matching is making the moment generating functions converge and hence the distribution functions are also converge. Regarding SQID it is intuitively quite reasonable because as quantiles being the basis for bring distributions closer also means that the distribution functions are also getting closer<sup>20</sup>.

<sup>18</sup>We have an analytic solution for the SDE

<sup>19</sup>Especially going to the true model by successively probability approximation for the true probability model.

<sup>20</sup>We follow an experimental methodology in the thesis where we assume that underlying laws could be experimentally discovered.

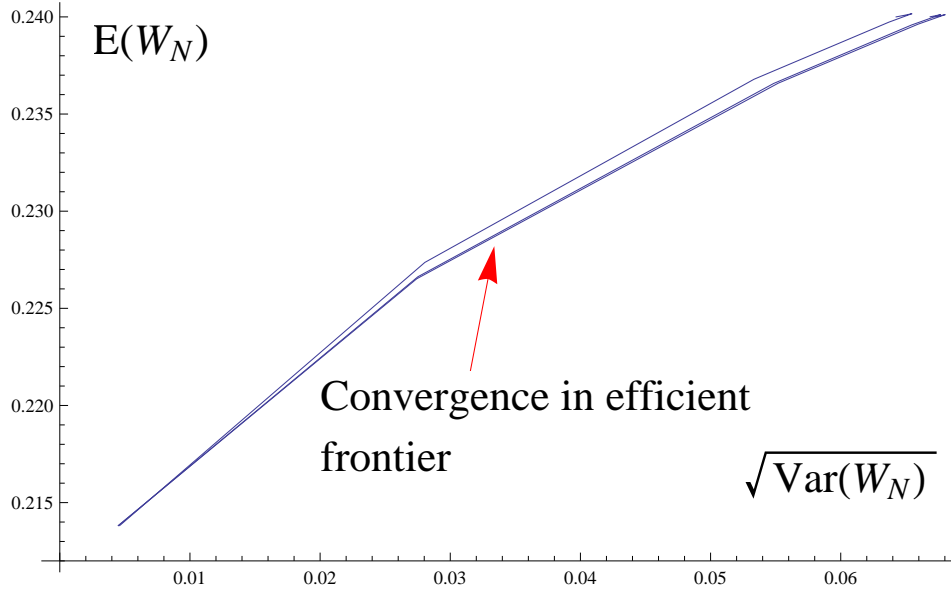


Figure 3.14: Deformation solution by varying  $\gamma_\ell = \frac{1}{5}, \frac{1}{10}, \frac{1}{15}, \frac{1}{20}$  for efficient frontier for a jump diffusion problem with parameters  $T = 1, N = 4, \omega = 0.07, s = e^{\omega\Delta T}, m = 0.14, \sigma = 0.3, \theta = 0.1, \delta = 0.05$ . Where  $T$  is the time horizon for investment,  $N$  is the number of re-balancing nodes.  $\omega$  is the continuous time risk-free rate,  $(\lambda, \mu)$  are transaction cost factors,  $s$  is the risk free growth over the interval,  $m$  is the drift for continuous time GBM and  $\sigma$  is the volatility for the continuous time GBM. The continuous time GBM implies a risky growth for the risky asset over the interval  $\Delta T$ .  $\gamma_\ell$  is the deformation parameter.

We provide some graphs to illustrate the resulting convergent behavior. Figure 3.13 shows convergence using SQID scheme to true value function for the problem considered in Section 3.5. Similarly, Figure 3.14-3.18 illustrate the convergence behavior for different SDE for risky growth and utility functions for the problem. We used geometric Brownian motion and jump diffusion model for risky growth. For utility functions we chose log utility and CRRA utility.

In Chapter 9 we will use deformation schemes to approximately meet portfolio constraints.

### 3.10 Towards robust and efficient lattice algorithms

Deformation schemes help us solve portfolio problems over a larger interval  $\Delta T$ .

Suppose we wish to obtain a continuous time solution from an approximate solution obtained with  $\Delta T$ . Now we can choose  $\Delta T$  to be arbitrary and large enough then solve the problem with  $M_1$  time steps. This will help us avoid interpolation errors and reduce computational time. Then we compute the solution again with  $M_2$  time steps where  $M_2 > M_1$ . We will continue to do so obtaining a list of pairs involving the solution and time steps. Following a suitable basis set we can express the continuation behavior and find the limiting behavior when we approach a continuous time behavior. By continuation behavior we mean projecting our discrete solution sets to the required solution. This is discussed in detail in Chapter 5.

In general for an efficient algorithm it is important to be able to utilize the *continuation* of

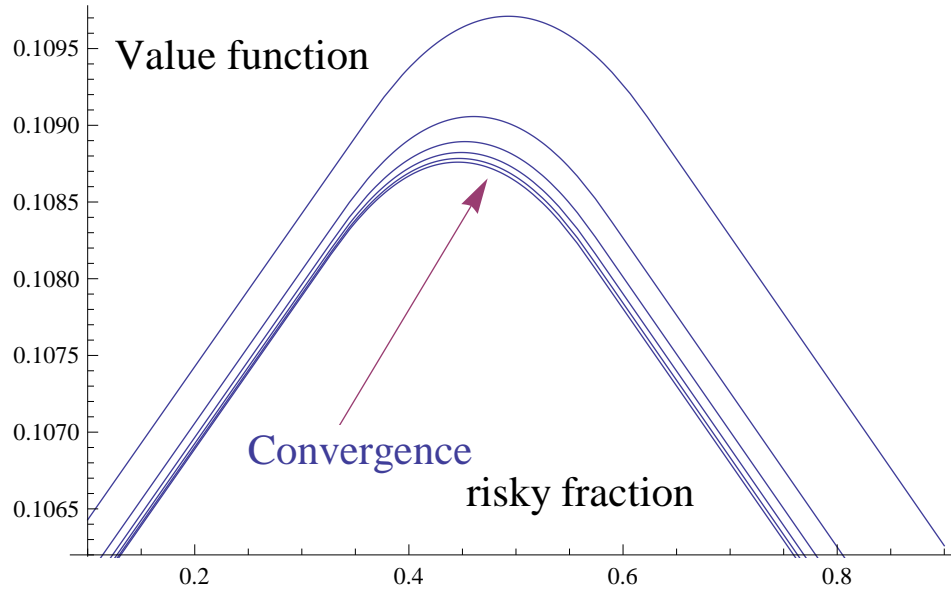


Figure 3.15: Deformation solution of value function with log-utility at  $t = 0$  by varying  $\gamma_\ell = \frac{1}{5}, \dots, \frac{1}{30}$  and parameters  $T = 1, N = 4, \omega = 0.1, \lambda = \mu = 0.01, s = e^{\omega\Delta T}, m = 0.14, \sigma = 0.3$ . Where  $T$  is the time horizon for investment,  $N$  is the number of re-balancing nodes.  $\omega$  is the continuous time risk-free rate,  $(\lambda, \mu)$  are transaction cost factors,  $s$  is the risk free growth over the interval,  $m$  is the drift for continuous time GBM and  $\sigma$  is the volatility for the continuous time GBM. The continuous time GBM implies a risky growth for the risky asset over the interval  $\Delta T$ .  $\gamma_\ell$  is the deformation parameter.

the value function ( or optimal control law ) with respect to the problem parameters:

- A**-Discretization of time space
- B**-Discretization of state space
- C**-Discretization of probability model

The deformation schemes discussed earlier deal with discretization of probability model for risky growth. However, time space and state space introduce interesting continuation behavior the value of which should be exploited in an efficient algorithm to determine a continuous time solution. Probability deformation schemes help us solve over an arbitrary  $\Delta T$ , easing the pain of interpolation errors. This was the outermost loop in gaining *numerical* efficiency. In the inner loop we would seek continuation in time space. And in the innermost loop we would seek continuation in state space to determine the value function (or optimal control law ). As a result we now have three nested loops !

The above ideas are summarized in algorithmic form below:

---

```

For  $i = 1, 2, \dots, N$ 
  For  $j = 1, 2, \dots, M$ 
    For  $k = 1, 2, \dots, L$ 
       $P = \{(\frac{1}{i}, \frac{1}{j}, \frac{1}{k}), \psi(\gamma_i, t_j, S_k)\}$ 
      Insert  $P$  in a list  $\mathcal{L}$ .

```



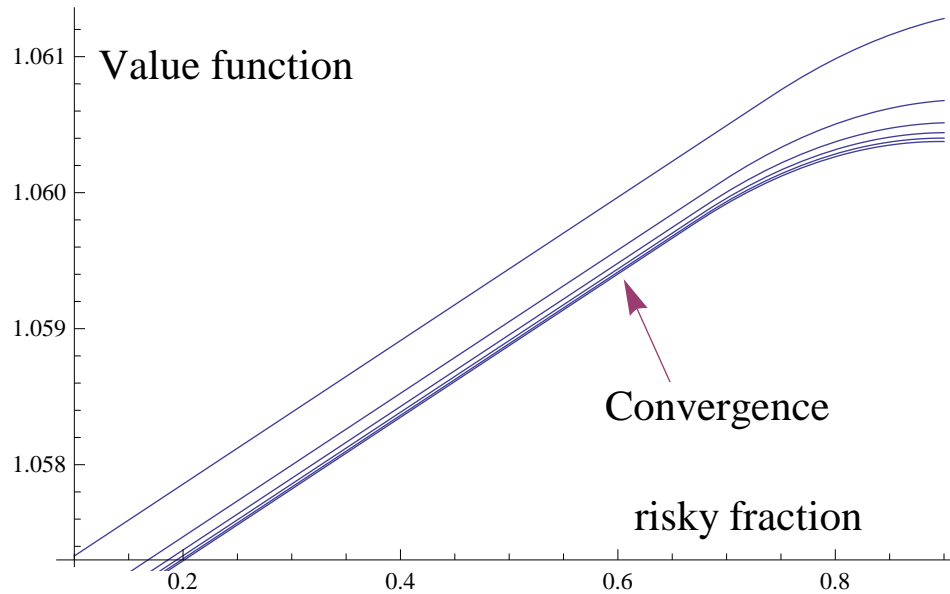


Figure 3.16: Deformation solution of value function with CRRA utility at  $t = 0$  by varying  $\gamma_\ell = \frac{1}{5}, \dots, \frac{1}{30}$  and parameters  $T = 1, N = 4, \omega = 0.1, \lambda = \mu = 0.01, s = e^{\omega\Delta T}, m = 0.14, \sigma = 0.3, V = 0.5$ . Where  $T$  is the time horizon for investment,  $N$  is the number of re-balancing nodes.  $\omega$  is the continuous time risk-free rate,  $(\lambda, \mu)$  are transaction cost factors,  $s$  is the risk free growth over the interval,  $m$  is the drift for continuous time GBM and  $\sigma$  is the volatility for the continuous time GBM. The continuous time GBM implies a risky growth for the risky asset over the interval  $\Delta T$ .  $\gamma_\ell$  is the deformation parameter.

Next k  
Next j  
Next i  
Interpolate the list  $\mathcal{L}$  and find  $\mathcal{L}(0, 0, 0)$

In the above algorithm  $\psi$  denotes the value function. Also we have  $i$ -th point discrete probability approximation,  $j$ -th point discrete time space approximation and  $k$ -th point state space approximation. So as when  $(\frac{1}{i}, \frac{1}{j}, \frac{1}{k}) \rightarrow (0, 0, 0)$  we have the required solution under an exact probability model and continuous-time domain. In simple words, we would make the discrete probability approximation, the time space division and state space division finer to see the corresponding continuous time solution.

In the thesis the state variables will typically be discretized using grids and the value function numerically represented using polynomial basis via the grids. This definitely is the curse of dimensionality as far as state space is concerned because numerical representation of value function is  $O(N^s)$  where  $s$  is the number of state variables<sup>21</sup>. Note the curse of dimensionality can never be *removed*. It can only be *tamed* by introducing an interesting set of new numerical issues to attain the desired accuracy which we must then deal with.

<sup>21</sup>Radial basis functions could make this process  $O(N)$  !

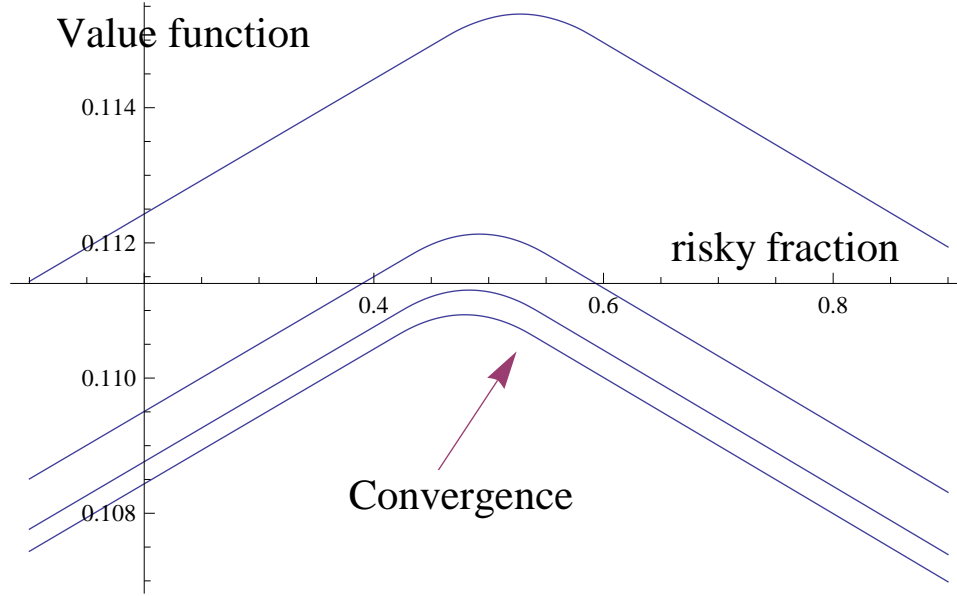


Figure 3.17: Deformation solution of value function with log-utility and jump diffusion model at  $t = 0$  by varying  $\gamma_\ell = \frac{1}{5}, \dots, \frac{1}{20}$  and parameters:  $T = 1, N = 4, \omega = 0.1, \lambda = \mu = 0.01, s = e^{\omega\Delta T}, m = 0.14, \sigma = 0.6, \theta = 0.1, \delta = 0.05$ . Where  $T$  is the time horizon for investment,  $N$  is the number of re-balancing nodes.  $\omega$  is the continuous time risk-free rate,  $(\lambda, \mu)$  are transaction cost factors,  $s$  is the risk free growth over the interval,  $m$  is the drift for continuous time GBM and  $\sigma$  is the volatility for the continuous time GBM. The continuous time GBM implies a risky growth for the risky asset over the interval  $\Delta T$ .  $\gamma_\ell$  is the deformation parameter.

It is also very important to frame a problem in the right state variables to allow decomposability for the value function of the *dynamic problems*. For example, consider the same problem set-up as in section 3.7 but with CARA or exponential utility.

Let  $X_{k+1}^-$  denote the wealth in the risky asset immediately before re-balancing and  $Y_{k+1}^-$  the wealth in the risk-free asset. We assume the investor is allowed to both borrow and lend risk-free asset. Under singular controls the state evolution equations could be described by:

$$X_{k+1}^- = (X_k^- + \Delta_k^1 - \Delta_k^2)\alpha_k \quad (3.67)$$

$$Y_{k+1}^- = (W_k^- - X_k^- - (1 + \lambda_k)\Delta_k^1 + (1 - \mu_k)\Delta_k^2)s_k \quad (3.68)$$

$$W_{k+1}^- = s \circ W_k^- + F(X_k^-) \quad (3.69)$$

where the stochastic functional  $F(X_k^-)$  represents the investor behavior of buying, selling or choosing no to re-balance.

Define the value function as:

$$\mathcal{J}_k(W_k^-, X_k^-) = \max_{\mathcal{S}} E^P(-e^{-zW_N} | \mathcal{F}_k) \quad (3.70)$$

Consider the last stage of the problem:

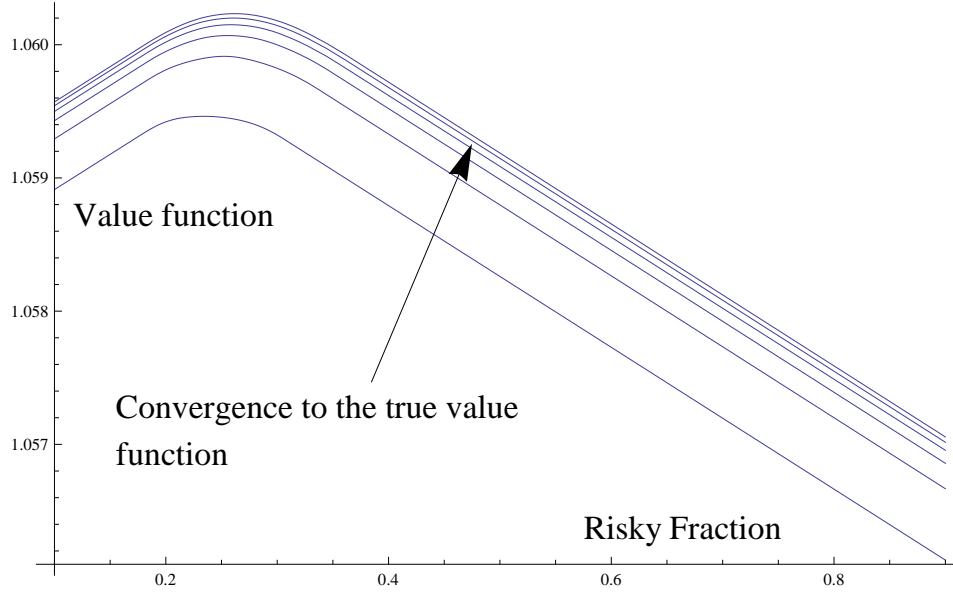


Figure 3.18: Deformation solution of value function with CRRA utility and jump diffusion model at  $t = 0$  by varying  $\gamma_\ell = \frac{1}{5}, \dots, \frac{1}{20}$  and parameters:  $T = 1, N = 4, \omega = 0.1, \lambda = \mu = 0.01, s = e^{\omega\Delta T}, m = 0.14, \sigma = 0.3, \theta = 0.1, \delta = 0.05, V = 0.5$ . Where  $T$  is the time horizon for investment,  $N$  is the number of re-balancing nodes.  $\omega$  is the continuous time risk-free rate,  $(\lambda, \mu)$  are transaction cost factors,  $s$  is the risk free growth over the interval,  $m$  is the drift for continuous time GBM and  $\sigma$  is the volatility for the continuous time GBM. The continuous time GBM implies a risky growth for the risky asset over the interval  $\Delta T$ .  $\gamma_\ell$  is the deformation parameter.

$$\mathcal{J}_{N-1}(W_{N-1}^-, X_{N-1}^-) = \max_s E^P(-e^{-z(sW_{N-1}^- + F(X_{N-1}^-))} | \mathcal{F}_k) \quad (3.71)$$

$$= e^{-zsW_{N-1}^-} \mathcal{J}^{(1)}(X_{N-1}^-) \quad (3.72)$$

We will show for CRRA utility in Chapter 6 that a similar decomposability with respect to the wealth occurs. In any case recursion  $k$  times would lead to the following:

$$\mathcal{J}_{N-k}(W_{N-k}^-, X_{N-k}^-) = e^{-zs^k W_{N-k}^-} \mathcal{J}^{(k)}(X_{N-k}^-) \quad (3.73)$$

Let us use the above example to summarize the numerical solution method in a few steps:

---

I- Find the relevant state variables. In the above they are  $(W_k^-, X_k^-)$ .

II- Sometimes we can simplify the problem in state space. In the above problem for instance the optimal control law depends only on  $X_k^-$  as amply illustrated by the structure of the problems.

III- Create a lattice / grid structure to carry out dynamic programming recursion using the state space selected in II. In the above problem, for instance, the relevant lattice contains only

$X_k^-$ . We set the lower and upper limits so that the no-transaction boundaries always lie inside them. It turns out that the *Merton* line for the time varying CARA problem (see [23]) is  $\frac{m-\omega}{2\sigma^2 e^{\omega(T-t)}}$  so if  $m \geq \omega$  for continuous time risk free rate  $\omega$  then we could chose the lower bound as being zero or less than zero. The upper bound would need to be set to a sufficiently high level with some experimentation to see for last stage whether no-transaction region lies inside the grid or not.

IV- Create an approximate discrete model for risky growth.

V- To avoid extrapolation errors the grid in the previous stage of dynamic program needs to be a factor lower than the next grid. Let  $(1+g)$  is the maximum factor by which the discrete probability approximation could grow for all the branches on the approximation. If  $L^{(k)}$  is the length of our grid at time  $k$  then  $L^{(0)} = \frac{L^{(N)}}{(1+g)^N}$ . This is because the relevant state variable  $X_k^-$  is directly tied to risky growths and at the upper boundary of the grid we are going to sell the risky asset rather than buy it.

VI- Starting from the last stage carry out recursion using the dynamic programming formalism. We find optimal controls and value functions for each stage going all the way to the initial time.

---

We provide an approximate solution in Figure 3.19 for CARA utility using a fairly coarse grid. We set the lower boundary to 5, the upper boundary to 2000 and state space division length to 10. The purpose of this coarse grid is to illustrate the numerical solution. It is seen that the center of risky fraction boundaries is decreasing as we move closer to the initial time. Indeed this should be the case, since, under the no-transaction cost the optimal amount of wealth to hold in risky asset in continuous time is  $\frac{m-\omega}{2\sigma^2 e^{\omega(T-t)}}$  where  $s$  is the continuous time risk free rate. In fact, for the parameters we chose in Figure 3.18 the no-transaction *Merton* amount of  $\approx 632$  lies in the center of no-transaction region at  $t = 0$ . This serves to show in many cases we can provide some intuitive validation for the numerical solution we have obtained via results in the academic literature.

The thesis will avoid the use of Monte-Carlo and PDE-based solution to dynamic portfolio problems. Monte-Carlo methods have been touted as being great in high dimensions. Stable numerical schemes to solve the non-linear PDEs associated with these set of problems are usually challenging to implement.

## 3.11 Analysis of continuous time dynamic trading strategies

### 3.11.1 Risk analysis of strategies

The thesis seeks to provide a framework under which we could do risk analysis of terminal wealth distribution for trading strategies under transaction costs. VaR, CVaR, skewness, kurtosis etc are some risk measures for the terminal wealth distribution. Suppose the investor has already determined the singular control for an investment objective and needed to analyze some characteristics of the terminal wealth distribution  $f(W_N)$ . Our lattice based framework provides simple and easily implementable framework for a robust analysis.

To summarize, the important solution steps are:

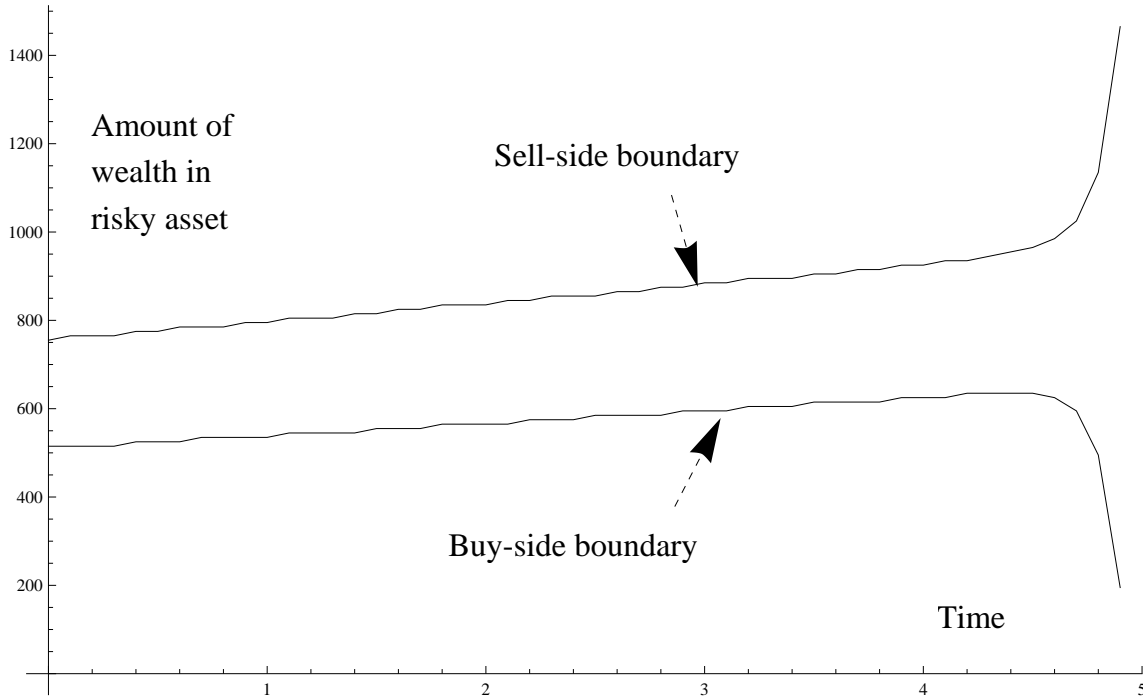


Figure 3.19: Finite time solution to the CARA utility problem:  $T = 5, N = 50, \omega = 0.05, s = e^\omega, m = 0.18, \sigma = 0.4, \lambda = \mu = 0.01, z = 0.01$  using a risky growth discrete probability approximation with 15 branches using a deformation parameter  $= \frac{1}{15}$ . Where  $T$  is the time horizon for investment,  $N$  is the number of re-balancing nodes.  $\omega$  is the continuous time risk-free rate,  $(\lambda, \mu)$  are transaction cost factors,  $s$  is the risk free growth over the interval,  $m$  is the drift for continuous time GBM and  $\sigma$  is the volatility for the continuous time GBM. The continuous time GBM implies a risky growth for the risky asset over the interval  $\Delta T$ .  $\gamma_\ell$  is the deformation parameter.

---

**A-Step 1:** Determine the optimal feed-back control law  $\vec{\zeta}$  by using the dynamic programming principle.

**B-Step 2:** Analyze the distribution of terminal wealth implied by  $\vec{\zeta}$  via the law of iterated expectations. This will be discussed in section 4.3.

---

The accuracy of the output can be easily verified using exact probability distributions. The criteria to judge upon could be closeness in value function or optimal control law. In Figures 3.20-3.23 the dynamic investor maximized a certain investment objective and got controls  $\vec{\zeta}$ . Via the law of iterated expectations the controls imply a probability distribution of terminal wealth  $W_N$ . We computed  $P(W_N < K) = \phi(K)$  via the law of iterated expectations since

$P(W_N < K) = E[1_{W_N < K}]$  to get the distribution function from which the probability distribution could be extracted via a simple numerical differentiation<sup>22</sup>.

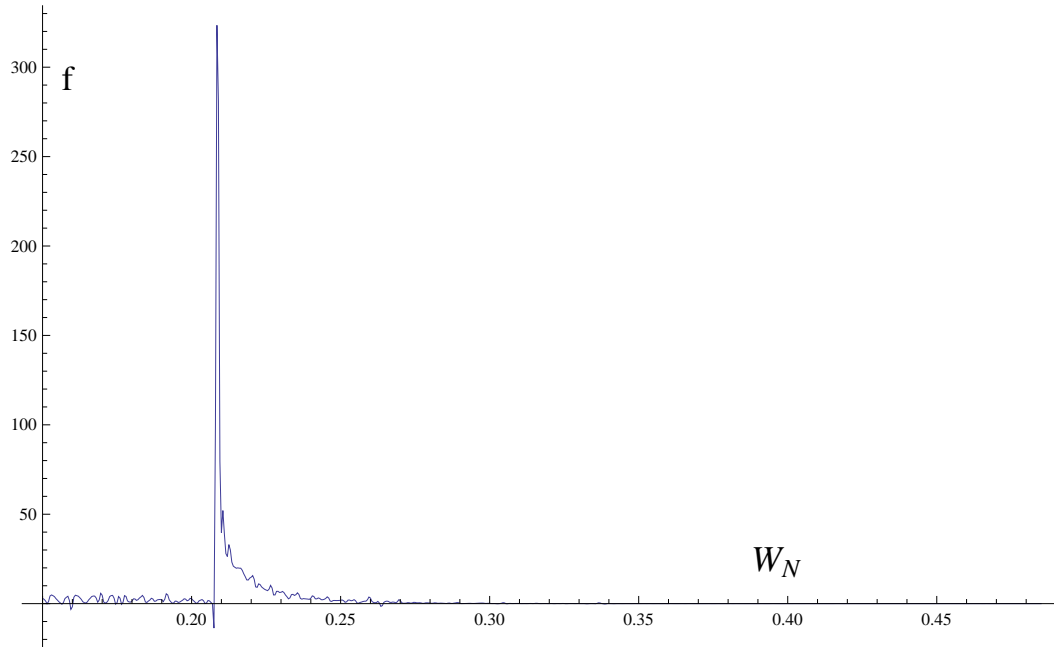


Figure 3.20: Terminal wealth distribution for an investor maximizing  $E[Pr(W_N > K)]$  with parameters:  $T = 0.5$ ,  $N = 5$ ,  $\omega = 0.05$ ,  $s = e^{\omega\Delta T}$ ,  $m = 0.12$ ,  $\sigma = 0.5$ ,  $\lambda = \mu = 0.001$ ,  $K = 0.208$ . Where  $T$  is the time horizon for investment,  $N$  is the number of re-balancing nodes.  $\omega$  is the continuous time risk-free rate,  $(\lambda, \mu)$  are transaction cost factors,  $s$  is the risk free growth over the interval,  $m$  is the drift for continuous time GBM and  $\sigma$  is the volatility for the continuous time GBM. The continuous time GBM implies a risky growth for the risky asset over the interval  $\Delta T$ .  $\gamma_\ell$  is the deformation parameter.

### 3.11.2 On the value of re-balancing

Re-balancing a portfolio has value because:

- 1- The portfolio is brought to the most optimal state vector for a particular investment objective.
- 2- In practice, although often not in theory, model parameter values get updated so that the optimal re-balancing state vector also changes.

However, re-balancing also introduces transaction costs and so there is a trade-off. This trade-off is solved by a heuristic such as by only re-balancing if we go far away from the most optimal no-transaction cost re-balancing state vector.

In this thesis, the dynamic investor will have  $N$  re-balancing points at which he could decide to re-balance or not. We assume the value of re-balancing could be encapsulated in the form of a value function so that tools of standard dynamic programming could be used for analysis.

<sup>22</sup>Smoothness algorithms might need to be applied to the output from numerical differentiation.

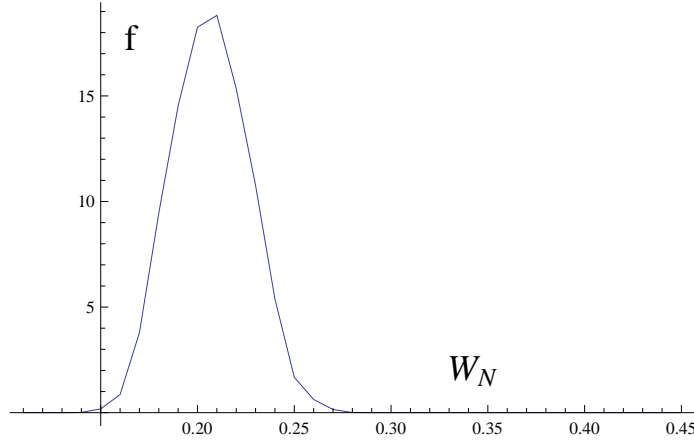


Figure 3.21: Terminal wealth distribution for an investor minimizing variability of wealth around a target level so that we minimize  $E[(W_N - b)^2]$  with parameters:  $T = 0.5, N = 5, \omega = 0.05, s = e^{\omega \Delta T}, m = 0.12, \sigma = 0.5, \lambda = \mu = 0.001, b = 0.4$ . Where  $T$  is the time horizon for investment,  $N$  is the number of re-balancing nodes. Here  $b$  is the target level,  $\omega$  is the continuous time risk-free rate,  $(\lambda, \mu)$  are transaction cost factors,  $s$  is the risk free growth over the interval,  $m$  is the drift for continuous time GBM and  $\sigma$  is the volatility for the continuous time GBM. The continuous time GBM implies a risky growth for the risky asset over the interval  $\Delta T$ .  $\gamma_\ell$  is the deformation parameter.

The value function takes a different form depending upon the investment objective. For the growth rate maximization problem it is:

$$\mathcal{J}(W_k^-, A_k^-) = \max E^P[\text{Log}(W_N) | \mathcal{F}_k] \quad (3.74)$$

The transaction cost in Figure 3.24 is proportional to the amount traded. The value function in this case becomes asymptotic because the investor has the option not to re-balance.

If the dynamic investor is stripped of his right not to re-balance the value function could become downward sloping. This could be seen in Figure 3.26.

In this chapter we provided a brief layout of our modeling framework and also discussed discrete probability approximation construction. In the next chapter we discuss the numerical implementation in Mathematica.

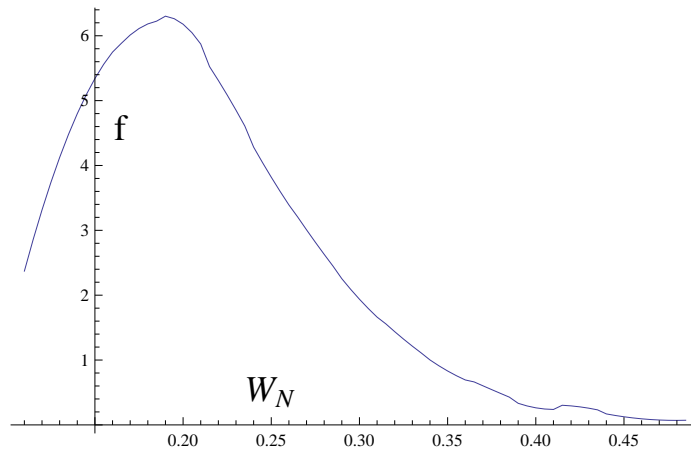


Figure 3.22: Terminal wealth distribution for an investor maximizing  $E[\frac{W_N^\gamma}{V}]$  with parameters:  $T = 0.5, N = 5, \omega = 0.05, s = e^{\omega\Delta T}, m = 0.12, \sigma = 0.5, \lambda = \mu = 0.001, V = 0.5$ . Where  $T$  is the time horizon for investment,  $N$  is the number of re-balancing nodes.  $\omega$  is the continuous time risk-free rate,  $(\lambda, \mu)$  are transaction cost factors,  $s$  is the risk free growth over the interval,  $m$  is the drift for continuous time GBM and  $\sigma$  is the volatility for the continuous time GBM. The continuous time GBM implies a risky growth for the risky asset over the interval  $\Delta T$ .  $\gamma_\ell$  is the deformation parameter.

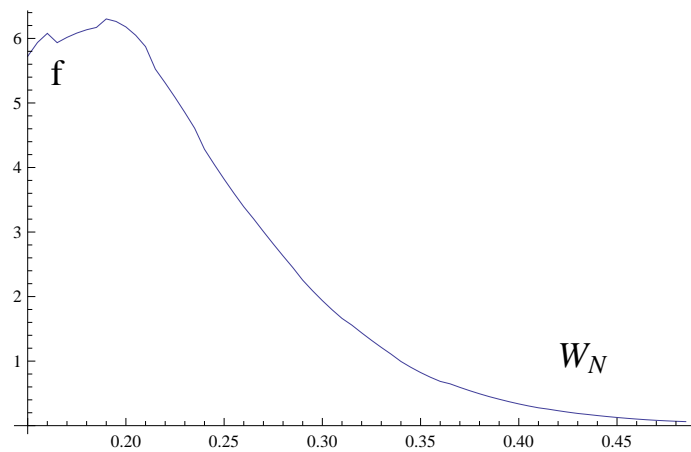


Figure 3.23: Terminal wealth distribution for an investor maximizing  $E[\frac{W_N^{\gamma_1}}{V_1} + \frac{W_N^{\gamma_2}}{V_2}]$  with parameters:  $T = 0.5, N = 5, \omega = 0.05, s = e^{\omega\Delta T}, m = 0.12, \sigma = 0.5, \lambda = \mu = 0.001, V_1 = \frac{1}{3}, V_2 = \frac{2}{3}$ . Where  $T$  is the time horizon for investment,  $N$  is the number of re-balancing nodes.  $\omega$  is the continuous time risk-free rate,  $(\lambda, \mu)$  are transaction cost factors,  $s$  is the risk free growth over the interval,  $m$  is the drift for continuous time GBM and  $\sigma$  is the volatility for the continuous time GBM. The continuous time GBM implies a risky growth for the risky asset over the interval  $\Delta T$ .  $\gamma_\ell$  is the deformation parameter.



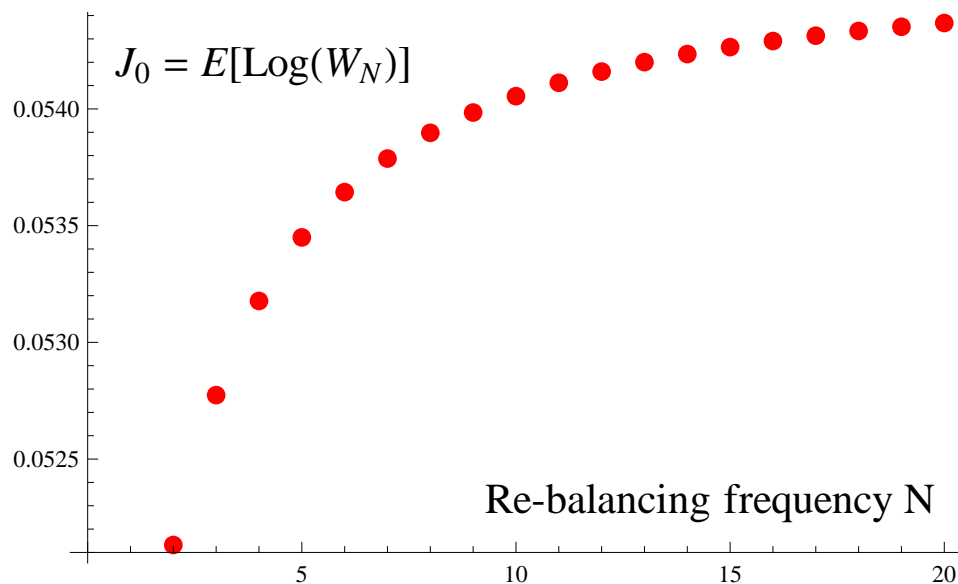


Figure 3.24: Variation of value function at time 0 with re-balancing frequency  $N$  for some choice of parameters:  $T = 1$ ,  $\omega = 0.05$ ,  $\lambda = \mu = 0.01$ ,  $s = e^{\omega\Delta T}$ ,  $m = 0.14$ ,  $\sigma = 0.7$ . Where  $T$  is the time horizon for investment,  $N$  is the number of re-balancing nodes.  $\omega$  is the continuous time risk-free rate,  $(\lambda, \mu)$  are transaction cost factors,  $s$  is the risk free growth over the interval,  $m$  is the drift for continuous time GBM and  $\sigma$  is the volatility for the continuous time GBM. The continuous time GBM implies a risky growth for the risky asset over the interval  $\Delta T$ .  $\gamma_\ell$  is the deformation parameter.

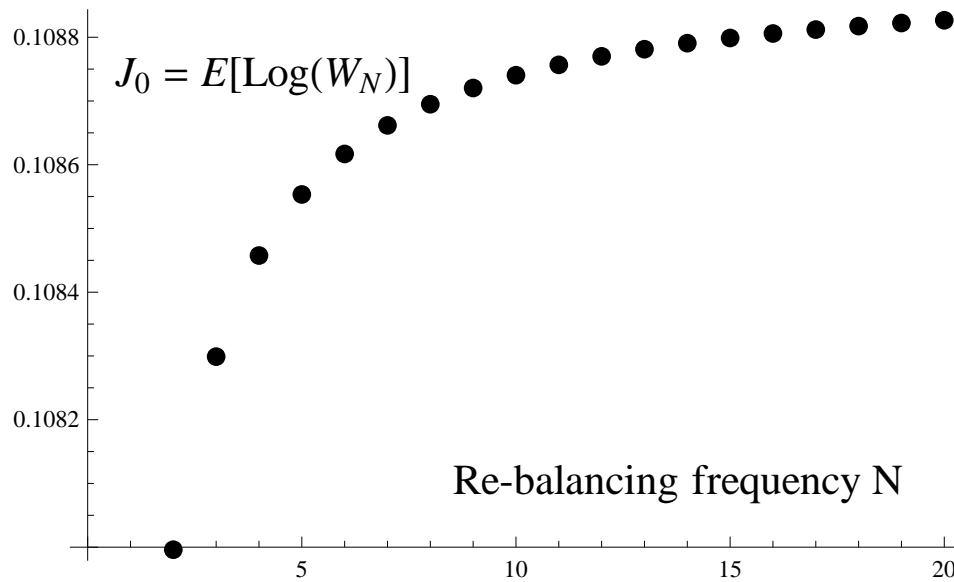


Figure 3.25: Variation of value function at time 0 with re-balancing frequency  $N$  with portfolio management fee for some choice of parameters:  $T = 1$ ,  $\omega = 0.07$ ,  $\lambda = \mu = 0.001$ ,  $s = e^{\omega\Delta T}$ ,  $m = 0.182$ ,  $\sigma = 0.4$ . Where  $T$  is the time horizon for investment,  $N$  is the number of re-balancing nodes.  $\omega$  is the continuous time risk-free rate,  $(\lambda, \mu)$  are transaction cost factors,  $s$  is the risk free growth over the interval,  $m$  is the drift for continuous time GBM and  $\sigma$  is the volatility for the continuous time GBM. The continuous time GBM implies a risky growth for the risky asset over the interval  $\Delta T$ .  $\gamma_\ell$  is the deformation parameter.

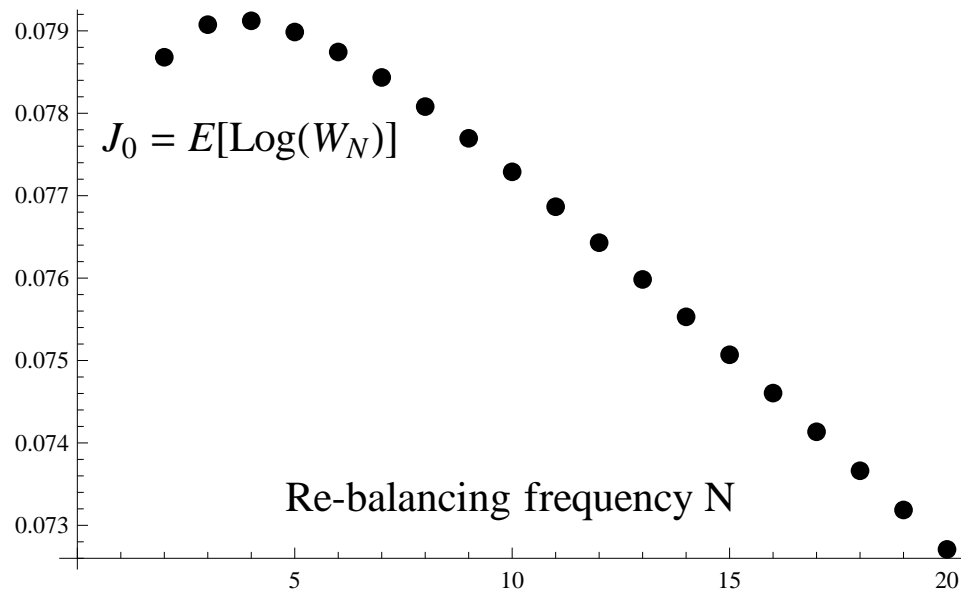


Figure 3.26: Variation of value function at time 0 with re-balancing frequency  $N$  with portfolio management fee when investor *always* has to re-balance for some choice of parameters:  $T = 1$ ,  $\omega = 0.07$ ,  $\lambda = \mu = 0.005$ ,  $s = e^{\omega\Delta T}$ ,  $m = 0.182$ ,  $\sigma = 0.4$ . Where  $T$  is the time horizon for investment,  $N$  is the number of re-balancing nodes.  $\omega$  is the continuous time risk-free rate,  $(\lambda, \mu)$  are transaction cost factors,  $s$  is the risk free growth over the interval,  $m$  is the drift for continuous time GBM and  $\sigma$  is the volatility for the continuous time GBM. The continuous time GBM implies a risky growth for the risky asset over the interval  $\Delta T$ .  $\gamma_\ell$  is the deformation parameter.

# Chapter 4

## Overview of *Mathematica* Implementations

This chapter provides a brief overview of the basic structure of numerical algorithms implemented in the Mathematica language. Mathematica provides a uniquely integrated and automated environment for parallel computing. With little configuration cost, a high degree of interactivity, and easy local and network operation, the symbolic character of the Mathematica language allows immediate support of a variety of existing and new parallel programming paradigms and data-sharing models. Mathematica also provides a rich set of mathematical and statistical functions which greatly helped in the numerical implementation of our algorithms. Appendices presenting Mathematica code for different sections of the chapter are supplied at the end of the document.

Most of our code was implemented on a 24-core machine with 16 kernels<sup>1</sup> utilized at a time for parallel implementations using the built-in **Parallelize[]** command. The results in Chapter 6 were obtained using a 2-core machine with 2 kernels utilized at a time. There are several variations in the way **Parallelize[]** could be used. We could apply it directly to the outer layer of the program or instead use individual parallelization of structures for instance by using the **ParallelTable[]** command.

The basic structure of almost all our problems can be broken down in to three main steps :

- 1- Probability Approximation via discrete multinomial discrete probability approximation.
- 2- Subsequent recursion using dynamic programming.
- 3- Saving the optimal controls obtained in step 2 and using them for further analysis.

We discuss each of the above three steps systematically.

### 4.1 Tree construction

As discussed earlier in Chapter 3 discrete probability approximation could be constructed either through moment matching or via a more general probability deformation.

---

<sup>1</sup>We only used 16 kernels because of the limitation of our Mathematica license.

### 4.1.1 Moment/Cross-moment matching

Moment matching typically results in a set of equations that must be solved numerically.

This can result in non-uniqueness in the sense that the solution set is essentially the same, but permuted with respect to the variables. As an example we provide in Appendix A the code for constructing a discrete probability approximation in 2-D. It could be seen that the discrete probability approximation has hierarchies. The discrete probability approximation at the highest level is used to obtain an equation that matched the cross-moment. The discrete probability approximation at a lower level is used to match the individual moments (up to order 2). We had five unknowns in our original discrete probability approximation and now we have five equations which could be solved using Mathematica's powerful root finding routine `NSolve[]`. This has already been discussed in detail in the Section 3.7.3 on discrete probability approximation construction in Chapter 3.

### 4.1.2 Trees via more general probability deformation

As discussed earlier we have several schemes that could help us create a more general class of discrete probability approximation. *Mathematica* has a rich set of statistical functions to help us achieve our goals.

Lets discuss the code for constructing discrete probability approximation via SQID scheme. It relies on using quantiles to create a probability approximation. `InverseCDF[]` was used to obtain quantiles and then `NIntegrate[]` used to obtain mean on a particular interval. In our 2-D code for SQID we chose to use Mathematica's `NIntegrate[]` on the transformed random variables.

If the risky growth is dependent upon a state variable we could easily accommodate for that by having discrete probability approximation dependent upon the state variable<sup>2</sup>. There are many variations in the way discrete probability approximations are created in our thesis. The lines of code in the appendix A are only for the purpose of illustration.

This section illustrated discrete probability approximations. However, we could easily work with `NIntegrate[]` to work with exact distributions. The latter turns out to be much more computationally demanding to achieve a desired level of accuracy.

## 4.2 Dynamic programming computations

### 4.2.1 Parallel computing in Mathematica

The recursive framework in dynamic programming is highly amenable to parallel computation. This is because the determination of value function at a point in state space  $S$  at time  $k$  only need only know the value function in state space one time step ahead<sup>3</sup>. The value function  $J_k$  at time  $k$  for different points in state space could, therefore, be computed in parallel across the entire grid. The idea is illustrated in Figure 4.1. We need not manually create clusters /grids in our 24 core machine. Mathematica will automatically create the grid structure and

<sup>2</sup>As in Chapter 8 where transaction costs are dependent on the volatility of the market.

<sup>3</sup>Seems similar to explicit finite difference methods for solving PDEs!

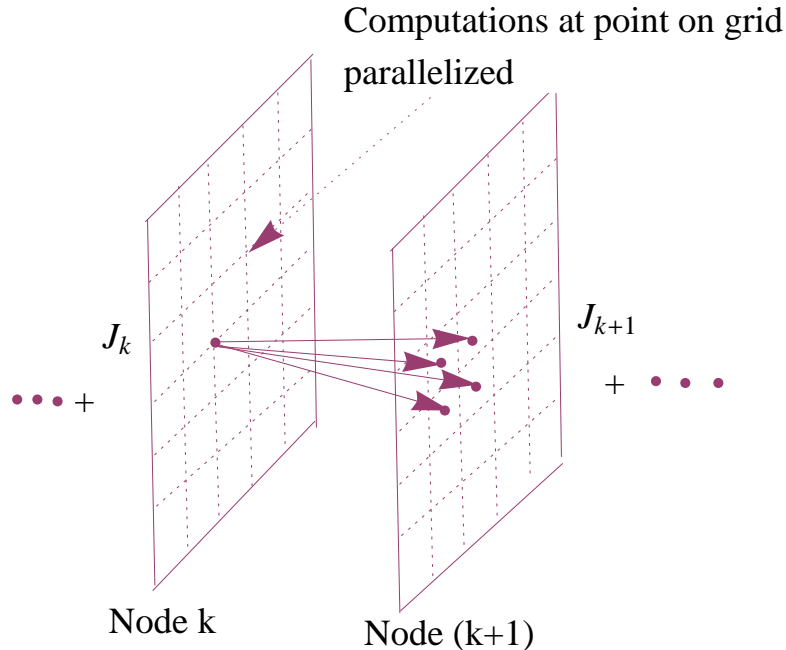


Figure 4.1: Parallel computation on grids. Value function computation at a point in node  $k$  only needs to know the value function surface at node  $(k + 1)$ .

distribute tasks in parallel. To do this we could either apply **Parallelize[]** to the outer layer of our program or use **ParallelTable[]** instead of **Table[]**.

## 4.2.2 Recursion via dynamic programming

Once a discrete probability approximation is constructed the stage is now set for recursively carrying out the dynamic programming methodology. **NestList[]** helps us carry out the recursion while **Interpolation[]** helps us numerically represent a value at each stage of the dynamic program over the state space domain. Depending upon the problem one could try adjusting the order of interpolation so as to achieve a desired level of accuracy. At each stage we could use *Mathematica's* **Parallelize[]** command to increase speed because the value function at a point in state space only needs to know the value function at the previous stage which is already computed and subsequently represented numerically. To determine optimal controls we used *Mathematica's* built-in routines or created custom optimization routines such as bisection which could utilize the special nature of the value function such as its concavity or convexity.

For example, to solve the type of transaction cost problems we present in Chapter 6, the Mathematica code in appendix A illustrates the initial recursion by proceeding from the last stage. We highlight the salient features of this initial recursion. Here the list **tlist1** stores for each point in state space the value function and the associated optimal control law (optimal re-balancing point, whether we should re-balance etc). Subsequently **JN1** is the numerical representation of the value function obtained after recursion in initial stage.

In this way we then proceed sequentially all our way up to the initial time to determine the value function and optimal control law at all the stages.

At each stage we store the optimal control law for each point in state space. This would be helpful in any analysis we would like to carry out. For instance, we might be interested in determining the no-transaction boundaries at a particular stage. The **ConvexHull[]** function in Mathematica could be useful in 1-D or 2-D provided the no-transaction region is convex. In higher dimensions or for non-convex regions there are third party programs. We have also built our own program for determining the boundaries that relies on constructing small ‘balls’ at points in the no-transaction region and seeing if they are inside the region or not. A large number of ‘balls’ each with a very small radius are constructed at evenly spaced points throughout the no-transaction region domain. If the entire ball lies inside the transaction region then its center is counted as part of the domain of the no-transaction region.

### 4.2.3 Analysis of the optimal control law

The optimal feedback control law at time step  $k$  denoted by  $\vec{\zeta}_k$  is now stored and ready for analysis. As discussed in Section 4.1 it is stored as a function of the state variable in list form as illustrated by the codes in the appendix A. This could easily be achieved by associating each point in state space with a label. So for a point in state space where we buy the point is labeled as **1**, a point where we sell is labeled as **2** and a point where we do nothing is labeled as **0**. By labeling here we mean the internal computer code architecture so that our code knows the optimal control law at each point in state space. Later in the thesis, for example in Figure 9.3 and Figure 9.4, we provide a visual depiction for such an internal labeling for our code. Knowing the optimal control law is very useful, and this allows us to visualize the law by plotting it in asset space. In this way we depict whether the optimal control for the investor is to buy, sell or do no transaction and analyze the resulting geometry.

Storing the control law opens up many potentially useful analyses via the *law of iterated expectations*. Say we are interested in determining the efficient frontier for the problem described in Section 3.3 of Chapter 3. We have a lattice with state space  $(\mathcal{A}_k^-, W_k^-)$  and the relevant variables already defined. To determine efficient frontier we require  $E[W_\tau|\mathcal{F}_0]$  and  $Var[W_\tau|\mathcal{F}_0]$  for the control law determined by solving the benchmark problem as described. Notice the efficient frontier depends upon  $\mathcal{F}_0$  and thus the wealth and risky fraction at initial time. As discussed in Section 3.3 by varying  $\gamma$  we generate the efficient frontier for a particular wealth and risky fraction at the initial time. For a particular value of gamma, risky fraction and wealth at initial time we have a set controls for the solved benchmark problem which we can denote by  $\zeta^*$ .

To obtain a point on the efficient frontier all we must now do is to define  $\phi_k(\mathcal{A}_k^-, W_k^-) = E[W_\tau|\mathcal{F}_k]$  and use the fact  $\phi_k = E[\phi_{k+1}|\mathcal{F}_k]$  where the expectation is carried under the controls  $\zeta^*$  already determined. We will do recursion on the lattice already described in Section 3.3 but know in this recursion we already know the controls.

Similarly, we can find  $Var[W_\tau|\mathcal{F}_0]$  once  $E[W_\tau|\mathcal{F}_0]$  has been determined by letting  $\Theta = E[W_\tau|\mathcal{F}_0]$  and recursion with the new objective  $Var[W_\tau|\mathcal{F}_0]$  but the same controls  $\zeta^*$ .

In brief, three possible ways of computing efficient frontier are :

I- Once the control law  $\vec{\zeta}_k$  has been determined compute  $E[W_\tau^2|\mathcal{F}_0]$  and  $E[W_\tau|\mathcal{F}_0]$  using the law of iterated expectations separately. Use these to get the pair  $(Var[W_\tau|\mathcal{F}_0], E[W_\tau|\mathcal{F}_0])$ .

II- Using the control law determine  $\Theta = E[W_\tau|\mathcal{F}_0]$  and then use it to figure out  $Var[W_\tau|\mathcal{F}_0] = E[(W_\tau - \Theta)^2|\mathcal{F}_0]$  via the law of iterated expectations.

III. Since  $E[(W_\tau - \gamma)^2|\mathcal{F}_0] = E[W_\tau^2|\mathcal{F}_0] - 2\gamma E[W_\tau|\mathcal{F}_0] + \gamma^2$ . Compute  $E[W_\tau^2|\mathcal{F}_0]$  or  $E[W_\tau|\mathcal{F}_0]$  and then use  $E[(W_\tau - \gamma)^2|\mathcal{F}_0]$  to find the pair  $(Var[W_\tau|\mathcal{F}_0], E[W_\tau|\mathcal{F}_0])$ .

There are many possible variations in the *Mathematica* implementation of our models and this chapter only highlighted the basics of the implementation <sup>4</sup>.

In the next chapter we will provide schemes under which solution from a discrete probability approximation is used to get the solution from the exact distribution.

---

<sup>4</sup>As in Chapter 9 we have constraints and in Chapter 11 we deal with a real-life trading strategy.



# Chapter 5

## Probability deformation continuation schemes

In the academic literature most of the portfolio theory under transaction cost literature is restricted to a continuous-time framework which results in *quasi-variational* Partial Differential Equations (PDEs). The objective of this chapter is to create a *generic* robust and efficient framework that could handle both discrete and continuous models simultaneously. The discrete time formulation is a special case of continuous-time formulation. The chapter proposes probability deformation schemes and examines their efficiency. Analysis is restricted to the popular transaction cost frameworks introduced in [28] and [81]. The investment objectives in these papers are different but the transaction cost structure is the same. Transaction cost is proportional to the amount traded.

### 5.1 Introduction

The fundamental philosophy of deformation solutions is to continuously march our solution from problems that can be easily solved to problems that can't be easily solved. In particular solving portfolio problems involving exact probability distributions can be a very daunting numerical task. Using exact distributions results in an increase in the computational complexity required to attain the desired accuracy in output. There is a work around for this however. Instead of solving problems using exact distributions we will solve problems via discrete approximations of the exact continuous time distributions. The discrete approximations are successively deformed<sup>1</sup> so that they provide convergence to the real problem with exact distribution in some probabilistic sense. This is in essence, the central theme of the chapter as illustrated in Figure 5.1. We are interested in the questions : By making probability models get closer are we making the output from these two models getting close ? Could we determine the output from the target probability model by making the approximate probability model get closer to the target probability model ? This chapter deals with these questions.

Discrete approximations to continuous probability distributions has been active area in *decision science* ( see [47], [46], [79]). An  $n$ -point discrete-distribution approximation consists of

---

<sup>1</sup>The word "deformed" would be used a lot by us. Basically we term the approximation of a continuous distribution as a *deformation process*.

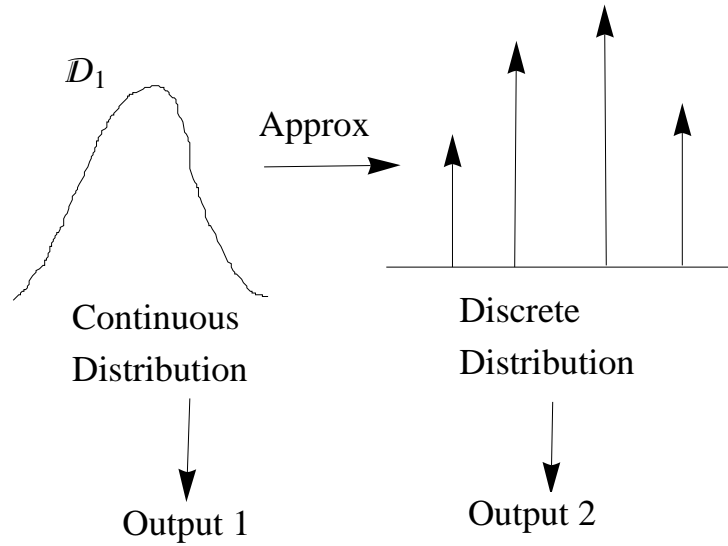


Figure 5.1: Two distributions going as an input to the numerical method. They both give an output to the model using same the numerical method. How close are the two outputs ?

$n$  values  $x_1, x_2, \dots, x_n$  and corresponding probabilities of occurrence  $p_1, p_2, \dots, p_n$  chosen to approximate the PDF for an underlying continuous random variable  $\mathcal{X}$ . The approximation could rely on specific features of the original distribution. It could rely on properties like moments or quantiles. Most of the common methods have names like *bracket mean*, *bracket median* and *moment matching* ( see [47], [46], [79]). The one dimensional definition in the academic literature could easily be extended to higher dimensions.

The chapter only focuses on the analysis of *probability deformation schemes*.

## 5.2 Probability deformation schemes

Suppose we have a multi-period portfolio problem with  $\mathcal{J}_k$  being the value function and  $\zeta_k$  being the control law under the exact probability structure  $p$ . Suppose we have  $p_\ell$  as an  $\ell$ -point approximation for  $p$  such that  $p_\ell \mapsto p$  in some probabilistic sense (i.e. convergence in probability, almost sure or in distribution ). Then we speculate  $\mathcal{J}_k^\ell \mapsto \mathcal{J}_k$  and  $\zeta_k^\ell \mapsto \zeta_k$  as  $\ell \mapsto \infty$ . We tighten the above speculation in the form of the conjecture :

**Conjecture :** Provided  $\mathcal{J}_k^\ell(\bullet)$  is *bounded* and *continuous* then  $p_\ell \xrightarrow{\mathcal{D}} p$  implies  $\mathcal{J}_k^\ell \xrightarrow{\mathcal{D}} \mathcal{J}_k$  for a *suitable state space grid setting*.

Note the condition *suitable state space grid setting* in the above conjecture. This is because the conjecture would hold only if we are free from interpolation and extrapolation errors in our dynamic programming recursion. This will happen only for a suitable grid setting as discussed in section 7 of chapter 3.

It is numerically very convenient to express the continuation behavior of the value function (or control law) in terms of the deformation parameter  $\gamma_\ell = \vartheta(\frac{1}{\ell})$  to get the desired solution with

respect to the original problem. So with a deformation parameter of  $\gamma_\ell$  we have a corresponding discrete probability approximation represented as an  $\ell$  point discrete approximation of our target probability model. Here  $\vartheta$  is a *monotonically* increasing function such that  $\lim_{a \rightarrow 0} \vartheta(a) = 0$ . In the rest of the chapter we will chose  $\vartheta(a) = a$ . We will later show that the *power law* and *polynomials* provide a good *basis set* to express the continuation behavior. By the continuation behavior we mean that, by changing the value of  $\gamma_\ell$ , how does the output change so that we can figure out the output from the target probability model.

The fact that the approximating probability distribution converges to the exact probability distribution of the model along the continuation path means the problem constraints also converge in some *probabilistic sense*.

## 5.3 Deformation schemes for a portfolio model in 1-D

### 5.3.1 Model description

The transaction cost model we will analyze is the simple growth rate model we had earlier considered in chapter 3. In particular this 1-D model is chosen because of its simplicity and popularity in the academic literature (See [28] and [72]). The investor shifts his wealth between risky and non-risky assets subject to a control strategy given his terminal investment objective. There are  $N$  periods and an investment horizon of length  $T$  years.

The model we will consider is the same model considered in Section 3.5. In that model the dynamic investor allocates wealth between risky and risk free asset and faces transaction cost proportional to the amount traded. Let us illustrate a transaction process involving two assets. It is popular in academic literature to have the first asset as risky and the second asset as risk-free (that finances the trades). Let  $X_k^+$  be the wealth in the risky asset immediately after re-balancing and  $Y_k^+$  in the risk-free asset.

If asset 1 is bought :

$$X_k^+ = \mathcal{A}_k^- W_k^- + \Delta_k = \epsilon_k^+ W_k^- \quad (5.1)$$

$$Y_k^+ = (1 - \mathcal{A}_k^-) W_k^- - (1 + \lambda_k) \Delta_k \quad (5.2)$$

$$\mathcal{A}_{k+1}^- = \frac{\epsilon_k^+ r_k}{\epsilon_k^+ r_k + ((1 - \mathcal{A}_k^-) - (1 + \lambda_k)(-\mathcal{A}_k^- + \epsilon_k^+)) s_k} \quad (5.3)$$

If asset 1 is sold :

$$X_k^+ = \mathcal{A}_k^- W_k^- - \Delta_k = \epsilon_k^+ W_k^- \quad (5.4)$$

$$Y_k^+ = (1 - \mathcal{A}_k^-) W_k^- + (1 - \mu_k) \Delta_k \quad (5.5)$$

$$\mathcal{A}_{k+1}^- = \frac{\epsilon_k^+ r_k}{\epsilon_k^+ r_k + ((1 - \mathcal{A}_k^-) + (1 - \mu_k)(\mathcal{A}_k^- - \epsilon_k^+)) s_k} \quad (5.6)$$

If no transaction is made :

$$X_k^+ = \mathcal{A}_k^- W_k^- \quad (5.7)$$

$$Y_k^+ = (1 - \mathcal{A}_k^- W_k^-) \quad (5.8)$$

$$A_{k+1}^- = \frac{\mathcal{A}_k^- r_k}{\mathcal{A}_k^- r_k + (1 - \mathcal{A}_k^-) s_k} \quad (5.9)$$

Consider a portfolio consisting of risky assets with the risky asset growing at a rate  $r_k$  over the  $k^{\text{th}}$  period. The investor has an initial endowment of  $\bar{W}$ . Let  $W_k^-$  be the wealth immediately before and  $W_k^+$  be the wealth immediately after re-balancing for the  $k^{\text{th}}$  period. Let  $X_k$  be the amount and  $\mathcal{A}_{i,k}^-$  be the fraction of wealth for the  $i^{\text{th}}$  risky asset relative to base wealth before re-balancing.

The value function takes a different form depending upon the investment objective.

For the growth rate (or log-utility) problem it is :

$$J(W_k^-, A_k^-) = E^P[\text{Log}(W_N^-) | \mathcal{F}_k] \quad (5.10)$$

Also,

$$\begin{aligned} \mathcal{J}_{N-k}(W_{N-k}^-, \mathcal{A}_{N-k}^-) &= \text{Log}(W_{N-k}^-) + \text{Max}_S E^{\mathbb{P}}[\mathcal{J}_{N-k+1}^{(k-1)}(\mathcal{A}_{N-k+1}^-) \\ &\quad + \text{Log}(\mathbb{F}_{N-k}(\mathcal{A}_{N-k}^-)) | \mathcal{F}_{N-k}] \\ &= \text{Log}(W_{N-k}^-) + \mathcal{J}_{N-k}^{(k)}(\mathcal{A}_{N-k}^-) \end{aligned} \quad (5.11)$$

Where the stochastic functional  $\mathbb{F}_{N-k}(A_{N-k}^-)$  encapsulating the control is represented as :

$$\mathbb{F}_{N-k}(A_{N-k}^-) = \begin{cases} (\epsilon_{N-k}^+ s_{N-k} + ((1 - A_{N-k}^-) - (1 + \lambda_{N-k})(-A_{N-k}^- + \epsilon_{N-k}^+)) \alpha_{N-k}) & \text{if risky asset bought} \\ (\epsilon_{N-k}^+ s_{N-k} + ((1 - A_{N-k}^-) + (1 - \mu_{N-k})(A_{N-k}^- - \epsilon_{N-k}^+)) \alpha_{N-k}) & \text{if risky asset sold} \\ A_{N-k}^- s_{N-k} + (1 - A_{N-k}^-) \alpha_{N-k} & \text{no trading} \end{cases}$$

Let the continuous time risky growth vector  $(\mathbf{1} + \mathbf{g})$  follow a multivariate GBM. Now  $\log(\mathbf{1} + \mathbf{g})$  is multi-variate normal. Also  $r_k$  is the corresponding discrete time risky growth for a risky asset. The domain of risky growth is infinite dimensional, however, we chose to truncate using appropriate algorithms to  $[0, r^*]$ . Where  $r^*$  now represents the truncated upper bound for the risky growth.

### 5.3.2 Numerical analysis of probability deformation schemes

We will restrict our numerical analysis to a certain state space domain for the value function. In the numerical experimentation we chose to have the initial wealth = 1 but the initial risky fraction changes and the appropriate value is given in the caption. See Tables 5.1-5.3. The value function under exact probability could be calculated using exact integration in dynamic programming. This is compared the value function we get using deformation schemes.

There are many possible discretization schemes. We will analyze three possible deformation schemes with respect to the deformation parameter  $\gamma = \frac{1}{\ell}$  :

**1- Simple interval division (SID) :** This will involve dividing the domain of the random variable into  $\ell$  equidistant chunks to form  $\ell$  intervals and finding the mid-point of the variable in the interval.

**2- Simple quantile interval division (SQID):** This will involve dividing the domain of random variable by using  $\ell$  quantiles using the quantile function and finding the mean of variable in the interval. A probability of  $\frac{1}{\ell}$  is assigned to each mean to get a discrete probability approximation.

**3- Moment division (MD):**

i)-Using an approximate moment matching algorithm using *Gaussian quadrature* as in [65] so that if the  $\ell$  the number of points for *Gaussian quadrature* the accuracy of distribution matching increases.

ii)- Instead of *Gaussian quadrature* we could match moments using standard discrete probability approximation construction as in Section 3.7.3.

Lets illustrate in a simple algorithmic way, the solution procedure in 1-D in a few steps:

---

**Step 1.** Chose whether to use SID, SQID or MD. Set  $i = 0$ . We construct a discrete approximation for risky growth over an interval  $\Delta T$ . The schemes SID, SQID and MD will give different discrete probability approximations. We then chose a deformation scheme with a particular value of  $\ell$ . This further implies the deformation parameter  $\gamma_\ell = \frac{1}{\ell}$ .

**Step 2.** We solve our 1-D model via dynamic programming to get the value function  $J_0^\ell$  at time  $t = 0$ . We have a pair  $P_i = (\gamma_\ell, J_0^\ell)$ .

**Step 3.** Increment the value of  $\ell$  and repeat step 2. Increment  $i$ . Insert  $P_i$  in the list  $L$ . If  $i > i^*$  go to step 4. Where  $i^*$  is a predefined termination level.

**Step 4.** Use the final list  $L$  as the data for continuation i.e. determining the limit  $\gamma_\ell \rightarrow 0$  using power law or polynomial basis. Under the power law the basis for an arbitrary real  $a$  are  $\{1, \gamma_\ell^a\}$ . Under polynomial basis we fit polynomial curves between successive data points. Mathematica's built-in function **Interpolation[]** was used. The default setting of cubic polynomial was used in all our numerical experimentation.

---

In each case of deformation we approach our required model by letting  $\frac{1}{\ell} \mapsto 0$ . This could be seen in Figures 5.2-5.4. The schemes are seen to march on to the true solution either monotonically increasing or decreasing for the choice of parameters in the figures. For different schemes we vary the deformation parameter and then use a continuation law. It is seen that all the three schemes land very close to the exact continuous time solution in the figure. The exact solution is marked by the solid circle at  $\gamma_\ell = 0$  in Figure 5.2-5.4. The other circles represent the solutions obtained for different deformation parameters.

For a particular choice of parameter it is always possible to compute the exact solution (as measured by the value function or the optimal control law). Results show that MD and SQID fare much better than SID. A power law is also seen to be a better continuation law compared to polynomial law in *general* shown in from the numerical experimentations shown in the next sections.

Method/Law	polynomial	power law
SID	-0.0341%	0.000920%
SQID	0.00271%	0.00458%
MD	-0.00757%	0.00177%

Table 5.1: Relative percentage error in value function with initial wealth=1, initial risky fraction=0.2, varying deformation from  $\ell = 15$  to 25 and parameter choice:  $\lambda = \mu = 0.01$ ,  $s = e^{0.1*\Delta T}$ ,  $m = 0.14$ ,  $\sigma = 0.3$ ,  $\gamma_\ell = \frac{1}{\ell}$ . Where  $T$  is the time horizon for investment,  $N$  is the number of re-balancing nodes.  $\omega$  is the continuous time risk-free rate,  $(\lambda, \mu)$  are transaction cost factors,  $s$  is the risk free growth over the interval,  $m$  is the drift for continuous time GBM and  $\sigma$  is the volatility for the continuous time GBM. The continuous time GBM implies a risky growth for the risky asset over the interval  $\Delta T$ .  $\gamma_\ell$  is the deformation parameter.

Method/Law	polynomial	power law
SID	0.0165%	0.000920%
SQID	-0.00552%	0.00552%
MD	0.00276%	0.00184%

Table 5.2: Relative percentage error in value function with initial wealth=1, initial risky fraction=0.5, varying deformation from  $\ell = 15$  to 25 and parameter choice:  $\lambda = \mu = 0.01$ ,  $s = e^{0.1*\Delta T}$ ,  $m = 0.14$ ,  $\sigma = 0.3$ ,  $\gamma_\ell = \frac{1}{\ell}$ . Where  $T$  is the time horizon for investment,  $N$  is the number of re-balancing nodes.  $\omega$  is the continuous time risk-free rate,  $(\lambda, \mu)$  are transaction cost factors,  $s$  is the risk free growth over the interval,  $m$  is the drift for continuous time GBM and  $\sigma$  is the volatility for the continuous time GBM. The continuous time GBM implies a risky growth for the risky asset over the interval  $\Delta T$ .  $\gamma_\ell$  is the deformation parameter.

Method/Law	polynomial	power law
SID	-0.109%	0.0265%
SQID	-0.00587%	0.0113%
MD	-0.00206%	0.00175%

Table 5.3: Relative percentage error in value function with initial wealth=1, initial risky fraction=0.9, varying deformation from  $\ell = 15$  to 25 and parameter choice:  $\lambda = \mu = 0.01$ ,  $s = e^{0.1*\Delta T}$ ,  $m = 0.14$ ,  $\sigma = 0.3$ ,  $\gamma_\ell = \frac{1}{\ell}$ . Where  $T$  is the time horizon for investment,  $N$  is the number of re-balancing nodes.  $\omega$  is the continuous time risk-free rate,  $(\lambda, \mu)$  are transaction cost factors,  $s$  is the risk free growth over the interval,  $m$  is the drift for continuous time GBM and  $\sigma$  is the volatility for the continuous time GBM. The continuous time GBM implies a risky growth for the risky asset over the interval  $\Delta T$ .  $\gamma_\ell$  is the deformation parameter.

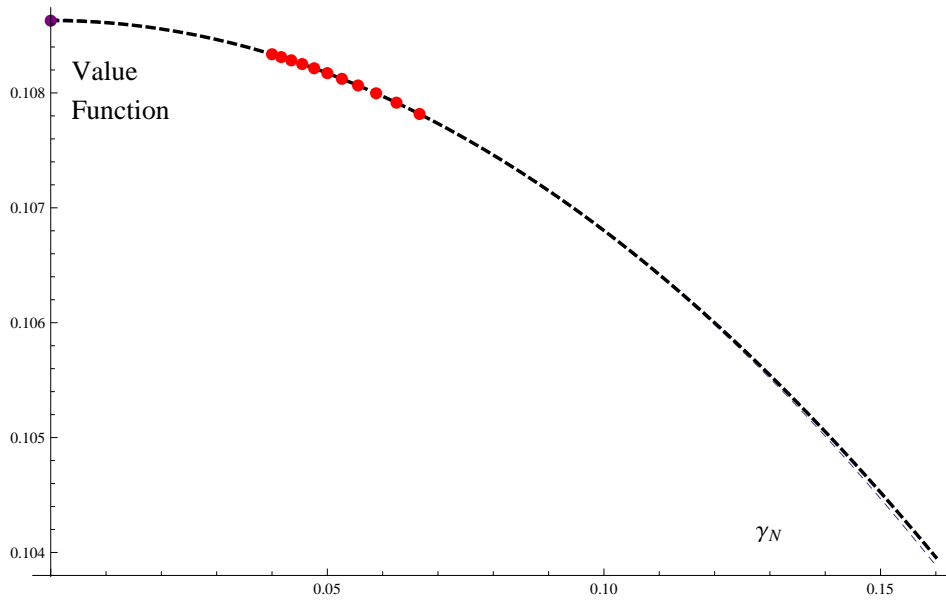


Figure 5.2: Value function in SID scheme with initial wealth=1, initial risky fraction=0.5, varying deformation from  $\ell=15$  to 25 and parameter choice:  $\lambda = \mu = 0.01$ ,  $s = e^{0.1*\Delta T}$ ,  $m = 0.14$ ,  $\sigma = 0.3$ ,  $T = 1$ ,  $N = 4$ ,  $\gamma_\ell = \frac{1}{\ell}$ . Where  $T$  is the time horizon for investment,  $N$  is the number of re-balancing nodes.  $\omega$  is the continuous time risk-free rate,  $(\lambda, \mu)$  are transaction cost factors,  $s$  is the risk free growth over the interval,  $m$  is the drift for continuous time GBM and  $\sigma$  is the volatility for the continuous time GBM. The continuous time GBM implies a risky growth for the risky asset over the interval  $\Delta T$ .  $\gamma_\ell$  is the deformation parameter.

## 5.4 Deformation schemes for a portfolio model in 2-D

### 5.4.1 Model description

The transaction cost model considered is the same as in 1-D but instead of the second asset being risk-free asset it is a risky asset. This slight change increases the dimensionality of the risky growth process by one. The investor now chooses to transfer wealth between two risky assets so as to maximize his growth rate over the time horizon<sup>2</sup>. The risky growth rates in this case present an interesting multivariate distribution to deform with respect to the parameter  $\gamma_\ell = \frac{1}{\ell}$ .

Let the risky growth vector  $(1 + g_1, 1 + g_2)$  follow a multivariate GBM. Now  $(\log(1 + g_1), \log(1 + g_2))$  is multivariate normal. Let  $\varpi$  denote the pdf of  $(1 + g_1, 1 + g_2)$  then deformation is done on the domain of the original distribution. Instead of an interval in 1-D we will have square grids in the domain. The domain is infinite dimensional, however, we chose to truncate using appropriate algorithms to  $[0, r_1^*] \times [0, r_2^*]$ .

The word *dimensionality* in the chapter denotes the dimension of the probability model. For as in an  $H$ -dim model we would encounter an  $H$ -dim risky growth vector  $g^* = (1 + g_1, 1 + g_2, \dots, 1 + g_H)$  over the interval  $\Delta T$  as a result of risky assets following a multi-variate **GBM**.

<sup>2</sup>This problem shares a great deal of similarity with the Mapleridge capital style asset management in which the hedge fund manager transfers wealth between trading strategies.

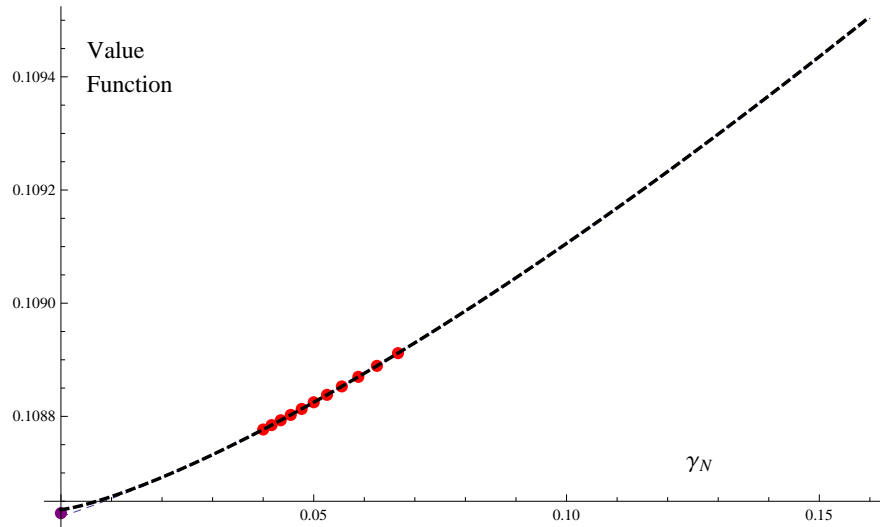


Figure 5.3: Value function in SQID scheme with initial wealth=1, initial risky fraction=0.5, varying deformation from  $\ell=15$  to 25 and parameter choice:  $\lambda = \mu = 0.01$ ,  $s = e^{0.1*\Delta T}$ ,  $m = 0.14$ ,  $\sigma = 0.3$ ,  $T = 1$ ,  $N = 4$ ,  $\gamma_\ell = \frac{1}{\ell}$ . Where  $T$  is the time horizon for investment,  $N$  is the number of re-balancing nodes.  $\omega$  is the continuous time risk-free rate,  $(\lambda, \mu)$  are transaction cost factors,  $s$  is the risk free growth over the interval,  $m$  is the drift for continuous time GBM and  $\sigma$  is the volatility for the continuous time GBM. The continuous time GBM implies a risky growth for the risky asset over the interval  $\Delta T$ .  $\gamma_\ell$  is the deformation parameter.

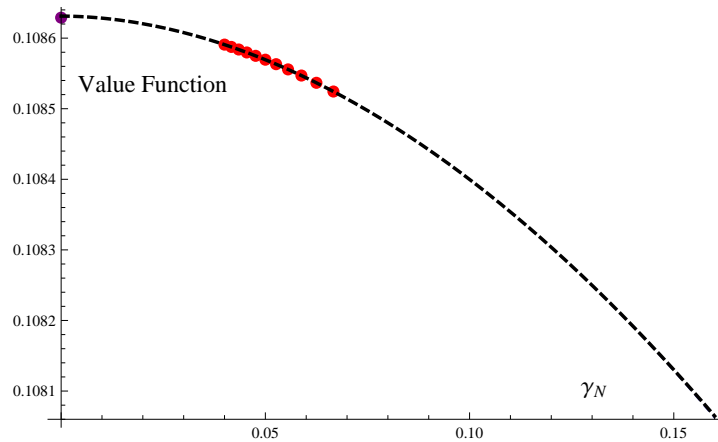


Figure 5.4: Value function in MD scheme with initial wealth=1, initial risky fraction=0.5, varying deformation from  $\ell=15$  to 25 and parameter choice:  $\lambda = \mu = 0.01$ ,  $s = e^{0.1*\Delta T}$ ,  $m = 0.14$ ,  $\sigma = 0.3$ ,  $T = 1$ ,  $N = 4$ ,  $\gamma_\ell = \frac{1}{\ell}$ . Where  $T$  is the time horizon for investment,  $N$  is the number of re-balancing nodes.  $\omega$  is the continuous time risk-free rate,  $(\lambda, \mu)$  are transaction cost factors,  $s$  is the risk free growth over the interval,  $m$  is the drift for continuous time GBM and  $\sigma$  is the volatility for the continuous time GBM. The continuous time GBM implies a risky growth for the risky asset over the interval  $\Delta T$ .  $\gamma_\ell$  is the deformation parameter.



Method/Law	polynomial	power law
SID	*	1.058%
<b>SQID</b>	0.202%	0.0257%

Table 5.4: relative percentage error in value function with initial wealth=1, initial risky fraction=0.5, varying deformation from  $\ell=8$  to 15 and parameter choice:  $\lambda = \mu = 0.05, T = 1, N = 4, \mu_1 = 0.08, \sigma_1 = 0.2, \mu_2 = 0.14, \sigma_2 = 0.8, \rho = 0.1, \gamma_\ell = \frac{1}{\ell}$ . Where  $T$  is the time horizon for investment,  $N$  is the number of re-balancing nodes.  $\omega$  is the continuous time risk-free rate,  $(\lambda, \mu)$  are transaction cost factors,  $s$  is the risk free growth over the interval,  $m$  is the drift for continuous time GBM and  $\sigma$  is the volatility for the continuous time GBM. The continuous time GBM implies a risky growth for the risky asset over the interval  $\Delta T$ .  $\gamma_\ell$  is the deformation parameter.

Accordingly,  $g^* = (\log(1 + g_1), \log(1 + g_2), \dots, \log(1 + g_H))$  is multi-variate normal over  $\Delta T$ . Then  $\varpi^H$  is the pdf of  $g^*$  upon which deformation is performed. The truncated domain will be  $[0, r_1^*] \times [0, r_2^*] \times \dots \times [0, r_H^*]$ .

### 5.4.2 Numerical analysis

A moment based scheme in higher dimensions is not explored here because of lack of proper algorithms at present to handle the computational complexity. In particular, we don't make general statements about  $N > 1$  but we still present some higher dimension results. It is not very straightforward to apply in higher dimensions the Gaussian *quadrature* based procedure which was possible in case of 1-D. It is still possible to create moment matching discrete probability approximation in higher dimensions where we match individual moments as well as cross-moments. We will discuss more about this in the final concluding chapter.

As expected SQID fares much better than a naive SID based upon the percentage errors. Extrapolation does not always work well when using polynomial in the continuation scheme because of the possible *wiggles*: irregular behavior observed while extrapolating the data interpolated using a polynomial basis.

We provide some numerical results for our earlier 2-D example in Table 2.4 for SQID and SID schemes. Further Figure 5.5 and Figure 5.6 provide a visual depiction of the continuation behavior under the SQID and SID schemes.

The basic numerical algorithm is the same as we highlighted for the 1-D case in Section 5.3.2. However, the risky growth is now two dimensional. We now work in a 2-D grid instead of an interval. Figure 5.7 shows how grids are created in 2-D space. For SQID scheme, for instance, we will use quantiles of the individual risky growths separately in the direction of the axis to create grids. The mean of the risky growth vectors inside the squared sized grids could easily be computed using numerical integration.

Based upon the tables and figures in this chapter it appears the power law works better than polynomial law in both the 1-D and 2-D cases.

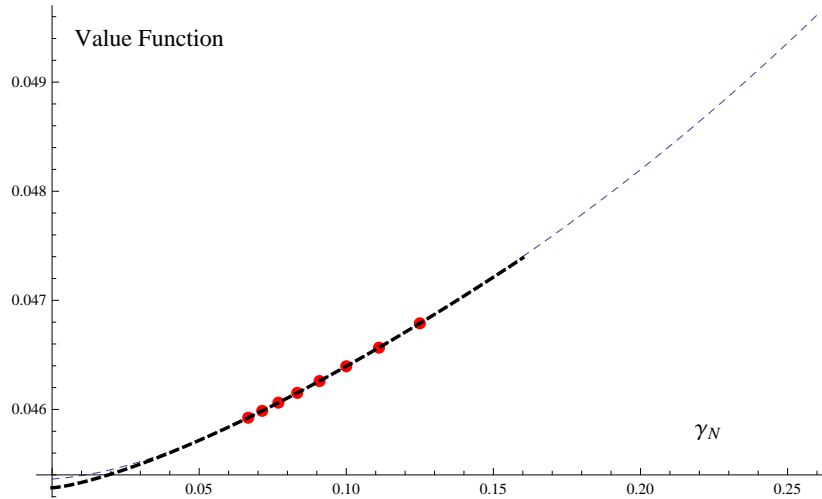


Figure 5.5: Value function in SID scheme with initial wealth=1, initial risky fraction=0.5, varying deformation from  $\ell=8$  to 15 and parameter choice:  $\lambda = \mu = 0.05, T = 1, N = 4, m_1 = 0.08, \sigma_1 = 0.2, m_2 = 0.14, \sigma_2 = 0.8, \rho = 0.1, \gamma_\ell = \frac{1}{\ell}$ . Where  $T$  is the time horizon for investment,  $N$  is the number of re-balancing nodes.  $\omega$  is the continuous time risk-free rate,  $(\lambda, \mu)$  are transaction cost factors,  $s$  is the risk free growth over the interval,  $m$  is the drift for continuous time GBM and  $\sigma$  is the volatility for the continuous time GBM. The continuous time GBM implies a risky growth for the risky asset over the interval  $\Delta T$ .  $\gamma_\ell$  is the deformation parameter.

## 5.5 Some remarks on moment division deformation

In 1-D it is a straightforward exercise to use Gaussian quadrature to create moment matching approximations as in [65]. It is possible to extend ideas to other quadratures. In higher dimensions we need to match cross-moments along with the individual moments. Let  $(X_i)$  denote a set of random variables so that suppose we wish to create a *MD* approximation up to an order  $A$ . Then we need to match  $(E(X_i^a)_{a \leq A}, E(X_i^k X_j^{a-k})_{a \leq A, k \leq a})$ . In one dimension it was easy to use quadrature based method as in [65], however, extending quadrature based method in higher dimension would be interesting.

As discussed earlier using enumerative discrete probability approximation we could still have a discrete probability approximation that matches individual as well as cross-moments. This has already been discussed in Chapter 3 but let's put the ideas in the more formal notation of this chapter. Let  $U$  be the order of MD approximation involved in matching the moments of monomial basis set with certain preferential ordering. Take the case of 2-D. How could we create a deformation scheme based on moment matching? This is by successively making the structure *richer*. A structure is considered richer if it has more model parameters to describe it. Examine the 2-D discrete probability approximation in Figure 5.8. The parent discrete probability approximation describes the joint evolution of risky growths and the sub-trees the individualized evolution. It has seven parameters and we would match the moments in lexicographic order as in table. Moments for set  $(x, y)$  would be matched first, then second moments  $(x^2, y^2, xy)$  and so on. We call this discrete probability approximation of cardinality  $M = 7$  richness. If we are to match third order moments we would consider the set  $(x^3, y^3, x^2y, y^2x)$ . To

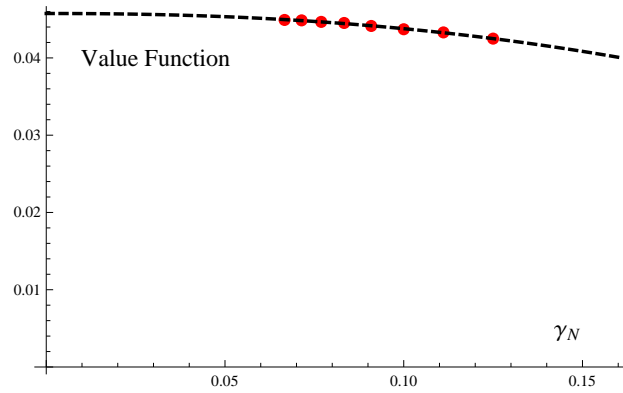


Figure 5.6: Value function in SQID scheme with initial wealth=1, initial risky fraction=0.5, varying deformation from  $\ell= 8$  to 15 and parameter choice:  $\lambda = \mu = 0.05, T = 1, N = 4, m_1 = 0.08, \sigma_1 = 0.2, m_2 = 0.14, \sigma_2 = 0.8, \rho = 0.1, \gamma_\ell = \frac{1}{\ell}$ . Where  $T$  is the time horizon for investment,  $N$  is the number of re-balancing nodes.  $\omega$  is the continuous time risk-free rate,  $(\lambda, \mu)$  are transaction cost factors,  $s$  is the risk free growth over the interval,  $m$  is the drift for continuous time GBM and  $\sigma$  is the volatility for the continuous time GBM. The continuous time GBM implies a risky growth for the risky asset over the interval  $\Delta T$ .  $\gamma_\ell$  is the deformation parameter.

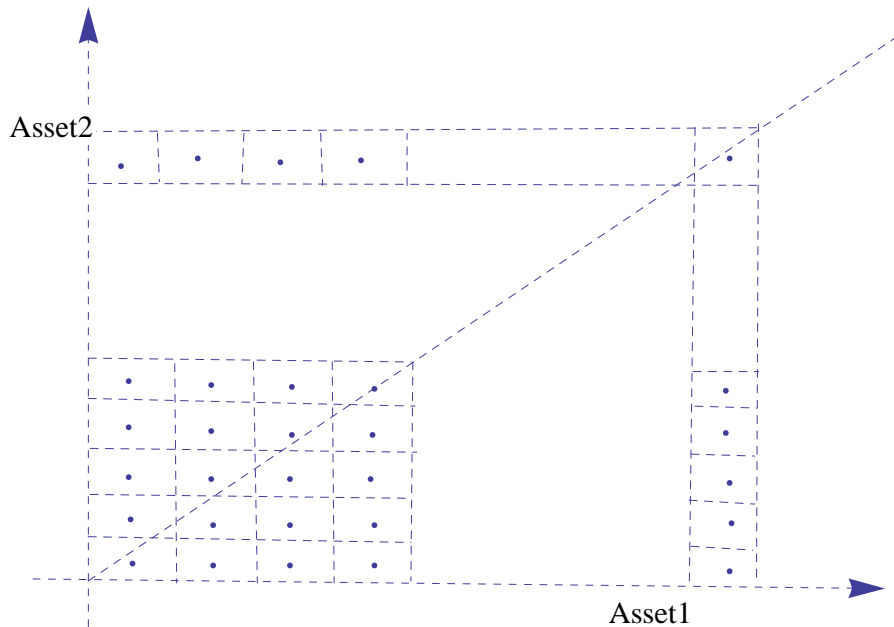


Figure 5.7: A possible deformation stencil in 2-D.

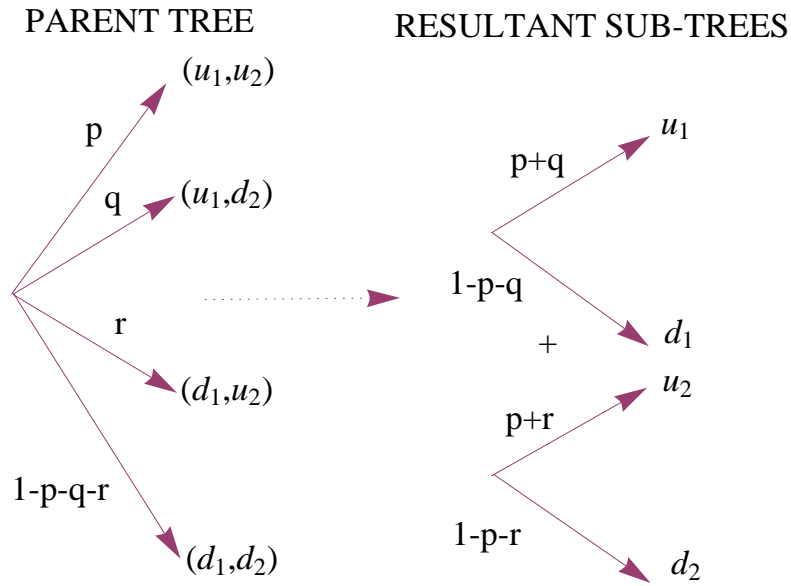


Figure 5.8: Tree in 2-D.

<b>Level I</b>	$(x, y)$
<b>Level II</b>	$(x^2, y^2, xy)$
<b>Level III</b>	$(x^3, y^3, x^2y, y^2x)$

Table 5.5: Lexicographic ordering of a monomial set in 2-D

seek continuation we must create a slightly richer discrete probability approximation by having more branches and then noting down the cardinality of the discrete probability approximation. We would then seek continuation of the problem through the parameter  $\gamma_I = \frac{1}{I}$ .

A richer discrete probability approximation has more parameters which are found by moving from one level to a higher level:

$$\text{Level I} < \text{Level II} < \text{Level III} < \dots$$

The structure could be made richer and hence closer to our target distribution by progressively moving from one level to a higher one.

<b>Level I</b>	$(x, y, z)$
<b>Level II</b>	$(x^2, y^2, z^2, xy, yz, xz)$
<b>Level III</b>	$(x^3, y^3, z^3, xy^2, xz^2, x^2y, x^2z, y^2z, yz^2, xyz)$

Table 5.6: Lexicographic ordering of a monomial set in 3-D

## 5.6 Applicability to a wide class of stochastic processes for risky growth

Our deformation methodology is easily applicable to wide range of stochastic processes.

Consider the popular *jump diffusion* model for risky asset  $i$

$$\frac{dS_t^{(i)}}{S_t^{(i)}} = \alpha^{(i)} dt + \sigma^{(i)} dZ_t + dq_t \quad (5.13)$$

in which the Poisson process  $dq_t$ , is characterized by jump intensity  $\lambda$  as well as jump size  $Y$  which is assumed independently log-normally distributed i.e.  $\log(Y) \sim N(\theta, \delta^2)$ .

The logarithm of the risky growth over an interval  $\Delta T$ , thereupon, follows

$$\log\left(\frac{S_{t+\Delta T}^{(i)}}{S_t^{(i)}}\right) = (\alpha^{(i)} - \frac{(\sigma^{(i)})^2}{2})\Delta T + \sigma^{(i)} \sqrt{\Delta T} Z_t + \sum_{t=1}^{n_t} \log(Y_t) \quad (5.14)$$

where  $n_t$  is the number of jumps in the interval  $\Delta T$ .

Further, let  $f(x)$  denote the density of  $\log\left(\frac{S_{t+\Delta T}^{(i)}}{S_t^{(i)}}\right)$

$$f(x) = \sum_{n=0}^{\infty} \frac{e^{-\lambda\Delta T} (\Delta T)^n}{n!} N\left(x; (\alpha^{(i)} - \frac{(\sigma^{(i)})^2}{2})\Delta T + n\theta, (\sigma^{(i)})^2\Delta T + n(\delta)^2\right) \quad (5.15)$$

We now have an analytic representation for the distribution of  $\log(1 + g)$  which does not rely on  $\Delta T$  being small because we have an analytics solution. The desired  $(1 + g)$  is obviously a monotonic transformation (apart from the fact the *quantiles* get monotonically transformed ) and we could easily work numerically with our deformation schemes as mentioned.

## 5.7 Towards a distribution-free approach

Our approach can be easily applied when the actual probability distribution model is unknown. In this case we could fit a smooth kernel distribution to our historical data and then apply deformation scheme on it. This would be particularly useful when analytical forms for multi-dimensional distribution could not be expressed in terms of a simple mathematical formula. We note that *Mathematica's* `SmoothKernelDistribution[]` returns a data distribution object that can be used like any other probability distribution, and hence could be useful in providing a distribution free approach.

## 5.8 Concluding remarks

Numerical results of this chapter show deformation schemes to be remarkably accurate for a fraction (about 1/10 to 1/20) of the computational cost required to obtain the exact solution. The exact solution using the exact distribution in dynamic programming is computationally intensive. This chapter explored a few possible schemes. In 2-D, for instance, a host of other

schemes are possible utilizing quantiles along the diagonal of the random variable domain. Many other statistical features could be similarly exploited.

The technique of successively deforming probability models towards the exact model was experimentally shown to converge to the exact probability model in this chapter. In the case of jump diffusion models deformation schemes have been found to be numerically very robust. In the next chapter we will show that moment based methods for discrete probability approximation construction are reasonably accurate by considering some popular academic models in transaction cost literature.

## Chapter 6

# Moment based discrete probability approximation of transaction cost models

The problem of optimizing portfolios in the presence of transaction costs has attracted significant interest. In this chapter we consider a discrete-time formulation of the models introduced by Morton and Pliska in [69] and Davis and Norman in [28]. We examine the applicability of the numerical discrete probability approximation as an alternative approach to solve transaction cost problems. The approach is able to solve a model in dimensions of less than or equal to three and non-standard geometries. Using the exact probability model in context of dynamic programming is computationally intensive as it involves root finding and optimization of complicated integrals. We provide a computational study of discrete probability approximation method on transaction cost models and highlight its many advantages.

The outline of the chapter is as follows: Section 1 considers discrete probability approximations for fixed transaction cost model in [69]. Section 2 considers analysis of discrete probability approximations for mean-variance problems. Section 3 considers discrete probability approximation for the proportional transaction cost models described in [28].

### 6.1 Tree approximations for fixed transaction cost model

As described in chapter 2, the question of optimal portfolio allocation was introduced in continuous time by *Merton* in his seminal 1969 study under a no-transaction cost assumption. The optimal policy proposed by *Merton* continuously transacts to hold a fixed fraction of wealth in each stock if the utility is logarithmic or CRRA. This results in infinite transactions on a finite interval. With transaction costs, the investor can only afford to make finitely many transactions. Intuitively, the investor would trade only if the fraction of stock holding is sufficiently far away from the *Merton* point. In 1990, Davis and Norman solved the Merton portfolio problem with proportional transaction costs for one stock case. In models of these type an investor makes minimal transactions to return the risky fraction on the boundary of the region of inaction if it wanders outside. In [84] a numerical scheme to iteratively find the viscosity solutions of such problems has been given. Some progress has been made in high dimensions for problems involving transaction costs. Reference [3] uses asymptotic analysis around the *Merton* point to obtain optimal policies for multiple stocks by maximizing asymptotic growth rate under an

infinite horizon. Reference [1] considers the same model as in [28] but their numerical scheme is shown to only work numerically for two stocks.

This section considers the optimal investment strategy of an investor who invests in one risk-free and multiple risky assets. The price evolution of risky assets is modeled by a multi-dimensional geometric Brownian motion. The discrete-time formulation allows the investor to bring his portfolio to the most optimal fraction of wealth in each asset while incurring fixed transaction costs of the management fee type as considered in [69], [6] and [3]. Thus at each stage he decides to re-balance or do nothing by comparing the value of each decision. The terminal utility at the end of the investment horizon is denoted by  $u(W_N)$  where  $W_N$  is the wealth at the terminal node. The focus in the quantitative finance literature has been on the infinite horizon framework which makes the problem time independent. Liu and Lowenstein [56] first studied the finite horizon problem considering some analytic approximations and some probabilistic arguments. Dai and Yi [25] considered the same problem albeit in a more formal PDE based framework. A more recent paper by Dai and Zhong [24] applies penalty based numerical methods on PDEs characterizing problems of these types.

In this section we provide a computational study on this simple model to provide solutions to its continuous time counterpart as in [69]. The solution is generally an optimal policy characterized by a *region of inaction* where admissible policies are regions in the set of all possible controls described by  $\mathcal{R}$ . A point dubbed the *Merton point* lies inside this region. When the proportion of investor's wealth lies inside the region, the investor does not transact. When the fluctuations in the risky price processes drive the proportions of wealth (*risky fraction process*) to the boundary of the *region of inaction* the investor transacts to bring it back to the *Merton point* if transaction costs are proportional to the amount of wealth. In the finite horizon problem both the region of inaction is time dependent in contrast to the infinite horizon case as solved and discussed in [69].

We use a discrete probability approximation approach to solve the model in one, two and three dimensions<sup>1</sup>. While only a simple transaction and utility structure is considered we see these simple discrete probability approximation methods as a promising tool for more higher dimensional complex transaction cost problems in a world where parallel programming and vast computer resources exist. Tree-based methods have been reasonably successful in the context of option pricing. Notable work in this regard are [15] and [21]. Our results show that they are reasonably accurate. Tree methods allow the solution of both finite and infinite horizon problems the analysis of which would be difficult otherwise. In most problems involving dynamic portfolio choice, the characterizing PDE can be discretized so as the resulting scheme gives a stable, consistent and convergent solution with convergence in sense of viscosity solution - an idea pioneered by Crandall, Ishii and Lions (1992) [43] and Fleming and Soner (1993) for non-linear partial differential equations [33]. Under suitable moment matching for probability model and a sufficiently fine discretization for the state variables our discrete probability based numerical algorithms show a stable and convergent behavior. An issue to be explored further is with respect to which the moments are matched and up to what degree so that the discrete probability approximation solution converges to the viscosity solution of the PDE characterizing the problem. A discrete probability based approximation can be equivalent to an approximate explicit finite difference scheme for the corresponding PDE.

---

<sup>1</sup>In general we could solve for arbitrary dimensions given sufficient computational power.



The problem in multi-dimensions has been well studied as in [73] and [71] for a different transaction cost structure. For instance, [51] uses a boundary update procedure to converge to the region of inaction and it has been proved to theoretically work in one dimension. Its ability to handle more complex geometries for *region of inaction* is questionable because of the requirement that the actual region of inaction lie inside the initial boundary approximation. Asymptotic methods considered in [6], [3] and [66] construct an approximate solution around the *Merton* point. Asymptotic techniques require transaction costs to be small and these methods are found to be relatively inaccurate. For instance, as noted in [3], for some parameters sets the estimated *Merton* point for asymptotic expansion could lie outside the simplex of the state variable domain. The ability of asymptotic techniques to handle more complex geometries for the *inaction region* is also questionable. Tree-based method can be seen as alternative approach given these pitfalls of the existing methods. They are simple to implement, reasonably accurate given certain conditions and computationally less intensive for reasonable dimensions.

This section considers the simple model of portfolio management type as in [69]. The solution of the problem is characterized by free-boundary ordinary differential equations (ODEs) and Partial Differential Equations (PDEs) which determine the risky fraction boundaries of the *region of inaction*. Real-world transaction costs are unpredictable with both fixed and random components in the form of bid-ask spread. In more complex geometries where PDE free boundary characterization results in numerically stiff problems we believe asymptotic methods become fairly inaccurate and existing solution schemes might fail to converge. Monte Carlo based methods in low dimensions for such kind of problems could be relatively inaccurate and time consuming. Tree-based methods are simple to implement and may be applied to different transaction cost paradigms. We have successfully applied it to models of the type as proposed as in [28] and with much more complex time inconsistent objectives.

### 6.1.1 The model

We will consider a simple transaction cost structure to illustrate the general idea behind the approximation methodology.

Consider a portfolio consisting of one risk-free asset growing at a rate of  $s_k$  over the  $k^{\text{th}}$  period i.e.  $(k, k + 1]$ . It also contains  $N$  risky assets with the  $i^{\text{th}}$  risky asset growing at a rate of  $r_{i,k}$  over the  $k^{\text{th}}$  period<sup>2</sup>.

The wealth in each risky asset  $i$  follows a geometric Brownian motion. In a continuous time framework  $S_{i,k}$  the stock price corresponding to the  $i^{\text{th}}$  risky asset is:

$$\frac{dS_i}{S_i} = m_i dt + \sigma_i dZ_t^i \quad (6.1)$$

The investor has an initial endowment of  $\bar{W}$  and at the beginning of each period he has the option to re-balance or not. Let  $W_k^-$  be the wealth immediately before and  $W_k^+$  be the wealth immediately after re-balancing for the  $k^{\text{th}}$  period. If the investor decides to re-balance then a certain fraction  $\lambda_k$  of the portfolio, termed the portfolio management fee, is extracted from the portfolio and the portfolio is subsequently brought to the most optimal fraction of wealth in

---

<sup>2</sup>Note  $(1 + g)$  is the continuous-time analogue of discrete time risky growth  $r_{i,k}$

each asset. Let  $X_{i,k}^-$  be the amount and  $\mathcal{A}_{i,k}^-$  be the fraction of wealth for the  $i^{\text{th}}$  risky asset relative to base wealth before re-balancing. We let  $Y_k$  denote the total amount of wealth in the risk-free asset in the period  $k$ . The fact that the transaction cost is independent of the initial risky fraction means the optimal re-balancing point (also called the *Merton point* or the *Merton line* for time varying optimal re-balancing point as in the case of CARA utility ) is independent of the initial risky fraction

The investment has a finite time horizon of  $T$ . There are  $N$  periods each of length  $\Delta T = \frac{T}{N}$  and  $k = 1, 2, \dots, N$ . The investment objective is to maximize the utility of final bequest  $E^{\mathbb{P}}[\mathbb{U}(W_N)]$ . Our model has the ability to accommodate both random and deterministic time horizons. For simplicity we will assume a deterministic time horizon  $T$ . We model an infinite horizon by letting  $T \rightarrow \infty$  yielding the infinite horizon policy  $p^*$  as a by-product.

Here  $\mathbb{U}(W_N) = \frac{W_N^V}{V}$  corresponds to CRRA utility with a risk aversion co-efficient of  $V$  with  $0 \leq V \leq 1$  and  $\mathbb{U}(W_N) = \frac{\text{Log}(W_N)}{T}$  corresponds to growth rate maximization with the limit  $N \rightarrow \infty$  for the asymptotic growth rate. The growth rate objective allows for *separability in wealth*. The limit  $\Delta T \rightarrow 0$  helps us obtain a continuous time solution of a model known in the transaction cost literature as the Pliska model (see [69], [6] and [3]). This simple transaction cost model has the virtue of being well studied and so allows for numerical validation against limiting and existing asymptotic results.

With the above stochastic framework we can represent the portfolio evolution in the form of a stochastic system. At the beginning of period  $k$  we have  $W_k^- = \sum X_{i,k}^- + Y_k^-$ . At the beginning of each period, if re-balancing is selected then the following system of equation hold:

$$X_{i,k+1}^- = (1 - \lambda_k) W_k^- \mathcal{A}_{i,k}^+ r_{i,k} \quad (6.2)$$

$$Y_{k+1}^- = (1 - \lambda_k) W_k^- \left( 1 - \sum \mathcal{A}_{i,k}^+ \right) s_k \quad (6.3)$$

$$\mathcal{A}_{i,k+1}^- = \frac{\mathcal{A}_{i,k}^+ r_{i,k}}{\sum \mathcal{A}_{i,k}^+ r_{i,k} + \left( 1 - \sum \mathcal{A}_{i,k}^+ \right) s_k} \quad (6.4)$$

If re-balancing is not selected then the following system holds :

$$X_{i,k+1}^- = W_k^- \mathcal{A}_{i,k}^- r_{i,k} \quad (6.5)$$

$$Y_{k+1}^- = W_k^- \left( 1 - \sum \mathcal{A}_{i,k}^- \right) s_k \quad (6.6)$$

$$\mathcal{A}_{i,k+1}^- = \frac{\mathcal{A}_{i,k}^- r_{i,k}}{\sum \mathcal{A}_{i,k}^- r_{i,k} + \left( 1 - \sum \mathcal{A}_{i,k}^- \right) s_k} \quad (6.7)$$

At the beginning of each period the investor decides to re-balance or not to re-balance keeping in view his dynamic objective for the terminal wealth  $W_N$  as previously considered. We require the constraint  $X_{i,k+1}^- \geq 0$  (no-shorting of risky asset allowed),  $Y_{k+1}^- \geq 0$ . We note that such constraints alter the geometry of the state variable domain  $\Omega_k$ . In two dimensions, for instance, the risky fraction domain takes the shape of a triangle shaped simplex. The fact

that a fraction of the wealth of the investor gets paid as the transaction cost and the investor takes only long position in the risky asset implies that the investor always remains solvent. The investor could, however, in theory become bankrupt if he takes a short position in the risky asset. Note that log-utility has a built in mechanism to control for bankruptcy because it approaches negative infinity for small amounts of wealth. We assume the utility structure allows separability in wealth thereupon working with the state space  $(W_k^-, \mathcal{A}_{i,k}^-)$  and truncating the state space vector  $\mathcal{A}_{i,k}^-$  to some reasonable lower and upper bounds. We assume that the risky fraction always lies in the interval  $[0, 1]$ <sup>3</sup>. In short a finite state approximation for all the possible states to be attained at beginning of period  $k$  is constructed so that our state variable always remains within the domain  $\Omega$ . Figure 6.1 illustrates the idea with the *region of inaction* embedded in risky fraction co-ordinate space  $\prod \mathcal{A}_{i,k}^-$ . The risky fraction space chosen to be large enough so that the *region of inaction* is always embedded inside it. The existence of a no-transaction region in risky fraction space is intuitively reasonable because:

A- The risky fraction process is a *mean reverting process* about *Merton* point for log-utility will be shown in Chapter 8.

B- The value of re-balancing is greater the further we are from the optimal re-balance point. We must state that the optimal re-balance point might not necessarily be the same as *Merton* point for the no-transaction cost case. *Merton* point for a problem for instance is transaction cost and utility structure dependent.

We will create a discrete-time, discrete probability approximation for the risky growth vector  $r_{i,k}$  so that the respective mean vector and variance-covariance matrix  $\Sigma$  over a period  $\Delta T$  match with the approximate moments of the continuous-time evolution of vector  $S_k$ . In the limit  $\Delta T \rightarrow 0$  the discrete-time approximation converges in distribution to the continuous-time distribution.

The exact distribution of  $r_{i,k}$  over a time step  $\Delta T$  is log-normal with mean of  $e^{(m-\frac{\sigma^2}{2})\Delta T + \frac{1}{2}\sigma^2\Delta T}$  and variance of  $\left( (e^{\sigma^2\Delta T} - 1) e^{2(m-\frac{\sigma^2}{2})\Delta T + \sigma^2\Delta T} \right)$ . As can be seen from the discretized version of equation 6.1, for sufficiently small  $\Delta T$ , the risky growth vector is also approximately multivariate normally distributed with a mean  $1 + m\Delta T$  and a variance-covariance matrix  $\Sigma$ . The choice of  $\Delta T$  will impact the accuracy of the solution given a certain utility and transaction cost structure. With this moment matching up to a certain order we can create a binomial, trinomial or an appropriate multi-nomial discrete probability approximation for risky growth vector  $r_{i,k}$ .

There is no unique way to create a discrete probability approximation. Chapter 3 highlighted the basics of discrete probability and now we will give some specific examples. In one dimension, for example, the binomial discrete probability approximation has two branches with the risky growth increasing to  $u$  with a probability  $p$  and decreasing to  $d$  with a probability  $1 - p$ . The trinomial approximation for the risky growth has three branches with the risky growth increasing to  $u$  with a probability  $p$ , going to  $l$  with a probability  $q$  and decreases to  $d$  with a probability  $1 - p - q$ . Risky growth evolution is time independent in our model. The

<sup>3</sup>However, by using suitable penalty adjustments in our dynamic programming formalism, we could accommodate generalized liquidity/portfolio constraints of the form  $-a \leq \mathcal{A}_{i,k}^- \leq a$  for some  $a \in \mathcal{R}$ . Our model could easily accommodate constraints of the type  $Y_{k+1}^- + \sum X_{i,k+1}^- \geq 0$  or perhaps even  $Y_{k+1}^- + (1-\lambda_k) \sum X_{i,k+1}^- \geq 0$  for more generalized transaction cost structures. This could be handled by suitable adjustments to the dynamic programming methodology by invoking some constraints or applying a penalty to the value function. We will discuss in detail in chapter 9.

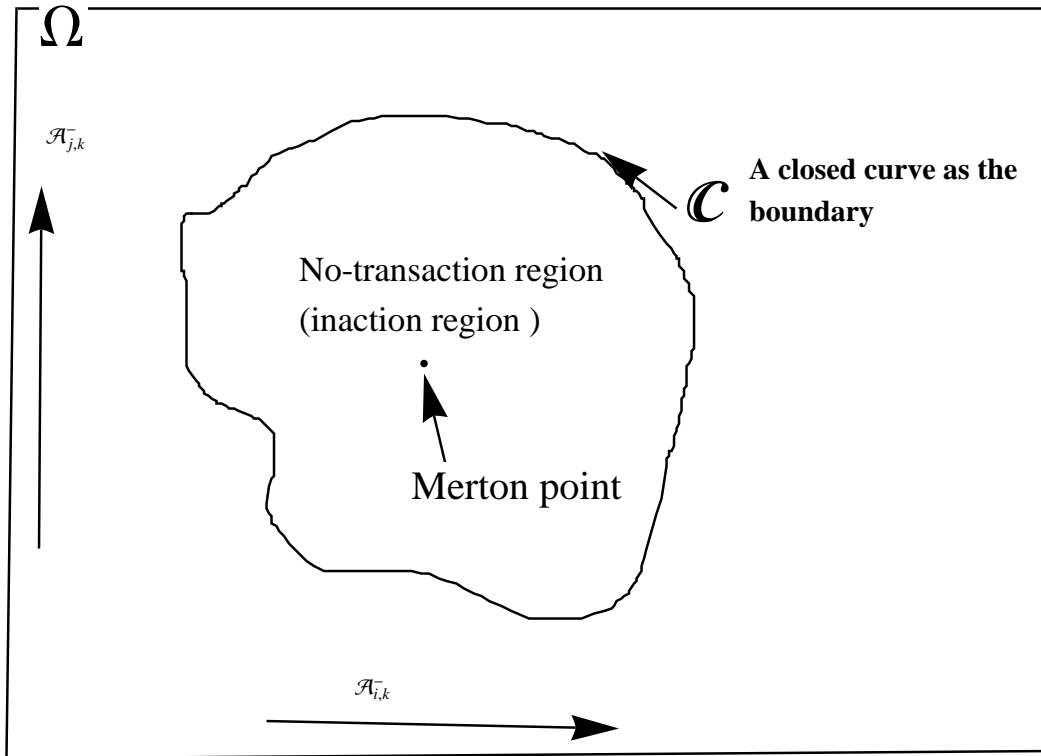


Figure 6.1: No-transaction region embedded in state variable space at node  $k$ .

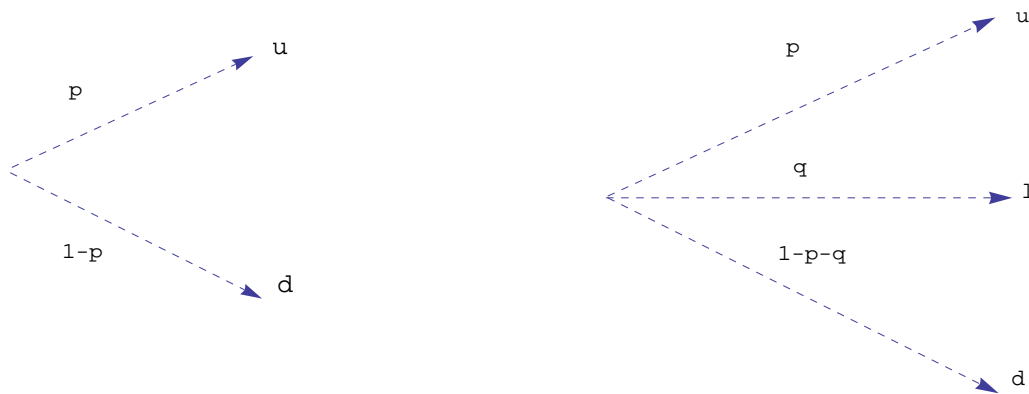


Figure 6.2: Binomial and Trinomial discrete probability approximations for risky growth in one dimension.

stochastic drift and volatility case we could easily accommodate for *non-stationary* discrete probability approximations which we do in chapter 11. We can denote  $((p, u), (1 - p, d))$  or  $((p, u), (q, l), (1 - p - q, d))$  as being an approximate discrete probability model for the contin-

uous stock price risky growth distribution.

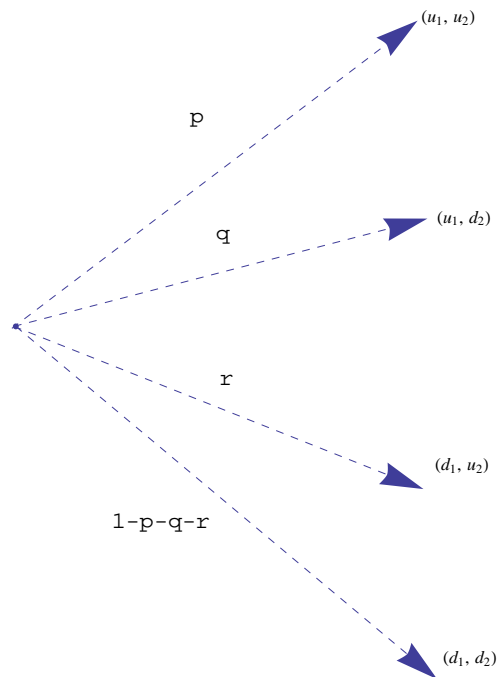


Figure 6.3: Binomial discrete probability approximation for a pair of risky growth in 2-dimensions.

In two dimensions the binomial approximation for the risky growth has four branches. Here we need to incorporate the two risky growths as a pair, as depicted in Figure 6.3. In one dimension for instance choosing  $u = \frac{1}{d} = 1 + g$  or  $u = \frac{1}{d} = 1 + g, l = 1$  gives reasonable results for some choice of parameters. We could have no restrictions on the branching factors  $u, l, d, \dots$  and build an approximate probability model by matching moments up to an order  $k$ . In Figure 6.2 the binomial discrete probability approximation has three parameters and so allows us to match first three moments of risky growth. The trinomial discrete probability approximation has four parameters and allows us to match the first four moments.

The binomial approximation for risky growth in  $N$ -dimensions can have  $2^N$  branches.

We could chose either log returns, simple returns or the actual stock price itself for moment matching purposes. Selection of the appropriate stochastic variable in the model with respect moment matching is to be done is an interesting question. For instance, by using moment matching with respect to log-returns [45] creates multinomial approximating models for  $k$  state variables by writing  $S_i(k + \Delta T) = S_i(k) e^{\zeta_i(k)}$  where  $e^{\zeta_i(k)}$  is the risky growth factor. Under a GBM model for stock prices we know that  $\zeta_i(k) = (m_i - \frac{\sigma_i^2}{2}) \Delta T + \sigma_i \sqrt{\Delta T} Z_k$  where  $Z_k$  is the Wiener process. Also,  $E[\zeta_i(k)] = (m_i - \frac{\sigma_i^2}{2}) \Delta T$  and  $\text{Var}[\zeta_i(k)] = \sigma_i^2 \Delta T$  and we can use moment matching to create a discrete time risky growth pair evolution.

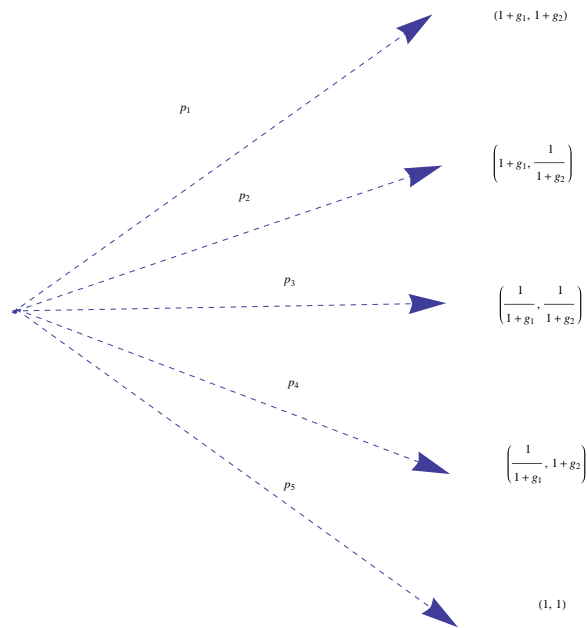


Figure 6.4: A possible approximation in 2-dimensions.

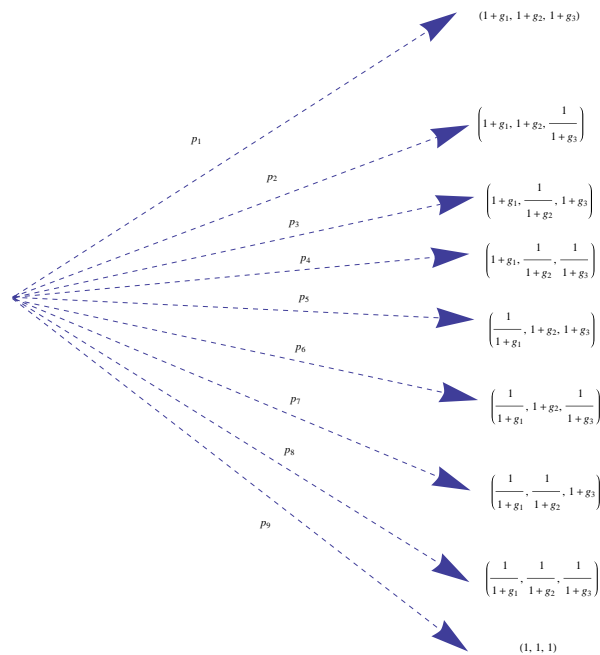


Figure 6.5: A multinomial approximation in three dimensions.

In two dimensions the risky growth pair is depicted in Figures 6.3 and 6.4. In three dimension the evolution of risky growth triplet is depicted in Figure 6.5. We can see with  $k$  dimensions we have  $2^k + 1$  branches in such constructions.

In our model the joint distribution of returns is either multi-variate normal or multi-variate log-normal. It turns out that if stock price is GBM then the risky growth over a small  $\Delta T$  has actually a log-normal distribution which could be approximated as being normal. In higher dimensions a simple procedure would seek to match the moments given by the mean vector and variance covariance matrix via  $E[X_i] = \mu_i, E[X_i X_j] = \rho_{ij}$ . Opportunity exists for creating better approximations by adding higher order moments  $E[X_i^r], E[X_i^r X_j^s]$  to our arsenal.

## 6.1.2 Approximation algorithm

The stage is now set to cast the above model in a dynamic programming framework so that discrete probability approximation method can be illustrated. We will consider CRRA and logarithmic utility functions separately.

Here the state space is the pair  $(W_k^-, \mathcal{A}_{i,k}^-)$  while the control is the vector  $(\mathcal{A}_{i,k}^+)$ .

**A-** First consider the CRRA utility. Let  $\mathcal{J}_N^{(i)}(\bullet)$  represent the portion *separable* from wealth in the value function  $\mathcal{J}_N(\bullet)$ .

Let  $\mathcal{J}_k(W_k^-, \mathcal{A}_k^-) = E^{\mathbb{P}}[\frac{W_N^V}{V} | \mathcal{F}_k]$  be the value function under the CRRA utility. Then under the control set  $\{\zeta\}$  we have:

$$\mathcal{J}_k(W_k^-, \mathcal{A}_k^-) = \max_{\{\zeta\}} E^{\mathbb{P}}[\mathcal{J}_{k+1}(W_{k+1}^-, \mathcal{A}_{k+1}^-) | \mathcal{F}_k]. \quad (6.8)$$

Now since  $\mathcal{J}_N(W_N^-, \mathcal{A}_N^-) = \frac{W_N^V}{V}$  we can write:

$$\mathcal{J}_N(W_N^-, \mathcal{A}_N^-) = \frac{W_{N-1}^V}{V} \mathbb{F}_{N-1}(\mathcal{A}_{i,N-1}^-)^V \quad (6.9)$$

where  $\mathbb{F}$  is a stochastic functional depicting the investor decision to re-balance or not at  $k = N - 1$  under the stochastic evolution as described earlier in section 6.1.2. Using equation (6.9) we can write:

$$\mathcal{J}_{N-1}(W_{N-1}^-, \mathcal{A}_{N-1}^-) = \frac{W_{N-1}^V}{V} \max_{\{\zeta\}} E^{\mathbb{P}}[\mathbb{F}_{N-1}(\mathcal{A}_{i,N-1}^-)^V | \mathcal{F}_{N-1}]. \quad (6.10)$$

The expression  $\mathbb{F}_{N-1}(\mathcal{A}_{i,N-1}^-)$  is:

$(1 - \lambda_{N-1}) (\sum \mathcal{A}_{i,N-1}^+ r_{i,N-1} + (1 - \sum \mathcal{A}_{i,N-1}^+) \circ s_{N-1})$  if the investor wants to re-balance and  
 $\sum \mathcal{A}_{i,N-1}^- r_{i,N-1} + (1 - \sum \mathcal{A}_{i,N-1}^-) \circ s_{N-1}$  if he decides to do nothing.

Letting  $\mathcal{J}_{N-1}(W_{N-1}^-, \mathcal{A}_{N-1}^-) = \frac{W_{N-1}^V}{V} \mathcal{J}_{N-1}^{(1)}(\mathcal{A}_{i,N-1}^-)$  we again use equation (6.10) to find that:

$$\mathcal{J}_{N-2}(W_{N-2}^-, \mathcal{A}_{N-2}^-) = \frac{W_{N-2}^V}{V} \max_{\zeta} E^{\mathbb{P}}[\mathcal{J}_{N-1}^{(1)}(\mathcal{A}_{i,N-1}^-) \mathbb{F}_{N-2}(\mathcal{A}_{i,N-2}^-)^V | \mathcal{F}_{N-2}] \quad (6.11)$$

$$= \frac{W_{N-2}^V}{V} \mathcal{J}_{N-2}^{(2)}(\mathcal{A}_{i,N-2}^-). \quad (6.12)$$

In general for  $k = 2, 3, \dots, N$  we can write:

$$\mathcal{J}_{N-k}(W_{N-k}^-, \mathcal{A}_{N-k}^-) = \frac{W_{N-k}^V}{V} \max_{\{s\}} E^{\mathbb{P}} [\mathcal{J}_{N-k+1}^{(k-1)}(\mathcal{A}_{i,N-k+1}^-) \circ \mathbb{F}_{N-k}(\mathcal{A}_{i,N-k}^-)^V | \mathcal{F}_{N-k}] = \frac{W_{N-k}^V}{V} \mathcal{J}_{N-k}^{(k)}(\mathcal{A}_{i,N-k}^-). \quad (6.13)$$

**B-** Next consider the logarithmic utility scaled with respect to the time horizon<sup>4</sup>.

Let  $\mathcal{J}_k(W_k^-, \mathcal{A}_k^-) = E^{\mathbb{P}}[\frac{\text{Log}(W_N^-)}{T} | \mathcal{F}_k]$  be the value function under the logarithmic utility. Then, under control set  $\{s\}$  we have:

$$\mathcal{J}_k(W_k^-, \mathcal{A}_k^-) = \max_{\{s\}} E^{\mathbb{P}} [\mathcal{J}_{k+1}(W_{k+1}^-, \mathcal{A}_{k+1}^-) | \mathcal{F}_k]. \quad (6.14)$$

Now since  $\mathcal{J}_N(W_N^-, \mathcal{A}_N^-) = \frac{1}{T} \text{Log}(W_N^-)$  we can write:

$$\mathcal{J}_N(W_N^-, \mathcal{A}_N^-) = \frac{1}{T} (\text{Log}(W_{N-1}^-) + \text{Log}(\mathbb{F}_{N-1}(\mathcal{A}_{i,N-1}^-))) \quad (6.15)$$

where  $\mathbb{F}$  is a stochastic functional depicting the investor behavior of re-balancing or not re-balancing at  $k = N - 1$  under the stochastic evolution as described earlier in section 6.1.2. Using equation (6.15) we can write:

$$\mathcal{J}_{N-1}(W_{N-1}^-, \mathcal{A}_{N-1}^-) = \frac{1}{T} (\text{Log}(W_{N-1}^-) + \max_{\{s\}} E^{\mathbb{P}} [\text{Log}(\mathbb{F}_{N-1}(\mathcal{A}_{i,N-1}^-)) | \mathcal{F}_{N-1}]). \quad (6.16)$$

The stochastic functional  $\mathbb{F}_{N-1}(\mathcal{A}_{i,N-1}^-)$  is:  $(1 - \lambda_{N-1}) (\sum \mathcal{A}_{i,N-1}^+ r_{i,N-1} + (1 - \sum \mathcal{A}_{i,N-1}^+) s_{N-1})$  if the investor wants to re-balance and  $\sum \mathcal{A}_{i,N-1}^- r_{i,N-1} + (1 - \sum \mathcal{A}_{i,N-1}^-) s_{N-1}$  if he decides to do nothing.

Letting  $\mathcal{J}_{N-1}(W_{N-1}^-, \mathcal{A}_{N-1}^-) = \frac{1}{T} (\text{Log}(W_{N-1}^-) + \mathcal{J}_{N-1}^{(1)}(\mathcal{A}_{i,N-1}^-))$  we again use equation (6.16) to find:

$$\begin{aligned} \mathcal{J}_{N-2}(W_{N-2}^-, \mathcal{A}_{N-2}^-) &= \frac{1}{T} (\text{Log}(W_{N-2}^-) + \max_{\{s\}} (E^{\mathbb{P}} [\mathcal{J}_{N-1}^{(1)}(\mathcal{A}_{i,N-1}^-) \\ &\quad + \text{Log}(\mathbb{F}_{N-2}(\mathcal{A}_{i,N-2}^-)) | \mathcal{F}_{N-2}]) \\ &= \frac{1}{T} (\text{Log}(W_{N-2}^-) + \mathcal{J}_{N-2}^{(2)}(\mathcal{A}_{i,N-2}^-)) \end{aligned} \quad (6.17)$$

In general for  $k = 2, 3, \dots, N$  we can write:

$$\begin{aligned} \mathcal{J}_{N-k}(W_{N-k}^-, \mathcal{A}_{N-k}^-) &= \frac{1}{T} (\text{Log}(W_{N-k}^-) + \max_{\{s\}} (E^{\mathbb{P}} [\mathcal{J}_{N-k+1}^{(k-1)}(\mathcal{A}_{i,N-k+1}^-) \\ &\quad + \text{Log}(\mathbb{F}_{N-k}(\mathcal{A}_{i,N-k}^-)) | \mathcal{F}_{N-k}]) \\ &= \frac{1}{T} (\text{Log}(W_{N-k}^-) + \mathcal{J}_{N-k}^{(k)}(\mathcal{A}_{i,N-k}^-)) \end{aligned} \quad (6.18)$$

■

<sup>4</sup>Scaling by time horizon does not impact the optimal controls obtained as we shall see.



**Lemma 6.1.1**  $\mathcal{J}_k(W_k^-, \mathcal{A}_k^-)$  has the property for  $\rho > 0$

(1)  $\mathcal{J}_k(\rho W_k^-, \mathcal{A}_k^-) = \rho^V \mathcal{J}_k(W_k^-, \mathcal{A}_k^-)$  for CARA utility.

(2)  $\mathcal{J}_k(\rho W_k^-, \mathcal{A}_k^-) = \log(\rho) + \mathcal{J}_k(W_k^-, \mathcal{A}_k^-)$  for log-utility by setting  $T = 1$ .

**Proof** Easily follows from separability of wealth in equations (6.12)-(6.17).

Using a change in variable notation we have for CARA utility:

$\mathcal{J}_k(W_k^-, \mathcal{A}_k^-) = \frac{W_k^V}{V} \mathcal{J}_k^*(\mathcal{A}_{i,k}^-)$ . So letting  $W_k^- \rightarrow \rho W_k^-$  the result follows from above.

■

In a discrete-time formalism our methodology tries to curb the dimensionality of the probability space. The expectation in equations (6.8)-(6.18) is carried under a discrete time probability space for risky growths. Under the limit  $\Delta T \rightarrow 0$  it converges to its continuous counterpart the solution of which is characterized by a PDE as in [69]. For instance, in the option pricing context Kushner and DiMasi (1978) have shown that, provided the diffusion co-efficient and option payoff are bounded, if a sequence of processes converges weakly to geometric brownian motion then the value functions for the optimal stopping problems also converge. In the next sections we validate the accuracy of discrete probability approximation based methodology by comparing our solutions to continuous time solutions that already exist in the literature. If  $T$  is finite then the model is a finite horizon time dependent problem. However, if we recurse infinitely in the recursion problems for equations (6.8)-(6.18) we solve the infinite horizon problem obtained by letting  $T \rightarrow \infty$ . In most cases the boundary changes very little if we are very far away from the terminal time and a finite boundary solution could be used to approximate an infinite boundary solution. For us, the point of the infinite horizon solution is to validate our discrete probability approximation based finite horizon solution. The solution to infinite horizon problem already exists in the quantitative finance literature and this will be the benchmark against which we will provide validation for the numerical discrete probability approximation solution.

### 6.1.3 Model output and validation

In this section logarithmic utility will be used for the purpose of calculations unless otherwise stated.

#### $N = 1$ risky assets

In this section we will provide some results for one risky asset and validate them against existing solution in the infinite horizon case by letting  $T \rightarrow \infty$ <sup>5</sup>. In all our subsequent results the parameters and the shape of the state variable simplex is chosen to be the same as in [69]. Figures 6.6 and 6.7 show output for parameters chosen to be  $\lambda = 0.001$ ,  $T = 5$ ,  $N = 500$ ,  $\Delta T = T/N$ ,  $s = e^{0.07\Delta T}$ ,  $m = 0.182$ ,  $\sigma = 0.4$ . The parameter values are the same as used in [69].

<sup>5</sup> Assuming a logarithmic utility and choosing  $u = e^{m\Delta T + \sigma\sqrt{\Delta T}}$ ,  $d = e^{m\Delta T - \sigma\sqrt{\Delta T}}$  and  $p = 1/2$  we create an approximation for Merton point using dynamic programming and find it to be  $a = -\frac{s(-\Delta T m + s - 1)}{\Delta T^2 m^2 + 2\Delta T m + \Delta T \sigma^2 + s^2 - 2\Delta T m s - 2s + 1}$ .

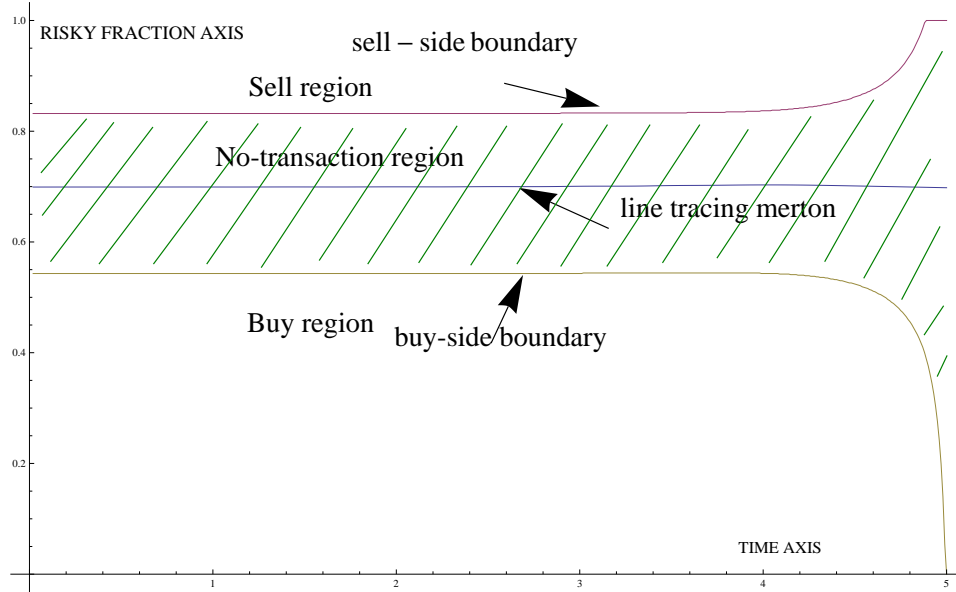


Figure 6.6: The sell-side and buy-side boundaries for the choice of parameters:  $\lambda = 0.001$ ,  $T = 5$ ,  $N = 500$ ,  $\Delta T = \frac{T}{N}$ ,  $s = e^{0.07\Delta T}$ ,  $m = 0.182$ ,  $\sigma = 0.4$ . Where  $T$  is the time horizon for investment,  $N$  is the number of re-balancing nodes.  $\omega$  is the continuous time risk-free rate,  $\lambda$  is the transaction cost factor,  $s$  is the risk free growth over the interval,  $m$  is the drift for continuous time GBM and  $\sigma$  is the volatility for the continuous time GBM. The continuous time GBM implies a risky growth for the risky asset over the interval  $\Delta T$ .

As seen by the graphs at infinite horizon discrete probability approximation solution implies risky fraction boundaries of  $(0.5425, 0.834)$  which is reasonably close to a solution of  $(0.54, 0.837)$  implied by solving a free-boundary problem as in [69] wherein the exact solution could be computed by solving a large system of nonlinear equations. The convergence to the infinite horizon solution took just few minutes with a simple discrete probability approximation in contrast to more elaborate and mathematically complex free-boundary solution procedure for high dimensions. Solution to corresponding continuous time PDEs could be fast too and the real advantage of discrete probability approximation lies in their simplicity and ease of implementation.

The exact distribution of risky growth as earlier stated is log-normal (and normal as  $\Delta T \rightarrow 0$ ) and this implies that we could exactly compute the risky fraction boundaries being estimated. However using the exact distribution is computationally very expensive. With just one period problem (which means  $\Delta T = 0.01$  and we iterate the dynamic programming equations just once) and the above choice of parameters as in Figure 6.6 and 6.7 the exact analytic distribution of risky growth implied risky fraction boundaries of  $(0.141, 1)$  which is reasonably close to that implied by discrete probability approximation  $(0.137, 1)$ . As  $\Delta T \rightarrow 0$  the approximation solution converges to the exact solution.

Figure 6.8 shows the variation of risky fraction boundaries with the transaction cost parameter. Plotting the width of no-transaction boundaries against  $\lambda$  in Figure 6.9 we observe the *boundary width* to be of  $O(\lambda^{1/4})$  by performing a least squares fit of the *width of boundary* against  $\text{Log}(\lambda)$ . The actual data is shown by dots and the smooth curve by the solid line.

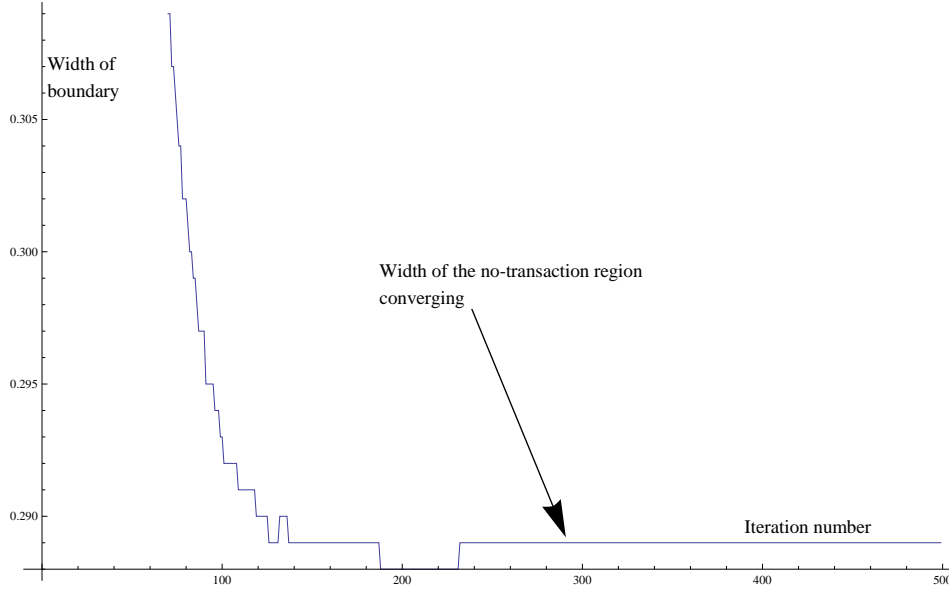


Figure 6.7: Width of no-transaction region plotted against iteration depth:  $\lambda = 0.001$ ,  $T = 5$ ,  $N = 500$ ,  $\Delta T = \frac{T}{N}$ ,  $s = e^{0.07\Delta T}$ ,  $m = 0.182$ ,  $\sigma = 0.4$ . The iterations are the same as in the dynamic programming equation. We start from the last stage to go to the initial time. Where  $T$  is the time horizon for investment,  $N$  is the number of re-balancing nodes.  $\omega$  is the continuous time risk-free rate,  $\lambda$  is the transaction cost factor,  $s$  is the risk free growth over the interval,  $m$  is the drift for continuous time GBM and  $\sigma$  is the volatility for the continuous time GBM. The continuous time GBM implies a risky growth for the risky asset over the interval  $\Delta T$ .

This provides a basis for asymptotic expansion in multi-dimensional PDEs characterizing the transaction cost problem.

The error in the value function (or optimal control law) determination at each stage of dynamic recursion comes from three sources:

(1) Discretization of state space ( number of steps required for a given accuracy is obviously transaction cost and utility structure dependent )

(2) Approximation of value function at each stage of optimization. Especially adjusting the termination accuracy goal of optimization will impact the accuracy of controls at each stage and hence the accuracy in the value function.

(3) Approximation of real probability model of risky growth evolution by a by a discrete probability approximation.

In Figure 6.10 it is seen that for some choice of parameters binomial and trinomial approximations give a pretty close solution. If  $l^{(m)}$  is the boundary based upon suitable discretization and  $m$  time step divisions then we hypothesize  $\|l^{(m)} - l^{(0)}\| \leq \frac{k}{m^\alpha}$  for some suitable constants  $k$  and  $\alpha$ .

### Results for $N \geq 2$ risky assets

Results are provided for both the cases of independent and correlated stock returns. As remarked in [69], [6] and [3] the *continuation region* is similar to an ellipse in two dimensions

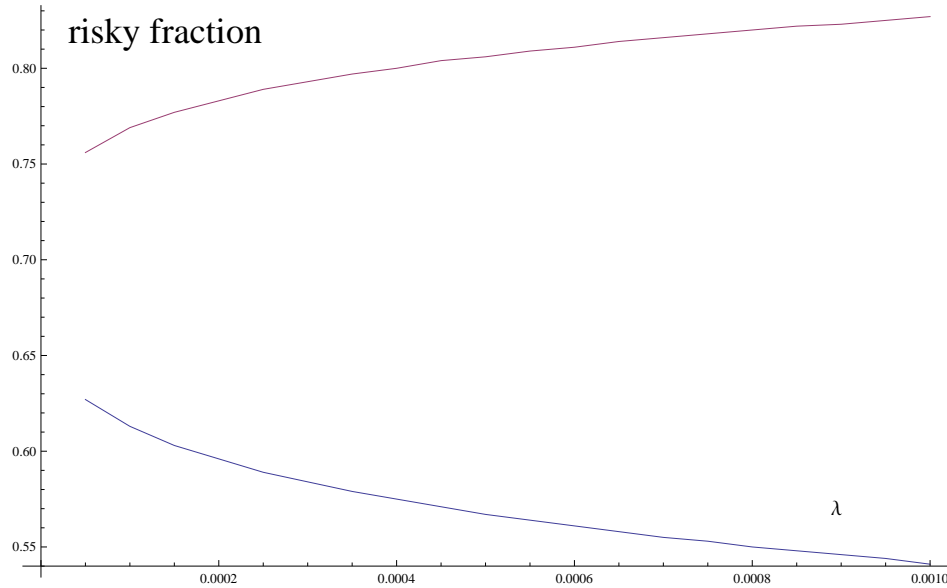


Figure 6.8: Risky fraction boundaries at initial time with respect to transaction cost parameter  $\lambda$ :  $\lambda = 0.001$ ,  $T = 3$ ,  $N = 500$ ,  $\Delta T = \frac{T}{N}$ ,  $s = e^{0.07\Delta T}$ ,  $m = 0.182$ ,  $\sigma = 0.4$ . Where  $T$  is the time horizon for investment,  $N$  is the number of re-balancing nodes.  $\omega$  is the continuous time risk-free rate,  $\lambda$  is the transaction cost factor,  $s$  is the risk free growth over the interval,  $m$  is the drift for continuous time GBM and  $\sigma$  is the volatility for the continuous time GBM. The continuous time GBM implies a risky growth for the risky asset over the interval  $\Delta T$ .

and ellipsoid in three dimensions. The correlation factor serves to stretch the ellipsoid. It seems that above a certain correlation factor the region hits risky fraction axis on either side. This might pose problems for existing methods to solve it as in [71], [6] and [83] for a constrained state variable simplex where the region of inaction is assumed to lie inside and not on the boundary of the simplex. Comparison of our result in the infinite horizon case is done using the method in [69] and gives a reasonably close answer. It is slightly off from the region implied by the asymptotic analysis of [6] and [3]. As depicted in Figure 6.16, our result for infinite horizon is sufficiently close to the exact result in the literature and reasonably close to approximate asymptotic results. This provides an argument in favor of discrete probability approximation methods as far as accuracy is concerned. Figure 6.14 and 6.15 show no-transaction boundaries at terminal time for independent and correlated stocks respectively. Figure 6.17 and 6.18 shows the geometry of *inaction* at infinite horizon for high *positive* correlation between two stocks. It is seen that the region drifts towards and eventually hits it the risky fraction axis as time progresses. This might pose problems for free boundary PDE solving procedures as the region has sharp boundaries and also for boundary update procedures since the the region lies on the boundary of risky fraction axis [51]. It must be mentioned in context of PDE solving procedures that the boundary of the solution is not known and must be computed as part of the solution itself.

This section provided results exclusively for the fixed cost transaction structure. However, discrete probability approximation based methods seem very promising for arbitrary transaction cost structures. For structures of the Davis Norman type as in [28] and the parameters as in

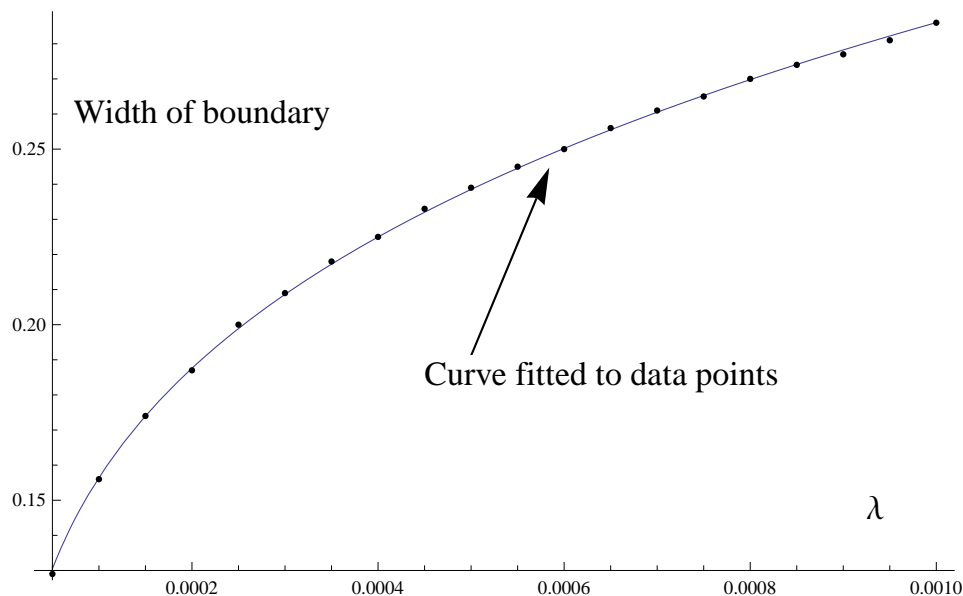


Figure 6.9: Variation of the width of risky fraction boundaries in the last stage with respect to transaction cost parameter and parameters:  $T = 3, N = 100, \Delta T = \frac{T}{N}, s = e^{0.07\Delta T}, m = 0.182, \sigma = 0.4$ . Mathematica's **FindFit[]** command used to directly do non-linear least squares optimization. Where  $T$  is the time horizon for investment,  $N$  is the number of re-balancing nodes.  $\omega$  is the continuous time risk-free rate,  $\lambda$  is the transaction cost factor,  $s$  is the risk free growth over the interval,  $m$  is the drift for continuous time GBM and  $\sigma$  is the volatility for the continuous time GBM. The continuous time GBM implies a risky growth for the risky asset over the interval  $\Delta T$ .

[72] the discrete probability approximation solution implies a solution with a fairly coarse time stepping which agrees with the infinite horizon solution through boundary update procedure as in [51]. An infinite horizon risky fraction boundary of  $(0.276, 0.606)$  implied by the probability approximation methodology was based upon a  $\Delta T = 3/40$  it just took couple of seconds for 80 iterations ! This is reasonably close to the value quoted as in [73]. We note that getting exact solution using analytic techniques could be very fast tough but discrete probability approximation based method possesses the advantage of being intuitive and easy to implement. We have also had promising results in higher dimensions using numerical probability approximation for problems of the Davis Norman type. We believe from the structure of problem that the ODEs and PDEs might become stiff for some parameters. This is supported by the fact that in Figure 6.18 shows a very small no transaction region for some choice of parameters which means the boundaries conditions are very rapidly changing! We note that if implicit PDE techniques are used stiffness is not an issue. However, implicit techniques for free-boundary problems might be very elaborate and complex. In contrast a discrete probability approximation method is simple, intuitive and easily implementable.

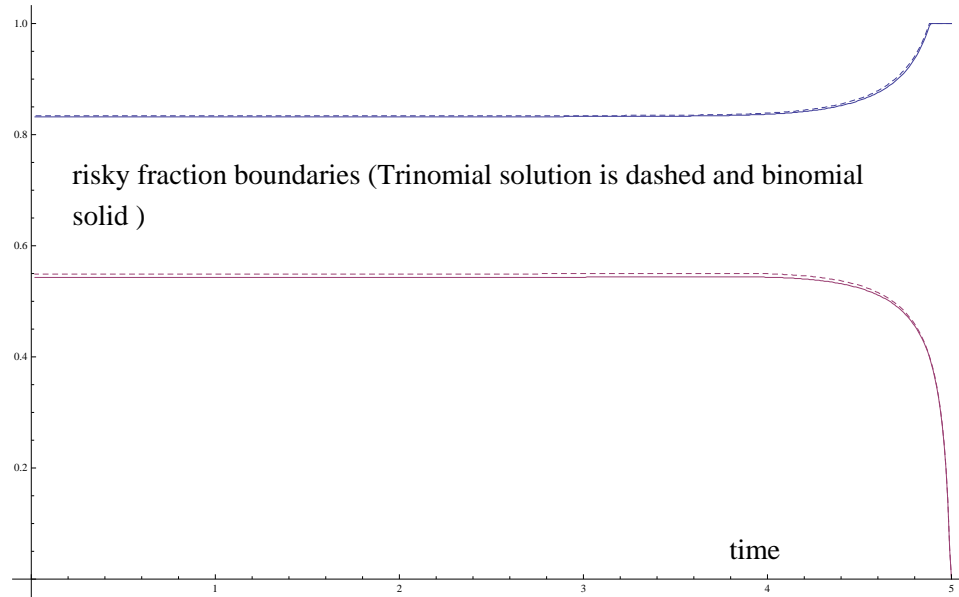


Figure 6.10: Risky boundary approximation: Comparing trinomial approximation for approximate normal with binomial approximation for exact log-normal with  $\lambda = 0.001$ ,  $T = 5$ ,  $N = 500$ ,  $\Delta T = \frac{T}{N}$ ,  $s = e^{0.07\Delta T}$ ,  $m = 0.182$ ,  $\sigma = 0.4$ . Where  $T$  is the time horizon for investment,  $N$  is the number of re-balancing nodes.  $\omega$  is the continuous time risk-free rate,  $\lambda$  is the transaction cost factor,  $s$  is the risk free growth over the interval,  $m$  is the drift for continuous time GBM and  $\sigma$  is the volatility for the continuous time GBM. The continuous time GBM implies a risky growth for the risky asset over the interval  $\Delta T$ .

#### 6.1.4 Model risk: optimal policies when risky portfolio growth follows an arbitrary distribution

In practice the theoretical distribution of risky growth is rarely known. We examine the cases where the actual distribution differs from a normal or log-normal distribution for an arbitrary small time interval. We examine the one-dimensional case and assume the distributions have the same first and second moments as if the risky growth were to follow a log-normal distribution. Results are provided in Tables 6.1 and 6.2.

It is interesting to note that the optimal policy in inverse gamma distribution case does not appear to be that distribution sensitive since a log-normal distribution with the same first and

<i>order</i>	risky fraction boundaries using inverse Gamma distribution
2	(0.137,1)
3	(0.144,1)
5	(0.142,1)
Exact inverse Gamma distribution	(0.142,1)

Table 6.1: same first and second moments as an equivalent log-normal with:  $\lambda = 0.001$ ,  $T = 0.04$ ,  $N = 1$ ,  $\Delta T = \frac{T}{N}$ ,  $s = e^{0.07\Delta T}$ ,  $m = 0.182$ ,  $\sigma = 0.4$ .

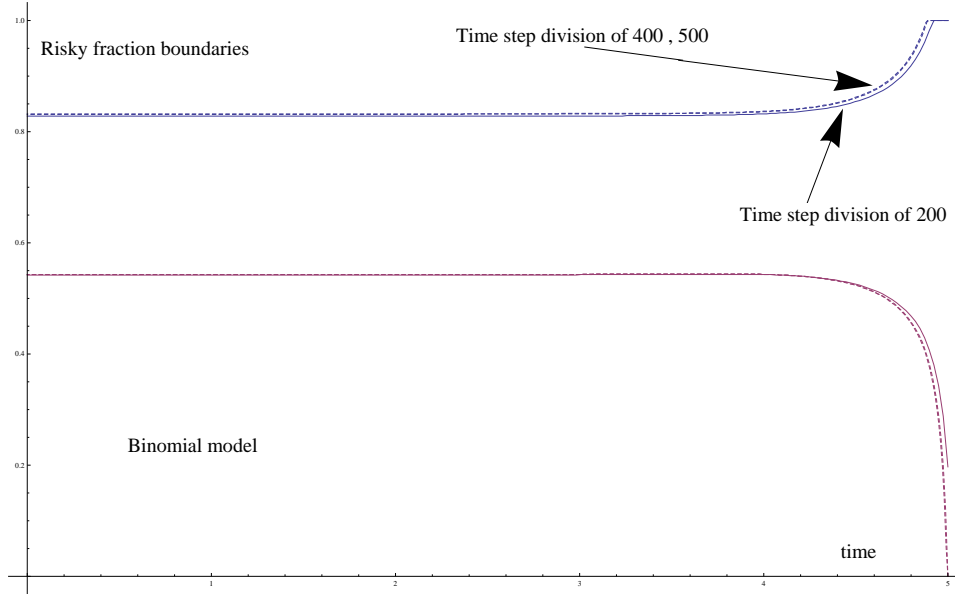


Figure 6.11: Risky boundary approximation: Varying time step divisions in Binomial approximation for exact log-normal with  $\lambda = 0.001, T = 5, N = 500, \Delta T = \frac{T}{N}, s = e^{0.07\Delta T}, m = 0.182, \sigma = 0.4$ . Where  $T$  is the time horizon for investment,  $N$  is the number of re-balancing nodes.  $\omega$  is the continuous time risk-free rate,  $\lambda$  is the transaction cost factor,  $s$  is the risk free growth over the interval,  $m$  is the drift for continuous time GBM and  $\sigma$  is the volatility for the continuous time GBM. The continuous time GBM implies a risky growth for the risky asset over the interval  $\Delta T$ .

second moments give risky fraction boundaries of  $(0.141, 1)$  at initial time.

Also the optimal policy in gamma distribution case does not appear to be that distribution sensitive since a log-normal distribution with the same first and second moments give risky fraction boundaries of  $(0.141, 1)$  at initial time.

By increasing the order of moment matching both distributions give boundaries exactly the same as given by exact distributions.

### 6.1.5 Analyzing finite horizon boundaries

It is always possible to compare the finite horizon solution we obtain under different probability deformations of the exact model and see their closeness. Probability deformation schemes

order	risky fraction boundaries using Gamma distribution
2	$(0.137, 1)$
3	$(0.141, 1)$
5	$(0.14, 1)$
Exact Gamma distribution	$(0.14, 1)$

Table 6.2: same first and second moments as an equivalent log-normal with:  $\lambda = 0.001, T = 0.04, N = 1, \Delta T = \frac{T}{N}, s = e^{0.07\Delta T}, m = 0.182, \sigma = 0.4$ .

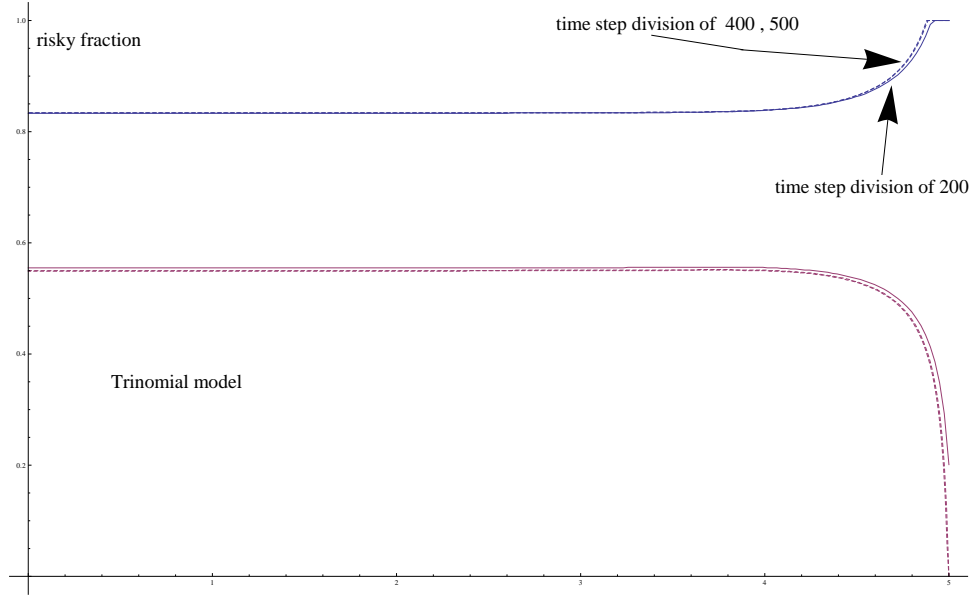


Figure 6.12: Risky boundary approximation: Varying time step divisions in Trinomial approximation for approximate normal with  $\lambda = 0.001, T = 5, N = 500, \Delta T = \frac{T}{N}, s = e^{0.07\Delta T}, m = 0.182, \sigma = 0.4$ . Where  $T$  is the time horizon for investment,  $N$  is the number of re-balancing nodes.  $\omega$  is the continuous time risk-free rate,  $\lambda$  is the transaction cost factor,  $s$  is the risk free growth over the interval,  $m$  is the drift for continuous time GBM and  $\sigma$  is the volatility for the continuous time GBM. The continuous time GBM implies a risky growth for the risky asset over the interval  $\Delta T$ .

(scheme,boundary)	lower boundary	upper boundary
SQID with $\gamma_\ell = 1/20$	0.5585	0.849
Moment deformation with $\gamma_\ell = 1/25$	0.547	0.8395
Moments of order 2 matched	0.543	0.8375

Table 6.3: Comparison of finite horizon no-transaction boundary obtained at  $T = 1$  with parameters:  $\lambda = 0.01, T = 1, N = 100, \Delta T = \frac{T}{N}, s = e^{0.07\Delta T}, m = 0.182, \sigma = 0.4$ .

were discussed in chapter 5. Figure 6.19 shows no-transaction boundary at  $T = 1$  using SQID scheme for some choice of parameters. The results are also summarized in Table 6.3.

### 6.1.6 Computational complexity and error analysis

If the number of time step divisions are  $l$  and state variable space divisions are  $n$  in  $d$  dimensions then we could hypothesize that the maximum time taken for program is  $O(ln^d)$ . However, as it is observed the solution changes much more the closer we are to terminal time ; in the context of optimization more computational effort might be expended here. Accordingly, the actual theoretical time taken would deviate from the maximum theoretical time. In reality the order is numerically found to scale as  $O(l^\alpha n^\eta)$  with  $\alpha$  and  $\eta$  in the interval  $[0, 1]$  for some range of parameters. This is based upon the numerical experimentation reported in Table 6.4 for some range of parameters. For a sufficiently fine discretization we believe interpolation order would



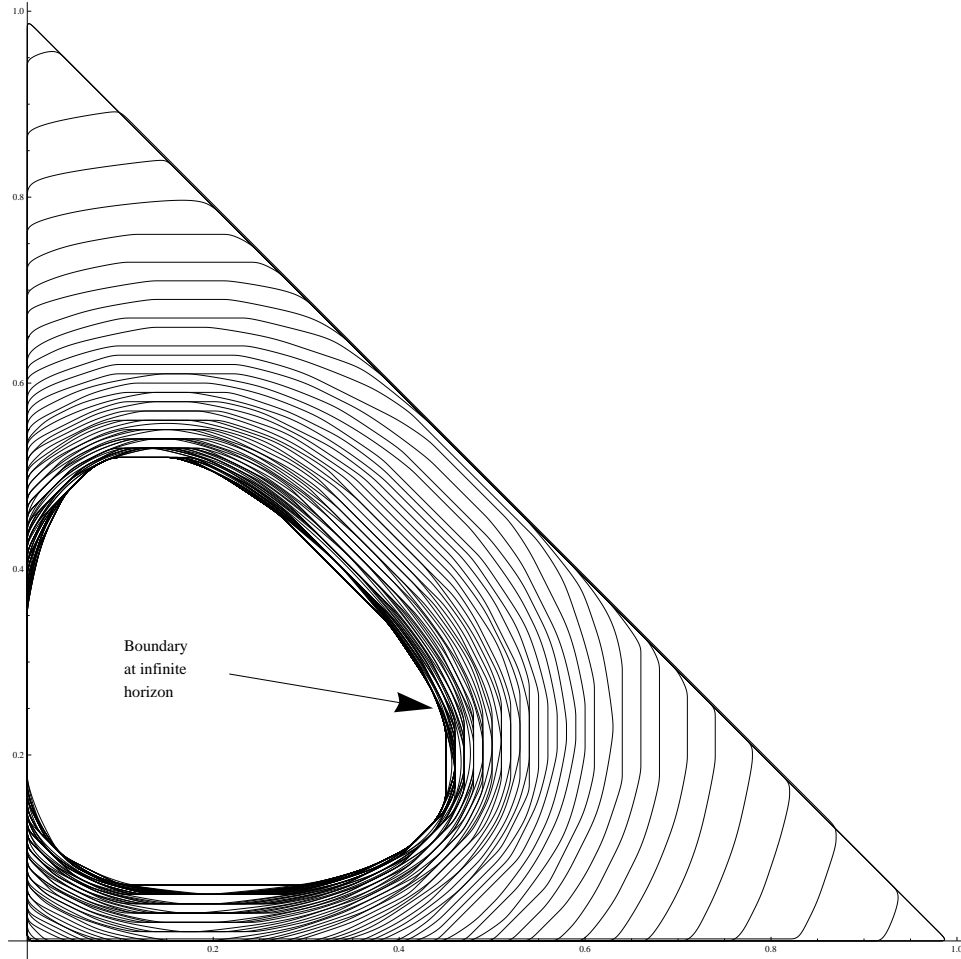


Figure 6.13: Independent stocks in 2-D. Horizontal axis is fraction of wealth in risky asset 1 and vertical axis is fraction of wealth in risky asset 2. Variation of the region of inaction with time:  $\lambda = 0.01$ ,  $T = 5$ ,  $N = 100$ ,  $\Delta T = \frac{T}{N}$ ,  $s = e^{0.10\Delta T}$ ,  $m_1 = 0.13$ ,  $\sigma_1 = 0.40$ ,  $m_2 = 0.15$ ,  $\sigma_2 = 0.44$ . Where  $T$  is the time horizon for investment,  $N$  is the number of re-balancing nodes.  $\omega$  is the continuous time risk-free rate,  $\lambda$  is the transaction cost factor,  $s$  is the risk free growth over the interval,  $m$  is the drift for continuous time GBM and  $\sigma$  is the volatility for the continuous time GBM. The continuous time GBM implies a risky growth for the risky asset over the interval  $\Delta T$ .

not contribute to significant error in our analysis. Such a belief is also an outcome of the study done by [34] in context of lattice based methods to price Asian options.

Several interesting features characterize the solution. However, we will assume from now on that the errors we will be measuring is the error in the no-transaction boundaries at some point in time. More specifically we concentrate on the risky fraction boundaries at the terminal time  $T$ . We will focus on one dimension and the parameter chosen are  $\lambda = 0.001$ ,  $T = 1$ ,  $s = e^{0.07\Delta T}$ ,  $m = 0.182$ ,  $\sigma = 0.4$  and we fit a probability model  $((p, u), (q, l), (1 - p - q, d))$  by matching the first  $k = 5$  moments of the stock price return distribution. There are 5 degrees of freedom and so 5 equations would be needed for moment matching. The actual exact risky fraction boundaries can be computed using dynamic programming principle with sufficiently

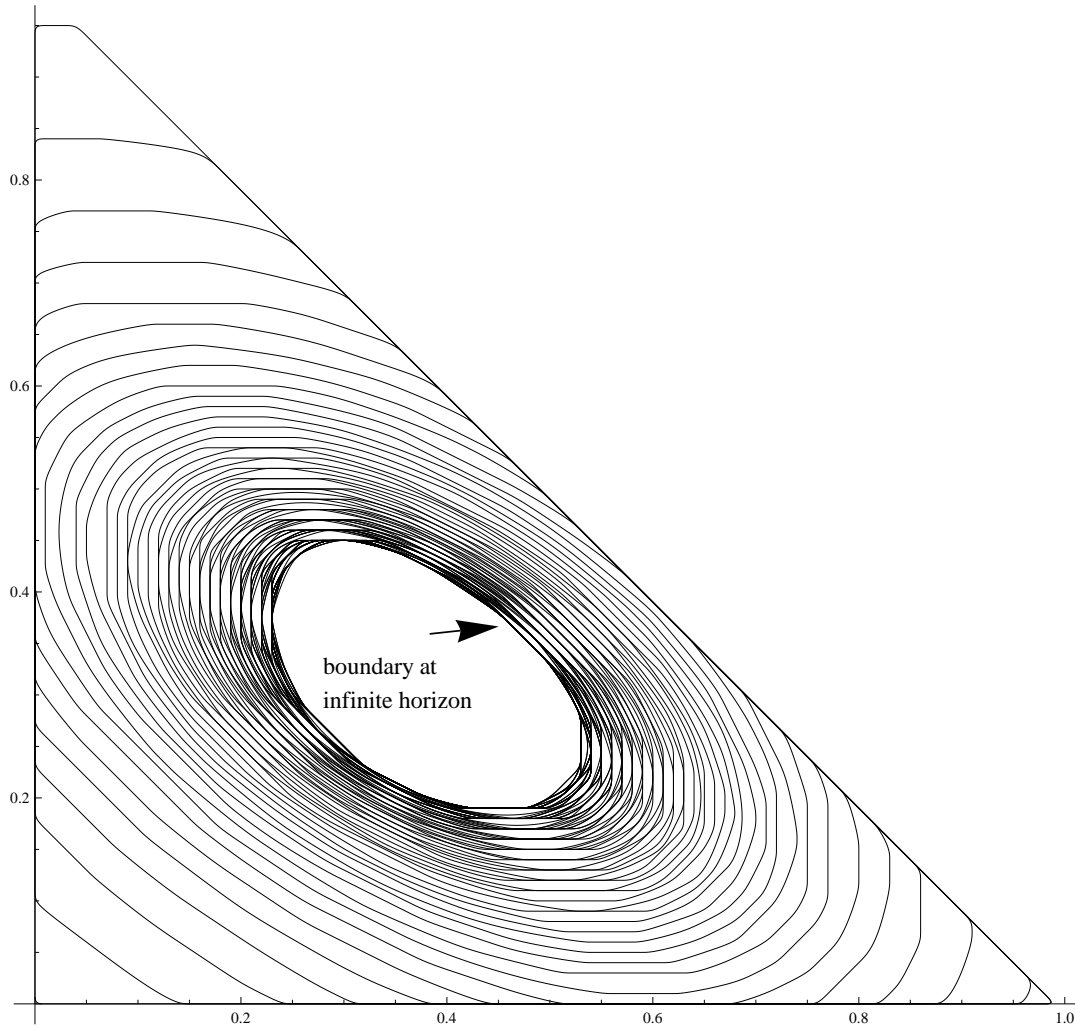


Figure 6.14: Horizontal axis is fraction of wealth in risky asset 1 and vertical axis is fraction of wealth in risky asset 2. Wealth fractions for two assets in a triangular simplex and correlated stocks in 2-D with:  $\lambda = 0.001, T = 2, N = 100, \Delta T = \frac{T}{N}, s = e^{0.07\Delta T}, m_1 = 0.13, \sigma_1 = \sqrt{0.1}, m_2 = 0.15, \sigma_2 = \sqrt{0.17}, \rho = \frac{0.07}{\sigma_1\sigma_2}$ . Here  $T$  is the time horizon for investment,  $N$  is the number of re-balancing nodes.  $\omega$  is the continuous time risk-free rate,  $\lambda$  is the transaction cost factor,  $s$  is the risk free growth over the interval,  $m$  is the drift for continuous time GBM and  $\sigma$  is the volatility for the continuous time GBM. The continuous time GBM implies a risky growth for the risky asset over the interval  $\Delta T$ .

small time stepping using the exact distribution. The error can then be suitably measured from the approximated and the exact values.

The logarithm of the absolute error in no transaction boundaries verses reciprocal of time stepping is observed to be roughly a straight line. A least squares fit can be used to obtain the order of the error. It is numerically observed that absolute error scales with  $\Delta T^\gamma$  for some  $0 \leq \gamma \leq 1$  for this range of parameters.

Similar numerical experiments were performed with the risky fraction space discretization

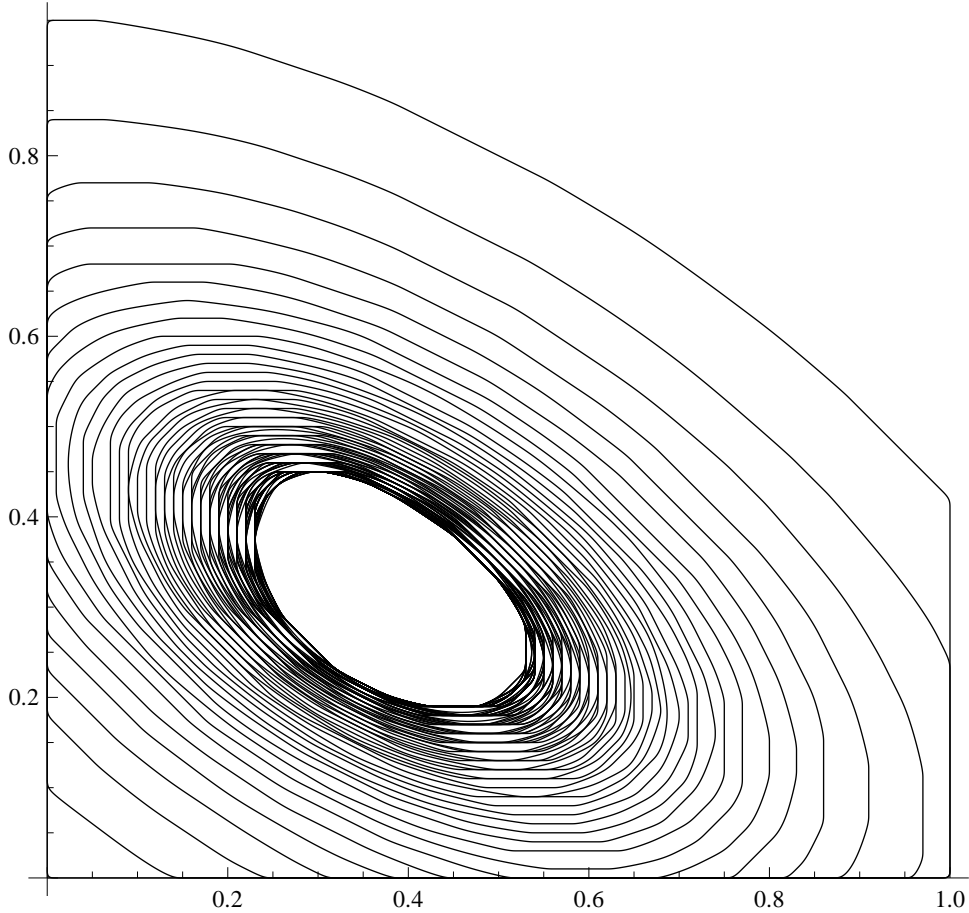


Figure 6.15: Horizontal axis is fraction of wealth in risky asset 1 and vertical axis is fraction of wealth in risky asset 2. Square simplex and correlated stocks in 2-D with:  $\lambda = 0.001$ ,  $T = 2$ ,  $N = 100$ ,  $\Delta T = \frac{T}{N}$ ,  $s = e^{0.07\Delta T}$ ,  $m_1 = 0.13$ ,  $\sigma_1 = \sqrt{0.1}$ ,  $m_2 = 0.15$ ,  $\sigma_2 = \sqrt{0.17}$ ,  $\rho = \frac{0.07}{\sigma_1\sigma_2}$ . Where  $T$  is the time horizon for investment,  $N$  is the number of re-balancing nodes.  $\omega$  is the continuous time risk-free rate,  $\lambda$  is the transaction cost factor,  $s$  is the risk free growth over the interval,  $m$  is the drift for continuous time GBM and  $\sigma$  is the volatility for the continuous time GBM. The continuous time GBM implies a risky growth for the risky asset over the interval  $\Delta T$ .

$da$  and errors are shown in the Table 6.9 below for some choice of parameters as previously mentioned.

Some error analysis for the value function has been done in 2-D in Table 6.10 and 6.11. Tree approximation have been found to be reasonably accurate.

It is also observed increasing the order of moment matching decreases the errors, as intuitively expected. With just a one stage problem and  $T = 0.04$  with the same parameters as chosen above the exact theoretical risky fraction boundary was found to be  $(0.141, 1)$ . The results of altering the order of the moment is shown in the Table 6.12. Figure 6.20 also provides a graphical depiction of how increasing the order of moment matching increases the accuracy in value function.

We note the parameter values chosen here were motivated the values in [69] and are not

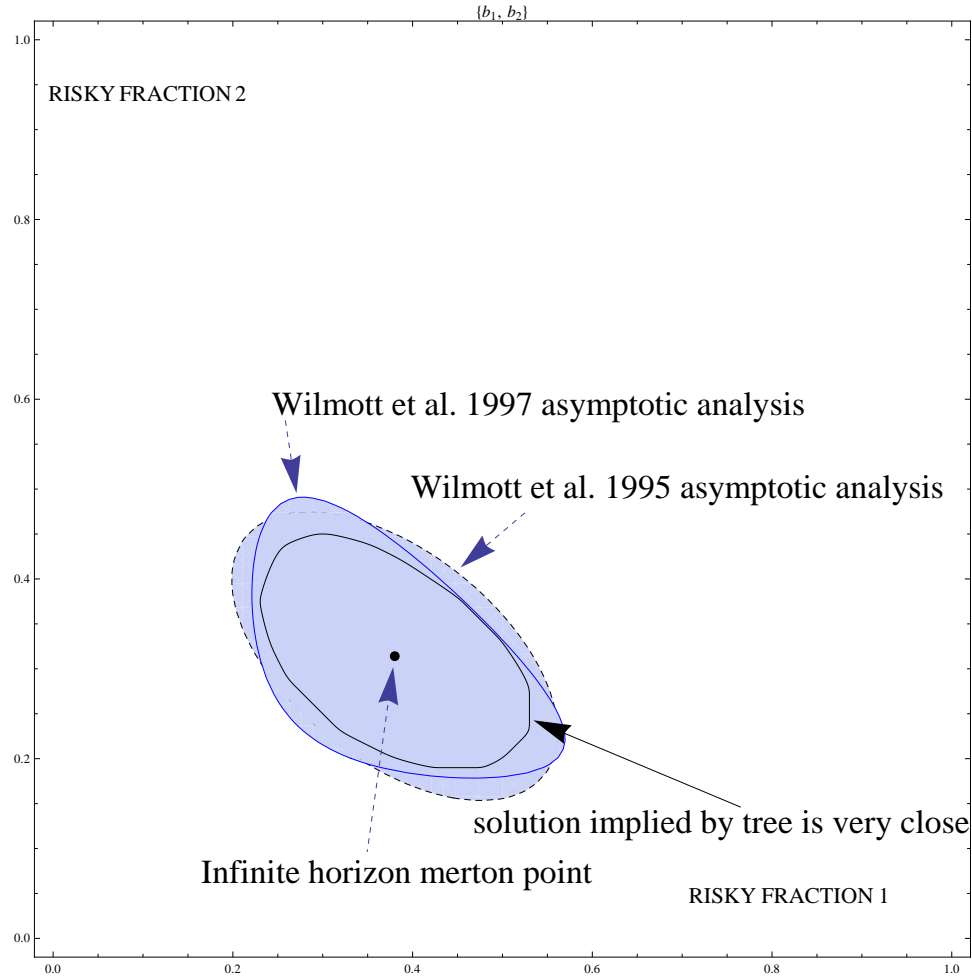


Figure 6.16: Triangle simplex and comparing discrete probability approximation solution to CASE I in [69]:  $\lambda = 0.001$ ,  $T = 2$ ,  $N = 100$ ,  $\Delta T = \frac{T}{N}$ ,  $s = e^{0.07\Delta T}$ ,  $m_1 = 0.13$ ,  $\sigma_1 = \sqrt{0.1}$ ,  $m_2 = 0.15$ ,  $\sigma_2 = \sqrt{0.17}$ ,  $\rho = \frac{0.07}{\sigma_1\sigma_2}$ . Where  $T$  is the time horizon for investment,  $N$  is the number of re-balancing nodes.  $\omega$  is the continuous time risk-free rate,  $\lambda$  is the transaction cost factor,  $s$  is the risk free growth over the interval,  $m$  is the drift for continuous time GBM and  $\sigma$  is the volatility for the continuous time GBM. The continuous time GBM implies a risky growth for the risky asset over the interval  $\Delta T$ .

necessarily the most accurate representation of reality.

## 6.2 Approximate dynamic mean-variance portfolio optimization under transaction costs

### 6.2.1 Introduction

The section considers optimal investment strategy of a *self-financing* investor who invests in risky hedge fund strategies. Risky strategies are modeled via a multi-dimensional geometric

parameters	$\alpha$	$\eta$
$m = 0.182, \sigma = 0.4$	0.567762	0.352002
$m = 0.3, \sigma = 0.8$	0.444675	0.260022
$m = 0.6, \sigma = 1$	0.365901	0.209622

Table 6.4: Scaling of time taken for some range of parameters with  $10 \leq l \leq 50$  and  $200 \leq n \leq 1000$ . Parameters:  $\lambda = 0.001, T = 1, \Delta T = \frac{T}{N}, s = e^{0.07\Delta T}$ .

parameters	$\gamma_1$	$\gamma_1$
$m = 0.182, \sigma = 0.4$	(0.708047, 0.627285)	(1.30029, 2.39293)
$m = 0.3, \sigma = 0.8$	(0.689466, 0.680646)	(0.789441, 0.941182)
$m = 0.6, \sigma = 1$	(0.843559, 0.547407)	(15.3268, -0.256201)

Table 6.5: Scaling of absolute error for some range of parameters. For  $\gamma_1$  we vary  $l$  and  $n$  kept to some large value. Similarly, for  $\gamma_2$  we vary  $n$  and  $l$  kept to some large value. Parameters chosen:  $\lambda = 0.001, T = 1, \Delta T = \frac{T}{N}, s = e^{0.07\Delta T}$ .

$l$	time taken (s)
10	1.578
20	2.719
30	4.203
40	5.578
50	7.047

Table 6.6: Time taken vs time division.  $\lambda = 0.001, T = 5, da = 0.001, \Delta T = \frac{T}{N}, s = e^{0.07\Delta T}, m = 0.182, \sigma = 0.4$ .

$n$	time taken (s)
200	2.75
250	2.578
333	3.266
500	4.328
1000	6.781

Table 6.7: Time taken vs state space division.  $\lambda = 0.001, T = 5, m = 500, \Delta T = \frac{T}{N}, s = e^{0.07\Delta T}, m = 0.182, \sigma = 0.4$ .

$l$	relative percentage error in lower boundary	relative percentage error in upper boundary
10	2.38%	0.834%
20	1.47%	0.596%
30	1.10%	0.477%
40	0.916%	0.358%

Table 6.8: relative percentage error vs time step division.  $\lambda = 0.001, T = 1, da = 0.001, \Delta T = \frac{T}{N}, s = e^{0.07\Delta T}, m = 0.182, \sigma = 0.4$ .

$da$	relative percentage error in lower boundary	relative percentage error in upper boundary
0.005	0.548%	0.358%
0.006	0.914%	0.48%
0.007	1.01%	0.597%

Table 6.9: Error vs state space division.  $\lambda = 0.001, T = 1, N = 100, \Delta T = \frac{T}{N}, s = e^{0.07\Delta T}, m = 0.182, \sigma = 0.4$ .

$(a_1, a_2)$	0.2	0.3	0.4	0.5	0.6
0.2	0.0467%	0.0462%	0.0509%	0.0694%	0.112%
0.3	0.0470%	0.0487%	0.0591%	0.0877%	*
0.4	0.0492%	0.0544%	0.0717%	*	*
0.5	0.0558%	0.0662%	*	*	*
0.6	0.0698%	*	*	*	*

Table 6.10: relative absolute percentage error at different nodal points in 2-D with 2nd order moment matching with:  $\lambda = 0.001, T = 0.05, N = 1, \Delta T = \frac{T}{N}, s = e^{0.07\Delta T}, m_1 = 0.13, \sigma_1 = \sqrt{0.1}, m_2 = 0.15, \sigma_2 = \sqrt{0.17}, \rho = \frac{0.07}{\sigma_1\sigma_2}$ .

$(a_1, a_2)$	0.2	0.3	0.4	0.5	0.6
0.2	0.00639%	0.0183%	0.0438%	0.0923%	0.178%
0.3	0.0135%	0.0309%	0.0652%	0.128%	*
0.4	0.0267%	0.0519%	0.0981%	*	*
0.5	0.0494%	0.0855%	*	*	*
0.6	0.0863%	*	*	*	*

Table 6.11: relative absolute percentage error at different nodal points in 2-D with 3rd order moment matching with:  $\lambda = 0.001, T = 0.05, N = 1, \Delta T = \frac{T}{N}, s = e^{0.07\Delta T}, m_1 = 0.13, \sigma_1 = \sqrt{0.1}, m_2 = 0.15, \sigma_2 = \sqrt{0.17}, \rho = \frac{0.07}{\sigma_1\sigma_2}$ .

order	risky fraction boundaries
2	(0.137,1)
3	(0.142,1)
5	(0.141,1)
Exact	(0.141,1)

Table 6.12: Accuracy dependent on order of moment matching with  $\lambda = 0.001, T = 0.04, N = 1, \Delta T = \frac{T}{N}, s = e^{0.07\Delta T}, m = 0.182, \sigma = 0.4$ .

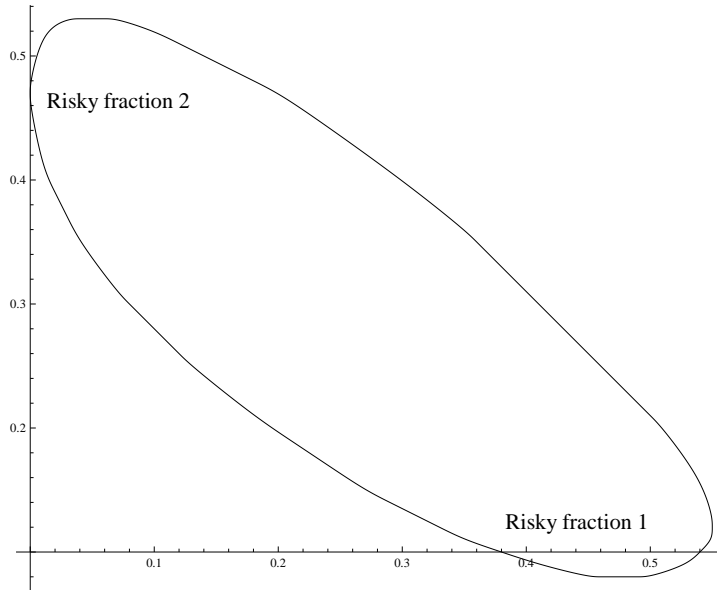


Figure 6.17: Triangle simplex and high correlation:  $\lambda = 0.001, T = 2, N = 100, \Delta T = \frac{T}{N}, s = e^{0.07\Delta T}, m_1 = 0.13\sigma_1 = \sqrt{0.1}, m_2 = 0.15, \sigma_2 = \sqrt{0.17}, \rho = 0.9$ . Where  $T$  is the time horizon for investment,  $N$  is the number of re-balancing nodes.  $\omega$  is the continuous time risk-free rate,  $\lambda$  is the transaction cost factor,  $s$  is the risk free growth over the interval,  $m$  is the drift for continuous time GBM and  $\sigma$  is the volatility for the continuous time GBM. The continuous time GBM implies a risky growth for the risky asset over the interval  $\Delta T$ .

Brownian motion. The discrete-time formulation under a finite horizon allows the investor to return his portfolio to the most optimal fraction of wealth in each asset but he also incurs transaction costs proportional to the amount traded as in [28]. At each stage he decides how much wealth to transfer from strategy  $i$  to strategy  $j$  depending upon the current configuration of wealth and the total amount of wealth. This is in contrast to the existing models where the risk free asset is used for financing. The investor, therefore, does not have significant exposure to the risk-free asset<sup>6</sup>.

The solution is generally an optimal policy characterized by a region of inaction  $\mathcal{R}$  which is expressed in terms of the state variables. When the fluctuations in the price processes drive the proportions of wealth (*risky fraction process*) outside the boundary of the region of inaction the investor transacts *sufficiently* to bring it back to the boundary of the region of inaction  $\partial\mathcal{R}$ . The structure of transaction cost structure and investment objective determines the shape of  $\mathcal{R}$ .

We use a discrete probability approximation approximation to solve the model in one, two and three dimensions. We will show that the discrete time model provides solutions that are reasonably close to its continuous time analogue. In discrete time we will subsequently provide salient features of the model from a financial standpoint.

To the best of our knowledge dynamic mean-ratio portfolio selection under transaction costs has not been suitably addressed in the academic literature using this numerical technique. Mean-variance characterization of problems also allow us to conduct a study from a Sharpe

<sup>6</sup>Applies to hedge funds who invest in risky strategies and want to maximize their Sharpe ratio.

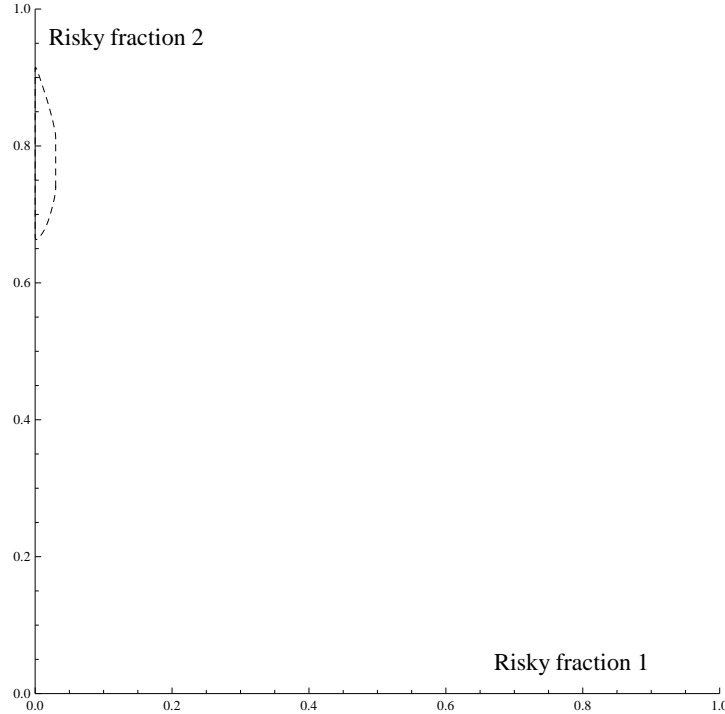


Figure 6.18: For some parameter choice boundaries could be rapidly changing. Triangle simplex and high correlation:  $\lambda = 0.001, T = 2, N = 100, \Delta T = \frac{T}{N}, s = e^{0.07\Delta T}, m_1 = 0.13, \sigma_1 = \sqrt{0.1}, m_2 = 0.15, \sigma_2 = \sqrt{0.17}, \rho = 0.96$ . Where  $T$  is the time horizon for investment,  $N$  is the number of re-balancing nodes.  $\omega$  is the continuous time risk-free rate,  $\lambda$  is the transaction cost factor,  $s$  is the risk free growth over the interval,  $m$  is the drift for continuous time GBM and  $\sigma$  is the volatility for the continuous time GBM. The continuous time GBM implies a risky growth for the risky asset over the interval  $\Delta T$ .

ratio optimization stand point. The paper [22] has studied mean-variance problems under no-transaction cost setting which allows for analytic derivation of the efficiency frontier. Fairly recently, [26] have considered mean-variance problems under transaction in only one dimension albeit in a much different setting involving a risk-free asset. Reference [26] also characterizes the optimal strategy, via a *Skorohod* problem in which a trader tries to keep a certain adjusted bond-stock position, within a no-trade region. It is not clear whether the adjusted position phenomenology used there could be applied when the risk-free asset is absent from the model. The authors of [26] also show that an expected terminal return may not be achievable if the planning horizon is shorter than a critical length  $T^*$ . Our section in this chapter is exclusively devoted to a transfer of wealth model for hedge fund strategies which we will subsequently discuss in more detail.

### 6.2.2 The model

We first illustrate the model in two dimensional case.

Consider a portfolio consisting of risky strategies with the risky strategy  $i$  growing at



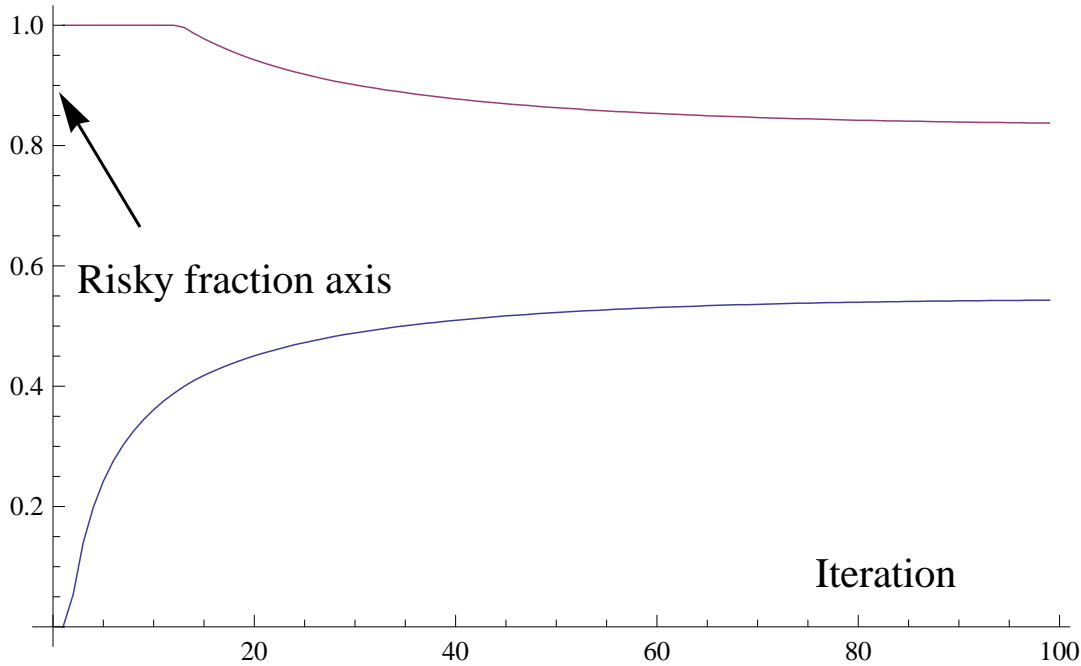


Figure 6.19: Finite horizon no-transaction boundary obtained at  $T = 1$  with parameters:  $\lambda = 0.01, T = 1, N = 100, \Delta T = \frac{T}{N}, s = e^{0.07\Delta T}, m = 0.182, \sigma = 0.4$ . Where  $T$  is the time horizon for investment,  $N$  is the number of re-balancing nodes.  $\omega$  is the continuous time risk-free rate,  $\lambda$  is the transaction cost factor,  $s$  is the risk free growth over the interval,  $m$  is the drift for continuous time GBM and  $\sigma$  is the volatility for the continuous time GBM. The continuous time GBM implies a risky growth for the risky asset over the interval  $\Delta T$ .

a rate  $s_{i,k}$  over the  $k^{\text{th}}$  period. The investor has an initial endowment of  $\bar{W}$ . At the beginning of each period he has the option to transfer wealth from one strategy to another. Let  $W_k^-$  be the wealth immediately before and  $W_k^+$  be the wealth immediately after re-balancing for the  $k^{\text{th}}$  period. If he decides to transfer a wealth  $\Delta_k$  from strategy  $i$  to strategy  $j$  then  $(1 + \lambda_k)\Delta_k$  is deducted from strategy  $i$  and only  $\Delta_k$  added to strategy  $j$  - in other words a certain fraction of his wealth gets lost in the transfer process. Let  $X_{i,k}^-$  be the amount and  $\mathcal{A}_{i,k}^-$  be the fraction of wealth for the  $i^{\text{th}}$  risky strategy relative to base wealth before re-balancing. All the strategies are risky and there are no risk free strategies in this transfer of wealth model.

Let  $\mathcal{M}(t)$  and  $\mathcal{L}(t)$  denote respectively the cumulative transfer of wealth from strategy  $i$  to  $j$  and from  $j$  to  $i$  respectively up to time  $t$ . Let  $\vartheta = (\mathcal{M}, \mathcal{L})$  denote an admissible strategy. Let  $\mathcal{W}^{x,y}(T)$  denote a set of net attainable wealths under transfer of wealth model starting with the initial strategy pair  $(x, y)$  under an admissible strategy.

The investment has a finite time horizon of  $T$ . There are  $N$  periods so that each period is of length  $\Delta T = \frac{T}{N}$  and  $k = 1, 2, \dots, N$ .

For instance for the *Sharpe ratio* problem (with pre-committed mean-variance controls ) the investment objective is:

$$\max \mathcal{S} = \frac{E^{\mathbb{P}}[W_N] - W_0 e^{rT}}{\sqrt{\text{Var}^{\mathbb{P}}[W_N]}} \tag{6.19}$$

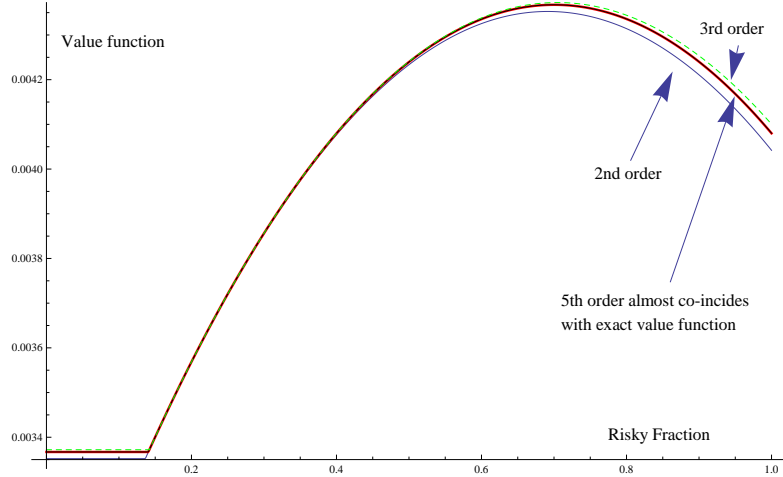


Figure 6.20: Value function approximation for one stage problem with different moment matching. Parameters:  $\lambda = 0.001$ ,  $T = 0.04$ ,  $N = 1$ ,  $\Delta T = \frac{T}{N}$ ,  $s = e^{0.07\Delta T}$ ,  $m = 0.182$ ,  $\sigma = 0.4$ . Where  $T$  is the time horizon for investment,  $N$  is the number of re-balancing nodes.  $\omega$  is the continuous time risk-free rate,  $\lambda$  is the transaction cost factor,  $s$  is the risk free growth over the interval,  $m$  is the drift for continuous time GBM and  $\sigma$  is the volatility for the continuous time GBM. The continuous time GBM implies a risky growth for the risky asset over the interval  $\Delta T$ .

Under pre-committed controls the optimal controls chosen at an initial time are not changed at a later date. Standard dynamic programming could not be applied to our objective in this form as it manifests itself as a *time inconsistent* control problem<sup>7</sup>.

With the above stochastic framework we can represent the portfolio evolution in the form of a stochastic system. At a period  $k$  we have  $W_k^- = \sum X_{\Theta,k}^-$  with  $\Theta = i, j$ . At the beginning of each period if he decides to transfer wealth from strategy  $j$  to strategy  $i$  then the following system of equation holds:

$$X_{i,k}^+ = \mathcal{A}_{i,k}^- W_k^- + \eta_k^{j,i,+} W_k^- \quad (6.20)$$

$$X_{j,k}^+ = \mathcal{A}_{j,k}^- W_k^- - (1 + \lambda_k) \eta_k^{j,i,+} W_k^- \quad (6.21)$$

$$\mathcal{A}_{i,k+1}^- = \frac{\mathcal{A}_{i,k}^+ s_{i,k}}{\mathcal{A}_{i,k}^+ s_{i,k} + (1 - \mathcal{A}_{i,k}^+) s_{j,k}} \quad (6.22)$$

In an analogous fashion we could write the system of equations that should hold if we transfer wealth from strategy  $i$  to strategy  $j$ :

$$X_{j,k}^+ = \mathcal{A}_{j,k}^- W_k^- + \eta_k^{i,j,+} W_k^- \quad (6.23)$$

$$X_{i,k}^+ = \mathcal{A}_{i,k}^- W_k^- - (1 + \lambda_k) \eta_k^{i,j,+} W_k^- \quad (6.24)$$

<sup>7</sup>Time consistency of control problems were discussed in chapter 3.

$$\mathcal{A}_{i,k+1}^- = \frac{\mathcal{A}_{i,k}^+ s_{i,k}}{\mathcal{A}_{i,k}^+ s_{i,k} + (1 - \mathcal{A}_{i,k}^+) s_{j,k}} \quad (6.25)$$

If he decides to do nothing:

$$X_{j,k}^+ = \mathcal{A}_{j,k}^- W_k^- \quad (6.26)$$

$$X_{i,k}^+ = \mathcal{A}_{i,k}^- W_k^- \quad (6.27)$$

$$\mathcal{A}_{i,k+1}^- = \frac{\mathcal{A}_{i,k}^- s_{i,k}}{\mathcal{A}_{i,k}^- s_{i,k} + (1 - \mathcal{A}_{i,k}^-) s_{j,k}} \quad (6.28)$$

At the beginning of each period he decides to transfer wealth from one strategy to another keeping in view his dynamic objective for the terminal wealth  $W_N$  as previously considered. The traditional *risk-return* trade off in finance means that the objective of Sharpe-ratio optimization over a horizon is actually a mean-variance optimization which pits out the highest sharper-ratio i.e. a point on the efficient frontier with the highest sharp-ratio over the given horizon.

His only constraint is  $\eta_{j,i,k}^+ \geq 0$  and  $\eta_{i,j,k}^+ \geq 0$  apart from the more obvious constraint  $W_k^-, W_k^+ \geq 0$ .

**Proposition 6.2.1**  $\mathcal{W}^{x,y}(T)$  is a convex set. Where  $x$  is the initial wealth in first risky asset and  $y$  in the second. Also  $\mathcal{W}^{x,y}(T)$  denotes the set of all attainable wealths at terminal time.

*Proof* The proof follows closely the arguments presented in [26].

Let the pair  $(X_i, Y_i)$  denote the evolution of wealth under the controls  $(M_i, L_i)$ .

Also  $W_1, W_2 \in \mathcal{W}^{x,y}(T)$  and we wish to show for any  $\phi \in [0, 1]$  that  $\phi W_1 + (1 - \phi)W_2 \in \mathcal{W}^{x,y}(T)$ .

Set  $X^{x,M,L} = \phi X_1 + (1 - \phi)X_2$  and  $Y^{x,M,L} = \phi Y_1 + (1 - \phi)Y_2$  if  $M = \phi M_1 + (1 - \phi)M_2$  and  $L = \phi L_1 + (1 - \phi)L_2$ .

Here  $(M_i, L_i)$  is associated with  $(X_i, Y_i)$

Hence,  $W^{x,y}(T) \geq \phi W_1 + (1 - \phi)W_2$ .

If a higher wealth is attainable so a lower wealth must also be attainable.

Thus,  $\phi W_1 + (1 - \phi)W_2 \in \mathcal{W}^{x,y}(T)$  and  $\mathcal{W}^{x,y}(T)$  is convex.

Convexity of attainable wealth is a requirement under which we could convert a constrained problem to an unconstrained problem ([87] and [26]). Dynamic Sharpe-ratio portfolio optimization is actually a *sub-problem* of mean-variance optimization.

Under mean-variance objective our problem is:

$$\begin{aligned} & \min \text{Var}^{\mathbb{P}}[W_N] \\ & \text{subject to } E^{\mathbb{P}}[W_N] = \kappa \end{aligned}$$

The above problem is feasible if there exists at least one admissible strategy satisfying  $E^{\mathbb{P}}[W_N] = \kappa$ . Given  $\kappa$  the optimal strategy  $\zeta^*$  is called an efficient strategy and the corresponding pair  $(E^{\mathbb{P}}[W_N], \text{Var}^{\mathbb{P}}[W_N])$  is called an *efficient pair* on a *smooth curve*  $\mathbf{C}(H, x, y)$ .

Convexity of attainable wealth implies that it is a *convex optimization problem*. By virtue of being a convex optimization problem and using Lagrange duality theorem [87] it could be re-written as:

$$\max_{\beta} \min(E^{\mathbb{P}}[(W_N - d)^2] + 2\beta E^{\mathbb{P}}[(W_N - d)]) \quad (6.29)$$

$$= \max_{\beta} \min E^{\mathbb{P}}[(W_N - b)^2] \quad \text{with} \quad b = d - \beta \quad (6.30)$$

As will be further illustrated below it is numerically more efficient to work with the related unconstrained problem:

$$\min E^{\mathbb{P}}[(W_N - \mathcal{H})^2] \quad (6.31)$$

Letting  $\mathcal{H} = d - \beta$  it is intuitively reasonable that problem (6.30) and (6.31) are equivalent in the sense of optimal control.

Time inconsistency of control problems was discussed in chapter 3. In all our subsequent discussion we will assume a *pre-committed* strategy with the controls estimated at  $t = 0$  and then subsequently held constant. Time-inconsistency implies that a straightforward application of the dynamic programming principle is not possible.

By choosing  $\mathcal{H}$  we are choosing a point on efficient frontier<sup>8</sup>. The problem is reduced to choosing a  $\mathcal{H}$  which maximize the time-horizon Sharpe ratio for a given initial wealth and risky fraction ratio.

Using the dynamic programming principle we can write:

$$\mathcal{J}(W_{k-1}^-, A_{k-1}^-) = \min_{(\zeta)} E^{\mathbb{P}}[\mathcal{J}(W_k^-, A_k^-) | \mathcal{F}_{k-1}] \quad (6.32)$$

Then for  $k = N$ :

$$\mathcal{J}(W_{N-1}^-, A_{N-1}^-) = \min_{(\zeta)} E^{\mathbb{P}}[(W_N^- - \mathcal{H})^2 | \mathcal{F}_{N-1}] \quad (6.33)$$

$$= \min_{(\zeta)} E^{\mathbb{P}}[(W_{N-1}^- \otimes F_{N-1}(A_{N-1}^-) - \mathcal{H})^2 | \mathcal{F}_{N-1}] \quad (6.34)$$

In a similar vein we could recursively go backwards and determine values for  $k = N - 2, N - 3, \dots, 2, 1$ .

The above problem is solved for a particular value of  $\mathcal{H}$  to yield an optimal control  $\zeta^*$  which is then used to obtain the pair  $(E^{\mathbb{P}}[W_N], \text{Var}^{\mathbb{P}}[W_N])$  by solving a system of equations involving  $E^{\mathbb{P}}[(W_N^- - \mathcal{H})^2]$  and  $E^{\mathbb{P}}[(W_N^- - \mathcal{H})]$  to give  $(E^{\mathbb{P}}[W_N], E^{\mathbb{P}}[(W_N)^2])$ . This was discussed in chapter 4. The desired value  $\mathcal{H}^*$  is one that maximizes the Sharpe-ratio over the finite horizon.

We postulate the existence of a Sharpe-ratio maximizing  $\mathcal{H}^*$ . The analytic curve  $\mathbf{C}(\lambda, x, y; \mathcal{H})$  is hypothesized to be a smooth curve monotonic with respect to  $\mathcal{H}$ . Figure 6.21 shows a possible curve traced out by  $\mathcal{H}$ .

<sup>8</sup>Though efficient frontier is a discrete time idea it is easy to generalize it to terminal wealth for a multi-period portfolio theory.

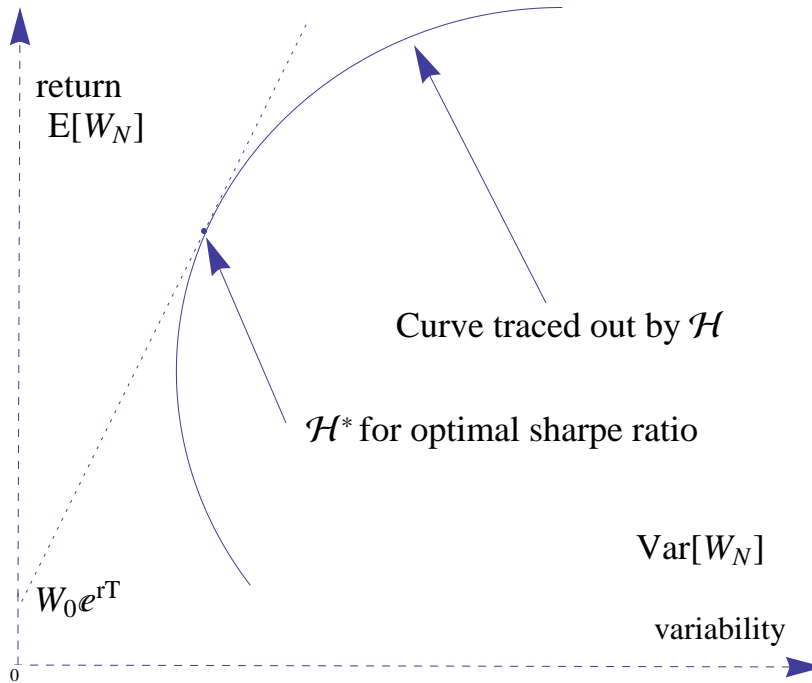


Figure 6.21: Analytic curve  $C(\lambda, x, y; \mathcal{H})$  and Sharpe-ratio maximization

We postulate  $\mathcal{H} \in \mathfrak{R}$  traces out the entire efficient frontier. With  $\overline{\mathcal{H}} = d - \beta^*$  where  $\beta^*$  is optimal by problem 6.30 then  $\mathcal{H} = \overline{\mathcal{H}}$  in 6.31 yields the same efficient point on  $C(\lambda, x, y; \mathcal{H})$ . Also  $d \uparrow$  results in  $\beta^* \downarrow$  so that  $\overline{\mathcal{H}} \uparrow$  and vice versa. We postulate  $\overline{\mathcal{H}} = f(d) = g(\beta^*)$  where  $f$  and  $g$  are continuous monotonic functions.

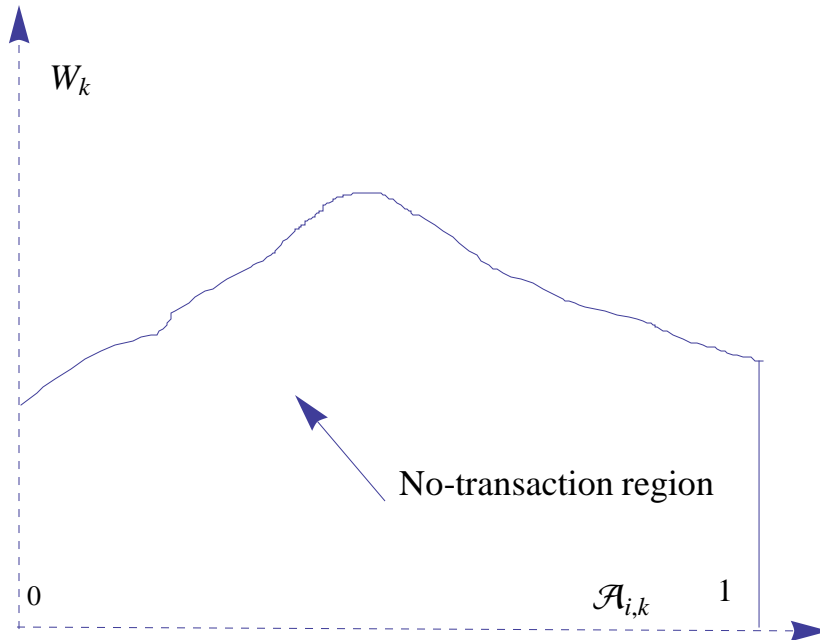
In our discrete framework the risky growth distribution is discretized and bounded so all possible expected returns will not be realized.

The utility structure does not allow separability in wealth so we work with the state space  $(W_k^-, \mathcal{A}_k^-)$  and truncate the state space vectors to reasonable lower and upper bounds. In short a finite state approximation for all the possible states to be attained at beginning of period  $k$  is constructed so that our state variable always remains within the domain  $\Omega$ .

The value of wealth in each risky strategy  $i$  follows Geometric Brownian motion. In a continuous time framework, if  $S_i$  is the value corresponding to the risky strategy  $i$  we have:

$$\frac{dS_i}{S_i} = m_i dt + \sigma_i dZ_t^i \tag{6.35}$$

In discrete-time we will create a discrete probability approximation approximation for the risky growth vector  $s_{i,k}$  so that the respective mean vector  $m$  and covariance matrix  $\Sigma$  over a period  $\Delta T$  match with the continuous-time evolution of vector  $S$ . In the limit  $\Delta T \rightarrow 0$  the discrete-time approximation converges in distribution to the continuous-time distribution.

Figure 6.22: No-transaction region  $\mathcal{R}$  at a time slice

### 6.2.3 Numerical method

The risky fraction is always confined inside  $[0, 1]$  because we only take positions in the risky assets in the interval  $[0, 1]$ . However, the wealth immediately before re-balancing is stochastic because of risky growths and careful attention needs to be paid to its domain.

Two important issues to be addressed are:

- 1- Interpolation errors.
- 2- Extrapolation errors.

The details of how to deal with interpolation and extrapolation error are discussed in section 3.10.

Also say if we are interested in the value function at an initial wealth of  $W_0$  then assuming the risky growth over an interval  $T$  is log-normal with probability density say  $r(T)$  we could choose  $w_{\max} = w_{\max}^0 L \sqrt{\text{Var}(r(T))}$  for  $L \geq 5$  where  $w_{\max}^0$  is the maximum amount of wealth in the two dimensional grid at initial time. It is important to note the wealth is always bounded below by zero. The investor can never go bankrupt if he is not allowed to take short positions under admissible controls.

Figure 6.23 shows a grid in  $(W_k^-, \mathcal{A}_k^-)$  space. The grid is very similar to the kind of finite difference grid used for solving PDEs. By construction, our grid only has restrictions on grid setting as far as interpolation and extrapolation errors are concerned (See [34]). Stability of the dynamic recursion in terms of the relative size of the state variable and time stepping should not be too much of a concern.

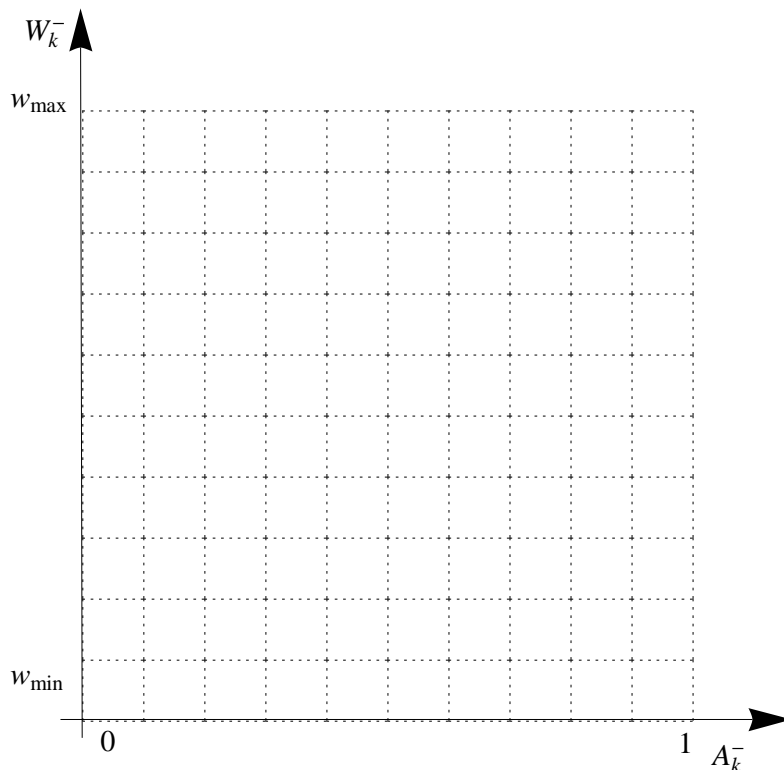


Figure 6.23: Grid of lattice approximation at a time snapshot.

#### 6.2.4 No-transaction regions with time and efficiency frontiers

It is observed, as expected, that the no-transaction regions shrinks going backwards in time. Furthermore, increasing the wealth decreases the risky fraction boundaries in state space. Above a certain wealth level the upper and lower side boundaries collapse to a line. See Figure 6.24 for a visual depiction of the no-transaction region.

Figure 6.25 depicts the intuitively reasonable result that transaction costs shrink the upper part of the efficient frontier inwards. In single period portfolio problems efficient frontiers are a branch of a parabola in risk-return space. Our multi-period model gives efficient frontiers of similar shape. Note, however, the optimal controls were pre-committed. In chapter 7 we will show that pre-committed multi-period efficient frontiers are slightly superior to single period efficient frontiers and hence the value of re-balancing is depicted.

#### 6.2.5 Sharpe ratio time series

As discussed earlier solving mean-variance problems helps us solve Sharpe ratio problems. After having found controls that yield maximum Sharpe ratio it is possible to see the time series behavior of Sharpe ratio in this framework. Let  $S_N$  be the Sharpe ratio measured at initial time with respect to the node  $N$  and  $N \leq T$ . Then we show in Figures 6.26-6.27 the Sharpe ratio behavior of the optimal portfolio compared to myopic portfolios. It is experimentally observed

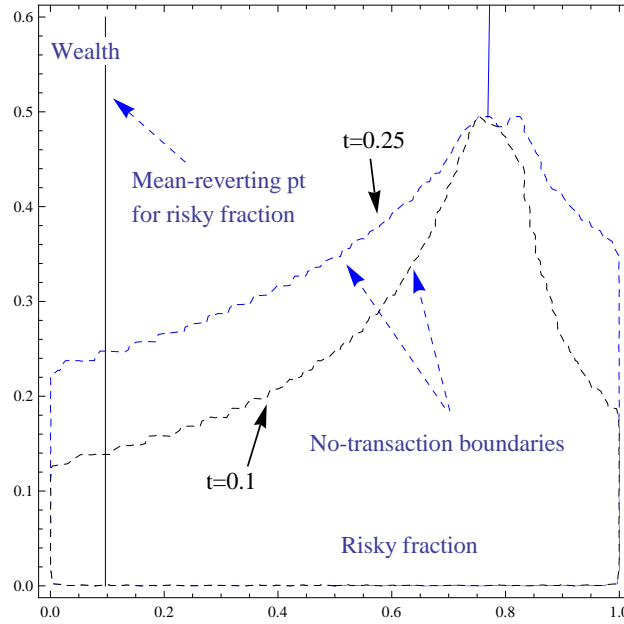


Figure 6.24: Time variation of risky fraction boundaries with parameters  $\lambda = \mu = 0.05$ ,  $T = 0.5$ ,  $N = 10$ ,  $s = e^{0.05\Delta T}$ ,  $m_1 = 0.08$ ,  $\sigma_1 = 0.42$ ,  $m_2 = 0.14$ ,  $\sigma_2 = 0.8$ ,  $\rho = 0.05$ . Where  $T$  is the time horizon for investment,  $N$  is the number of re-balancing nodes.  $\omega$  is the continuous time risk-free rate,  $(\lambda, \mu)$  are transaction cost factors,  $s$  is the risk free growth over the interval,  $m_i$  is the drift for continuous time GBM and  $\sigma_i$  is the volatility for the continuous time GBM. The continuous time GBM implies a risky growth for the risky asset over the interval  $\Delta T$ .

that the Sharpe ratio series shows some improvement compared to a myopic investment in individual risky assets.

## 6.2.6 Comparison of solution with model using the exact distribution

The discrete time solution is observed to be close to that obtained from a model built using an exact distribution. However, along a certain strip where  $W_k = \mathcal{H}$  the deviation is found to be relatively higher. Elsewhere the deviation is low. This highlights the possibility of constructing discrete probability approximation algorithms which give a solution that is close to that implied by exact distributions by ignoring some regions (i.e. strips) along state space and then interpolating.

Table 6.13 shows our discrete probability approximation based solution to be remarkably close to a solution using an exact distribution. This should not be too surprising because for a one period mean-variance problem, discrete probability approximation using second order moment matching give exactly the same solution as one using exact distribution.

Consider just a one period problem in which we invest in a risky assets for which the objective is:



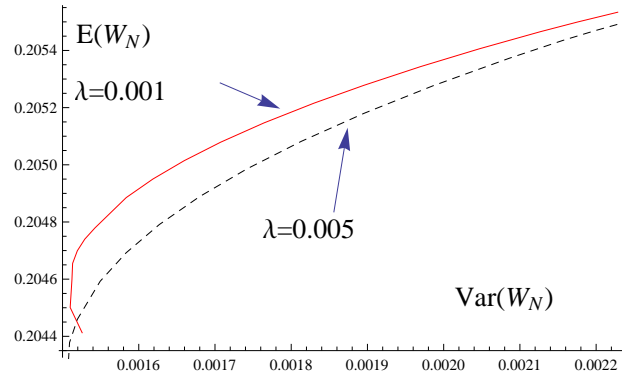


Figure 6.25: Impact of transaction cost on dynamic efficiency frontier with parameters  $T = 0.3, N = 6, s = e^{0.05\Delta T}, m_1 = 0.08, \sigma_1 = 0.42, m_2 = 0.14, \sigma_2 = 0.8, \rho = 0.05$ . Where  $T$  is the time horizon for investment,  $N$  is the number of re-balancing nodes.  $\omega$  is the continuous time risk-free rate,  $(\lambda, \mu)$  are transaction cost factors,  $s$  is the risk free growth over the interval,  $m_i$  is the drift for continuous time GBM and  $\sigma_i$  is the volatility for the continuous time GBM. The continuous time GBM implies a risky growth for the risky asset over the interval  $\Delta T$ .

$(A_k, W_k)$	0.1	0.3	0.5	0.7	0.9
0.1	0.0000165%	$4.30 \times 10^{-6}\%$	$6.90 \times 10^{-6}\%$	$7.24 \times 10^{-7}\%$	$8.87 \times 10^{-7}\%$
0.3	0.0000157%	$4.26 \times 10^{-6}\%$	$6.81 \times 10^{-6}\%$	$7.24 \times 10^{-7}\%$	$8.81 \times 10^{-7}\%$
0.5	0.0000516%	$4.23 \times 10^{-6}\%$	$6.76 \times 10^{-6}\%$	$2.96 \times 10^{-8}\%$	$8.75 \times 10^{-7}\%$
0.7	0.0000153%	$9.35 \times 10^{-6}\%$	$6.66 \times 10^{-6}\%$	$2.19 \times 10^{-8}\%$	$8.69 \times 10^{-7}\%$
0.9	0.0000148%	$1.74 \times 10^{-6}\%$	$6.78 \times 10^{-6}\%$	$3.72 \times 10^{-7}\%$	$2.86 \times 10^{-6}\%$

Table 6.13: Relative absolute percentage error in the value function at time  $t = 0$  different nodal points in 2-D with parameters  $\lambda = \mu = 0.005, T = 0.25, N = 5, s = e^{0.05\Delta T}, m_1 = 0.08, \sigma_1 = 0.42, m_2 = 0.14, \sigma_2 = 0.8, \rho = 0.05$ .

$$\min_{(\zeta)} E^{\mathbb{P}} [(W_{N-1}^- \circ F_{N-1}(\mathcal{A}_{N-1}^-) - \mathcal{H})^2] \tag{6.36}$$

But  $F_{N-1}(\mathcal{A}_{N-1}^-)$  is linear in the risky growths in the framework we had discussed earlier. This means provided the probability model matches the first two moments for risky growths we will get the correct optimal control  $\zeta^*$ .

### 6.2.7 Concluding remarks

The section used lattice based discrete probability approximation approximations to highlight some salient features of *pre-committed* dynamic mean-variance portfolio theory under transaction costs. The modeling framework can be extended to realistic portfolio issues as we shall see in chapter 10.

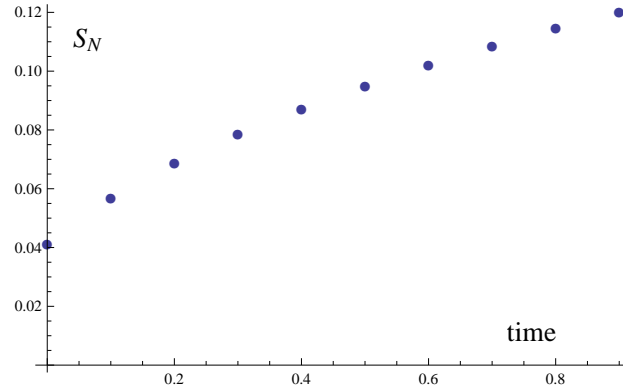


Figure 6.26: Sharpe ratio time series evaluated at  $t = 0$ , initial fraction in asset one =0.5, initial wealth =0.2, for different times with parameters  $\lambda = \mu = 0.005$ ,  $T = 1$ ,  $N = 10$ ,  $s = e^{0.05\Delta T}$ ,  $m_1 = 0.08$ ,  $\sigma_1 = 0.42$ ,  $m_2 = 0.14$ ,  $\sigma_2 = 0.8$ ,  $\rho = 0.05$ . Where  $T$  is the time horizon for investment,  $N$  is the number of re-balancing nodes.  $\omega$  is the continuous time risk-free rate,  $(\lambda, \mu)$  are transaction cost factors,  $s$  is the risk free growth over the interval,  $m_i$  is the drift for continuous time GBM and  $\sigma_i$  is the volatility for the continuous time GBM. The continuous time GBM implies a risky growth for the risky asset over the interval  $\Delta T$ .

### 6.3 Tree approximation of proportional transaction cost model

In this section we consider the discrete time version of the proportional transaction cost model. This model is the most widely used and popular model in the academic literature ( e.g. see [28]). We will try to experiment with the closeness of the discrete time optimal control problems in the finite horizon implied by discrete probability approximation and the exact infinite horizon optimal control. We will try to compute the infinite horizon solution in discrete time by letting  $T \rightarrow \infty$ . Fortunately the infinite horizon solution in continuous time could be computed by the boundary update procedures of the corresponding PDEs [72]. See Figure 2.8 for convergence in boundaries using the boundary update procedure. See Table 6.14 for a comparison of infinite horizon solutions.

The dynamic portfolio choice problem is similar to the model considered in chapter 5. The investor shifts his wealth between assets subject a control strategy given his terminal investment objective.

Consider a simple model where our portfolio consist of a risky and non-risky asset. The investor shifts his wealth between assets subject a control strategy given his terminal investment objective. There are  $N$  periods and an investment horizon of length  $T$  years.

Let us illustrate a transaction process involving two assets. Let  $X_k^+$  be the wealth in the risky asset immediately after re-balancing and  $Y_k^+$  for the risk-free. Also  $\mathcal{A}_k^-$  is the fraction of wealth in the risky asset immediately before re-balancing. Let  $\Delta_k$  be the amount of wealth transferred and transaction cost is incurred which is illustrated by the system of equations below. Denote  $r_k$  as the growth rate of the risky asset and  $s_k$  as the growth rate of risk-free asset.

If asset 1 is bought:

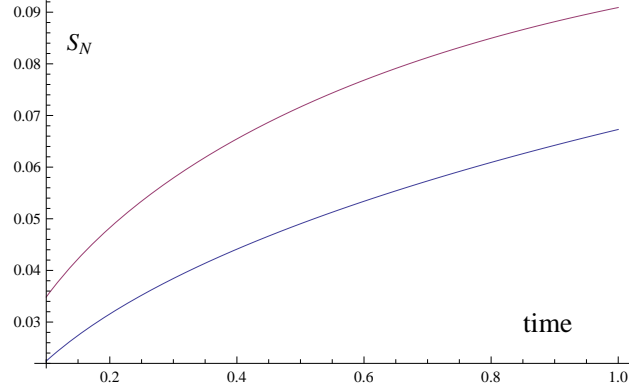


Figure 6.27: Sharpe ratio series with myopic investment in individual assets evaluated at  $t=0$  for different times with parameters  $\lambda = \mu = 0.005$ ,  $T = 1$ ,  $N = 10$ ,  $s = e^{0.05\Delta T}$ ,  $m_1 = 0.08$ ,  $\sigma_1 = 0.42$ ,  $m_2 = 0.14$ ,  $\sigma_2 = 0.8$ ,  $\rho = 0.05$ . Where  $T$  is the time horizon for investment,  $N$  is the number of re-balancing nodes.  $\omega$  is the continuous time risk-free rate,  $(\lambda, \mu)$  are transaction cost factors,  $s$  is the risk free growth over the interval,  $m_i$  is the drift for continuous time GBM and  $\sigma_i$  is the volatility for the continuous time GBM. The continuous time GBM implies a risky growth for the risky asset over the interval  $\Delta T$ .

$$X_k^+ = \mathcal{A}_k^- W_k^- + \Delta_k = \epsilon_k^+ W_k^- \quad (6.37)$$

$$Y_k^+ = (1 - \mathcal{A}_k^-) W_k^- - (1 + \lambda_k) \Delta_k \quad (6.38)$$

$$\mathcal{A}_{k+1}^- = \frac{\epsilon_k^+ r_k}{\epsilon_k^+ r_k + ((1 - \mathcal{A}_k^-) - (1 + \lambda_k)(-\mathcal{A}_k^- + \epsilon_k^+)) s_k} \quad (6.39)$$

If asset 1 is sold:

$$X_k^+ = \mathcal{A}_k^- W_k^- - \Delta_k = \epsilon_k^+ W_k^- \quad (6.40)$$

$$Y_k^+ = (1 - \mathcal{A}_k^-) W_k^- + (1 - \mu_k) \Delta_k \quad (6.41)$$

$$\mathcal{A}_{k+1}^- = \frac{\epsilon_k^+ r_k}{\epsilon_k^+ r_k + ((1 - \mathcal{A}_k^-) + (1 - \mu_k)(\mathcal{A}_k^- - \epsilon_k^+)) s_k} \quad (6.42)$$

If re-balancing is not selected:

$$X_k^+ = \mathcal{A}_k^- W_k^- \quad (6.43)$$

$$Y_k^+ = (1 - \mathcal{A}_k^-) W_k^- \quad (6.44)$$

$$\mathcal{A}_{k+1}^- = \frac{\mathcal{A}_k^- r_k}{\mathcal{A}_k^- r_k + (1 - \mathcal{A}_k^-) s_k} \quad (6.45)$$

The value function takes different form depending upon the investment objective.

time stepping and moment order	lower boundary	upper boundary
10,3	0.304	0.618
20,3	0.292	0.615
50,3	0.283	0.616
60,2	0.275	0.609
Exact	0.2754	0.61596

Table 6.14: Infinite horizon upper and lower boundaries computed using discrete probability approximation with parameters  $m = 0.14$ ,  $\sigma = 0.3$ ,  $\lambda = \mu = 0.05$ ,  $\omega = 0.1$ ,  $s = e^{\omega\Delta T}$ .

For growth rate problem it is:

$$J(W_k^-, A_k^-) = \max E^P \left[ \frac{1}{T} \text{Log}(W_N) | \mathcal{F}_k \right] \quad (6.46)$$

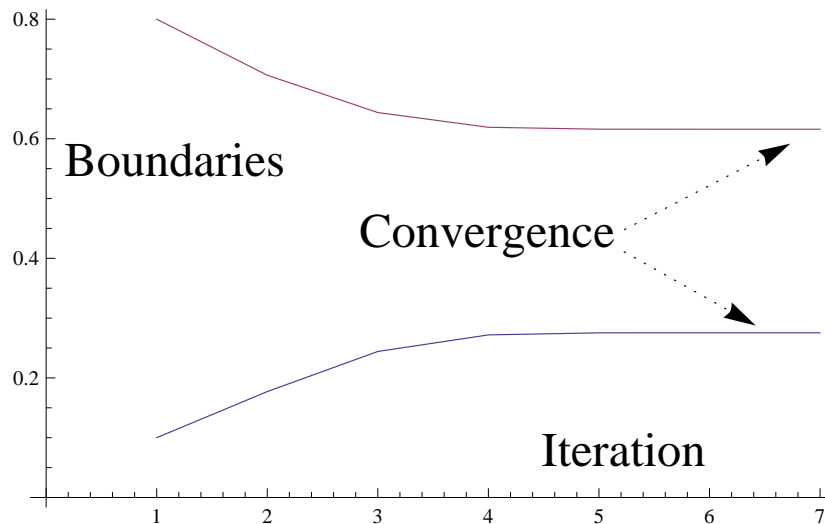


Figure 6.28: Obtaining infinite horizon solution using boundary update numerical methods with parameters  $m = 0.14$ ,  $\sigma = 0.3$ ,  $\lambda = \mu = 0.05$ ,  $\omega = 0.1$ ,  $s = e^{\omega\Delta T}$ . Where  $T$  is the time horizon for investment,  $N$  is the number of re-balancing nodes.  $\omega$  is the continuous time risk-free rate,  $(\lambda, \mu)$  are transaction cost factors,  $s$  is the risk free growth over the interval,  $m$  is the drift for continuous time GBM and  $\sigma$  is the volatility for the continuous time GBM. The continuous time GBM implies a risky growth for the risky asset over the interval  $\Delta T$ .

Let's analyze at a particular time instead of infinite horizon. It is always possible to compute the solution with  $\Delta T$  time stepping using exact distribution and see how close it is to a discrete probability approximation based solution. Interestingly for a realistic parameter choice the solution is very close as implied by the extreme closeness in no-transaction boundaries. Results are shown in Figure 6.29 where the buy and sell side boundaries almost coincide with the exact solutions.

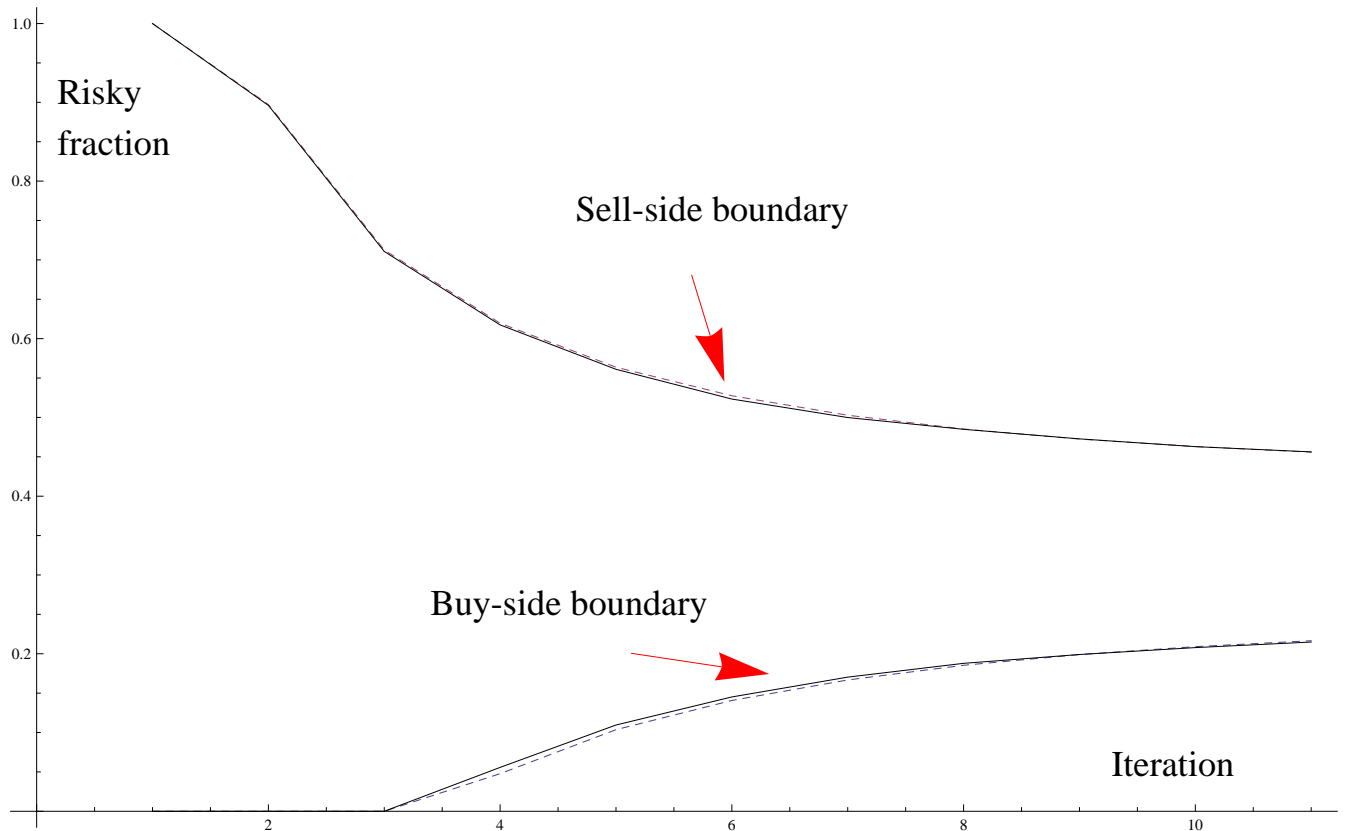


Figure 6.29: Obtaining finite horizon no-transaction boundaries with parameters  $T = 1, N = 10, m = 0.08, \sigma = 0.42, \lambda = \mu = 0.01, \omega = 0.05, s = e^{\omega\Delta T}$ . Here iteration corresponds to the iteration in dynamic programming. Where  $T$  is the time horizon for investment,  $N$  is the number of re-balancing nodes.  $\omega$  is the continuous time risk-free rate,  $(\lambda, \mu)$  are transaction cost factors,  $s$  is the risk free growth over the interval,  $m$  is the drift for continuous time GBM and  $\sigma$  is the volatility for the continuous time GBM. The continuous time GBM implies a risky growth for the risky asset over the interval  $\Delta T$ .

## 6.4 Concluding remarks

Using an exact probability model is computationally intensive. Using discrete probability approximations as an alternative to get approximate solutions is computationally cheap and gives reasonable accuracy for suitable state space discretization. We find discrete probability approximation methods to be a promising tool to solve more advanced problems in the rapidly growing literature on transaction costs. See chapters 8, 9 and 10 for further promising results. In the next chapter we will use solution for an exact distribution to examine the value of re-balancing.

## Chapter 7

# Value of re-balancing portfolios under transaction costs

Computational examples will be provided for an investor investing in a market with GBM assets, the parameters of which switch following a hidden Markov model process. The investor is assumed have perfect foresight about the parameters which will apply over the subsequent rebalance period. The investment horizon is finite and we consider different objectives including growth rate maximization, CRRA utility maximization, CARA utility maximization and mean-variance optimization. A high re-balancing frequency could degrade portfolio performance in the presence of transaction costs if we do not have the option of not re-balancing. The chapter examines the value of re-balancing under different market parameter and investment objectives. It is found that growth rate, CRRA and CARA utility objectives are fairly insensitive to increasing re-balancing frequency. Also the value of re-balancing is highly dependent upon the parameters of the model like investment horizon, volatility etc. We also find that mean-variance problems are slightly more sensitive to re-balancing in the presence of transaction costs. In such situations, we assert the primary reason for an investor to re-balance is not to bring the portfolio to the most optimal *Merton* portfolio state vector which is the optimal fraction of wealth in risky asset or the amount of wealth in risky asset. Instead the primary reason is to update his beliefs about the market parameters.

Indeed computational examples will be provided for an investor with perfect foresight<sup>1</sup> but the market parameters switch over the horizon. In the mean-variance case the investor would be concerned about both - the relative value of parameter change compared to re-balancing to optimal portfolio state vector dependent upon the market parameters. The chapter concludes with an analysis of the stochastic differential equation (SDE) for the relevant state variable processes and provides some intuitive explanations for the aforementioned numerical results.

The main results of this chapter can be summarized by few important points. We provide experimental evidence for most common utility functions like Logarithmic, CRRA, CARA and mean-variance that re-balancing portfolios has a value which quickly saturates with increased re-balancing frequency. Log-utility investors are observed to be the least sensitive to increased re-balancing frequency, while CRRA, CARA, and mean variance investors are slightly more responsive. Our numerical experiments demonstrate that the true the true value of re-balancing

---

<sup>1</sup>By perfect foresight we mean a market analyst with perfect ability to estimate/forecast future parameters.

is one that allows changes in the investment environment to be exploited. Most common academic models assume the drift and volatility for a risky asset to be constant over a time horizon. In reality the drift and volatility are themselves stochastic. If a financial analyst could predict the growth and volatility of a stock over a horizon this would have a great deal of value in the way investment portfolios should be dynamically allocated over time. In fact, for a reasonably short horizon the relevant portfolio state vector for realistic parameter choice would not deviate sufficiently from the most optimal re-balancing point to warrant a transaction. Accurate forecasts of the way model parameters change could add significant value to re-balancing.

The main results of this chapter can be summarized in a few main points:

1-For common utility functions and realistic constant model parameters re-balancing has a value which soon saturates with increased re-balancing frequency.

2-Predicting the expected growth and volatility of risky assets has significant value in improving investment performance via increased re-balancing value.

3-The chapter provides a framework under which a dynamic investor could forecast his changing environment and accordingly dynamically allocate portfolio for best performance given his investment goals.

## 7.1 Introduction

In continuous time portfolio theory re-balancing is done all the time. In stark contrast the Markowitz framework assumes that one portfolio is chosen and the investor goes to sleep until the time horizon is reached. How often should portfolios be re-balanced? Unfortunately only a small number of quantitative studies have been done to address this important issue. To measure value of re-balancing, [50] considers a model with growth rate maximization albeit without transaction costs. Reference [48] considers a model with transaction costs under stochastic volatility using Monte-Carlo techniques stepping forward in time. The set-up of both [50] and [48] is rather restrictive because the actual trading frequency equals the number of available observation points. This means the set-up does not allow the investor the option of not re-balancing. Also [48] considers only HARA utility and [50] the Kelly criterion.

The chapter seeks to provide an analysis under transaction costs for different investment objectives. The trading frequency is less than or equal to the number of observation points thus making our model flexible enough to enable the investor to trade less frequently than the number of observation points. Our model is more computationally extensive because including transaction costs adds to the dimensionality of the state space. We consider the optimal investment strategy of a self-financing investor who invests both in a risky and risk free asset.

## 7.2 Investment model

In all our subsequent analysis we consider the simple investment model already discussed in chapter 5. We briefly present the model again. The investor shifts his wealth between assets subject a control strategy given his terminal investment objective. There are  $N$  periods and an investment horizon of length  $T$  years.

Let us illustrate a transaction process involving two assets. Let  $X_k^+$  be the wealth in the risky asset immediately after re-balancing and  $Y_k^+$  for the risk-free asset. If asset 1 is bought:

$$X_k^+ = \mathcal{A}_k^- W_k^- + \Delta_k = \epsilon_k^+ W_k^- \quad (7.1)$$

$$Y_k^+ = (1 - \mathcal{A}_k^-) W_k^- - (1 + \lambda_k) \Delta_k \quad (7.2)$$

$$\mathcal{A}_{k+1}^- = \frac{\epsilon_k^+ r_k}{\epsilon_k^+ r_k + ((1 - \mathcal{A}_k^-) - (1 + \lambda_k)(-\mathcal{A}_k^- + \epsilon_k^+)) s_k} \quad (7.3)$$

If asset 1 is sold:

$$X_k^+ = \mathcal{A}_k^- W_k^- - \Delta_k = \epsilon_k^+ W_k^- \quad (7.4)$$

$$Y_k^+ = (1 - \mathcal{A}_k^-) W_k^- + (1 - \mu_k) \Delta_k \quad (7.5)$$

$$\mathcal{A}_{k+1}^- = \frac{\epsilon_k^+ r_k}{\epsilon_k^+ r_k + ((1 - \mathcal{A}_k^-) + (1 - \mu_k)(\mathcal{A}_k^- - \epsilon_k^+)) s_k} \quad (7.6)$$

If no transaction occurs:

$$X_k^+ = \mathcal{A}_k^- W_k^- \quad (7.7)$$

$$Y_k^+ = (1 - \mathcal{A}_k^-) W_k^- \quad (7.8)$$

$$\mathcal{A}_{k+1}^- = \frac{\mathcal{A}_k^- r_k}{\mathcal{A}_k^- r_k + (1 - \mathcal{A}_k^-) s_k} \quad (7.9)$$

Consider a portfolio consisting of risky and risk free assets. The risky assets grows at a rate  $r_k$  over the  $k^{\text{th}}$  period. The investor has an initial endowment of  $\bar{W}$ . Let  $W_k^-$  be the wealth immediately before and  $W_k^+$  be the wealth immediately after re-balancing for the  $k^{\text{th}}$  period.

The value function takes different form depending upon the investment objective.

**A-**For the growth rate problem it is:

$$\mathcal{J}(W_k^-, A_k^-) = \max E^P[\text{Log}(W_N) | \mathcal{F}_k]$$

**B-**For CRRA utility problem it is:

$$\mathcal{J}(W_k^-, A_k^-) = \max E^P\left[\frac{W_N^V}{V} | \mathcal{F}_k\right]$$

**C-**For the pre-committed mean variance problem it is:

$\mathcal{J}(W_k^-, A_k^-) = \max E^P[(W(N) - b)^2 | \mathcal{F}_k]$  where we vary  $b$  to get a point on a *mean-variance efficient* frontier.

**D-**For CARA utility problem it is:

$\mathcal{J}(W_k^-, A_k^-) = \max E^P[-e^{-zW_N} | \mathcal{F}_k]$ . This means for the CARA objective the value function at all time nodes will always be negative.

The dynamic programming recursion and modeling framework has already been highlighted in detail in chapters 3, 5 and 6. Tree based approximation on lattices has also been extensively discussed in chapters 5 and 6. In the Logarithmic and CRRA utilities the state space is always confined to the risky fraction space  $[0, 1]$  while in the case of CARA the state



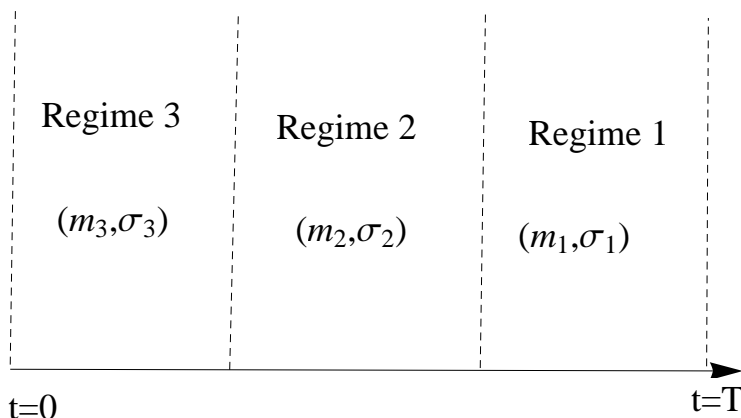


Figure 7.1: Parameters switching over the investment horizon. The three regimes have different drift and volatility for GBM of the risky asset.

space is “the amount of wealth” and is not bounded. For numerical solution purposes we could confine it to an interval  $[0, L]$  where  $L$  is a sufficiently large positive real number. In the earlier chapter 6 we had shown CRRA and log-utility show separability with respect to wealth albeit in a slightly different way. In section 3.10 it was shown CARA utility also possesses separability with respect to wealth. However, mean-variance problems do not allow separability in wealth so the state space contains both wealth and the risky fraction as discussed in chapter 6. While the risky fraction always remains within  $[0, 1]$  the stochastic wealth process need not always be confined to the truncated state space domain. In this chapter we will use the exact probability model over the interval  $\Delta T$  for computations.

For the most part in the chapter we have models in which the parameters are constant over the investment horizon. However, for analysis in some sections we will also consider a very simple regime switching model. In such a switching model the parameters like the drift  $m_i$  and volatility  $\sigma_i$  over the investment horizon are regime dependent. Moreover, we assume that the investor has perfect foresight in terms of estimation ability and knows in advance what the parameters will be in different regimes. In figure 7.1 for instance, regime 1 has parameters  $(m_1, \sigma_1)$ , regime 2 has parameters  $(m_2, \sigma_2)$  and regime 3 has parameters  $(m_3, \sigma_3)$ . The switching mean and volatility means that the discrete approximation for risky growth is different if different regimes. This model will be used in later sections for some analysis in the value of re-balancing.

### 7.3 Numerical analysis of the value of re-balancing

It will be assumed subsequently that the value of re-balancing is embedded in the value function. In CRRA, CARA, log-utility and mean-variance case it depends upon the initial wealth

and risky fraction.

Throughout this chapter *re-balancing frequency* denotes the number of observation points available for re-balancing. The investor has the right to re-balance or not to re-balance at an observation point given the cost benefit analysis encapsulated via dynamic programming. In the numerical example we will use a mix of realistic and unrealistic parameter choices. It is seen that for unrealistic volatility values of above 100 percent the value of re-balancing is much higher compared to realistic values. We apply our framework to realistic values estimated from real-time data for a stock.

### 7.3.1 Log-utility case

We report a few interesting results in this case. First, it is observed that the value of re-balancing in growth rate maximization is not that high given realistic parameter choices. This is shown by figures 7.2-7.5. All the four figures show little value of re-balancing, saturating as soon as re-balancing frequency is increased. However, the value significantly increases if the volatility or time horizon of investment increases. We change the parameters in figures to illustrate these ideas. Clearly volatility of 100 percent is unrealistic and the objective was to show that value of re-balancing is much lower for realistic parameter values.

Interestingly, we also observe formulating the problem as single dynamic optimization as in figure 7.6 yields controls which yield essentially the same value function as one that uses dynamic programming for growth maximization over small intervals in the investment horizon.

We also show a numerical example in figure 7.7 in which investor has limited rights of re-balancing in a problem in which asset mean and variances switch over the horizon. The value of re-balancing is accordingly shown by graphs. This example serves to illustrate that apart from the value of re-balancing to the most optimal state risky fraction - encapsulating re-balancing also has a lot of value for a market in which parameters are non-constant over the investment horizon. The example shows the primary reason for investor to re-balance is encode the most recent parameters in his investment behavior.

### 7.3.2 CRRA case

The results of the CARA are similar to the log-utility case, although it appears that CARA utility shows more increase in value for re-balancing for a similar parameter choice, as measured in absolute value terms. This phenomenon is depicted by figures 7.8-7.13. All these figures show a small value of re-balancing. Increasing the volatility and length of the horizon is found to significantly impact the value of re-balancing.

Similar to the log-utility case we also show a numerical example in figure 7.14 in which the investor has limited rights of re-balancing in a problem in which asset mean and variances switch over the horizon. Exploiting the information of market belief of parameters like switch in drift/volatility carries a value in re-balancing which could be measured in our theoretical framework.

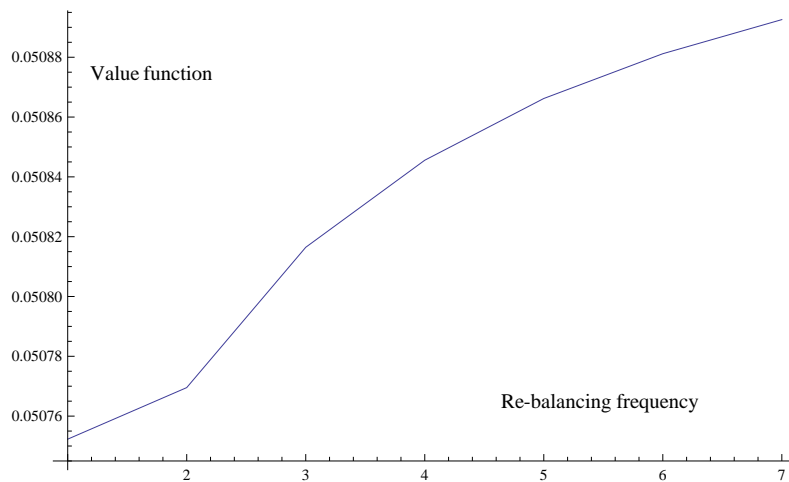


Figure 7.2: Value of re-balancing for log-utility with initial risky fraction=0.5 and wealth =1 the parameters  $\lambda = \mu = 0.05$ ,  $s = e^{0.05\Delta T}$ ,  $a_{min} = 0.001$ ,  $a_{max} = 0.999$ ,  $da = 0.01$ ,  $T = 1$ ,  $m = 0.14$ ,  $\sigma = 0.6$ . Where  $T$  is the time horizon for investment,  $N$  is the number of re-balancing nodes.  $\omega$  is the continuous time risk-free rate,  $(\lambda, \mu)$  are transaction cost factors,  $s$  is the risk free growth over the interval,  $m$  is the drift for continuous time GBM and  $\sigma$  is the volatility for the continuous time GBM. The continuous time GBM implies a risky growth for the risky asset over the interval  $\Delta T$ .  $(a_{min}, a_{max})$  are the bounds for risky fraction state space.

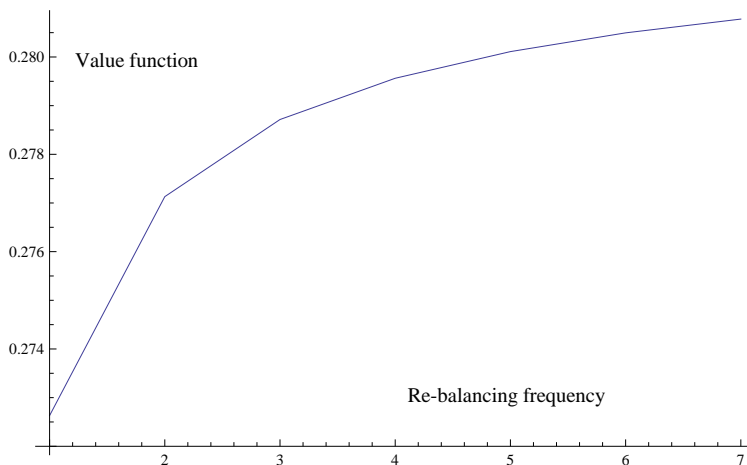


Figure 7.3: Value of re-balancing for log-utility with initial risky fraction=0.5 and wealth =1 the parameters  $\lambda = \mu = 0.05$ ,  $s = e^{0.05\Delta T}$ ,  $a_{min} = 0.001$ ,  $a_{max} = 0.999$ ,  $da = 0.01$ ,  $T = 5$ ,  $m = 0.14$ ,  $\sigma = 0.6$ . Where  $T$  is the time horizon for investment,  $N$  is the number of re-balancing nodes.  $\omega$  is the continuous time risk-free rate,  $(\lambda, \mu)$  are transaction cost factors,  $s$  is the risk free growth over the interval,  $m$  is the drift for continuous time GBM and  $\sigma$  is the volatility for the continuous time GBM. The continuous time GBM implies a risky growth for the risky asset over the interval  $\Delta T$ .  $(a_{min}, a_{max})$  are the bounds for risky fraction state space.

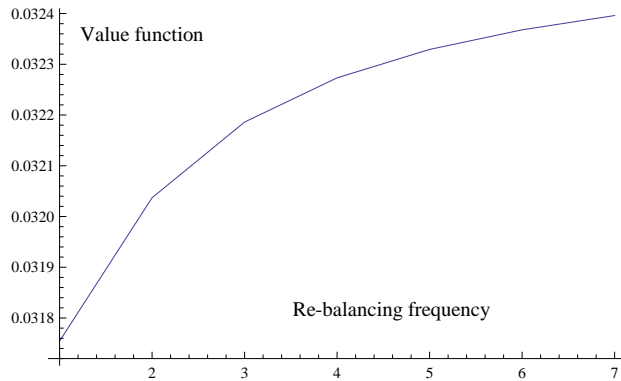


Figure 7.4: Value of re-balancing for log-utility with initial risky fraction=0.5 and wealth =1 the parameters  $\lambda = \mu = 0.05$ ,  $s = e^{0.05\Delta T}$ ,  $amin = 0.001$ ,  $amax = 0.999$ ,  $da = 0.01$ ,  $T = 1$ ,  $m = 0.14$ ,  $\sigma = 1.0$ . Where  $T$  is the time horizon for investment,  $N$  is the number of re-balancing nodes.  $\omega$  is the continuous time risk-free rate,  $(\lambda, \mu)$  are transaction cost factors,  $s$  is the risk free growth over the interval,  $m$  is the drift for continuous time GBM and  $\sigma$  is the volatility for the continuous time GBM. The continuous time GBM implies a risky growth for the risky asset over the interval  $\Delta T$ .  $(amin, amax)$  are the bounds for risky fraction state space.

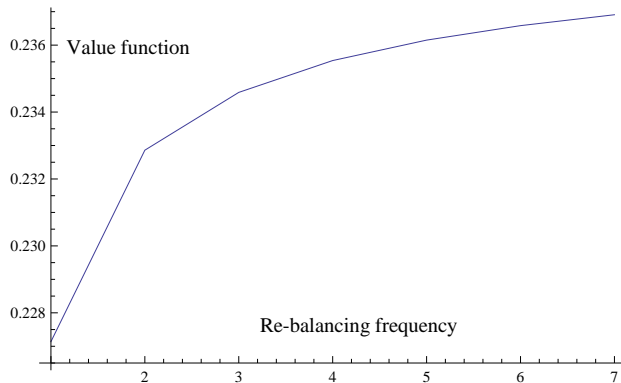


Figure 7.5: Value of re-balancing for log-utility with initial risky fraction=0.5 and wealth =1 the parameters  $\lambda = \mu = 0.05$ ,  $s = e^{0.05\Delta T}$ ,  $amin = 0.001$ ,  $amax = 0.999$ ,  $da = 0.01$ ,  $T = 5$ ,  $m = 0.14$ ,  $\sigma = 0.6$ . Where  $T$  is the time horizon for investment,  $N$  is the number of re-balancing nodes.  $\omega$  is the continuous time risk-free rate,  $(\lambda, \mu)$  are transaction cost factors,  $s$  is the risk free growth over the interval,  $m$  is the drift for continuous time GBM and  $\sigma$  is the volatility for the continuous time GBM. The continuous time GBM implies a risky growth for the risky asset over the interval  $\Delta T$ .  $(amin, amax)$  are the bounds for risky fraction state space.

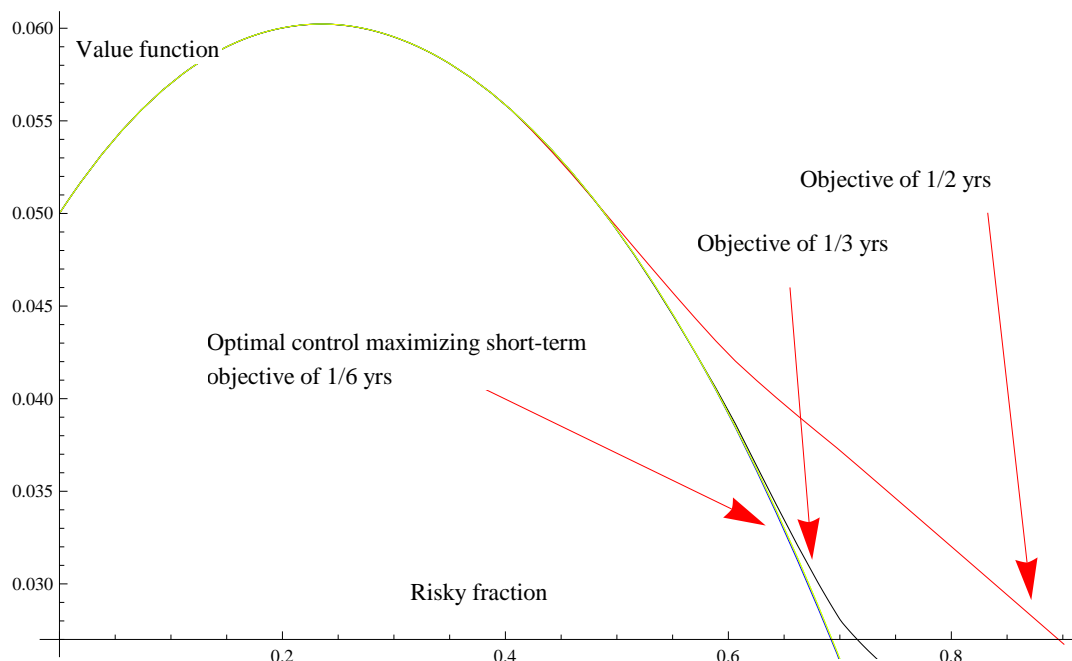


Figure 7.6: Value of re-balancing when objective function is decomposed over small time horizons to yield controls which are then applied to long-term value function with parameters  $\lambda = \mu = 0.05$ ,  $s = e^{0.05\Delta T}$ ,  $amin = 0.001$ ,  $amax = 0.999$ ,  $da = 0.1$ ,  $T = 1$ ,  $m = 0.14$ ,  $\sigma = 0.6$ . Where  $T$  is the time horizon for investment,  $N$  is the number of re-balancing nodes.  $\omega$  is the continuous time risk-free rate,  $(\lambda, \mu)$  are transaction cost factors,  $s$  is the risk free growth over the interval,  $m$  is the drift for continuous time GBM and  $\sigma$  is the volatility for the continuous time GBM. The continuous time GBM implies a risky growth for the risky asset over the interval  $\Delta T$ .  $(amin, amax)$  are the bounds for risky fraction state space.

### 7.3.3 CARA case

Over small horizons CARA utility shows almost no value of re-balancing as was with the case with logarithmic and CRRA utility. Over larger horizons there seems to be a greater than log/CRRA or greater than short-horizon re-balancing value in relative terms. See figures 7.15-7.16.

### 7.3.4 Mean-variance case

For the mean-variance case we chose to have two risky assets. It is observed to show a relatively greater value of re-balancing as depicted by the shift in efficient frontier. These ideas are shown in figure 7.17. However, the value of re-balancing is still not that much! The main reason for this being that we have pre-committed controls in which investor does not change his controls with the arrival of new information.

For added realism we performed analysis on the AMAZON stock. It was assumed to follow GBM so the dynamics could be discretized as:

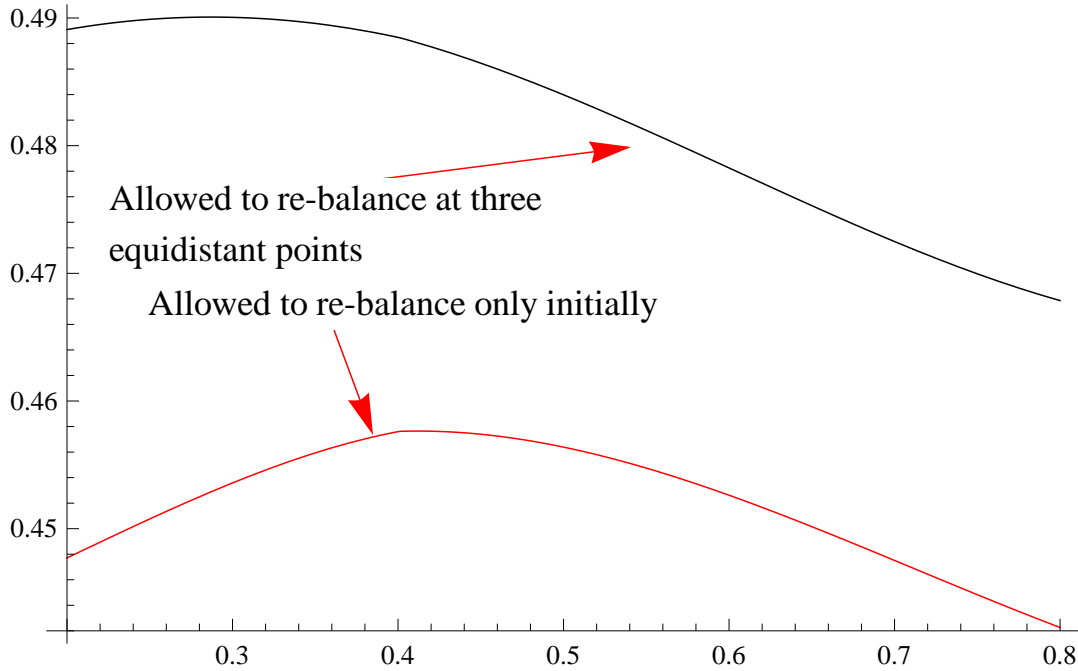


Figure 7.7: Value of re-balancing with parameters that switch over the horizon -investor has perfect foresight. Each regime is of length  $5/3$  years. Parameters for first  $m = 0.4, \sigma = 0.8$ ; for second  $m = 0.3, \sigma = 0.7$ ; and for third  $m = 0.14, \sigma = 0.6$ . Also  $T = 5, \lambda = \mu = 0.05, s = e^{0.05\Delta T}, amin = 0.001, amax = 0.999$ . Where  $T$  is the time horizon for investment,  $N$  is the number of re-balancing nodes.  $\omega$  is the continuous time risk-free rate,  $(\lambda, \mu)$  are transaction cost factors,  $s$  is the risk free growth over the interval,  $m$  is the drift for continuous time GBM and  $\sigma$  is the volatility for the continuous time GBM. The continuous time GBM implies a risky growth for the risky asset over the interval  $\Delta T$ .  $(amin, amax)$  are the bounds for risky fraction state space.

$$\frac{\Delta S}{S} = m\Delta T + \sigma \sqrt{\Delta T} Z_t \quad (7.10)$$

for a Brownian motion  $Z_t$ .

Then estimated values are:

$$\hat{m} = \frac{E[\frac{\Delta S}{S}]}{\Delta T} \quad (7.11)$$

$$\hat{\sigma}^2 = \frac{Var[\frac{\Delta S}{S}]}{\Delta T} \quad (7.12)$$

Using a 180 days look back starting from 1st of May 2012 estimated values were  $\hat{m} = 0.18, \hat{\sigma} = 0.4$ . The value of re-balancing under different scenarios are shown for different utilities are shown. In this example we always form a portfolio with risky and risk free asset. Log-utility, CRRA and mean-variance case (we have AMAZON stock and one risk free asset now ) show a minute value of re-balancing. CARA shows a relatively greater value. We see

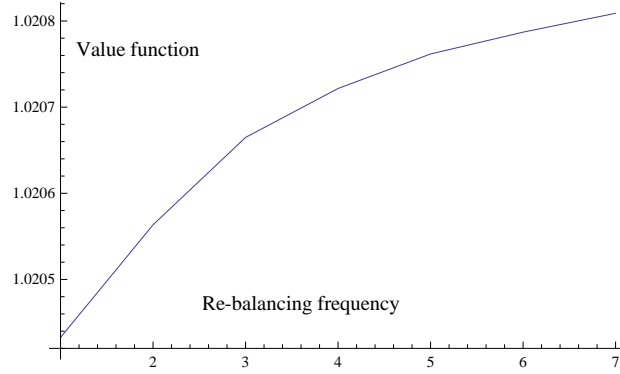


Figure 7.8: Value of re-balancing for CRRA utility with initial risky fraction=0.5 and wealth =1 the parameters  $V = 0.5, \lambda = \mu = 0.05, s = e^{0.05\Delta T}, amin = 0.001, amax = 0.999, da = 0.01, T = 1, m = 0.14, \sigma = 1.0$ . Where  $T$  is the time horizon for investment,  $N$  is the number of re-balancing nodes.  $\omega$  is the continuous time risk-free rate,  $(\lambda, \mu)$  are transaction cost factors,  $s$  is the risk free growth over the interval,  $m$  is the drift for continuous time GBM and  $\sigma$  is the volatility for the continuous time GBM. The continuous time GBM implies a risky growth for the risky asset over the interval  $\Delta T$ .  $(amin, amax)$  are the bounds for risky fraction state space.

once again there is almost little or no value of re-balancing for realistic parameter choices given they remain constant over the horizon. The results are shown in figure 7.18-7.21.

## 7.4 Intuitive explanation of results using the state variable SDE

Let  $X_t$  be the amount of wealth in the risky asset (following GBM ) and  $Y_t$  be the amount of wealth in risk-free asset.

Define the risky fraction as  $\Psi_t = \frac{X_t}{X_t + Y_t}$  where

$$dY_t = \omega Y_t dt \quad (7.13)$$

$$dX_t = X_t(mdt + \sigma dZ_t) \quad (7.14)$$

Using Ito's lemma it can be easily shown that:

$$d\Psi_t = \sigma^2 \Psi(1 - \Psi) \left( \frac{m - \omega}{\sigma^2} - \Psi \right) dt + \sigma \Psi(1 - \Psi) dZ_t \quad (7.15)$$

Similarly, using separability of wealth in the associated HJB equation for no-transaction cost case ( $\lambda = \mu = 0$ ) it is a simple exercise to show the most optimal risky fraction for CRRA case is  $\frac{(m-\omega)}{\sigma^2(1-V)}$  implies  $\frac{(m-\omega)}{\sigma^2}$  as optimal point for growth rate case in the limit.

Similarly, let  $X_t$  be the amount of wealth in the risky asset 1 (following GBM ) and  $Y_t$  be the amount of wealth in risky asset 2 (following GBM ) then if  $\Psi_t = \frac{X_t}{X_t + Y_t}$  we can easily show using Ito's lemma:

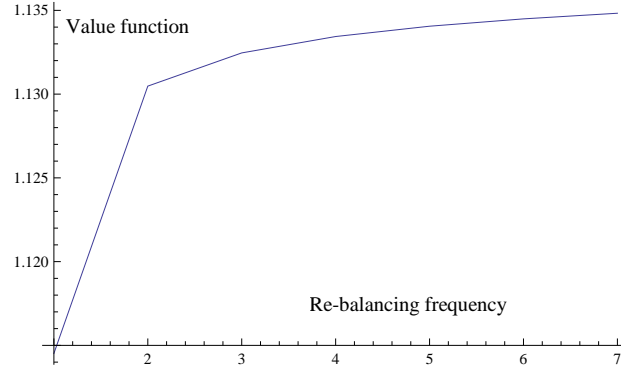


Figure 7.9: Value of re-balancing for CRRA utility with initial risky fraction=0.5 and wealth =1 the parameters  $V = 0.5, \lambda = \mu = 0.05, s = e^{0.05\Delta T}, amin = 0.001, amax = 0.999, da = 0.01, T = 5, m = 0.14, \sigma = 1.0$ . Where  $T$  is the time horizon for investment,  $N$  is the number of re-balancing nodes.  $\omega$  is the continuous time risk-free rate,  $(\lambda, \mu)$  are transaction cost factors,  $s$  is the risk free growth over the interval,  $m$  is the drift for continuous time GBM and  $\sigma$  is the volatility for the continuous time GBM. The continuous time GBM implies a risky growth for the risky asset over the interval  $\Delta T$ .  $(amin, amax)$  are the bounds for risky fraction state space.

$$d\Psi_t = (\sigma_2^2 - \sigma_1^2 - \rho\sigma_1\sigma_2)\Psi(1-\Psi)\left(\Psi - \frac{m_2 - m_1 - \rho\sigma_1\sigma_2}{\sigma_2^2 - \sigma_1^2 - \rho\sigma_1\sigma_2}\right)dt + \Psi(1-\Psi)(\sigma_1 dZ_t^1 - \sigma_2 dZ_t^2) \quad (7.16)$$

It is clear from the SDE in equation (7.16) that increasing the volatility increases the strength of *mean-reversion* to the risky fraction point. For log-utility case this is also the most optimal *Merton* point. However, as discussed for CRRA, this is at some distance from the optimal *Merton* point. Interestingly, increasing volatility also increases randomness in the SDE hence increasing the frequency at which the risky fraction hovers around the mean-reversion point. The overall effect it has on the value of re-balancing could be more rigorously explored analytically for the SDEs given.

As the time horizon becomes longer we are more likely to deviate from the optimal *Merton* point and hence the value of re-balancing increases.

The simple results above can be depicted in no-transaction geometries for Growth rate, CRRA utility, CARA utility and mean-variance case respectively. Clearly, if the mean reverting point for risky fraction line is closer to the no-transaction region the smaller is the value of re-balancing.

We had observed in the log-utility case that the value of re-balancing under transaction cost was very small. This can easily be explained by the fact the mean-reverting point for the risky fraction is always inside the no-transaction region (this mean-reverting point coincides with the *Merton* point and so is hence situated *symmetrically* inside the region). These ideas are depicted in figure 7.22.

The CRRA case is an interesting case in point. As highlighted earlier and shown in figure 7.23 the mean-reverting risky fraction point lies inside the no-transaction the closer we are to terminal time but when we go far away it lies at some distance from the *centre of gravity* of the no-transaction region. Clearly, if the time horizon is small enough then the value of



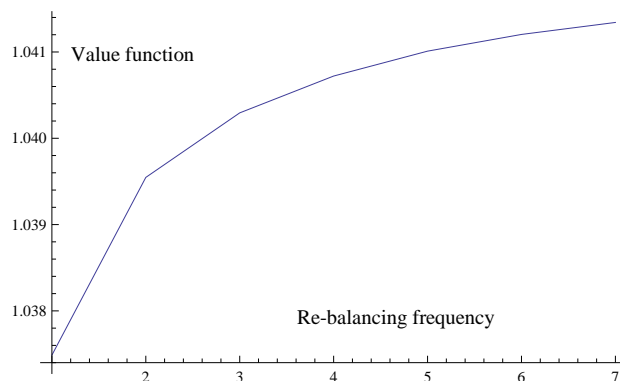


Figure 7.10: Value of re-balancing for CRRA utility with initial risky fraction=0.5 and wealth =1 the parameters  $V = 0.5, \lambda = \mu = 0.05, s = e^{0.05\Delta T}, amin = 0.001, amax = 0.999, da = 0.01, T = 1, m = 0.4, \sigma = 1.5$ . Where  $T$  is the time horizon for investment,  $N$  is the number of re-balancing nodes.  $\omega$  is the continuous time risk-free rate,  $(\lambda, \mu)$  are transaction cost factors,  $s$  is the risk free growth over the interval,  $m$  is the drift for continuous time GBM and  $\sigma$  is the volatility for the continuous time GBM. The continuous time GBM implies a risky growth for the risky asset over the interval  $\Delta T$ .  $(amin, amax)$  are the bounds for risky fraction state space.

re-balancing for CRRA case is small and would become larger the longer is the time horizon. Similarly, we could explain the case for volatility of the market. These ideas are illustrated in the diagram of figure 7.20.

CARA is the most interesting case of all. In the case of AMAZON stock it showed relatively greater value of re-balancing compared to other utility functions. Perhaps the reason for this is that under no-transaction cost the most optimal re-balancing point for CARA utility is to keep a certain amount of wealth in the risky asset and this amount varies with time. We will call this optimal time varying re-balancing under no-transaction cost case as the *Merton* line for CARA utility. In [23] the time varying line is shown to be  $\frac{m-\omega}{\eta\sigma^2 e^{\omega(T-t)}}$ . Under transaction costs we will have buy and sell side boundaries around this line. In any case it seems now that we no longer have a mean-reverting relevant state variable process. On average a GBM asset wealth process would drift away from this line as depicted in Figure 7.24

The mean-variance case for two risky assets discussed in section 7.3.4 is the most interesting because the no-transaction geometry. The problem was solved for a particular point on the efficiency frontier to yield the transaction boundaries as highlighted. The boundaries depend upon the level of wealth and above a certain level of wealth collapse to a *Merton* point. The mean-reverting risky fraction is shown by a line in Figure 7.2.6. It is easily seen that it can be quite far away from the no-transaction region for certain levels of wealth. This agrees closely with our numerical result in which for a particular choice of initial wealth and risky fraction the efficiency frontier showed a slight shift.

This section attempted to explain the numerical results in the above sections intuitively using *no-transaction* geometries.

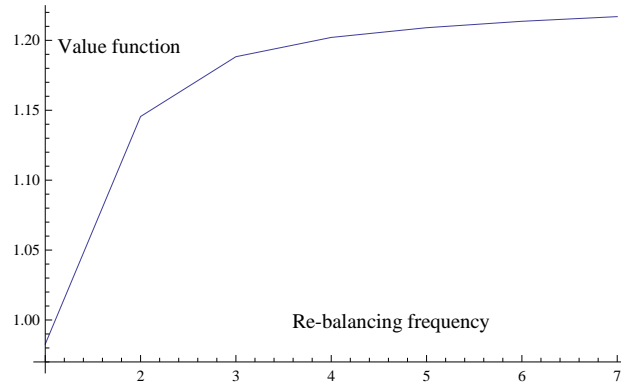


Figure 7.11: Value of re-balancing for CRRA utility with initial risky fraction=0.5 and wealth =1 the parameters  $V = 0.5, \lambda = \mu = 0.05, s = e^{0.05\Delta T}, amin = 0.001, amax = 0.999, a = 0.01, T = 5, m = 0.4, \sigma = 1.5$ . Where  $T$  is the time horizon for investment,  $N$  is the number of re-balancing nodes.  $\omega$  is the continuous time risk-free rate,  $(\lambda, \mu)$  are transaction cost factors,  $s$  is the risk free growth over the interval,  $m$  is the drift for continuous time GBM and  $\sigma$  is the volatility for the continuous time GBM. The continuous time GBM implies a risky growth for the risky asset over the interval  $\Delta T$ .  $(amin, amax)$  are the bounds for risky fraction state space.

## 7.5 Concluding remarks

The chapter highlighted a theoretical framework for the value of re-balancing portfolios. We provided some numerical results and tried to explain them intuitively.

The SDEs analysis in last section opens up a *Pandora's* box for some interesting theoretical analysis. For instance, if  $\phi^-$  and  $\phi^+$  are the no-transaction boundaries then it will be interesting to explore the fraction of time the risky fraction *SDE* stays inside the no-transaction region. It will also be interesting to explore the frequency of barrier hitting of the risky fraction when subjected to the optimal control trading rule. These analytic results could shed interesting ideas on to the subject of value of re-balancing. We could introduce a stopping time random variable as the time the risky fraction process takes to hit the no-transaction boundary given we started from the *Merton* point. An analysis on the probability distribution of this random variable could shed some theoretical results on the value of re-balancing under different investment objectives.

It is possible to make our modeling framework more elaborate by including fixed costs  $F_k$  incurred immediately after re-balancing. That is:

$$W_k^{++} = W_k^+ - \psi_k \quad (7.17)$$

A more economic direction could be sought by comparing the expected marginal utility of re-balancing to the expected marginal dis-utility of not re-balancing. In the next chapter we provide a framework for an investor faced with uncertain transaction costs and the loss of utility suffered as a result of uncertainty.

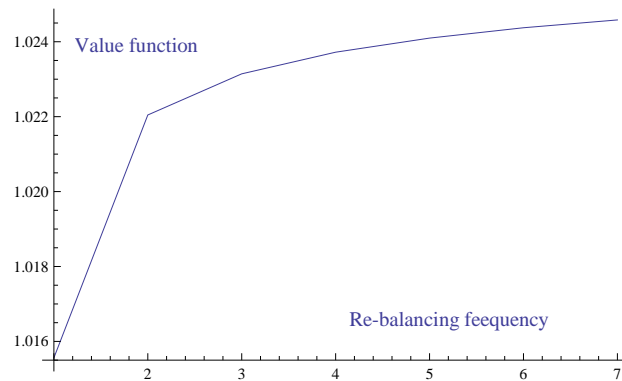


Figure 7.12: Value of re-balancing for CRRA utility with initial risky fraction=0.5 and wealth =1 the parameters  $V = 0.5, \lambda = \mu = 0.05, s = e^{0.05\Delta T}, amin = 0.001, amax = 0.999, da = 0.01, T = 1, m = 0.4, \sigma = 2.0$ . Where  $T$  is the time horizon for investment,  $N$  is the number of re-balancing nodes.  $\omega$  is the continuous time risk-free rate,  $(\lambda, \mu)$  are transaction cost factors,  $s$  is the risk free growth over the interval,  $m$  is the drift for continuous time GBM and  $\sigma$  is the volatility for the continuous time GBM. The continuous time GBM implies a risky growth for the risky asset over the interval  $\Delta T$ .  $(amin, amax)$  are the bounds for risky fraction state space.

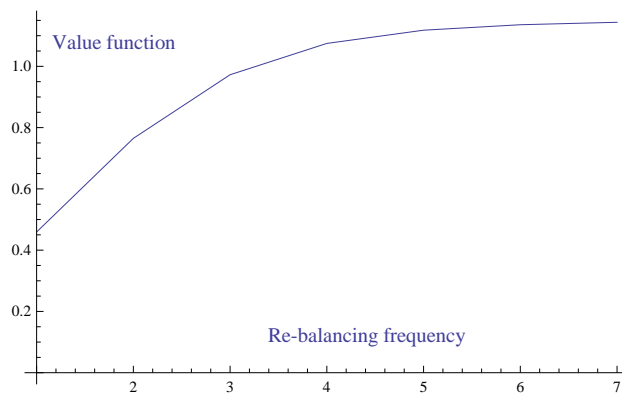


Figure 7.13: Value of re-balancing for CRRA utility with initial risky fraction=0.5 and wealth =1 the parameters  $V = 0.5, \lambda = \mu = 0.05, s = e^{0.05\Delta T}, amin = 0.001, namax = 0.999, da = 0.01, T = 5, m = 0.4, \sigma = 2$ . Where  $T$  is the time horizon for investment,  $N$  is the number of re-balancing nodes.  $\omega$  is the continuous time risk-free rate,  $(\lambda, \mu)$  are transaction cost factors,  $s$  is the risk free growth over the interval,  $m$  is the drift for continuous time GBM and  $\sigma$  is the volatility for the continuous time GBM. The continuous time GBM implies a risky growth for the risky asset over the interval  $\Delta T$ .  $(amin, amax)$  are the bounds for risky fraction state space.

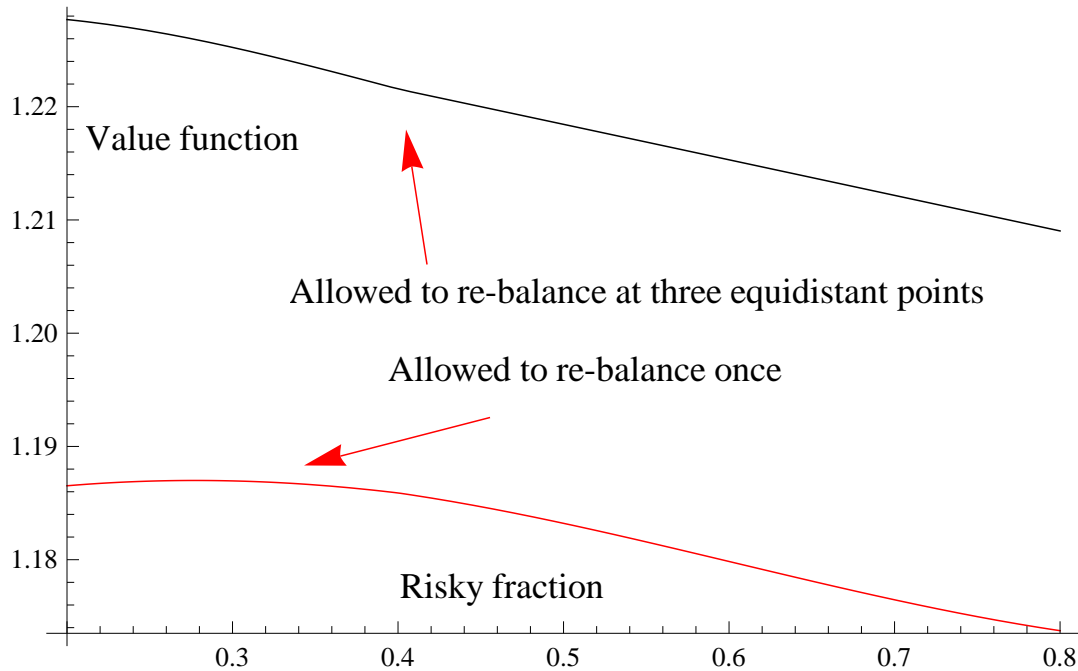


Figure 7.14: Value of re-balancing with parameters that switch over the horizon -investor has perfect foresight. Each regime is of length  $5/3$  years. Parameters for first  $m = 0.4, \sigma = 1.2$ ; for second  $m = 0.3, \sigma = 1.1$ ; and for third  $m = 0.14, \sigma = 1.0$ . Also  $V = 0.5, T = 5, \lambda = \mu = 0.05, s = e^{0.05\Delta T}, amin = 0.001, amax = 0.999$ . Where  $T$  is the time horizon for investment,  $N$  is the number of re-balancing nodes.  $\omega$  is the continuous time risk-free rate,  $(\lambda, \mu)$  are transaction cost factors,  $s$  is the risk free growth over the interval,  $m$  is the drift for continuous time GBM and  $\sigma$  is the volatility for the continuous time GBM. The continuous time GBM implies a risky growth for the risky asset over the interval  $\Delta T$ .  $(amin, amax)$  are the bounds for risky fraction state space.

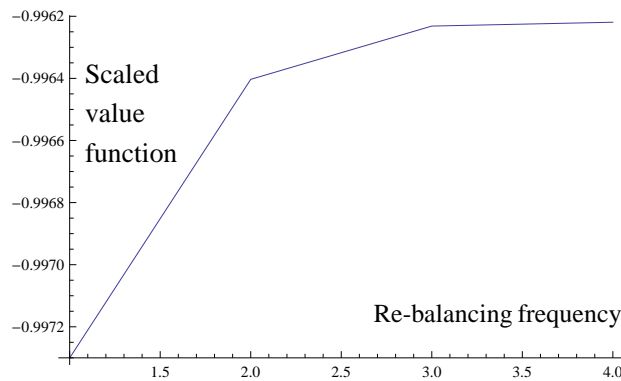


Figure 7.15: Scaled value of re-balancing for CARA utility with initial wealth in risky asset =100 the parameters  $\lambda = \mu = 0.05$ ,  $s = e^{0.05\Delta T}$ ,  $amin = 0.001$ ,  $amax = 0.999$ ,  $da = 0.01$ ,  $T = 1$ ,  $m = 0.14$ ,  $\sigma = 0.6$ . Where  $T$  is the time horizon for investment,  $N$  is the number of re-balancing nodes.  $\omega$  is the continuous time risk-free rate,  $(\lambda, \mu)$  are transaction cost factors,  $s$  is the risk free growth over the interval,  $m$  is the drift for continuous time GBM and  $\sigma$  is the volatility for the continuous time GBM. The continuous time GBM implies a risky growth for the risky asset over the interval  $\Delta T$ .  $(amin, amax)$  are the bounds for risky fraction state space.

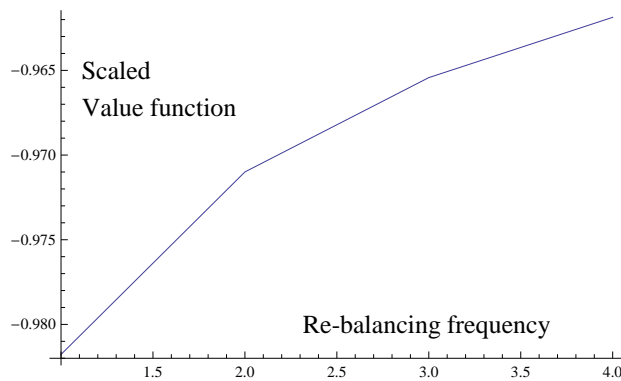


Figure 7.16: Scaled value of re-balancing for CARA utility with initial wealth in risky asset =100 the parameters  $\lambda = \mu = 0.05$ ,  $s = e^{0.05\Delta T}$ ,  $amin = 0.001$ ,  $amax = 0.999$ ,  $da = 0.01$ ,  $T = 5$ ,  $m = 0.14$ ,  $\sigma = 0.6$ . Where  $T$  is the time horizon for investment,  $N$  is the number of re-balancing nodes.  $\omega$  is the continuous time risk-free rate,  $(\lambda, \mu)$  are transaction cost factors,  $s$  is the risk free growth over the interval,  $m$  is the drift for continuous time GBM and  $\sigma$  is the volatility for the continuous time GBM. The continuous time GBM implies a risky growth for the risky asset over the interval  $\Delta T$ .  $(amin, amax)$  are the bounds for risky fraction state space.

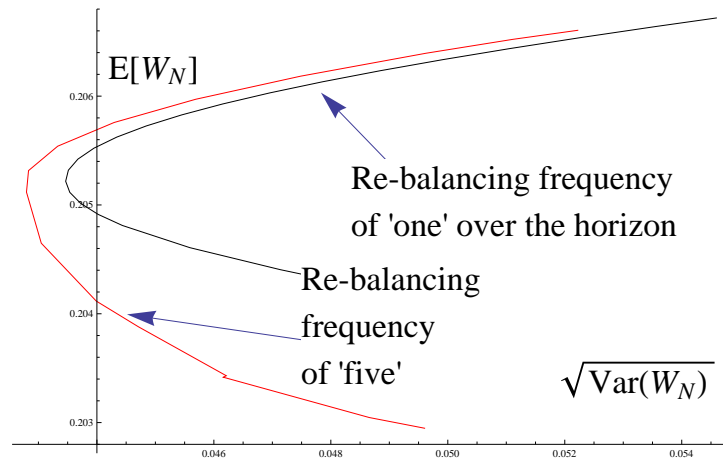


Figure 7.17: Value of re-balancing depicted by a shift in the efficiency frontier calculated for the initial wealth =0.2 and initial risky fraction =0.5. Parameters are chosen as:  $T = 0.3, \lambda = \mu = 0.005, s = e^{0.05\Delta T}, m_1 = 0.08, \sigma_1 = 0.42, m_2 = 0.14, \sigma_2 = 0.8, \rho = 0.05, a_{min} = 0.001, a_{max} = 0.999$ .

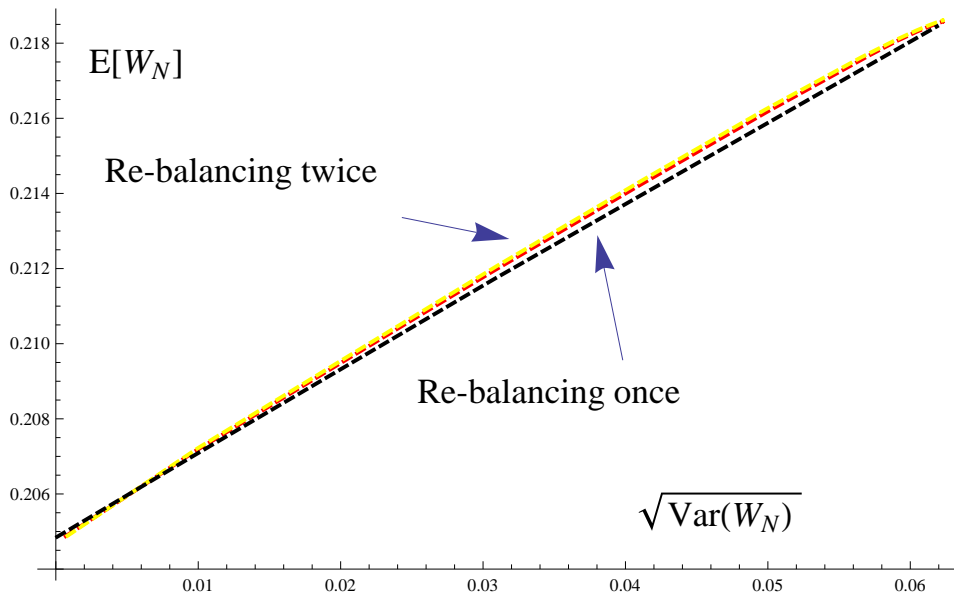


Figure 7.18: Mean variance CASE for AMAZON stock by forming a portfolio with risk free asset and AMAZON stock with parameters  $\lambda = \mu = 0.01, s = e^{0.05\Delta T}, T = 0.5, m = 0.18, \sigma = 0.4, \lambda = \mu = 0.01$ . Where  $T$  is the time horizon for investment,  $N$  is the number of re-balancing nodes.  $\omega$  is the continuous time risk-free rate,  $(\lambda, \mu)$  are transaction cost factors,  $s$  is the risk free growth over the interval,  $m$  is the drift for continuous time GBM and  $\sigma$  is the volatility for the continuous time GBM. The continuous time GBM implies a risky growth for the risky asset over the interval  $\Delta T$ .

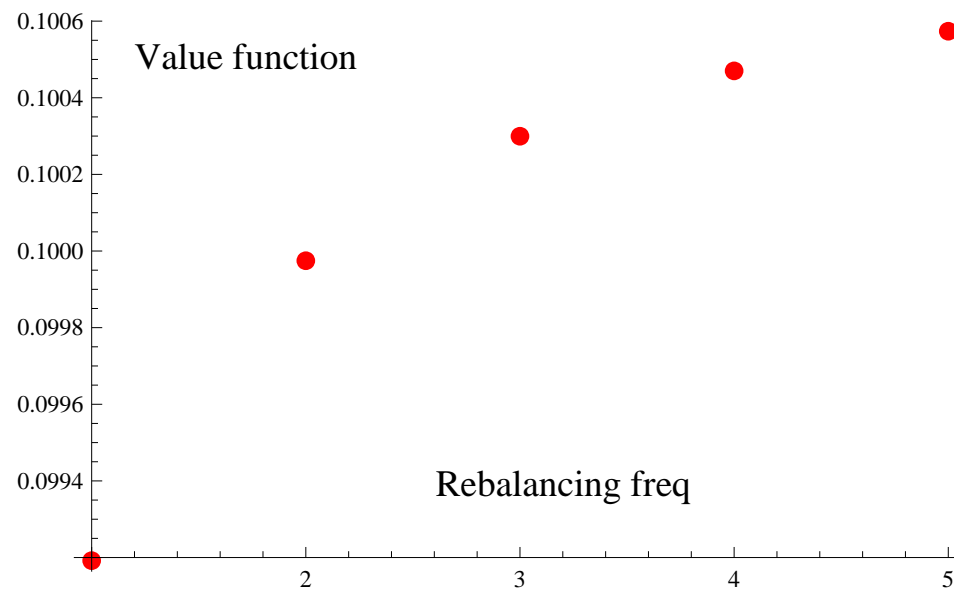


Figure 7.19: Log utility CASE for AMAZON stock by forming a portfolio with risk free asset and AMAZON stock with parameters  $\lambda = \mu = 0.01$ ,  $s = e^{0.05\Delta T}$ ,  $T = 1$ ,  $m = 0.18$ ,  $\sigma = 0.4$ ,  $\lambda = \mu = 0.01$ . Where  $T$  is the time horizon for investment,  $N$  is the number of re-balancing nodes.  $\omega$  is the continuous time risk-free rate,  $(\lambda, \mu)$  are transaction cost factors,  $s$  is the risk free growth over the interval,  $m$  is the drift for continuous time GBM and  $\sigma$  is the volatility for the continuous time GBM. The continuous time GBM implies a risky growth for the risky asset over the interval  $\Delta T$ .

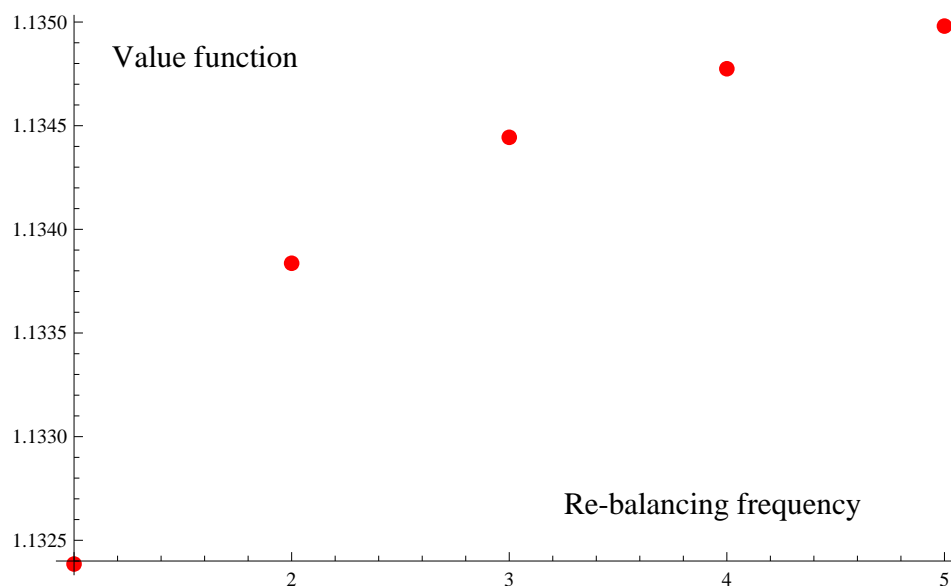


Figure 7.20: CRRA utility CASE for AMAZON stock by forming a portfolio with risk free asset and AMAZON stock with parameters  $\lambda = \mu = 0.01$ ,  $s = e^{0.05\Delta T}$ ,  $T = 1$ ,  $m = 0.18$ ,  $\sigma = 0.4$ ,  $\lambda = \mu = 0.01$ . Where  $T$  is the time horizon for investment,  $N$  is the number of re-balancing nodes.  $\omega$  is the continuous time risk-free rate,  $(\lambda, \mu)$  are transaction cost factors,  $s$  is the risk free growth over the interval,  $m$  is the drift for continuous time GBM and  $\sigma$  is the volatility for the continuous time GBM. The continuous time GBM implies a risky growth for the risky asset over the interval  $\Delta T$ .



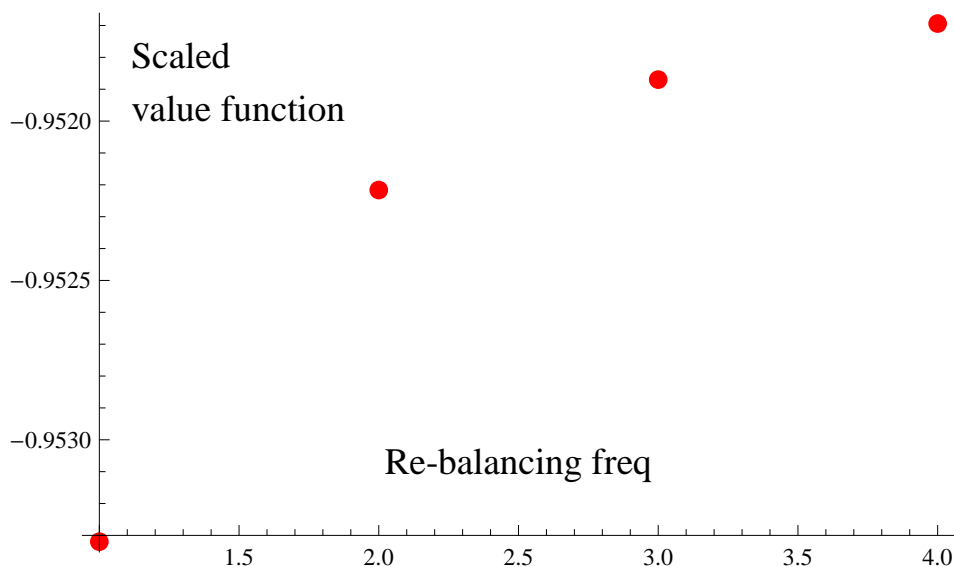


Figure 7.21: CARA utility CASE for AMAZON stock by forming a portfolio with risk free asset and AMAZON stock with parameters  $\lambda = \mu = 0.01, s = e^{0.05\Delta T}, T = 1, m = 0.18, \sigma = 0.4, \lambda = \mu = 0.01, z = 0.01$ . Value function is scaled and evaluated with initial wealth in risky asset =100. Where  $T$  is the time horizon for investment,  $N$  is the number of re-balancing nodes.  $\omega$  is the continuous time risk-free rate,  $(\lambda, \mu)$  are transaction cost factors,  $s$  is the risk free growth over the interval,  $m$  is the drift for continuous time GBM and  $\sigma$  is the volatility for the continuous time GBM. The continuous time GBM implies a risky growth for the risky asset over the interval  $\Delta T$ .

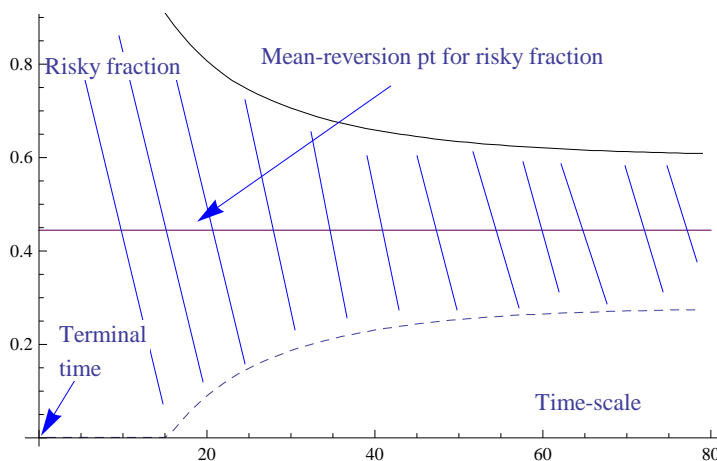


Figure 7.22: Log-utility CASE: Phase geometry of no-transaction region with respect to *Merton* point and mean-reversion of risky fraction with parameters  $\lambda = \mu = 0.05, s = e^{0.1\Delta T}, T = 6, N = 80, amin = 0.001, amax = 0.999, da = 0.001, m = 0.14, \sigma = 0.3$ .

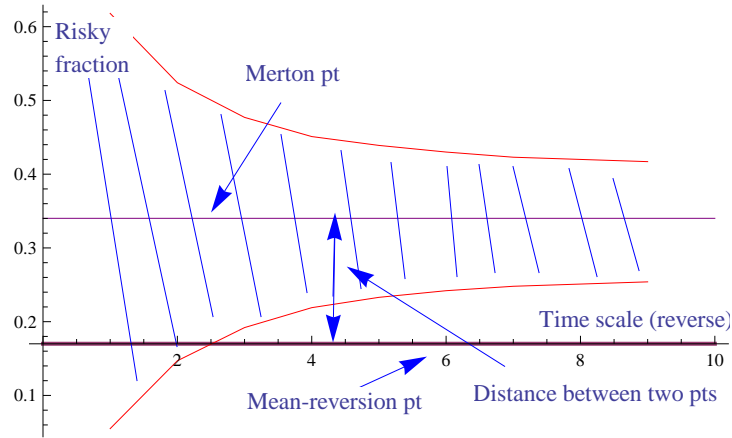


Figure 7.23: CRRA utility CASE: Phase geometry of no-transaction region with respect to *Merton* point and mean-reversion of risky fraction with parameters  $V = 0.5, \lambda = \mu = 0.005, s = e^{0.05\Delta T}, T = 1, N = 10, amin = 0.001, amax = 0.999, da = 0.001, m = 0.08, \sigma = 0.42$ .

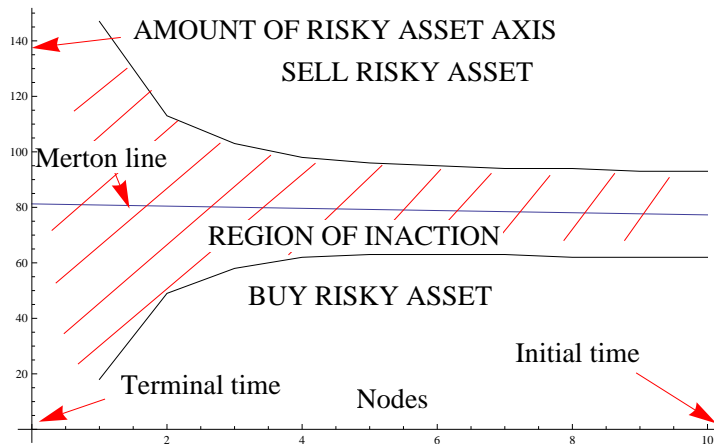


Figure 7.24: CARA-utility CASE: Phase geometry of no-transaction region with respect to *Merton* line with parameters  $\lambda = \mu = 0.01, s = e^{0.05\Delta T}, T = 1, N = 10, xmin = 5, xmax = 600, dx = 1, \eta = 0.01, m = 0.18, \sigma = 0.4, z = 0.01$ . Here  $[xmin, xmax]$  denotes the bounds for amount of wealth in risky asset state space. Using the same parameters as estimated for AMAZON stock in this chapter.

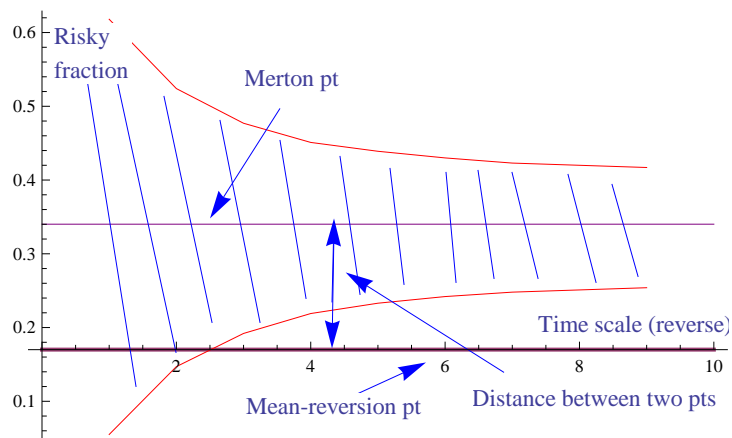


Figure 7.25: CARA utility CASE: Phase geometry of no-transaction region with respect to time varying Merton line  $\eta = 0.01, \lambda = \mu = 0.01, s = e^{0.05\Delta T}, T = 1, N = 10, x_{min} = 5, x_{max} = 600, dx = 1, m = 0.18, \sigma = 0.4, z = 0.01$ . Here  $[x_{min}, x_{max}]$  denotes the bounds for amount of wealth in risky asset state space

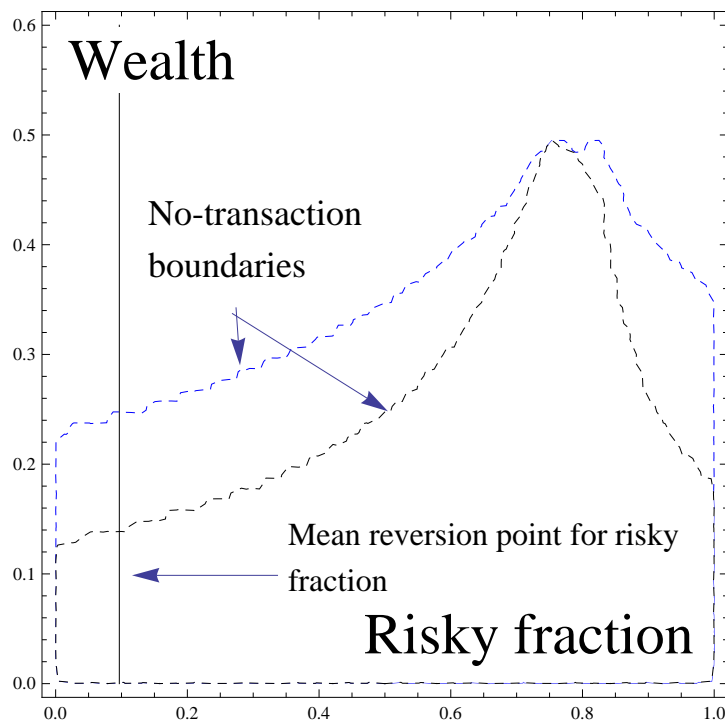


Figure 7.26: Mean-variance (*pre-committed* controls -also called 'benchmark' objective) CASE: Phase stencil of no-transaction topology with respect to mean-reversion of risky fraction. Parameters are chosen as:  $T = 0.3, N = 6, \lambda = \mu = 0.05, s = e^{0.05\Delta T}, m_1 = 0.08, \sigma_1 = 0.42, m_2 = 0.14, \sigma_2 = 0.8, \rho = 0.05, a_{min} = 0.001, a_{max} = 0.999$ .

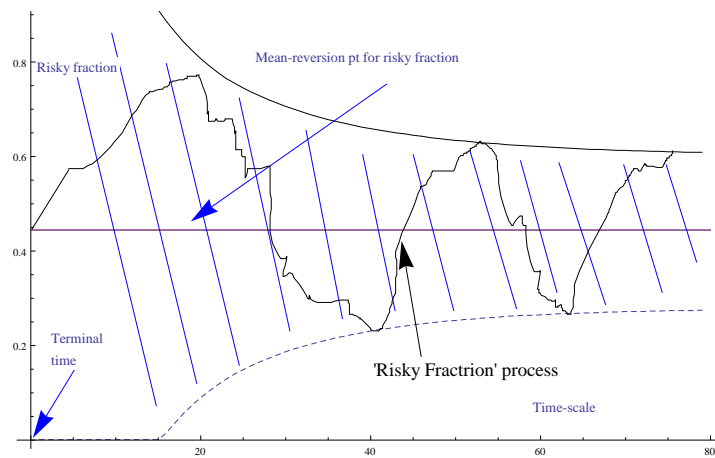


Figure 7.27: Reflection of the 'risky fraction' process about the no-transaction boundaries and the value of re-balancing.

# Chapter 8

## Lattice approximation for a dynamic stochastic transaction cost model

### 8.1 Introduction

This chapter provides a model for dynamic portfolio re-balancing under stochastic transaction cost in which transaction costs are perfectly correlated with market volatility. The volatility is assumed to follow a mean-reverting *Heston* model. We provide an approximate lattice approximation to derive the no-transaction region geometry. We will consider optimal investment strategy of a *self-financing* investor who invests in risky hedge fund strategies. It is shown that the expected loss in utility as a result of uncertain transaction cost could be significant.

Transaction costs include both a random and fixed component. Papers such as [82], [80] and [74] hint that the market maker responds to a more volatile market by widening the bid-ask spread. Econometric tests carried out by [14], [40] and [41] further support the positive relation. The relationship is further neatly quantified in paper by Gilles [88] who reports an exponential law (although almost linear) scaling between the bid-ask spread and volatility for LSE stocks. Later, [77] reports a logarithmic scaling relationship between bid-ask spread and volatility.

In broad brush the main ideas of the chapter are:

- 1- We provide a discrete framework of analysis for dynamic portfolio optimization under uncertain transaction costs.
- 2- Uncertain transaction costs could erode our investment performance in expected utility terms.
- 3- While it makes sense to re-balance in times of high volatility we are also faced with high transaction costs which could erode our investment performance.

### 8.2 Transaction cost model with stochastic volatility

We have  $X_t$  as the amount of wealth in the risky asset and  $Y_t$  be the amount of wealth in risk free asset.

Denote  $L_t$  and  $M_t$  as being non-decreasing processes such that  $L_t$  is the total amount of risky asset bought and  $M_t$  as being the total amount sold. Let  $\mathcal{J}(X, Y, \nu, t) = E[\phi(W(T))|\mathcal{F}_t]$

denote the value function.

Here the relevant *controlled SDEs* are:

$$dX = X(mdt + \sqrt{v}dZ_t^1) + dL_t - dM_t \quad (8.1)$$

$$dY = rYdt - (1 + \lambda)dL_t + (1 - \mu)dM_t \quad (8.2)$$

$$dv_t = (\theta - v_t)dt + \sigma \sqrt{v_t}dZ_t^2 \quad (8.3)$$

where  $dL_t = l_t dt$ ,  $dM_t = u_t dt$  and  $E[dZ_t^1 dZ_t^2] = \rho dt$ . Also the following is assumed:  $0 \leq l_s, u_s \leq \kappa$ .

Using the Bellman principle and simplifying we get:

$$\begin{aligned} \max_{l,u} (\mathcal{J}_t + mX\mathcal{J}_X + \frac{1}{2}vX^2\mathcal{J}_{XX} + rY\mathcal{J}_Y + \theta\mathcal{J}_v - v\mathcal{J}_v + \frac{1}{2}\mathcal{J}_{vv}\sigma^2v \\ + \sigma\rho vX\mathcal{J}_{Xv} + l_t(\mathcal{J}_X - (1 + \lambda)\mathcal{J}_Y) + u_t((1 - \mu)\mathcal{J}_Y - \mathcal{J}_X)) = 0 \end{aligned} \quad (8.4)$$

Using an argument similar to [28] we get the PDE defining the no-transaction region:

$$\mathcal{J}_t + mX\mathcal{J}_X + \frac{1}{2}vX^2\mathcal{J}_{XX} + rY\mathcal{J}_Y + \theta\mathcal{J}_v - v\mathcal{J}_v + \frac{1}{2}\mathcal{J}_{vv}\sigma^2v + \sigma\rho vX\mathcal{J}_{Xv} = 0 \quad (8.5)$$

with the boundary conditions ( BCs ):

$$\mathcal{J}_X - (1 + \lambda)\mathcal{J}_Y = 0 \quad (8.6)$$

$$(1 - \mu)\mathcal{J}_Y - \mathcal{J}_X = 0 \quad (8.7)$$

It is easy to see the derivation of BCs from the principle of smooth pasting. At the buy boundary, for instance, the following holds:  $\mathcal{J}(X + \Delta, Y - (1 + \lambda)\Delta) \approx \mathcal{J}(X, Y)$  where  $\Delta$  is very small. Using the first order expansion we get the boundary condition  $\mathcal{J}_X = (1 + \lambda)\mathcal{J}_Y$ . There are also economic reasons based upon *utilitarian* principles of why this should hold. Inside the buy region  $l_t$  is positive so  $\mathcal{J}_X \geq (1 + \lambda)\mathcal{J}_Y$  and in the sell region  $u_t$  is positive so  $(1 - \mu)\mathcal{J}_Y \geq \mathcal{J}_X$ .

The terminal condition for log-utility is:

$$\mathcal{J}(X, Y, v, T) = \text{Log}(X(T) + Y(T)) \quad (8.8)$$

## 8.3 Investment model under transaction costs

In the remainder of this chapter we consider a simple investment model. The investor shifts his wealth between risky and non-risky asset subject to a control strategy given his terminal investment objective of maximizing the growth rate. There are  $N$  periods and an investment horizon of length  $T$  years. It is the same transfer of wealth model as discussed in several earlier chapters and we will not provide details of it again.

For the growth rate problem considered in chapter 5 the value function takes the form:

$$\mathcal{J}(W_k^-, A_k^-) = E^P[\text{Log}(W_N)|\mathcal{F}_k] \quad (8.9)$$

Let  $\mathcal{M}_1(t)$  and  $\mathcal{M}_2(t)$  denote respectively the cumulative transfer of wealth from strategy  $i$  to  $j$  and from  $j$  to  $i$  respectively up to time  $t$ . Let  $\nu = (\mathcal{M}_1, \mathcal{M}_2)$  denote an admissible strategy. Let  $W^{x,y}(T)$  denote the net attainable wealth under transfer of wealth model starting with the initial strategy pair  $(x, y)$  under an admissible strategy.

The risky asset price  $S_k$  describing the the fundamental value, taken as the midpoint of the bid and ask prices, is assumed to follow a GBM with a drift  $m$  and volatility  $\sigma$ .

In particular, we have:

$$dS_t = mdt + \sqrt{\sigma_t}dZ_t \quad (8.10)$$

and a mean-reversion model for volatility:

$$d\sigma_t = \theta(\Lambda - \sigma_t)dt + \xi \sqrt{\sigma_t}dB_t \quad (8.11)$$

with  $Z_t, B_t$  being Brownian motions and  $E[dZ_t dB_t] = \rho dt$ .

For log-utility we have:

$$\begin{aligned} \mathcal{J}_{N-k}(W_{N-k}^-, \mathcal{A}_{N-k}^-, \sigma_{N-k}) &= \frac{1}{T} \text{Log}(W_{N-k}^-) + \max_s E^{\mathbb{P}}[(\mathcal{J}_{N-k+1}^{(k-1)}(\mathcal{A}_{i,N-k+1}^-, \sigma_{N-k+1})) \\ &\quad + \text{Log}(\mathbb{F}_{N-k}(\mathcal{A}_{i,N-k}^-)) | \mathcal{F}_{N-k}] \\ &= \frac{1}{T} \text{Log}(W_{N-k}^-) + \mathcal{J}_{N-k}^{(k)}(\mathcal{A}_{i,N-k}^-, \sigma_{N-k}) \end{aligned} \quad (8.12)$$

where the stochastic functional  $F_{N-k}(A_{N-k}^-)$  could be represented as:

$$\mathbb{F}_{N-k}(A_{N-k}^-) = \begin{cases} (\epsilon_{N-k}^+ s_{N-k} + ((1 - A_{N-k}^-) - (1 + \lambda_{N-k})(-A_{N-k}^- + \epsilon_{N-k}^+))\alpha_{N-k}) & \text{if risky asset bought} \\ (\epsilon_{N-k}^+ s_{N-k} + ((1 - A_{N-k}^-) + (1 - \mu_{N-k})(A_{N-k}^- - \epsilon_{N-k}^+))\alpha_{N-k}) & \text{if risky asset sold} \\ A_{N-k}^- s_{N-k} + (1 - A_{N-k}^-)\alpha_{N-k} & \text{no trading} \end{cases}$$

## 8.4 Formulation as a stochastic transaction cost model

Seeking inspiration from prior empirical work the chapter from now assumes that transaction costs are related to volatility under a simple *affine* function. We will assume:

$$\lambda_k = \sum_{i=0}^I a_i \sigma_k^i \quad (8.14)$$

where  $a_i$  is the weight and  $\sigma_k$  is the volatility at node  $k$ .

It is not the purpose of the chapter to estimate the relationship. The chapter only seeks to provide a theoretical framework under which stochastic transaction cost models could be analyzed. Mean reversion in volatility, therefore, implies mean reversion in transaction costs. In fact, a time snapshot of bid-ask spread might lead one to suspect it is mean-reverting but with a very high mean-reversion rate! For further details on dependence of bid-ask spread on market parameters see [63].

## 8.5 Lattice formulation of the model

Seeking inspiration from the continuous-time model we propose the discrete time model as:

$$g_{k+1,k} = 1 + \frac{\Delta S_k}{S_k} = 1 + m_k \Delta T + \sqrt{\sigma_k} \sqrt{\Delta T} Z_k^1 \quad (8.15)$$

$$\Delta \sigma_k = \theta(\Lambda - \sigma_k) \Delta T + \xi \sqrt{\sigma_k} \sqrt{\Delta T} Z_k^2 \quad (8.16)$$

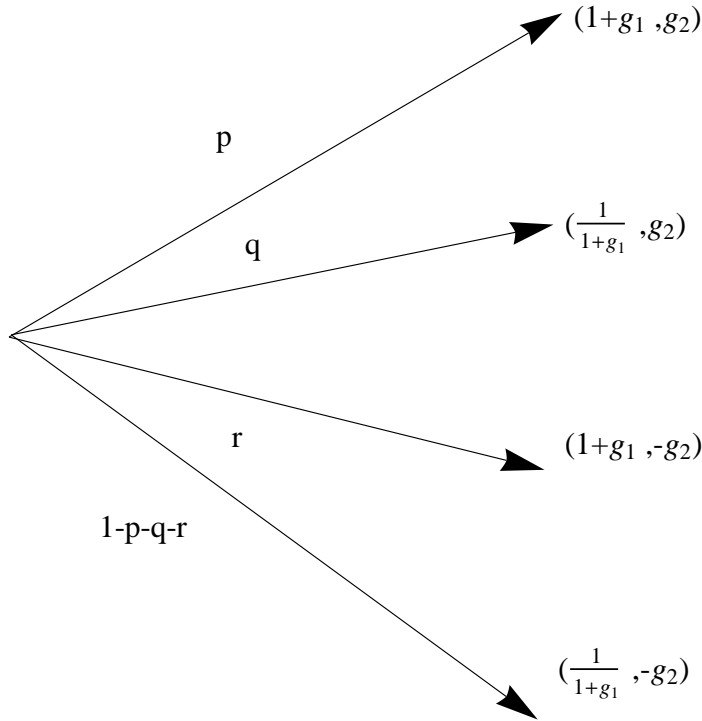


Figure 8.1: Joint evolution discrete probability approximation for (risky growth, change in volatility. )

Figure 8.1 shows the joint evolution of risky growth and volatility. Figures 8.2 and 8.3 then show the implied individual discrete probability approximation for risky growth and volatility. Figure 8.4 shows dynamic programming in action in the lattice framework. The transaction cost process is mean-reverting and is depicted diagrammatically in figure 8.5. We use the following moment matching to create a decision-tree for a framework of analysis:

$$E[g_{k+1,k}] = 1 + m_k \Delta T, \text{Var}[g_{k+1,k}] = \sigma_k \Delta T \quad (8.17)$$

$$E[\Delta \sigma_k] = \theta(\Lambda - \sigma_k) \Delta T, \text{Var}[\Delta \sigma_k] = \xi^2 \sigma_k \Delta T \quad (8.18)$$

$$\text{Cov}[g_{k+1,k}, \Delta \sigma_k] = \xi \sigma_k \rho \Delta T \quad (8.19)$$



*	risky frac=0.5, vol =0.5	risky frac=0.5, vol =0.6	risky frac=0.5, vol =0.7
$\lambda_t = 0.05$	0.0135	0.1023	0.00787
$\lambda_t = 0.025 + \frac{1}{16}\sigma_t$	0.0132	0.0089	0.00498

Table 8.1: Expected utility measured at  $t = 0$  as a result of uncertain transaction costs with parameters:  $m = 0.14, \theta = 0.1, \Lambda = 0.4, \xi = 0.5, T = 0.4, \rho = 0.1$ . We have  $\theta, \Lambda, \xi$  and  $\rho$  as the parameters for the joint evolution tree.

We will assume a no short sale constraint in the risky asset and so our risky fraction space is always restricted to  $[0, 1]$ . To avoid extrapolation errors in volatility we will truncate the volatility domain at each earlier time step by the maximum amount volatility could jump on a discrete probability approximation. This is to ensure that all our state variables remain within the domain of interpolation. Interpolation errors are taken care of by using a fine enough discretization that scales with discretization in time steps by a power law as discussed already in chapter 3. The continuous limit of value function could be found by assuming errors scale as  $O(n^\gamma)$ - where  $n$  denotes the fineness of discretization along state space and  $\gamma$  a scaling factor. The limit  $n \rightarrow \infty$  could be used to estimate continuous time solution.

The model provided in this chapter provides a framework for analyzing the expected utility a dynamic investor could suffer under uncertain transaction costs. To be precise assume there are two possible types of transaction cost processes:

- 1- Transaction cost is constant:  $\lambda_t = \bar{\lambda}$
- 2- Transaction cost is random, mean-reverting and related to volatility:  $\lambda_t = a + b\sigma_t$

The constants  $a$  and  $b$  are chosen so that the processes in (1) and (2) have the same mean-reverting level  $\bar{\lambda}$ .

How much is the expected utility of a dynamic investor faced with uncertain transaction costs compared to one with constant transaction costs? The answer is the *loss due to uncertainty could be significant* depending upon his initial wealth allocation and volatility levels. We summarize numerical results in table 8.1. Using the two types of transaction cost process we measure expected logarithmic utility at initial time for different configuration of state variables. It is found that investor with uncertain transaction costs faces a loss in expected logarithmic utility. It make sense to re-balance portfolios in times with high volatility as discussed in chapter 7 we are also faced with high transaction fees while would make re-balancing less attractive.

The chapter does not seek to assert that the discrete time solution converges to the continuous time solution. The objective of the chapter is to provide a framework of analysis in discrete time keeping in view its continuous time analogue. We will illustrate only numerically that the discrete time framework has solution that is remarkably close to the solution implied by exact distribution over the interval  $\Delta T$ . Closeness in value function is shown in table 8.2.

We will provide a numerical solution to the problem for some choice of parameters as shown by next couple of figures. Our numerical results are in close conformity with the no-transaction cost formulation because the *Merton* line always lies inside the no-transaction regions. See figures 8.6 and 8.7.

$(A_k, v_k)$	0.75	0.8	0.85
0.15	0.0316%	0.0327%	0.042%
0.3	0.292%	0.370%	0.454%
0.45	1.24%	1.50%	2.07%
0.6	2.44%	1.59%	1.27%
0.75	0.614%	0.526%	0.485%

Table 8.2: Relative absolute percentage error in the value function at time for different nodal points in 2-D with parameters  $m = 0.14, \theta = 0.1, \lambda = 0.8, \xi = 0.02, T = 0.04, \rho = 0.1, \sigma_{min} = 0.7, \sigma_{max} = 0.9, \mu = 0.01 + 0.01\sigma, \gamma = 2, L = 100N^\gamma, s = e^{0.05\Delta T}, N = 6, da = \frac{amax-amin}{L}, \Delta T = \frac{T}{N}, amin = 0.001, amax = 0.999$ . We have  $\theta, \Lambda, \xi$  and  $\rho$  as the parameters for the joint evolution tree. Also  $da$  represents the risky fraction space discretization with  $[amin, amax]$  being the bounds. Where  $T$  is the time horizon for investment,  $N$  is the number of re-balancing nodes.  $\omega$  is the continuous time risk-free rate,  $(\lambda, \mu)$  are transaction cost factors,  $s$  is the risk free growth over the interval,  $m$  is the drift for continuous time GBM and  $\sigma$  is the volatility for the continuous time GBM. The continuous time GBM implies a risky growth for the risky asset over the interval  $\Delta T$ .

## 8.6 Concluding remarks

The chapter proposed a simple transaction cost model and we used lattice approximation to solve it in discrete time. It will be interesting to explore different variants of volatility models like CEV, regime switching etc. In regime switching models, for instance, it is possible to model transaction cost as being dependent upon different volatility regimes. At the same time, it is possible to include more complex mean-reverting dynamics for transaction costs. The next chapter adds more realism to our framework by providing tools to solve dynamic portfolio choice problems under constraints.

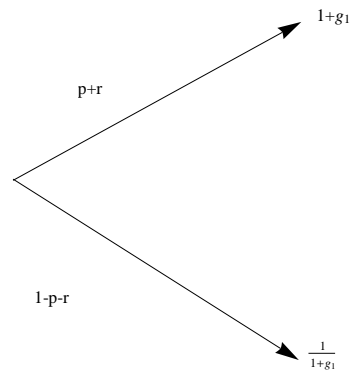


Figure 8.2: Evolution of risky growth.

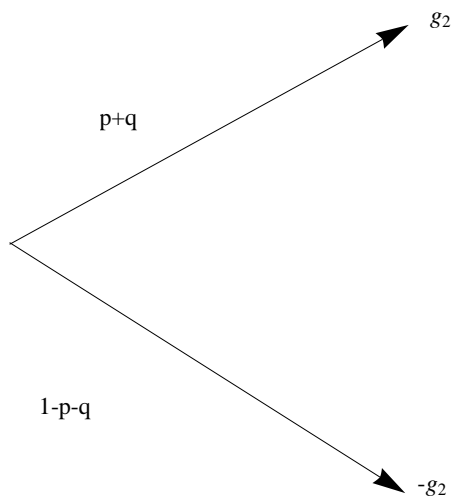


Figure 8.3: Evolution of change in volatility.

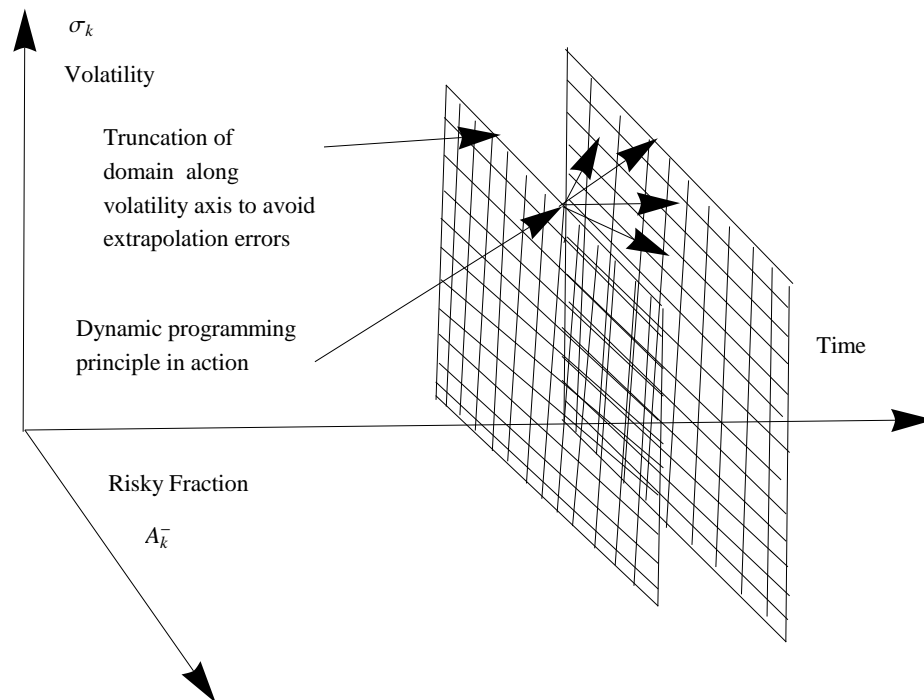


Figure 8.4: Dynamic programming on a grid and truncation on volatility axis to avoid extrapolation errors.

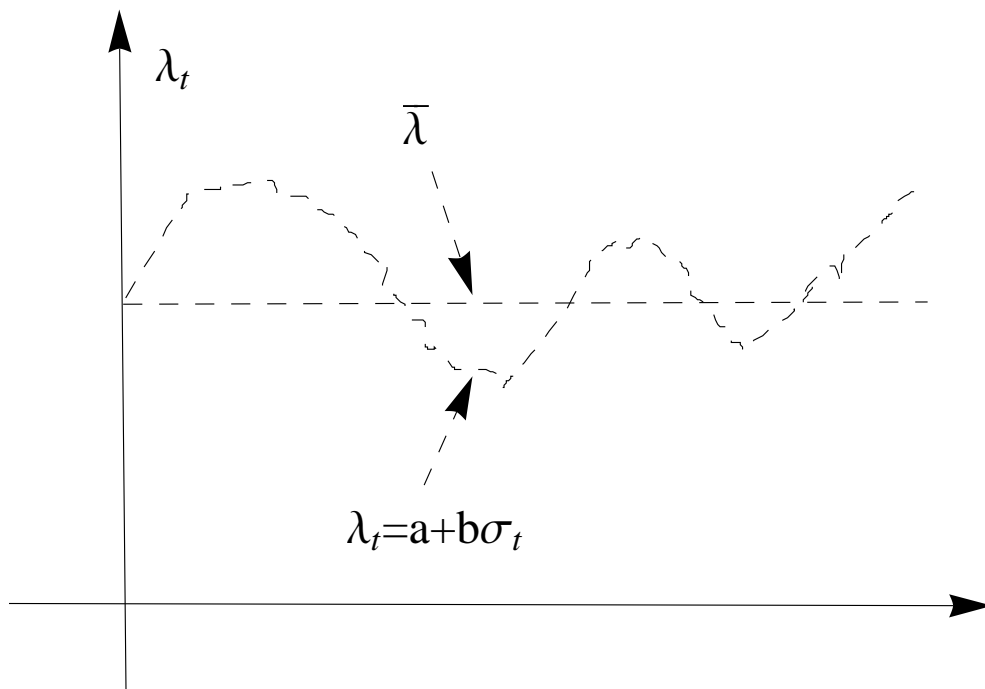


Figure 8.5: Transaction cost processes.

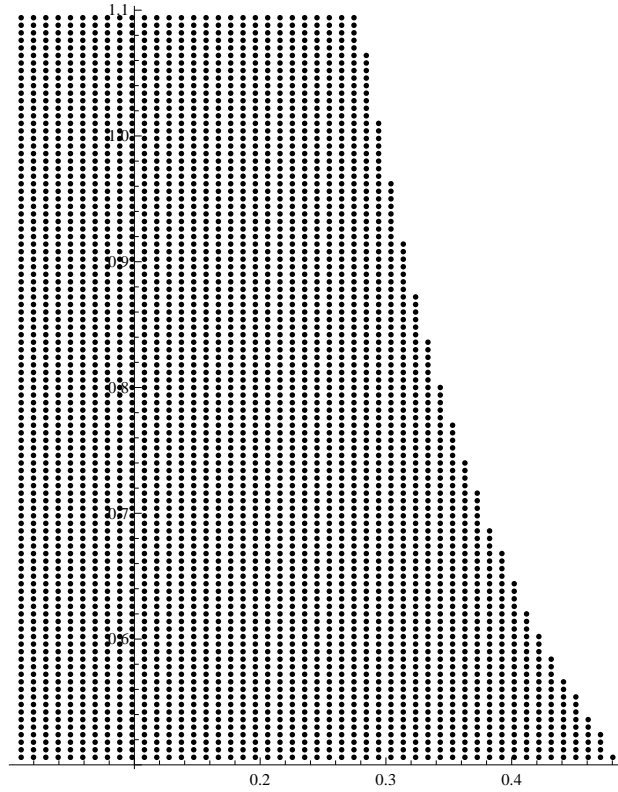


Figure 8.6: No-transaction topology at time  $t=0.45$  and parameters  $m = 0.14, \theta = 0.1, \Lambda = 0.8, \xi = 0.02, T = 0.5, \rho = 0.1, \sigma_{min} = 0.5, \sigma_{max} = 1.1, \lambda = \mu = 0.01 + 0.01\sigma, \gamma = 2, L = 10N^\gamma, s = e^{0.05\Delta T}, N = 10, da = \frac{amax-amin}{L}, \Delta T = \frac{T}{N}, amin = 0.001, amax = 0.999$ . Volatility axis horizontal and risky fraction axis vertical. We have  $\theta, \Lambda, \xi$  and  $\rho$  as the parameters for the joint evolution tree. Also  $da$  represents the risky fraction space discretization with  $[amin, amax]$  being the bounds. Where  $T$  is the time horizon for investment,  $N$  is the number of re-balancing nodes.  $\omega$  is the continuous time risk-free rate,  $(\lambda, \mu)$  are transaction cost factors,  $s$  is the risk free growth over the interval,  $m$  is the drift for continuous time GBM and  $\sigma$  is the volatility for the continuous time GBM. The continuous time GBM implies a risky growth for the risky asset over the interval  $\Delta T$ .

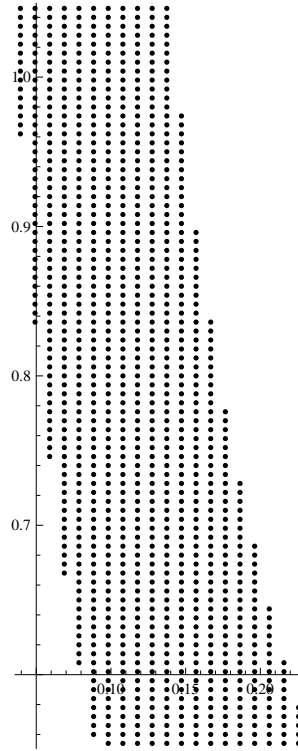


Figure 8.7: No transaction geometry at time  $t=0.1$  and parameters  $m = 0.14, \theta = 0.1, \Lambda = 0.8, \xi = 0.02, T = 0.5, \rho = 0.1, \sigma_{min} = 0.5, \sigma_{max} = 1.1, \lambda = \mu = 0.01 + 0.01\sigma, \gamma = 2, L = 10N^\gamma, s = e^{0.05\Delta T}, N = 10, da = \frac{amax-amin}{L}, \Delta T = \frac{T}{N}, amin = 0.001, amax = 0.999$ . Volatility axis horizontal and risky fraction axis vertical. We have  $\theta, \Lambda, \xi$  and  $\rho$  as the parameters for the joint evolution tree. Also  $da$  represents the risky fraction space discretization with  $[amin, amax]$  being the bounds. Where  $T$  is the time horizon for investment,  $N$  is the number of re-balancing nodes.  $\omega$  is the continuous time risk-free rate,  $(\lambda, \mu)$  are transaction cost factors,  $s$  is the risk free growth over the interval,  $m$  is the drift for continuous time GBM and  $\sigma$  is the volatility for the continuous time GBM. The continuous time GBM implies a risky growth for the risky asset over the interval  $\Delta T$ .

# Chapter 9

## Portfolio optimization under transaction costs incorporating realistic constraints

### 9.1 Introduction

This chapter seeks to illustrate robust numerical methods to dynamically allocate portfolio assets under realistic problem constraints. Two important constraints that are discussed are the *draw-down constraint* and *portfolio insurance* constraint. Our methodology is combined with *probability deformation* methods so that the problem constraints are met in some *probabilistic* sense. More precisely, probability deformation schemes help us construct a *tree of evolution* for risky growth of an asset and optimal controls are obtained such that the portfolio constraints are satisfied *approximately*.

Most realistic portfolio problems are beset with constraints involving portfolio state variables. Let  $W(t)$  denote the wealth at any time  $t$ . Wealth is a very important portfolio state variable as far as constraints are concerned.

Current investment allocation most often requires some sort of downside protection (see [11], [52], [19]). More precisely this might require that the wealth at some point in time never falls below a certain value. This is also called *portfolio insurance*. Option-based portfolio insurance (OBPI) and Constant Proportion portfolio insurance (CPPI) are notable insurance strategies for pensions plans. The OBPI, introduced by Leland and Rubinstein (1976) (see [54]), consists of a portfolio invested in a risky asset covered by a listed put written on it. Whatever the value of risky asset at the terminal date, the portfolio value will be always greater than the strike of the put<sup>1</sup>. CPPI (see [12]) uses a simple strategy to allocate assets dynamically over time. The investor starts by setting a floor equal to the lowest acceptable value of the portfolio. Then, he computes the cushion as the excess of the portfolio value over the floor and determines the amount allocated to the risky asset by multiplying the cushion by a predetermined multiple. The *optimality* of these strategies might be questionable. To speak in mathematical terms it is an inequality to be met:

$$W(T) > K \quad \text{a.s.} \quad (9.1)$$

Another realistic constraint is the draw-down constraint which hedge funds often face (see

---

<sup>1</sup>If the put is not available in the market it could be synthetically manufactured.



[2],[9],[39]). It requires that the wealth at any point  $W(t)$  is always greater or equal to a certain fraction of the maximum wealth attained  $M(t)$ :

$$W(t) \geq \alpha M(t), \forall t \geq 0 \quad \text{a.s.} \quad (9.2)$$

We also assume that the investor is never allowed to go bankrupt i.e.  $W(t) \geq 0$ . Bankruptcy prohibition is another important constraint on its own. For example the nature of our portfolio could be such that bankruptcy never happens. A good example is when investor only takes long positions in stocks and bonds while making transactions that let him remain solvent. Log-utility is an interesting function because it has a built-in mechanism for inhibiting insolvency.

It is possible that a portfolio insurance constraint could never be met and we could write it instead as being  $P(W(T) > K) \geq \eta \equiv E[1_{W(T) > K}] \geq \eta$ .

The dynamic investor of this chapter invests only in a risky asset and risk free asset.

The main ideas of this chapter could be summarized as:

1- We observe through numerical examples when the constraints (in this case portfolio insurance and draw-down) involving portfolio state variables become tighter the fraction of wealth allocated to risky asset for CRRA utility decreases.

2- The chapter provides an approximate dynamic programming framework so that the investor is able to meet his portfolio constraints approximately.

## 9.2 The model

The transaction cost model we will analyze is the simple growth rate model we described in Chapter 5. We will not provide details of the model which had been discussed in Chapter 5. The investment objective in this chapter will, however, now be the CRRA (or power) utility. It is chosen because [38] in a no-transaction cost setting uses constant relative risk aversion utility function in his analysis and we could compare our results. Also the logarithmic utility could be seen a limiting case of power utility.

## 9.3 Solution methodology for constraints

We will consider two problem formulations for the purpose of illustration:

1- Portfolio insurance requiring  $W(T) > K$  **a.s.**

2- Maximum draw-down problem requiring  $W(t) \geq \alpha M(t)$  for every  $t \geq 0$  **a.s.**

In context of dynamic programming meeting a constraint almost surely is an interesting probabilistic situation. This means that the constraint must always be satisfied without a *doubt*. However, it would be more realistic to argue that the constraint could never be met given the probability model for the risky asset. This idea summarizes the central theme of this thesis which is *solving dynamic portfolio allocation problems approximately*. We will combine the idea of *probabilistic deformation* from earlier chapters with the idea of penalty to solve dynamic programming problem under constraints  $\{\eta\}$ .

The idea is to formulate the problem with the deformation parameter  $\gamma_\ell$ . Now with this discrete probability model we have a tree of evolution for risky growths having  $\ell$  branches. Any evolution which violates the constraint is assigned a high penalty (positive or negative

depending upon the value function) and multiplied by the probability of evolution in the dynamic programming equation<sup>2</sup>. In terms of dynamic programming language sitting at node  $k$  we will penalize any evolution of state variables that violates the state space constraints in the expectation of the value function at time node  $k$  (i.e. at time  $t + \Delta T$ ). Also any current state variable is highly penalized so that evolution at time node  $k - 1$  (i.e. at time  $t - \Delta T$ ) is aware of such a violation. Moreover, the deformation parameter in essence really gives a discrete approximation of a truncated version of continuous time probability model for risky growths. In the limit we are able to meet the constraints at least *approximately*.

Consider the bankruptcy prohibition constraint. Suppose we are at time  $t$ . Then seeing from tree of evolution of risky growths we can see all possible wealths. Any wealth at time  $t + \Delta T$  that violates non-negativity is assigned a penalty. Sitting at the current time, the value functions at next time step is really an expectation of a function of future evolution of wealth and risky fraction. So any negative future wealth is assigned penalty.

Take the portfolio insurance constraint as an example. If we require  $W(T) > K$  almost surely, as long as you have at least  $Ke^{-r\Delta T}$  in the risk free asset we would be fine. However, putting too much risk-free asset could be detrimental to portfolio performance. Even though the probability is low it remains a possibility that a risky asset can fall enough, over a finite time to violate the terminal portfolio insurance constraint if we do not have enough of risk free asset. Substantial transaction cost would be incurred if we eliminate the risky asset component from our portfolio. In such situations we would be interested in solving the constraint approximately. Our tree provides an approximate solution methodology. This is where deformation schemes are so useful.

Instead of:

$$P(W(T) > K) = 1 \quad (9.3)$$

In this thesis we consider:

$$P(W(T) > K) \geq \alpha \cong E^P[1_{W(T) > K}] \quad (9.4)$$

where  $\alpha$  is some number close to 1 .

It is easy to see that incorporating portfolio insurance constraints increases the dimensionality of our problems. For the portfolio insurance problem, for example, for any utility function we have  $(\mathcal{A}_k^-, \mathcal{W}_k^-)$  (i.e. risky fraction and wealth at node  $k$ ) as the relevant state variables. In particular, decomposability with respect to wealth no longer occurs. The constraint will usually be explicitly considered in the last stage of our dynamic programming problem because it is a constraint on the terminal wealth. The last stage is the initial recursion in dynamic programming!<sup>3</sup> .

For the maximum draw-down problem we now have the state variables as being the tuple  $(\mathcal{W}_k^-, \mathcal{M}_k^-, \mathcal{A}_k^-)$  where:

$$\mathcal{M}_{k+1}^- = \max\{\mathcal{M}_k^-, \mathcal{W}_{k+1}^-\} \quad (9.5)$$

Log-utility and CRRA can take both negative and positive values so any constraint violation is assigned a high negative value in our dynamic program. CRRA is positive if the risk aversion

<sup>2</sup>Logarithmic utility is a case in point because it contains a built-in mechanism for penalizing the wealth going close to zero by approaching negative infinity.

<sup>3</sup>As someone once said: “*Life can only be understood backwards but it must be lived going forwards!*”

co-efficient is in  $[0, 1]$  in which case we could assign *any* value less than or equal to zero as a penalty.

## 9.4 Numerical results for realistic problems

Analytic results for the *portfolio insurance* constraint problem do not exist in the financial mathematics literature. Analytic results do exist for the no transaction cost draw-down problem<sup>4</sup> (see [38]). The result states that the optimal investment in the risky asset is an explicit constant proportion of the difference between the current wealth  $W_k^-$  and the imposed fraction on the running maximum  $M_k^-$ . More precisely,

$$A_k^- = \psi_k(W_k^- - \alpha M_k^-), \psi_k \in \mathfrak{R}. \quad (9.6)$$

We provide a numerical illustration of our methodology via some figures to follow. The relevant control laws are encoded are provided in the caption of the figures.

Figures 9.1 and 9.2 show no-transaction regions for the portfolio insurance problem solved approximately. We constructed a risky growth tree with ten branches ( $\gamma_N = 10$ ) to solve the constrained problem approximately. The risky fraction is represented on horizontal axis and wealth on the vertical axis. Figure 9.1 shows the no-transaction region in the last stage of the problem. Figure 9.2 shows no-transaction region at initial time. As expected the no-transaction regions shrink as we move closer to the initial time using dynamic recursion. The geometries are seen to be slightly different for the last stage because that is when the portfolio insurance constraints come in to action. One fact is obvious from all the geometries: as the amount of wealth decreases ( the portfolio insurance constraint becomes tighter ) the center of no-transaction region has a lower fraction in the risky asset<sup>5</sup>.

Figures 9.3 and 9.4 show the no-transaction geometries for the draw-down constraint problem. The state space is three dimensional so we visualize it in a 2-D at a wealth slice. The risky fraction is on the horizontal axis and running maximum wealth on the vertical axis. The draw-down analytic result [38] is in close conformity with the no-transaction geometries we have obtained. In Figure 9.3 and Figure 9.4 the barrier between the buy and sell side boundary shifts *monotonically* to the left as the running maximum increases. Figure 9.3 is the geometry for the last stage of the program at a wealth slice and Figure 9.4 for the last stage. As the running maximum increases the center of no-transaction region has a lower fraction in the risky asset<sup>6</sup>.

Figure 9.5 shows the terminal wealth distribution for portfolio insurance constraint problem with the same parameters as in Figures 9.1 and 9.2 using the techniques of Chapter 3. It is seen to satisfy the portfolio insurance constraint level of  $K = 0.2$  very well.

<sup>4</sup>The analytic result of Grossman and Zhou [38] is in an infinite horizon framework with no intermediate consumption and the investment objective being CRRA utility.

<sup>5</sup>In Figures 9.1 and 9.2 the portfolio insurance constraint has  $K = 0.2$ .

<sup>6</sup>Because the draw-down constraint is becoming tighter!

## 9.5 Conclusion

The chapter was an excursion into the realm of solving portfolio allocation problems for hedge funds and pension plans. It is our hope to be able to extend our methodology to more interesting and challenging problems in dynamic asset allocation. We will turn our attention to exactly such a problem, of analyzing so-called pairs trading, in Chapter 10.

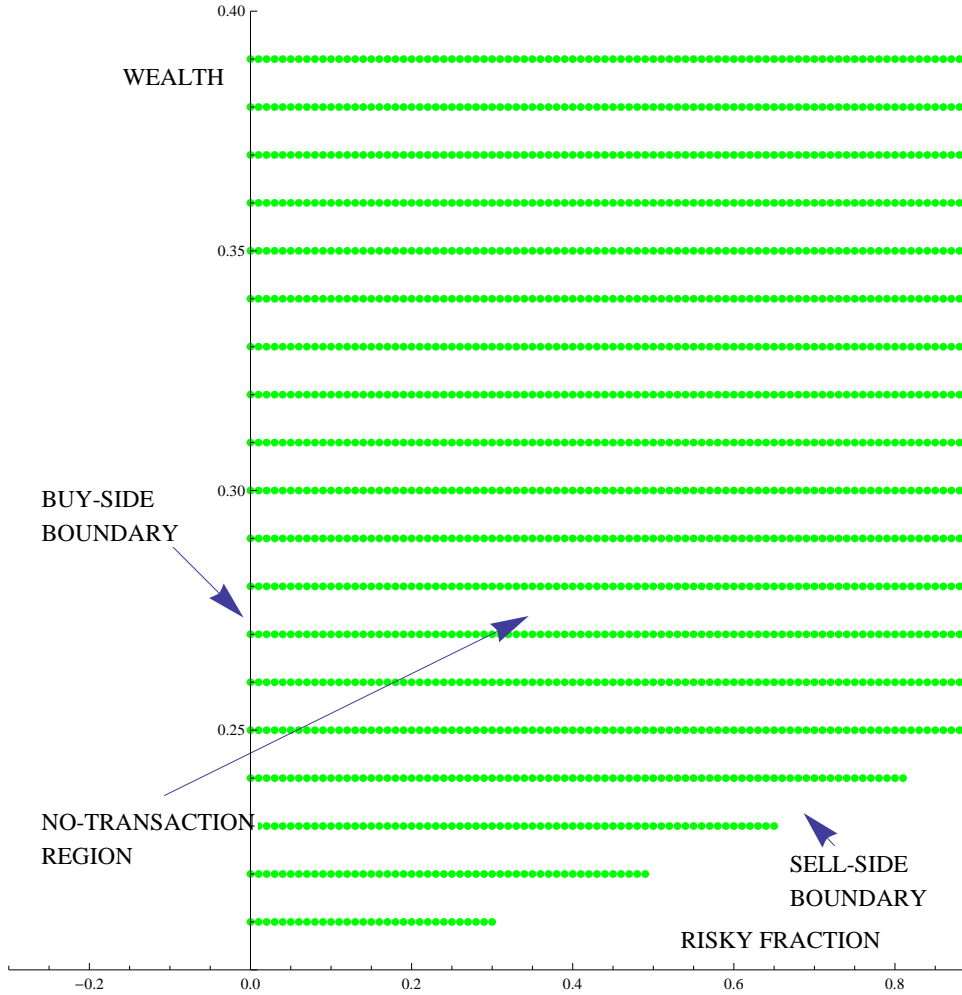


Figure 9.1: CRRA utility and no-transaction region for portfolio insurance constraint problem at time =0.75 yrs with parameters:  $\gamma_N = \frac{1}{10}$ ,  $T = 1$ ,  $N = 4$ ,  $\lambda = \mu = 0.01$ ,  $s = e^{0.1\Delta T}$ ,  $m = 0.14$ ,  $\sigma = 0.3$ ,  $K = 0.2$ ,  $V = 0.5$ . We denote  $K$  as the portfolio insurance level. Where  $T$  is the time horizon for investment,  $N$  is the number of re-balancing nodes.  $\omega$  is the continuous time risk-free rate,  $(\lambda, \mu)$  are transaction cost factors,  $s$  is the risk free growth over the interval,  $m$  is the drift for continuous time GBM and  $\sigma$  is the volatility for the continuous time GBM. The continuous time GBM implies a risky growth for the risky asset over the interval  $\Delta T$ .  $\gamma_t$  is the deformation parameter. Also  $V$  is the risk aversion co-efficient for CRRA utility.

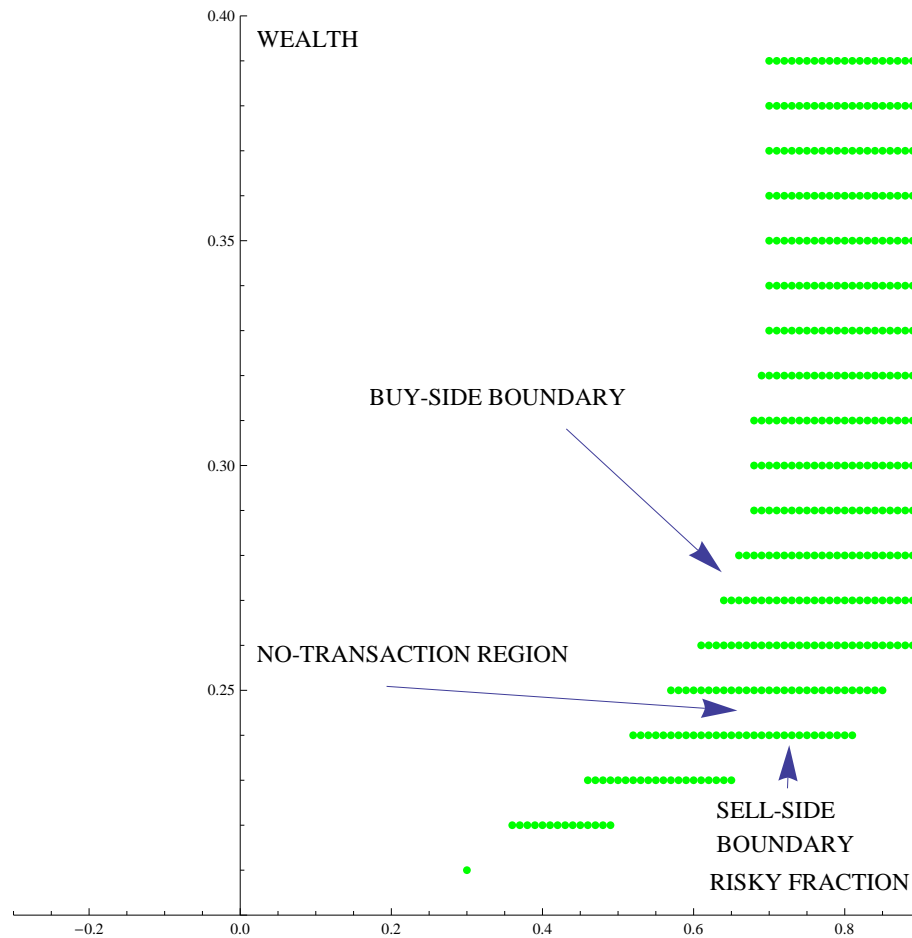


Figure 9.2: CRRA utility and no-transaction region for portfolio insurance constraint problem at time =0 yrs with parameters:  $\gamma_N = \frac{1}{10}$ ,  $T = 1$ ,  $N = 4$ ,  $\lambda = \mu = 0.01$ ,  $s = e^{0.1\Delta T}$ ,  $m = 0.14$ ,  $\sigma = 0.3$ ,  $K = 0.2$ ,  $V = 0.5$ . We denote  $K$  as the portfolio insurance level. Where  $T$  is the time horizon for investment,  $N$  is the number of re-balancing nodes.  $\omega$  is the continuous time risk-free rate,  $(\lambda, \mu)$  are transaction cost factors,  $s$  is the risk free growth over the interval,  $m$  is the drift for continuous time GBM and  $\sigma$  is the volatility for the continuous time GBM. The continuous time GBM implies a risky growth for the risky asset over the interval  $\Delta T$ .  $\gamma_t$  is the deformation parameter. Also  $V$  is the risk aversion co-efficient for CRRA utility.

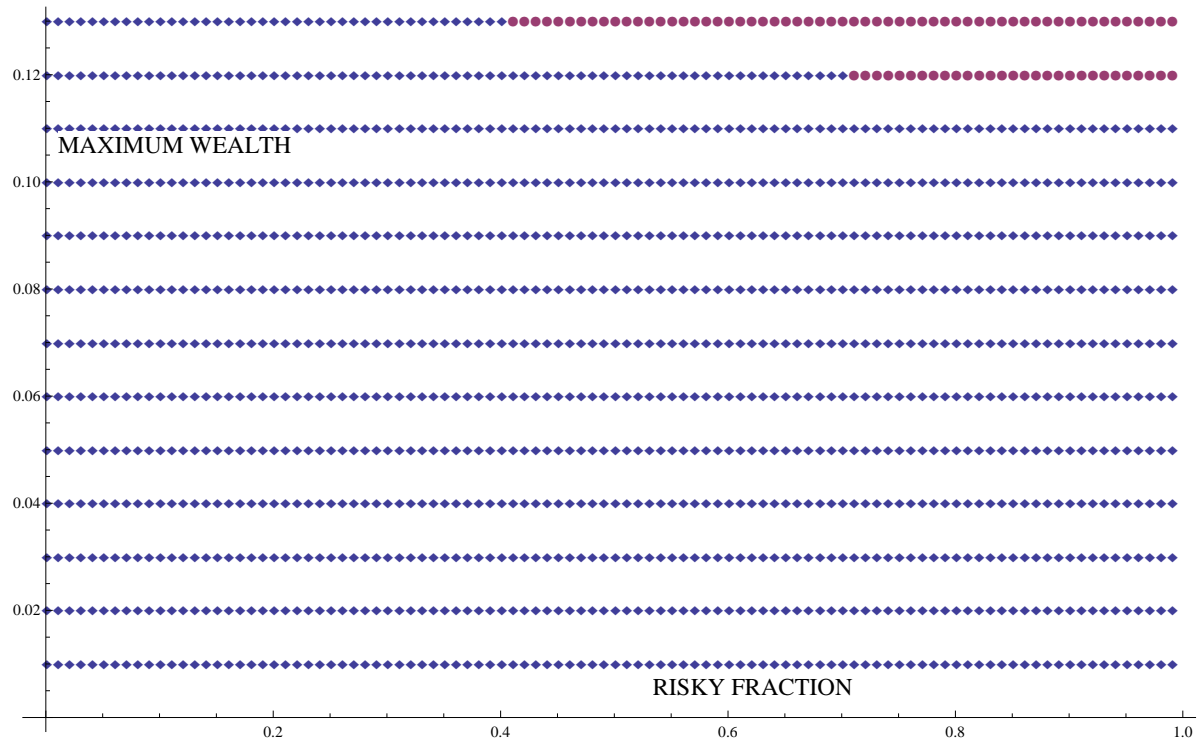


Figure 9.3: Here  $\star$  =BUY,  $\blacklozenge$  =DO-NOTHING and  $\bullet$  = SELL for no-transaction region geometry with CRRA utility for draw-down constraint problem at time =0.75 yrs and wealth =0.07 with parameters:  $\gamma_N = \frac{1}{10}$ ,  $T = 1$ ,  $N = 4$ ,  $\lambda = \mu = 0.01$ ,  $s = e^{0.1\Delta T}$ ,  $m = 0.14$ ,  $\sigma = 0.3$ ,  $\alpha = 0.25$ ,  $V = 0.5$ . We denote  $\alpha$  as important number in the draw-down constraint. Where  $T$  is the time horizon for investment,  $N$  is the number of re-balancing nodes.  $\omega$  is the continuous time risk-free rate,  $(\lambda, \mu)$  are transaction cost factors,  $s$  is the risk free growth over the interval,  $m$  is the drift for continuous time GBM and  $\sigma$  is the volatility for the continuous time GBM. The continuous time GBM implies a risky growth for the risky asset over the interval  $\Delta T$ .  $\gamma_\ell$  is the deformation parameter. Also  $V$  is the risk aversion co-efficient for CRRA utility.

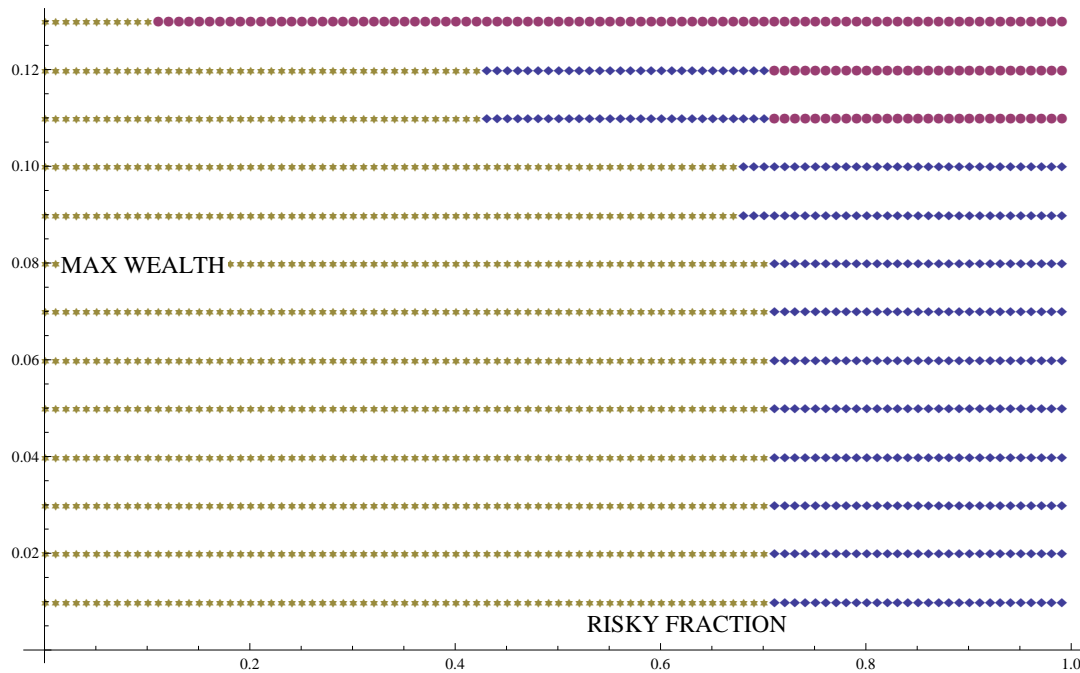


Figure 9.4: Here  $\star$  =BUY , $\diamond$  =DO-NOTHING and  $\bullet$  = SELL for no-transaction region geometry with CRRA utility for draw-down constraint problem at time =0 yrs and wealth =0.07 with parameters:  $\gamma_N = \frac{1}{10}, T = 1, N = 4, \lambda = \mu = 0.01, s = e^{0.1\Delta T}, m = 0.14, \sigma = 0.3, \alpha = 0.25, V = 0.5$ . We denote  $\alpha$  as important number in the draw-down constraint. Where  $T$  is the time horizon for investment,  $N$  is the number of re-balancing nodes.  $\omega$  is the continuous time risk-free rate,  $(\lambda, \mu)$  are transaction cost factors,  $s$  is the risk free growth over the interval,  $m$  is the drift for continuous time GBM and  $\sigma$  is the volatility for the continuous time GBM. The continuous time GBM implies a risky growth for the risky asset over the interval  $\Delta T$ .  $\gamma_t$  is the deformation parameter. Also  $V$  is the risk aversion co-efficient for CRRA utility.



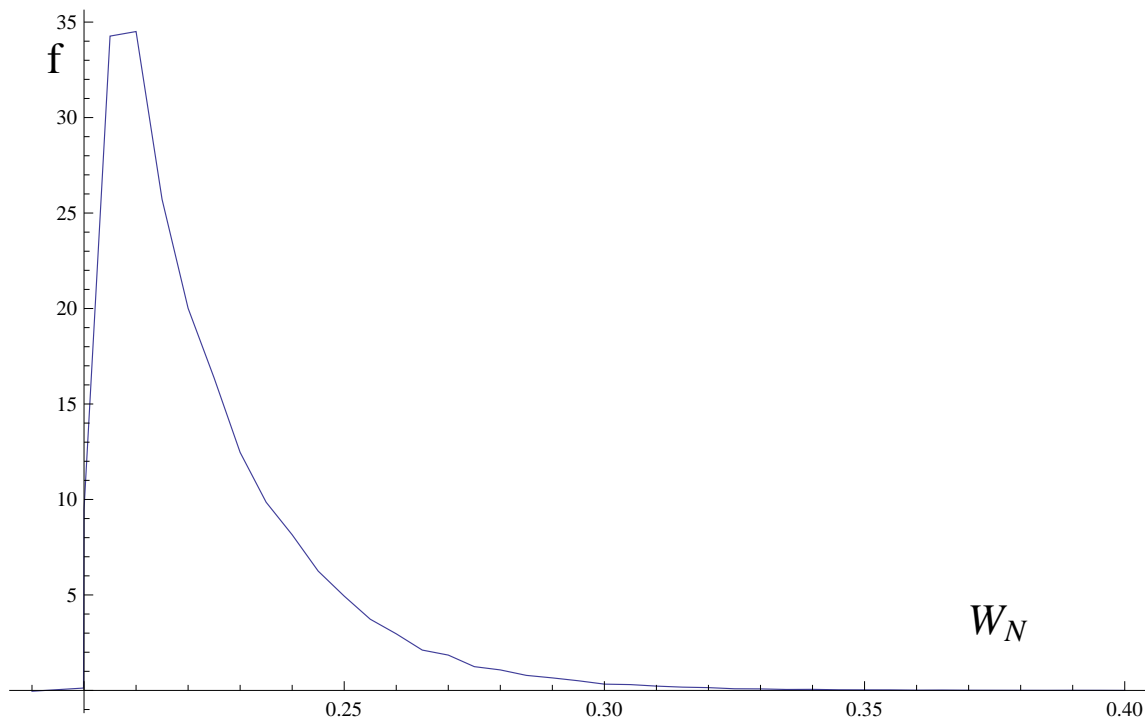


Figure 9.5: Initial wealth=0.5 and initial risky fraction=0.5. CRRA utility and terminal wealth distribution for portfolio insurance constraint problem with parameters:  $\gamma_N = \frac{1}{15}$ ,  $T = 1$ ,  $N = 4$ ,  $\lambda = \mu = 0.01$ ,  $s = e^{0.1\Delta T}$ ,  $m = 0.14$ ,  $\sigma = 0.3$ ,  $K = 0.2$ ,  $V = 0.5$ . Also  $V$  is the risk aversion co-efficient for CRRA utility.

# Chapter 10

## Lattice methods for pairs trading

Pairs trading is an investment strategy used by hedge funds in which equal, or roughly equal, amounts of capital in stocks, futures, options etc are simultaneously invested on both the long and short sides of the market. One reason for this strategy, in theory at least, is to make sure the result of the strategy is independent of broader market performance. Pairs are often selected for fundamental reasons for assets located in the same sector. Most of the literature on pairs trading, with notable papers being [32], [36] and [42], is devoted to discrete time signals in which the investor goes long the spread when it falls below a lower barrier and goes short the spread if it goes above an upper barrier. Analytical solutions were explored in [8]. Pairs trading is applicable to all asset classes and is an important class of algorithmic trading strategy practiced by hedge funds.

The chapter serves to give approximate lattice methods to analyze pairs trading models. In section 1 we provide lattice techniques to analyze pairs trading model based upon discrete time signals. In section 2 we provide techniques to model more dynamic versions of pairs trading models and also include transaction costs.

### 10.1 Dynamic pairs trading based upon discrete time signals

This section lays down the basic mathematical framework for the pairs trading methodology. Let  $A_k$  be the fundamental price of first stock and  $B_k$  be the fundamental price of the second stock. The fundamental price is the fair price of the stock. In this section of the thesis we will assume it as being the mid-point of bid-ask spread i.e.  $fundamental_t = \frac{1}{2}(bid_t + ask_t)$ .

A possible definition of the spread could be  $Z_k = A_k - \varpi_1 - \varpi_2 B_k$ . The investor shorts the spread if crosses an upper barrier and longs the spread if it falls below a lower barrier. In the Appendix B we highlight other possible pair trading schemes and the associated signals. The classical spread trading is based upon entry and exit signals. The process from going long to short or from short to long will be termed as a cycle in which the investor makes a profit equal to the difference in barrier levels. It is obvious that each completed cycle results in a profit and that the risk taken by an investor is that the cycle does not close.

### 10.1.1 Model

Let  $A_k$  and  $B_k$  be the price processes of the pairs and let  $Z_k$  be the process for the spread as defined earlier. There are  $N$  trading points over the time horizon and  $k = 1, 2, \dots, N$ . There are financial reasons for us to believe that the spread is mean-reverting. In the short-run the stocks may diverge from their fair prices but revert to their fundamental prices some time later which provides the basis for the spread to be mean-reverting. The trading period forward horizon  $T$  is of a sufficiently short so that arbitrage opportunities exist.

Due to its mean-reverting nature we will assume that the spread follows an Ornstein-Uhlenbeck (O-U) process<sup>1</sup>:

$$dZ_t = \kappa(\theta - Z_t)dt + \sigma dZ_t \quad (10.1)$$

where  $Z_t$  is a Brownian motion.

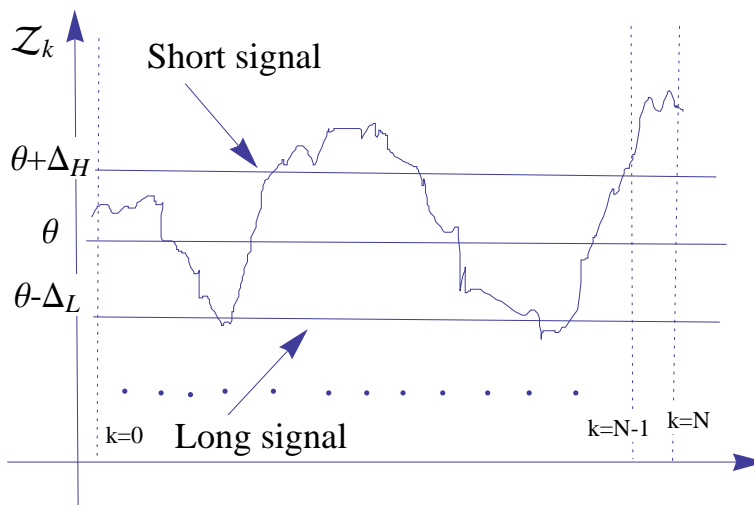
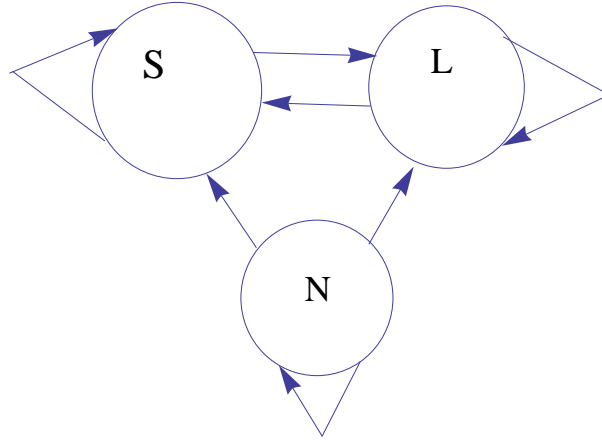


Figure 10.1: Trading Rule with entry and exit signals.

It can be observed from Figure 10.1 that we assume that the trading rule is fully encoded by the entry and exit signals. The optimal signals for that rule are one that yield maximum expected profits at the terminal time. We will denote  $S_k$  as the investor position on spread.  $S_k$  takes values in the set  $\{0, 1, 2\}$  where 0 means no position (**N**), 1 for short (**S**) and 2 for long (**L**). Also we will henceforth assume from now on that the upper and lower barrier for signals are both equidistant from the mean-reverting level (i.e.  $\Delta_H = \Delta_L$ ) and are also time independent.

We may describe the attainable values of  $S_k$  with the set  $\{\mathbf{N}, \mathbf{S}, \mathbf{L}\}$ . The state transitions under the trading rule is depicted in Figure 10.2.

<sup>1</sup>O-U process is stationary, Gaussian and Markovian. In particular, the stationarity assumption might not be satisfied very well in real life data. The primary motivation for choosing this process was its mean-reverting nature. As someone once said: "All models are wrong but some are useful."

Figure 10.2: Transition diagram for the state  $S_k \in \{\mathbf{N}, \mathbf{S}, \mathbf{L}\}$ .

Let  $\{\pi_k\}$  denote a non-decreasing process for the cumulative profits to date. So if  $\delta_k$  is the profit in the  $k^{\text{th}}$  period we could write:

$$\pi_k = \pi_{k-1} + \delta_k \quad (10.2)$$

We now frame the simple problem in value function formalism and define the value function to be:

$$V_k(\pi_k, \mathcal{Z}_k, S_k) = \mathbb{E}_{\Delta^*}[\pi_N | \mathcal{F}_k] \quad (10.3)$$

where  $\mathcal{F}_k$  is the filtration generated by Brownian motion and  $\Delta^*$  is the optimal parameter to be determined as part of optimization in dynamic programming.

It is easy to see that each cycle results in a profit of  $\Delta_L + \Delta_H = 2\Delta$ . The trading rule implies that  $S_k$  shifts state in the set  $\{0, 1, 2\}$ . The *evolution* of the state variables is described by:

$$\delta_k = (2\Delta) \mathbf{1}_{(S_{k-1}==1 \cap S_k==2) \cup (S_{k-1}==2 \cap S_k==1)} \quad (10.4)$$

$$S_k = \mathbf{1}_{(\mathcal{Z}_k > \theta + \Delta)} + 2 \cdot \mathbf{1}_{(\mathcal{Z}_k < \theta - \Delta)} + S_{k-1} \cdot \mathbf{1}_{(\theta - \Delta < \mathcal{Z}_k < \theta + \Delta)} \quad (10.5)$$

Starting from the terminal time:

$$V_{N-1}(\pi_{N-1}, \mathcal{Z}_{N-1}, S_{N-1}) = \mathbb{E}_{\Delta^*}[\pi_N | \mathcal{F}_{N-1}] \quad (10.6)$$

$$= \pi_{N-1} + \mathbb{E}_{\Delta^*}[\delta_N | \mathcal{F}_{N-1}] \quad (10.7)$$

$$= \pi_{N-1} + \mathcal{J}^{(1)}(\mathcal{Z}_{N-1}, S_{N-1}) \quad (10.8)$$

Going recursively backwards we see:

$$V_{N-k}(\pi_{N-k}, \mathcal{Z}_{N-k}, S_{N-k}) = \pi_{N-k} + \mathcal{J}^{(k)}(\mathcal{Z}_{N-k}, S_{N-k}) \quad (10.9)$$

The role of dynamic programming was to provide a scientific way to determine *optimal strategy* parameters without resorting to any simulation based technique. The  $\Delta^*$  is the same for all the periods and assumed to be time independent. We will chose a value for  $\Delta^*$  at initial state space configuration so as to maximize profits at the terminal time.

**Proposition 10.1.1** Equation (10.9) can be generalized to an extra parameter  $a$ :

$$V_{N-k}(a\pi_{N-k}, \mathcal{Z}_{N-k}, S_{N-k}) = (a - 1)\pi_{N-k} + V_{N-k}(\pi_{N-k}, \mathcal{Z}_{N-k}, S_{N-k}) \text{ for } a \in \mathfrak{R}.$$

**Proof** From equation (10.9) we have  $V_{N-k}(a\pi_{N-k}, \mathcal{Z}_{N-k}, S_{N-k}) = a\pi_{N-k} + \mathcal{J}^{(k)}(\mathcal{Z}_{N-k}, S_{N-k})$

Hence,

$$V_{N-k}(a\pi_{N-k}, \mathcal{Z}_{N-k}, S_{N-k}) = a\pi_{N-k} - \pi_{N-k} + \pi_{N-k} + \mathcal{J}^{(k)}(\mathcal{Z}_{N-k}, S_{N-k})$$

Thus,

$$V_{N-k}(a\pi_{N-k}, \mathcal{Z}_{N-k}, S_{N-k}) = (a - 1)\pi_{N-k} + V_{N-k}(\pi_{N-k}, \mathcal{Z}_{N-k}, S_{N-k})$$

■

## 10.1.2 Lattice based solution methodology

To apply our framework to a real life pair we have to estimate the spread process  $\mathcal{Z}_k$  using a historical look back from the start of the trading date and then apply to our dynamic programming framework to determine the optimal strategy parameter  $\Delta^*$ . The stock pair (LOW,HD) is a popular pair<sup>2</sup> in the industry and our analysis will subsequently be only restricted to it just for the sake of experimentation. A historical data set  $\mathcal{H}$  is chosen for estimation purposes with a certain look back from the start of the trading date.

The problem has separability in  $\pi_k$  so a grid is constructed in  $(\mathcal{Z}_k, S_k)$  space with  $S_k = 0, 1, 2$  and  $\mathcal{Z}_k \in [zmin, zmax]$ . The lower and upper limits of  $\mathcal{Z}_k$  are set to the 99 percent confidence interval in the historical data with the look back that is  $\mathcal{H}$ . Using the recursion equations (10.6-10.9) we could numerically determine the optimal control  $\Delta^*$  for the state variables at initial time. But to carry out the recursion we must first estimate the spread process  $\mathcal{Z}_k$  first using the data set  $\mathcal{H}$  !. If  $\mathcal{Z}_k = A_k - \varpi_1 - \varpi_2 B_k$  then by regressing  $A_k$  against  $B_k$  we estimate  $(\varpi_1, \varpi_2)$  yielding the residuals as the spread  $\mathcal{Z}_k$  which needs to be calibrate to O-U process. Calibration was done via the method of maximum likelihood<sup>3</sup>.

Setting the problem in our lattice framework we now cast the process  $\mathcal{Z}_k$  into a discrete probability approximation with  $E(\mathcal{Z}_k)$  and  $Var(\mathcal{Z}_k)$  dependent on  $\mathcal{Z}_k$ . This could be done using the probability deformation schemes we had already discussed in Chapter 5. Also for the application of probability deformation algorithms we have:

<sup>2</sup>Lowes (LOW) and Home Depot (HD) are both home improvement stores. They are located in the same industry and thus share similar sources of risks.

<sup>3</sup>We chose Maximum Likelihood from our various techniques to illustrate the method. Though there are so many other methods like brute force OLS on discretized SDE, brute force method of moments, generalized of method moments !

$$\eta_k = E(\mathcal{Z}_{k+1}|\mathcal{F}_k) = \mathcal{Z}_k e^{-\kappa\Delta T} + \theta(1 - e^{-\kappa\Delta T}) \tag{10.10}$$

$$\phi_k = Var(\mathcal{Z}_{k+1}|\mathcal{F}_k) = \frac{\sigma^2}{2\kappa}(1 - e^{-2\kappa\Delta T}) \tag{10.11}$$

$$\mathcal{Z}_{k+1}|\mathcal{F}_k \sim N(\eta_k, \phi_k) \tag{10.12}$$

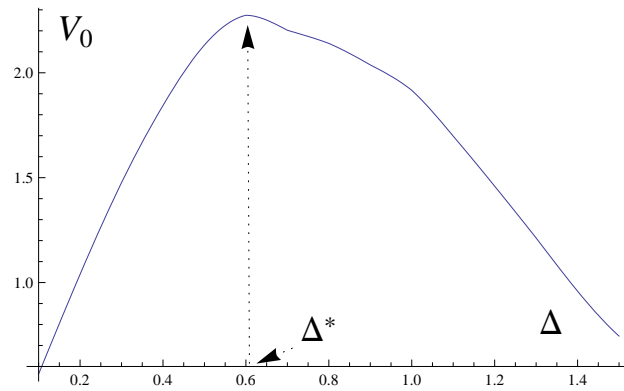


Figure 10.3: Value function at time  $t = 0$  for spread process calibrated to “LOW” and “HD” stock pair. At  $t = 0$  investor is short the spread with  $\mathcal{Z}_0 = 1.0$ . The time horizon for trading is 0.5 years with 10 observation points and data calibrated to history from May 2011 to May 2012.

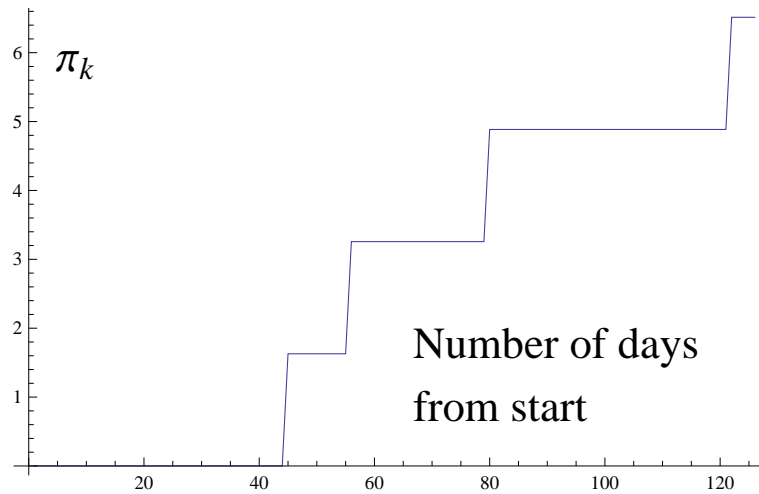


Figure 10.4: Simulation of gross realized profit (not including transaction costs) with trading starting at (2007,3,1) and look back of 500 days. The time horizon for trading is 0.5 years with 10 observation points and data calibrated with historical look back.

With a discrete probability approximation for  $\mathcal{Z}_k$  at hand we are ready to carry out the recursions in equations 10.6-10.9. Figure 10.3 shows our methodology applied to the pair

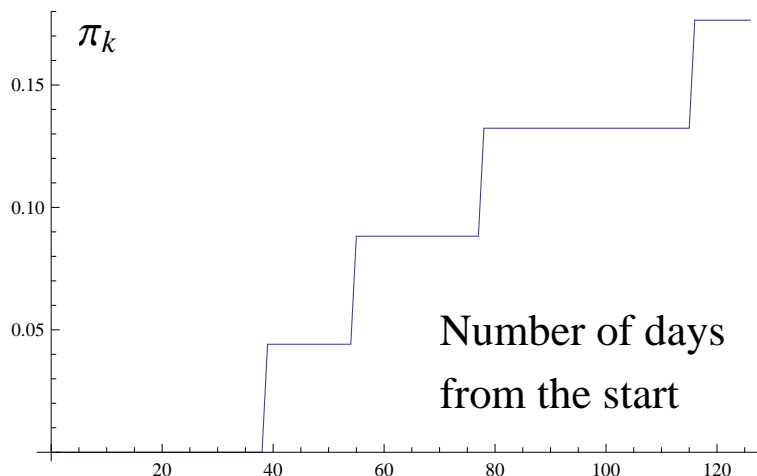


Figure 10.5: Simulation of gross realized profit (not including transaction costs) with trading starting at (2007,3,1) and look back of 100 days. The time horizon for trading is 0.5 years with 10 observation points and data calibrated with the historical look back.

(LOW,HD) to get the optimal  $\Delta^*$  for the forward trading horizon. The optimal strategy parameter  $\Delta^*$  is one that maximizes the value function at initial configuration of state variables. See Figure 10.3 for an illustration.

We also provide some simulations for our calibrated trading strategy  $\Delta^*$  for some randomly selected years. See Figure 10.4 and Figure 10.5.

Five years is a reasonable amount of time for back-test and was applied to our pair (LOW,HD). We applied our methodology to 24 equally spaced trading dates in the interval 2005-2011 so that we had 24 possible profits  $\pi_N$ . It is observed that in 6 out of 24 trades we had no profit at all which means that the cycle did not close! The results are summarized in the histogram in Figure 10.6.

To summarize main steps in optimal trading strategy design:

- 
- 1- Chose a look back from the start date. Get the historical data  $\mathcal{H}$  for estimation purposes.
  - 2- Estimate  $(\varpi_2^*, \varpi_1^*)$  in  $\mathcal{Z}_k = A_k - \varpi_1 - \varpi_2 B_k$  using  $\mathcal{H}$ .
  - 3- Fit an O-U process to the historical  $\{\mathcal{Z}_k\}$  obtained with  $\mathcal{H}$  using the estimates in 2.
  - 4- Use the O-U process in recursion equations to find the optimal  $\Delta^*$  for the forward trading horizon.
  - 5- Perform a 5 years back test on the so designed strategy.
- 

We note that in step 5 it is useful to analyze stability in the co-integration of the two pairs so that we are not subject to model risk problem. Also it is best to have as stationary as possible the historical spread data to have a *good* pair for profitable trading in the forward horizon. The broader vision of this section was to provide a lattice framework of analysis. We will discuss later in the conclusion that such a lattice framework allows us to embed complexity in our

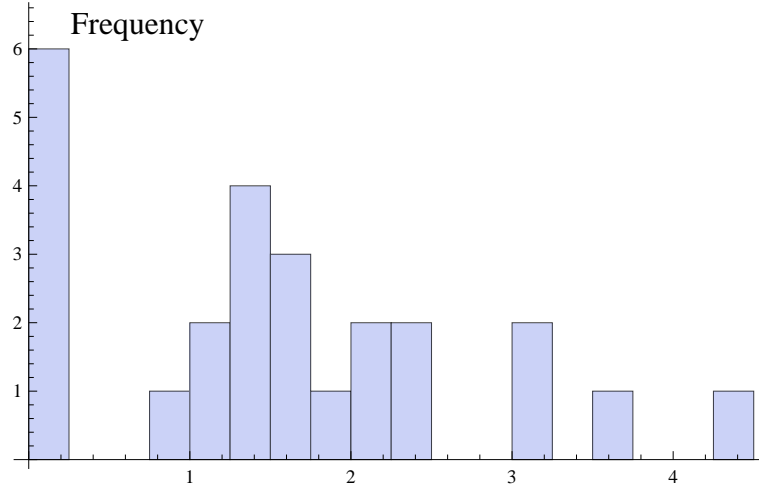


Figure 10.6: Histogram of realized profits for trading starting points chosen equally spaced in 2005-2011. Stock pair is (**LOW,HD**). Look back of 180 days and trading horizon of 180 days.

problem structure not possible by ordinary SDEs expressed in mathematical form (see [37] for a discussion on this issue).

We performed the analysis without transaction costs to simplify things. It is easy to factor in a transaction cost approximation. For the moment suppose the investor is long the spread at one point in time and then short the spread at a later time so that he makes profits. Also let  $(A_k^1, B_k^1)$  be the fundamental pair price initially and  $(A_k^2, B_k^2)$  be the fundamental pair price afterwards. We can express it as:

$$-A_k^1 + A_k^2 + \varpi_2 B_k^1 - \varpi_2 B_k^2 = 2\Delta \quad (10.13)$$

Let  $\alpha$  represent the bid-ask fraction symmetrically situated about the fundamental price. Then the total transaction costs  $C$  during the cycle equals:

$$C = \alpha(A_k^1 + A_k^2 + \varpi_2 B_k^1 + \varpi_2 B_k^2) \quad (10.14)$$

So far it appears the transaction cost for a cycle depends upon the fundamental prices which we have not factored into our model. But our objective is only to get an approximation and, assuming, the fundamental prices do not move too much during the interval we could put in average expected prices into our model approximating the transaction costs as :

$$C = 2\alpha(\bar{A} + \varpi_2 \bar{B}) \quad (10.15)$$

The realized profit is then  $2\Delta - C$ .

Most of the notable papers in academic literature for pairs trading are devoted to models involving discrete time signals. Moreover, the entry and exit signals for the trading strategy is based upon a *mean-reverting* spread process following an *Ornstein-Uhlenbeck* process. Unlike the previous literature this chapter seeks to provide an lattice based dynamic finite horizon framework under which trading strategies similar to trading pairs under transaction costs could be analyzed. We assume that there is a common state factor which drives the law of motion of



the pairs. Our framework also enables us to compare, analyze and subsequently rank the *risk - return* characteristics of trading strategies under transaction costs.

## 10.2 Lattice method for dynamic pairs trading under transaction costs

Most of the literature on pairs trading, with notable papers being [32], [36] and [42], is devoted to discrete time signals in which the investor goes long the spread when it falls below a lower barrier and goes short the spread if it goes above an upper barrier. Analytical solutions were explored in [8]. Pairs trading is applicable to all asset classes and is an important class of algorithmic trading strategy practiced by hedge funds.

Dynamic pairs trading has been first studied by [70]. This section seeks to give a more dynamic flavor to the trading strategy by adding a common factor in the expected return of the pairs and also including transaction costs. Experience suggests that successful pairs are most often located in the same industry. For example, Ford (F) and General Motors (GM) could be one example.

Let  $A_k$  be the stock price of F and  $B_k$  be the stock price of GM. One particular way of capturing the spread  $Z_k$  would be to define it as  $Z_k = \text{Log}(A_k) - \varpi_2 \text{Log}(B_k)$ . In general, the *co-integration* factor  $\varpi_2$  may be estimated from the historical data but for simplicity we will assume it to be close to one. Co-integration is a time series concept in which two time series are co-integrated if they share a common drift. Experience suggests that  $Z_k$  is most often mean-reverting for the pairs. Whether or not it is stationary could be questionable from a time series standpoint. We might suspect when  $Z_k$  becomes high or low its likelihood to revert to the equilibrium value increases.

Let  $(1 + g_k^1)$  be the growth rate of the first stock and  $(1 + g_k^2)$  be the growth rate of the second stock. This implies:  $Z_{k+1} = \text{Log}\left(\frac{1+g_k^1}{1+g_k^2}\right) + Z_k$ . Now if  $g_k^1 < g_k^2$  the spread  $Z_k$  decreases and vice versa.

This motivates us to create an endogenous system in which the expected returns on the stocks are linked to their own spreads. Figures 10.7 and 10.8 depict the idea. The expected returns are dependent on the stochastic *spread* with a differential sensitivity. The results is a differential in growth rates and hence the observed mean-reverting behavior in the stochastic spreads.

The standard CAPM model argues for expected returns of companies to be dependent on market risk premium. Other factor models include plausible factors as a source of risk premium. Our model argues there is a common factor in the two risky assets which contributes to the risk premium [36].

### 10.2.1 Intuition behind dynamic pairs trading

The idea behind the trading model is very simple. We would long /short the asset so as to bring our portfolio near the line of perfect hedge (shown by a straight line passing through the origin in Figure 10.10 ) as much as possible given the transaction costs. The intuition behind this is very simple.

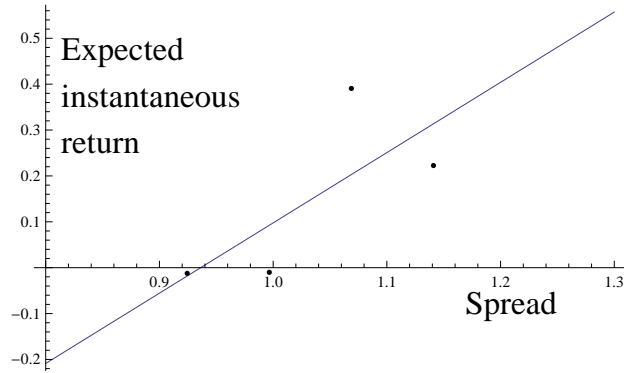


Figure 10.7: Approximate dependence expected return of the **MS** stock on the **(MS,GS)** stock pair spread using the daily closing stock prices from July 2005 to July 2006.

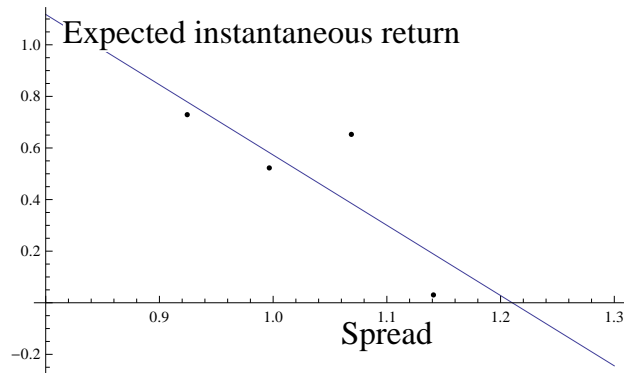


Figure 10.8: Approximate dependence expected return of the **GS** stock on the **(MS,GS)** spread using the daily closing stock prices from July 2005 to July 2006.

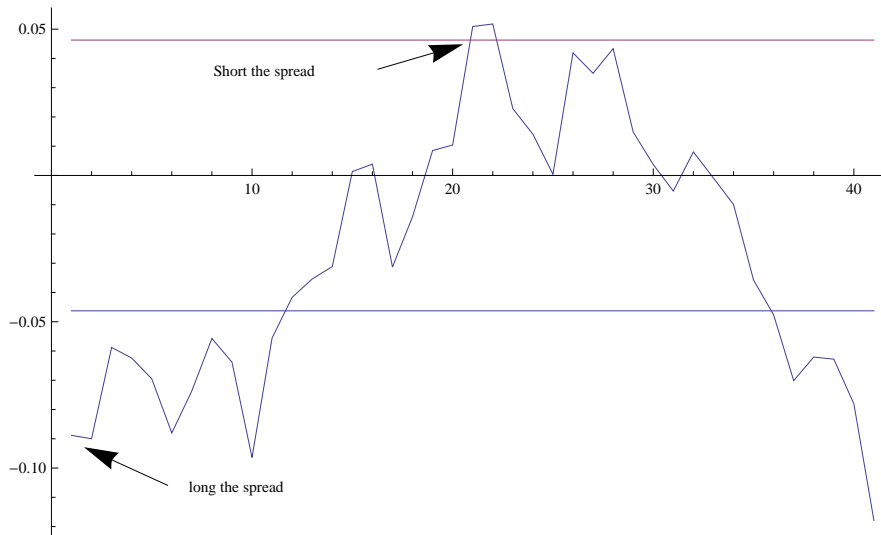


Figure 10.9: Pair trading signals - shorting when the spread falls below a barrier and longing when the spread goes above.

Suppose we have  $L_1$  amount in one risky asset and  $-L_2$  in the other. In other words we always take opposite positions in the risky assets. At the next time step our wealth grows to:  $(g_1 - g_2)Q + (L_1 - L_2)$  assuming  $L_1 \simeq L_2$ . But the expected growth rates are highly dependent on the spreads and so if we know the current value of spread we could predict the likely growth rates. We are very likely to make money thereupon. This is because of the mean-reverting behavior of the spreads and the dependence of the expected return on the spread.

We intuitively suspect that such a trading strategy would result in lower expected profits compared to an optimal unconstrained portfolio trading but with a lower variability.

Suppose the asset price of pairs follows a multi-variate GBM so that:

$$dA = (a + bZ_k)Adt + \sigma_1 AdW_t^1 \quad (10.16)$$

$$dB = (c + dZ_k)Bdt + \sigma_2 BdW_t^2 \quad (10.17)$$

Here  $W_t^i$  are standard Brownian motions with  $E[dW_t^1 dW_t^2] = \rho dt$ .

With  $Z_k = \text{Log}(\frac{A_k}{B_k})$ , using Ito's lemma the stochastic spread follows:

$$dZ_t = (d - b) \left( \frac{(a - c) - \frac{\sigma_1^2}{2} + \frac{\sigma_2^2}{2}}{d - b} - Z_t \right) dt + \sigma_1 dW_t^1 - \sigma_2 dW_t^2 \quad (10.18)$$

$$dZ_t = \kappa(\theta - Z_t)dt + \sigma dW_t^3 \quad (10.19)$$

Where  $\sigma = \sqrt{\sigma_1^2 + \sigma_2^2}$  and  $W_t^3$  is a standard Brownian motion.

As expected the spread process turns out to be mean-reverting.

Pairs trading is a highly successful class of algorithmic trading strategy even though its optimality from the point of view of Kelly criterion of maximizing the logarithm of growth rate could be questionable. We will compare the mean-variance optimality of the dynamic pairs trading strategy under transaction costs to an optimal trading rule implied by standard dynamic programming.

Standard dynamic portfolio theory implies that a growth rate maximizing investor keeps the fraction of wealth in risky assets equal to a constant fraction assuming a constant drift and volatility. Under transaction costs he has no-transaction boundaries around those risky fractions. In contrast, the dynamic pair trading model under transaction costs would bring our risky fraction to the line of no net exposure provided we go far away from that line and also dependent on the value of stochastic spread.

## 10.2.2 Dynamic programming formulation of the trading model

The investor puts his wealth in two risky assets and a risk-free asset so as to maximize the long-term growth rate. Consider a portfolio consisting of one risk-free asset growing at a rate of  $s_k$  over the  $k^{\text{th}}$  period. It also has two risky assets (pairs) with the  $i^{\text{th}}$  risky asset growing at a rate of  $r_{i,k}$  over the  $k^{\text{th}}$  period. The investor has an initial endowment of  $\bar{W}$ . At the beginning of each period he has the option to re-balance or not.

Let  $W_k^-$  be the wealth immediately before and  $W_k^+$  the wealth immediately after re-balancing for the  $k^{\text{th}}$  period. If he decides to re-balance then he faces transaction costs proportional to the

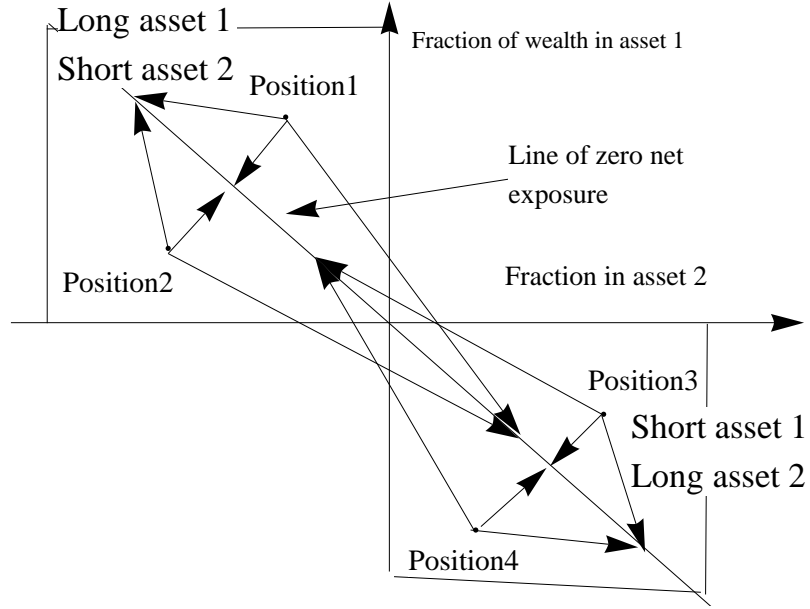


Figure 10.10: Dynamic pairs trading - pair trading quadrants with different controls illustrated.

amount traded. There are  $N$  periods so that each period is of equal length  $\Delta\mathcal{T} = \frac{\mathcal{T}}{N}$ . Such models were discussed in detail in Chapters 3, 5 and 6.

In this section we denote the vector  $\mathcal{A}_k^-$  as the fraction of wealth in risky assets respectively.

Let  $\mathcal{J}_k(W_k^-, \mathcal{A}_k^-, \mathcal{Z}_k^-) = E^{\mathbb{P}}[\frac{\text{Log}(W_N)}{T} | \mathcal{F}_k]$  be the value function under the logarithmic utility then under control set  $\{\zeta\}$  we have:

$$\mathcal{J}_k(W_k^-, \mathcal{A}_k^-, \mathcal{Z}_k^-) = \text{Max}_{\{\zeta\}} E^{\mathbb{P}}[\mathcal{J}_{k+1}(W_{k+1}^-, \mathcal{A}_{k+1}^-, \mathcal{Z}_{k+1}^-) | \mathcal{F}_k]. \quad (10.20)$$

Now since  $\mathcal{J}_N(W_N^-, \mathcal{A}_N^-, \mathcal{Z}_N^-) = \frac{1}{T} \text{Log}(W_N)$  we can write:

$$\mathcal{J}_N(W_N^-, \mathcal{A}_N^-, \mathcal{Z}_N^-) = \frac{1}{T} (\text{Log}(W_{N-1}^-) + \text{Log}(\mathbb{F}_{N-1}(\mathcal{A}_{i,N-1}^-, \mathcal{Z}_{i,N-1}^-))) \quad (10.21)$$

where  $\mathbb{F}$  is a stochastic functional depicting the investor behavior of re-balancing or not re-balancing at  $k = N - 1$  under the stochastic evolution. Further:

$$\mathcal{J}_{N-1}(W_{N-1}^-, \mathcal{A}_{N-1}^-, \mathcal{Z}_{N-1}^-) = \frac{1}{T} (\text{Log}(W_{N-1}^-) + \text{Max}_{\{\zeta\}} E^{\mathbb{P}}[\text{Log}(\mathbb{F}_{N-1}(\mathcal{A}_{i,N-1}^-, \mathcal{Z}_{i,N-1}^-)) | \mathcal{F}_{N-1}]). \quad (10.22)$$

In general for  $k = 2, 3, \dots, N$  we can write:

$$\begin{aligned} \mathcal{J}_{N-k}(W_{N-k}^-, \mathcal{A}_{N-k}^-, \mathcal{Z}_{N-k}^-) &= \frac{1}{T} (\text{Log}(W_{N-k}^-) + \text{Max}_{\zeta} E^{\mathbb{P}}[\mathcal{J}_{N-k+1}^{(k-1)}(\mathcal{A}_{i,N-k+1}^-, \mathcal{Z}_{i,N-k+1}^-) \\ &\quad + \text{Log}(\mathbb{F}_{N-k}(\mathcal{A}_{i,N-k}^-, \mathcal{Z}_{i,N-k}^-)) | \mathcal{F}_{N-k}]) \end{aligned} \quad (10.23)$$

$$= \frac{1}{T} (\text{Log}(W_{N-k}^-) + \mathcal{J}_{N-k}^{(k)}(\mathcal{A}_{i,N-k}^-, \mathcal{Z}_{i,N-k}^-)). \quad (10.24)$$

■

Our model is subject to *leverage* constraints of  $\alpha^*$ . A leverage constraint of 50 percent would mean the investor can not short or long more than 50 percent of his wealth at a point in time in a particular risky asset.

The optimality of pairs trading formulation using dynamic programming from the point of view of Kelly Criterion could be questionable. For instance, the optimal trading rule without restrictions under transaction costs would be to bring risky fraction as close as possible to the boundary of the no-transaction region. Under no-transaction costs the investor brings it to the *Merton* point. Under leverage constraints things will change somewhat but would be similar. In fact, under leverage constraints the *Merton* point is most likely to be on the boundary of the state simplex. We have no reason to believe that the *Merton* point always lies inside a constrained state space simplex. Under no-transaction cost case with risky assets following a multi-variate GBM we can easily prove the most optimal re-balancing point is  $\vec{\alpha} = \frac{1}{1-\gamma}\Sigma^{-1}(\vec{m} - r)$  for CRRA and  $\vec{\alpha} = \Sigma^{-1}(\vec{m} - r)$  for log-utility. With transaction costs being small we will have a no-transaction region surrounding this optimal point. The optimal policy under transaction cost would be to bring to the boundary of no-transaction region.

### 10.2.3 Evolution of portfolio state processes under a pairs trading model

The trading rule is summarized in Figure 10.10. There are several ways in which an investor can bring his portfolio to the line of zero net exposure depending upon his positioning in the quadrant. The arrows show the movement. For example if he is in position 1 then there are three possible ways to bring his portfolio to the line of zero net exposure. We provide the evolution equations for position 1 as depicted in Figure 10.10 and put the equations for rest of the positions in the Appendix B.

Also we denote:

$a_{i,k}^+$  = wealth in risky asset 1 immediately after re-balancing

$b_{i,k}^+$  = wealth in risky asset 2 immediately after re-balancing

$c_{i,k}^+$  = wealth in risky free asset immediately after re-balancing

**Position 1** -  $\mathcal{A}_{1,k}^- > 0, \mathcal{A}_{2,k}^- < 0$  with  $\mathcal{A}_{1,k}^- > |\mathcal{A}_{2,k}^-|$ :

**A-L - S** move (buy asset 1 and sell asset 2):

$$a_{i,k}^+ = \mathcal{A}_{1,k}^- \mathcal{W}_k^- + \Delta_k^1 = h \mathcal{W}_k^- \quad (10.25)$$

$$b_{i,k}^+ = \mathcal{A}_{2,k}^- \mathcal{W}_k^- - \Delta_k^2 = -h \mathcal{W}_k^- \quad (10.26)$$

$$c_{i,k}^+ = (1 - \mathcal{A}_{1,k}^- - \mathcal{A}_{2,k}^-) \mathcal{W}_k^- - (1 + \lambda_k) \Delta_k^1 + (1 - \mu_k) \Delta_k^2 \quad (10.27)$$

This implies that  $0 \leq \xi_k^1 \leq \alpha^* - \mathcal{A}_{1,k}^-$ . The second control can be expressed in terms of the first control via  $\xi_k^2 = \mathcal{A}_{2,k}^- + \mathcal{A}_{1,k}^- + \xi_k^1$ .

The state processes now evolve as:

$$\mathcal{A}_{1,k+1}^- = \frac{(\mathcal{A}_{1,k}^- + \xi_k^1) r_1}{\beta_{1,k}} \quad (10.28)$$

$$\begin{aligned}\beta_{1,k} &= (\mathcal{A}_{1,k}^- + \xi_k^1)r_1 - (\mathcal{A}_{1,k}^- + \xi_k^1)r_2 \\ &\quad + ((1 - \mathcal{A}_{1,k}^- - \mathcal{A}_{2,k}^-) - (1 + \lambda_k)\xi_k^1 + (1 - \mu_k)(\mathcal{A}_{2,k}^- + \mathcal{A}_{1,k}^- + \xi_k^1))s\end{aligned}\quad (10.29)$$

$$\mathcal{A}_{2,k+1}^- = \frac{-(\mathcal{A}_{1,k}^- + \xi_k^1)r_2}{\beta_{2,k}}\quad (10.30)$$

$$\begin{aligned}\beta_{2,k} &= ((\mathcal{A}_{1,k}^- + \xi_k^1)r_1 - (\mathcal{A}_{1,k}^- + \xi_k^1)r_2 \\ &\quad + ((1 - \mathcal{A}_{1,k}^- - \mathcal{A}_{2,k}^-) - (1 + \lambda_k)\xi_k^1 + (1 - \mu_k)(\mathcal{A}_{2,k}^- + \mathcal{A}_{1,k}^- + \xi_k^1))s\end{aligned}\quad (10.31)$$

**B- S - S** move (sell asset 1 and sell asset 2 ):

$$a_{i,k}^+ = \mathcal{A}_{1,k}^- \mathcal{W}_k^- - \Delta_k^1 = h\mathcal{W}_k^- \quad (10.32)$$

$$b_{i,k}^+ = \mathcal{A}_{2,k}^- \mathcal{W}_k^- - \Delta_k^2 = -h\mathcal{W}_k^- \quad (10.33)$$

$$c_{i,k}^+ = (1 - \mathcal{A}_{1,k}^- - \mathcal{A}_{2,k}^-)\mathcal{W}_k^- + (1 - \mu_k)\Delta_k^1 + (1 - \mu_k)\Delta_k^2 \quad (10.34)$$

This implies that  $0 \leq \xi_k^1 \leq \mathcal{A}^* + \mathcal{A}_k^1$ . The second control can be expressed in terms of the first control via  $\xi_k^2 = \mathcal{A}_k^2 + \mathcal{A}_k^1 - \xi_k^1$ .

The state processes now evolve as:

$$\mathcal{A}_{1,k+1}^- = \frac{(\mathcal{A}_{1,k}^- - \xi_k^1)r_1}{\beta_{1,k}} \quad (10.35)$$

$$\begin{aligned}\beta_{1,k} &= (\mathcal{A}_{1,k}^- - \xi_k^1)r_1 - (\mathcal{A}_{1,k}^- - \xi_k^1)r_2 \\ &\quad + ((1 - \mathcal{A}_{1,k}^- - \mathcal{A}_{2,k}^-) + (1 - \mu_k)\xi_k^1 + (1 - \mu_k)(\mathcal{A}_{2,k}^- + \mathcal{A}_{1,k}^- - \xi_k^1))s\end{aligned}\quad (10.36)$$

$$\mathcal{A}_{2,k+1}^- = \frac{-(\mathcal{A}_{1,k}^- - \xi_k^1)r_2}{\beta_{2,k}} \quad (10.37)$$

$$\begin{aligned}\beta_{2,k} &= (\mathcal{A}_{1,k}^- - \xi_k^1)r_1 - (\mathcal{A}_{1,k}^- - \xi_k^1)r_2 \\ &\quad + ((1 - \mathcal{A}_{1,k}^- - \mathcal{A}_{2,k}^-) + (1 - \mu_k)\xi_k^1 + (1 - \mu_k)(\mathcal{A}_{2,k}^- + \mathcal{A}_{1,k}^- - \xi_k^1))s\end{aligned}\quad (10.38)$$

**C- S - L** move (sell asset 1 and buy asset 2):

$$a_{i,k}^+ = \mathcal{A}_{1,k}^- \mathcal{W}_k^- - \Delta_k^1 = h\mathcal{W}_k^- \quad (10.39)$$

$$b_{i,k}^+ = \mathcal{A}_{2,k}^- \mathcal{W}_k^- + \Delta_k^2 = -h\mathcal{W}_k^- \quad (10.40)$$

$$c_{i,k}^+ = (1 - \mathcal{A}_{1,k}^- - \mathcal{A}_{2,k}^-)\mathcal{W}_k^- + (1 - \mu_k)\Delta_k^1 - (1 + \lambda_k)\Delta_k^2 \quad (10.41)$$

This implies that  $0 \leq \xi_k^1 \leq \mathcal{A}^* + \mathcal{A}_{1,k}^-$ . The second control can be expressed in terms of the first control via  $\xi_k^2 = -\mathcal{A}_{2,k}^- - \mathcal{A}_{1,k}^- + \xi_k^1$ .

The state processes now evolve as:

$$\mathcal{A}_{1,k+1}^- = \frac{(\mathcal{A}_{1,k}^- - \xi_k^1)r_1}{\beta_{1,k}} \quad (10.42)$$

$$\begin{aligned} \beta_{1,k} = & (\mathcal{A}_{1,k}^- - \xi_k^1)r_1 - (\mathcal{A}_{1,k}^- - \xi_k^1)r_2 \\ & + ((1 - \mathcal{A}_{1,k}^- - \mathcal{A}_{2,k}^-) + (1 - \mu_k)\xi_k^1 - (1 + \lambda_k)(-\mathcal{A}_{2,k}^- - \mathcal{A}_{1,k}^- + \xi_k^1))s \end{aligned} \quad (10.43)$$

$$\mathcal{A}_{2,k+1}^- = \frac{-(\mathcal{A}_{1,k}^- - \xi_k^1)r_2}{\beta_{2,k}} \quad (10.44)$$

$$\begin{aligned} \beta_{2,k} = & (\mathcal{A}_{1,k}^- - \xi_k^1)r_1 - (\mathcal{A}_{1,k}^- - \xi_k^1)r_2 \\ & + ((1 - \mathcal{A}_{1,k}^- - \mathcal{A}_{2,k}^-) + (1 - \mu_k)\xi_k^1 - (1 + \lambda_k)(-\mathcal{A}_{2,k}^- - \mathcal{A}_{1,k}^- + \xi_k^1))s \end{aligned} \quad (10.45)$$

**D- N - N (Do-nothing):**

$$a_{i,k}^+ = \mathcal{A}_{1,k}^- \mathcal{W}_k^- \quad (10.46)$$

$$b_{i,k}^+ = \mathcal{A}_{2,k}^- \mathcal{W}_k^- \quad (10.47)$$

$$c_{i,k}^+ = (1 - \mathcal{A}_{1,k}^- - \mathcal{A}_{2,k}^-) \mathcal{W}_k^- \quad (10.48)$$

State control constraints are absent here as state particles evolve with *complete freedom*.

The state processes now evolve as:

$$\mathcal{A}_{1,k+1}^- = \frac{\mathcal{A}_{1,k}^- r_1}{\mathcal{A}_{1,k}^- r_1 + \mathcal{A}_{2,k}^- r_2 + (1 - \mathcal{A}_{1,k}^- - \mathcal{A}_{2,k}^-)s} \quad (10.49)$$

$$\mathcal{A}_{2,k+1}^- = \frac{\mathcal{A}_{2,k}^- r_2}{\mathcal{A}_{1,k}^- r_1 + \mathcal{A}_{2,k}^- r_2 + (1 - \mathcal{A}_{1,k}^- - \mathcal{A}_{2,k}^-)s} \quad (10.50)$$

## 10.2.4 A generalized trading model

### Evolution of state particles without any pre-determined trading rule

In a generalized trading we don't have a predetermined heuristic to tell us what should be the evolution of state process. We let the dynamic programming principle help us decide.

In all the possible control *moves* for the state particle we always have a constraint  $-\alpha^* \leq h_k^{i,+} \leq \alpha^*$ . We only provide evolution equations for buying asset 1 and selling asset 2 and put rest of the equations in the appendix B.

**A-Buy Asset 1, Sell Asset 2:**

$$a_{i,k}^+ = \mathcal{A}_{1,k}^- \mathcal{W}_k^- + \Delta_k^1 = h_k^{1,+} \mathcal{W}_k^- \quad (10.51)$$

$$b_{i,k}^+ = \mathcal{A}_{2,k}^- \mathcal{W}_k^- - \Delta_k^2 = h_k^{2,+} \mathcal{W}_k^- \quad (10.52)$$

$$c_{i,k}^+ = (1 - \mathcal{A}_{1,k}^- - \mathcal{A}_{2,k}^-) \mathcal{W}_k^- - (1 + \lambda_k) \Delta_k^1 + (1 - \mu_k) \Delta_k^2 \quad (10.53)$$

The state particles now evolve as:

$$\mathcal{A}_{1,k+1}^- = \frac{h_k^{1,+} r_1}{\beta_{1,k}} \quad (10.54)$$

$$\begin{aligned} \beta_{1,k} = & h_k^{1,+} r_1 + h_k^{2,+} r_2 \\ & + ((1 - \mathcal{A}_{1,k}^- - \mathcal{A}_{2,k}^-) - (1 + \lambda_k)(h_k^{1,+} - \mathcal{A}_{1,k}^-) + (1 - \mu_k)(\mathcal{A}_{2,k}^- - h_k^{2,+})) s \end{aligned} \quad (10.55)$$

$$\mathcal{A}_{2,k+1}^- = \frac{h_k^{2,+} r_2}{\beta_{2,k}} \quad (10.56)$$

$$\begin{aligned} \beta_{2,k} = & h_k^{1,+} r_1 + h_k^{2,+} r_2 \\ & + ((1 - \mathcal{A}_{1,k}^- - \mathcal{A}_{2,k}^-) - (1 + \lambda_k)(h_k^{1,+} - \mathcal{A}_{1,k}^-) + (1 - \mu_k)(\mathcal{A}_{2,k}^- - h_k^{2,+})) s \end{aligned} \quad (10.57)$$

### 10.2.5 Solution methodology

We highlight the solution methodology in broad brush. Its main ingredients are grid construction and dynamic recursion as discussed in the previous section. The problem has separability in wealth  $\mathcal{W}_k^-$  as shown by equations 10.21-10.24. We will accordingly construct a 3D grid in  $(\mathcal{A}_{1,k}^-, \mathcal{A}_{2,k}^-, \mathcal{Z}_k)$  space. Lower and upper limits for  $\mathcal{A}_{i,k}^-$  are set to the leverage constraints. Lower and upper limits for  $\mathcal{Z}_k$  can be found from the underlying discrete probability approximation for  $\mathcal{Z}_k$ .

Since  $\mathcal{Z}_k = \text{Log}(A_k) - \text{Log}(B_k)$  we have  $\Delta \mathcal{Z}_k = \frac{1+g_A}{1+g_B}$ . Once a joint evolution 2-D discrete probability approximation for risky growth  $(1 + g_A, 1 + g_B)$  dependent upon the value of  $\mathcal{Z}_k$  is constructed the corresponding 1-D discrete probability approximation for  $\Delta \mathcal{Z}_k$  dependent upon  $\mathcal{Z}_k$  could easily be obtained. The upper limit for  $\mathcal{Z}_k$  are chosen by observing a value for  $\mathcal{Z}_k$  when  $\Delta \mathcal{Z}_k$  discrete probability approximation has a “very small” probability of going up and lower limit chosen when it has a “very small” probability of going down.

### 10.2.6 Numerical results for control law

We illustrate the results of pair trading rule in the state variable space. In Figures 10.11 10.12 we have the fraction of wealth in the risky assets in the horizontal and vertical axis respectively. The control law was encoded with symbols as shown in the captions. Such a picture lets a pair trader know what to do at a point in time.



For a certain choice of parameters it is seen that pair trading rule is quite off from the growth rate under a generalized trading rule. We display the terminal wealth distribution results in Tables 10.1-10.3.

Numerical results match our intuition very well. For dynamic pairs trading the investor is more likely to bring to the line of perfect hedge the more the spread is away from the equilibrium. Also he is less likely to do any transaction if the value of spread is close to its equilibrium. Also he trades much more in the pairs trading rule compared to the optimal trading rule implied by dynamic programming. In the optimal trading rule he trades much less and trading only if the spread is significantly away from the equilibrium.

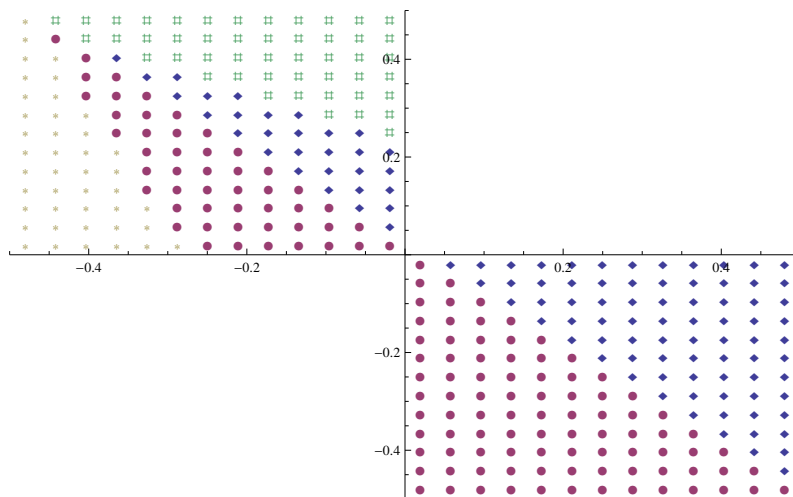


Figure 10.11: Optimal control law at time  $t = 0$  and spread = 0.25 under dynamic trading for the following choice of parameter which are already defined earlier :  $\lambda = \mu = 0.005, T = 0.2, N = 2, s = e^{0.05\Delta T}, a = 0.16, b = 0.1, \sigma_1 = 0.1, c = 0.1, d = 0.9, \sigma_2 = 0.2, \rho = 0.05$ . Also  $\diamond \mapsto SS, \bullet \mapsto SL, \star \mapsto LS, + \mapsto LL$  and  $\# \mapsto NN$ .

### 10.2.7 Mean-variance optimality of dynamic pairs trading:

Assuming  $W_N = W_0 e^{r_N T}$  then:

$$E[r_N] = \frac{E(\text{Log}(W_N)) - \text{Log}(W_0)}{T}, \text{Var}[r_N] = \frac{\text{Var}(\text{Log}(W_N))}{T^2} \tag{10.58}$$

The results tabulated in the following tables are in line with our intuition. Pairs trading has a lower variability in returns but at a cost of lower expected returns.

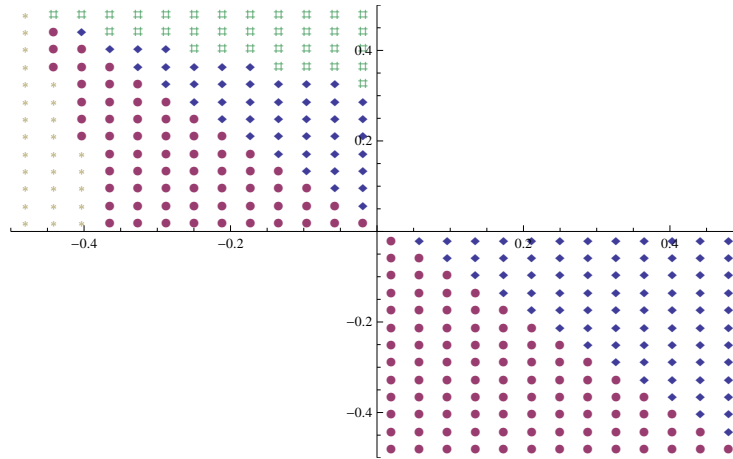


Figure 10.12: Optimal control law at time  $t = 0$  and spread = 0.5 under dynamic trading for the following choice of parameter which are already defined earlier:  $\lambda = \mu = 0.005, T = 0.2, N = 2, s = e^{0.05\Delta T}, a = 0.16, b = 0.1, \sigma_1 = 0.1, c = 0.1, d = 0.9, \sigma_2 = 0.2, \rho = 0.05$ . Also  $\diamond \mapsto$  SS,  $\bullet \mapsto$  SL,  $\star \mapsto$  LS,  $+$   $\mapsto$  LL and  $\# \mapsto$  NN.

trading rule	terminal wealth statistics	$E[\text{Log}(W_N)]$	$\text{Var}[\text{Log}(W_N)]$
pairs trading rule		0.132	0.0288
optimal trading rule		0.207	0.0366

Table 10.1: Terminal wealth distribution statistics initial risky fraction 1=0.2, initial risky fraction 2 =-0.2, stochastic spread=0.7, with parameter:  $\lambda = \mu = 0.005, T = 0.5, N = 5, s = e^{0.05\Delta T}, a = 0.16, b = 0.1, \sigma_1 = 0.1, c = 0.1, d = 0.9, \sigma_2 = 0.1, \rho = 0.2$

### 10.2.8 Concluding remarks

The section analyzed a particular class of algorithmic trading strategy by comparing it to an optimal trading rule implied by standard dynamic programming. Our objective was to provide a framework under which a rigorous risk-return analysis of dynamic trading strategies is possible.

trading rule	terminal wealth statistics	$E[\text{Log}(W_N)]$	$\text{Var}[\text{Log}(W_N)]$
pairs trading rule		0.1079	0.0262
optimal trading rule		0.176	0.0341

Table 10.2: Terminal wealth distribution statistics initial risky fraction 1=0.2, initial risky fraction 2 =-0.2, stochastic spread=0.55, with parameter:  $\lambda = \mu = 0.005, T = 0.5, N = 5, s = e^{0.05\Delta T}, a = 0.16, b = 0.1, \sigma_1 = 0.1, c = 0.1, d = 0.9, \sigma_2 = 0.2, \rho = 0.2$

trading rule	terminal wealth statistics	$E[\text{Log}(W_N)]$	$\text{Var}[\text{Log}(W_N)]$
pairs trading rule		0.0998	0.0254
optimal trading rule		0.165	0.033

Table 10.3: Terminal wealth distribution statistics initial risky fraction 1=0.2, initial risky fraction 2 =-0.2, stochastic spread=0.5, with parameter:  $\lambda = \mu = 0.005, T = 0.5, N = 5, s = e^{0.05\Delta T}, a = 0.16, b = 0.1, \sigma_1 = 0.1, c = 0.1, d = 0.9, \sigma_2 = 0.1, \rho = 0.2$

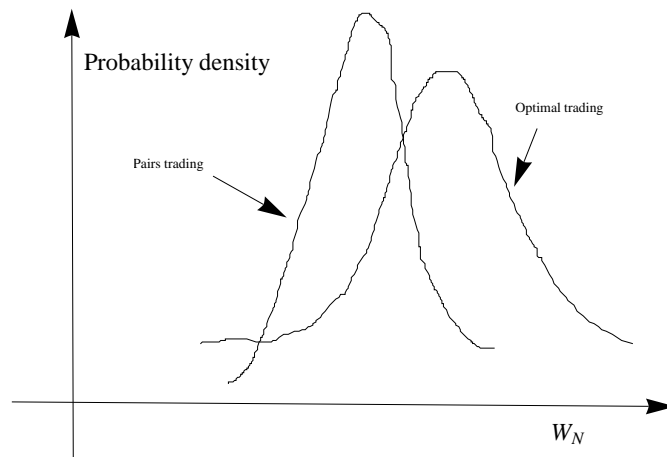


Figure 10.13: Probability distribution of terminal wealth.

# Chapter 11

## CONCLUSION

Our goal had been to present simple, intuitively appealing and easily implementable numerical algorithms to solve problems in portfolio theory. We apply this tool to build insight about a set of dynamic portfolio problems. Transaction costs were an essential feature of our models. We provided a discrete time lattice framework for analyzing dynamic portfolio problems. Discrete probability approximations were used as a fundamental tool for solving different variants of realistic portfolio problems in chapter 6 to chapter 10. Approximate methods were provided for handling portfolio constraints in chapter 9 and a real life pairs trading application of our framework was provided in chapter 10.

SDEs (mostly GBM ) in continuous time were approximated and embedded into our lattice framework. Amongst the ambitious goals for future work we would like to make our lattice apply to a discrete time dynamical system called *cellular automaton* (CA). Most mathematical models in science are based upon the assumption that time and space are continuous, whereas according to Stephen Wolfram “time and space are discrete” [37]. In future we would like to create CA like models which are capable of depicting the complex behavior displayed in real life. Consider the modeling in Chapter 10 for example. We assumed that the spread followed a well behaved continuous O-U process. However, in reality the spread follows a much more complex process no SDE could ever aim to model in a continuous framework. We believe our discrete time lattices could. We could in principle use data in real-life to embed complex probability structure in our lattices. The structure needs to interact with time and with other lattice structures denoted by  $\{\tilde{h}_{k,i}\}$  in the macro-economic environment.

The fact is that “real-world” processes have parameters which change with time. As we highlighted in Chapter 7 most of the value of re-balancing springs from the “non-stationarity” in risky growths. If we have a GBM with constant drift and volatility then re-balancing does not have a lot of value because the relevant portfolio state vectors for a utility function do not sufficiently deviate from our optimal positioning to warrant re-balancing under transaction costs. In this context, a financial analyst’s forecast about the drift and volatility of the stock has a lot of value. Forecasting economic conditions has a lot of value because this is tied to the performance of stocks. We provide a visualization in Figure 11.1 of no-transaction geometries over an investment horizon in which an investor could perfectly forecast<sup>1</sup> the drift and volatility of the stock in the three equidistant regimes<sup>2</sup> in a one year investment horizon. One can see

---

<sup>1</sup>Perfect foresight makes the dynamic programming problem *time consistent*.

<sup>2</sup>Each regime is of length  $\frac{1}{3}$  year. See Chapter 7 for a discussion on our regime model.

that no-transaction geometries under a parameter change model are quite different from the constant parameter models we saw in Chapter 6.

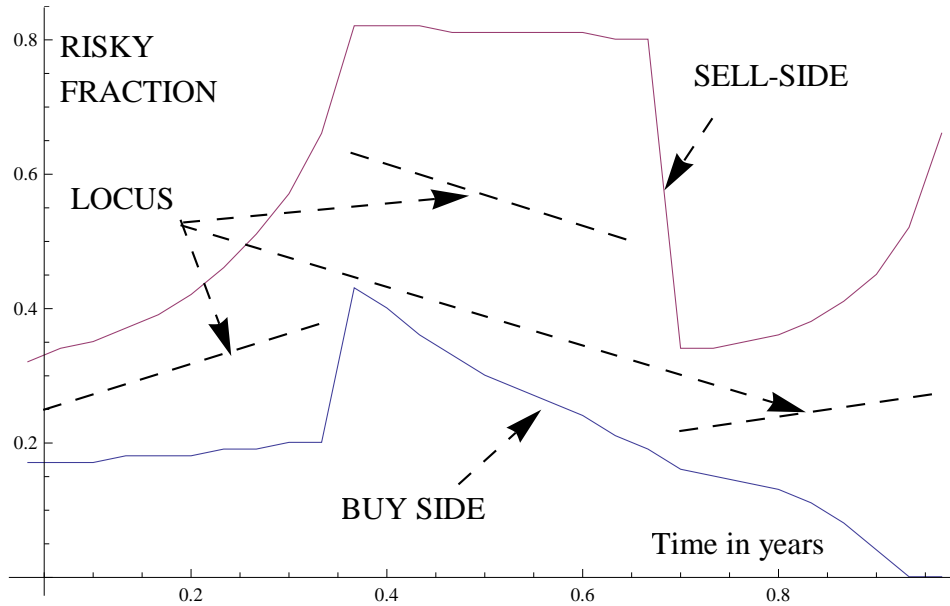


Figure 11.1: No-transaction geometries for growth rate maximization when parameters change over the horizon and investor has perfect foresight. Parameters:  $m_1 = 0.14, \sigma_1 = 0.6, m_2 = 0.2, \sigma_2 = 0.5, m_3 = 0.15, \sigma_3 = 0.45$ . Here  $(m_i, \sigma_i)$  is the drift and volatility for regime  $i$ .

Our approach in the thesis was based upon experimentation as a basis for discovery. Consider for instance, a famous problem you will most often encounter in stochastic calculus. Let us suppose  $W(t)$  is a standard Brownian motion and we are required to find the stopping time distribution where the stopping time  $\tau$  is defined for some positive real  $a$  as:

$$\tau = \min\{t : W(t) \geq a\} \quad (11.1)$$

Using principles of stochastic calculus we could derive the analytical form for the stopping time distribution.

However, the thesis provides techniques which could solve the problem numerically without resort to any detailed stochastic calculus principle. All we require is the law of iterated expectations and the principle of deformation. Our experimental lattice would be  $\mathcal{L} = (W_k, M_k)$ .

Here for  $W_0 = M_0 = 0$ :

$$\Delta W_k \sim N(0, \Delta T) \quad (11.2)$$

$$M_{k+1} = \max\{M_k, W_{k+1}\} \quad (11.3)$$

Now define:

$$\phi(T|\mathcal{F}_0) = P(\tau \leq T|\mathcal{F}_0) \quad (11.4)$$

$$= P(M(T) \geq a|\mathcal{F}_0) \quad (11.5)$$

$$= E(1_{\{M(T) \geq a\}}|\mathcal{F}_0) \quad (11.6)$$

We can now easily determine  $\phi$  via law of iterated expectations on a deformed probability structure and determine  $\phi'$  which is the approximated stopping time distribution. The results of our experimental lattices are reasonably accurate by comparing with exact analytic result for first passage time in continuous time. See Figures 11.2 and 11.3. In Figure 11.2 we use SQID scheme with 25 branches and in Figure 11.3 we matched first 19 moments of Standard Brownian Motion.

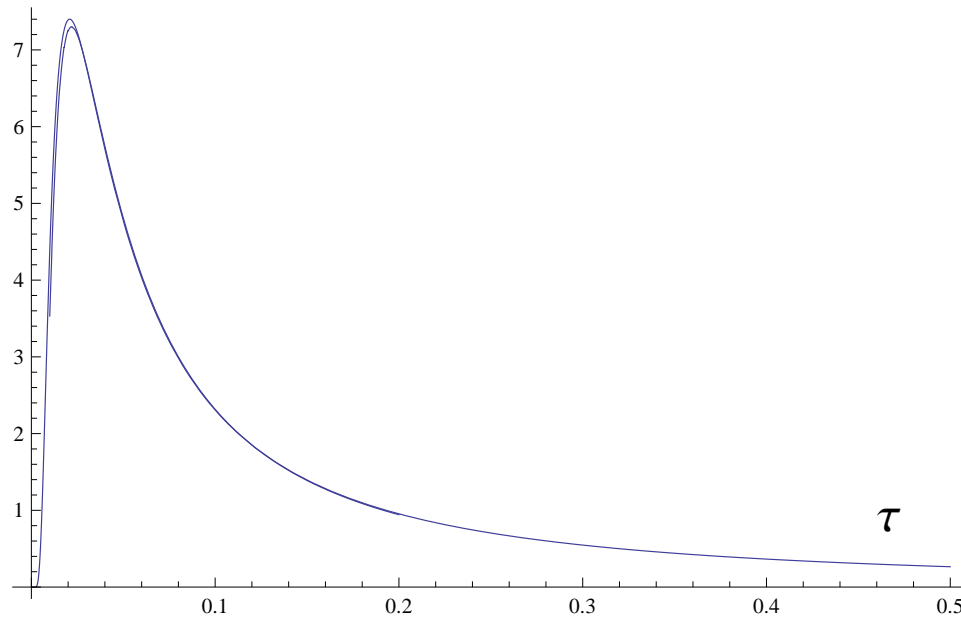


Figure 11.2: First passage time distribution using lattice compared to exact result. SQID scheme used to create 25 branches for Standard Brownian motion. Parameters:  $a = 0.25$ ,  $N = 90$ ,  $T = 0.2$ ,  $wmin = -1$ ,  $wmax = +1$ ,  $mmin = -1$ ,  $mmax = +1$ ,  $dw = 0.05$ ,  $dm = 0.05$ . Here  $a$  is the barrier,  $N$  is the number of time steps,  $T$  is the time period,  $(wmin, wmax)$  are the bounds for actual value of Standard Brownian motion,  $(mmin, mmax)$  are the bounds for attained maximum value of Standard Brownian motion,  $dw$  is the size of state step in  $W_k$ -space and  $dm$  is the size of state step in  $M_k$  space.

The fact is that real-world processes are much more complex and stochastic calculus principles might not exist to analyze them. However, our experimental lattices could provide a framework of analysis.

The thesis avoided any PDE based approach to the solutions which are popular for continuous time formulations in academic literature.

For instance, a PDE encountered in the transaction cost literature is:

$$V_t + rxV_x + \mu yV_y + \frac{1}{2}\sigma^2 y^2 V_{yy} = 0 \quad (11.7)$$

with  $V(x, y, t) := y^{\gamma-1}\phi(\frac{x}{y}, t)$  and  $V_x = V_y$  at  $\partial B$ ,  $(1 - \alpha)V_x = V_y$  at  $\partial S$ .

The above PDE can be transformed in to a nice linear PDE via  $z = \frac{x}{y}$  (reducing the order of PDE) and then  $w = \log(z)$ . This makes the PDE constant co-efficient perfectly linear and provides stability to a finite difference scheme that involves moving back in time. Solving

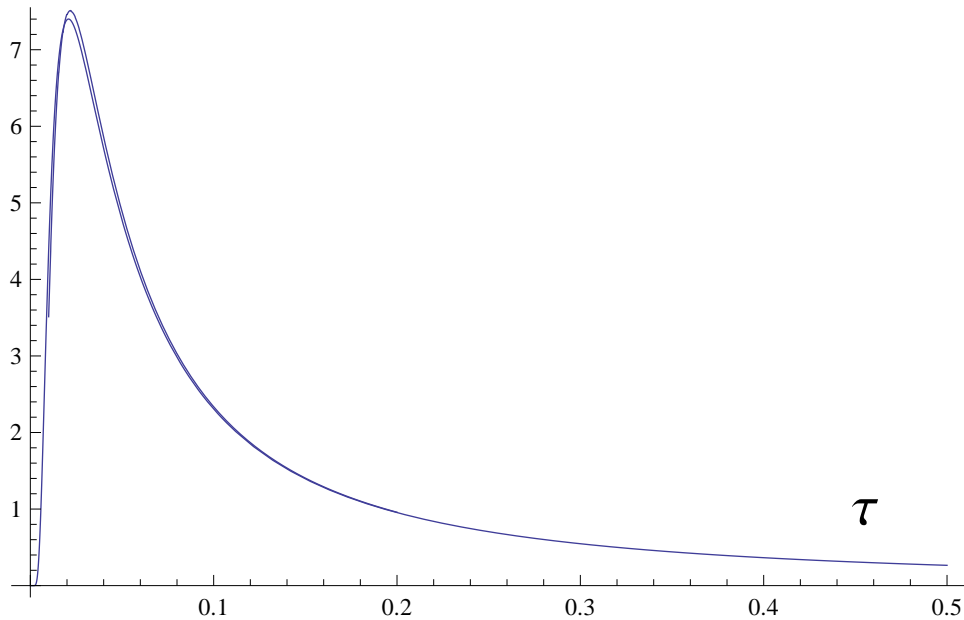


Figure 11.3: First passage time distribution using lattice compared to exact result. Moment matching of first 19 moments for Standard Brownian motion. Parameters:  $a = 0.25$ ,  $N = 90$ ,  $T = 0.2$ ,  $wmin = -1$ ,  $wmax = +1$ ,  $mmin = -1$ ,  $mmax = +1$ ,  $dw = 0.05$ ,  $dm = 0.05$ . Here  $a$  is the barrier,  $N$  is the number of time steps,  $T$  is the time period,  $(wmin, wmax)$  are the bounds for actual value of Standard Brownian motion,  $(mmin, mmax)$  are the bounds for attained maximum value of Standard Brownian motion,  $dw$  is the size of state step in  $W_k$ -space and  $dm$  is the size of state step in  $M_k$  space.

PDEs like these is quite of a challenge because HJB PDE is only valid inside the boundaries and we don't know the location of these boundaries. We do, however, know the behavior of the boundaries which can be exploited with small enough time stepping backwards in time. The choice of discretization in variables is observed to significantly impact the accuracy and stability of the PDE.

In the short subsections that follow we state and discuss our future goals:

## 11.1 Developing methods for improved computational speed

Furthermore, there are few useful tips that slightly improve computational speed. One is *homotopic perturbation scheme* that we are currently developing. This involves using the optimal control law in the time step ahead as a *feed* in to the optimal control search for previous time step.

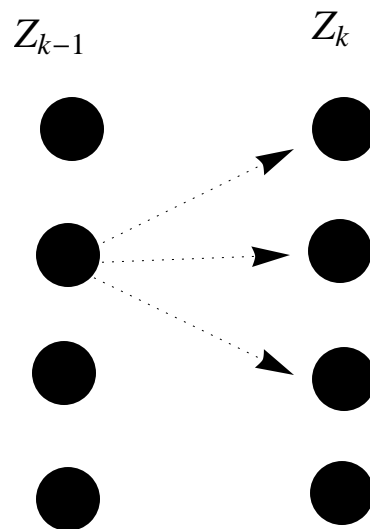


Figure 11.4: Lattice framework for spread evolution.

## 11.2 Extending our modeling framework to a wider range of asset classes

We want to extend our modeling framework outside the GBM model for stock prices. The algorithms in this thesis were specifically developed so that we could handle portfolios consisting of a wide variety of asset classes e.g. foreign exchange, options, futures etc. As discussed earlier we have schemes that could essentially handle a wide variety of stochastic processes for risky assets.

Take jump diffusion as an example. It can be used to model commodity prices, portfolios with exchange rate, energy portfolios, market crashes, systematic risk etc. For the purpose of illustrating jump diffusion models in action, consider a portfolio having money in different currencies for instance dollars and pounds. The basic modeling framework is the same as we had in our earlier series of manuscripts whereby the investor has some investment objective over a time horizon.

Let  $W_k$  : be the total amount of wealth in pounds for the dynamic investor

$X_k$  : be the amount of wealth in dollars

$Y_k$  : be the amount of wealth in pounds

$E_k$  : be the exchange rate for pounds (£) per dollar \$.



If the investor decides to transfer wealth from dollars to pounds then:

$$X_{k+1}^- = \frac{(A_k^- - \xi_k)W_k^- \circ r_1}{E_k} \quad (11.8)$$

$$Y_{k+1}^- = ((1 - A_k^-) + (1 - \mu)\xi_k)W_k^- \circ r_2 \quad (11.9)$$

$$W_{k+1}^- = (A_k^- - \xi_k)W_k^-(1 + g_k) \circ r_1 + ((1 - A_k^-) + (1 - \mu)\xi_k)W_k^- \circ r_2 \quad (11.10)$$

If he decides to transfer wealth from pounds to dollars then:

$$X_{k+1}^- = \frac{(A_k^- + \xi_k)W_k^- \circ r_1}{E_k} \quad (11.11)$$

$$Y_{k+1}^- = ((1 - A_k^-) - (1 + \lambda)\xi_k)W_k^- \circ r_2 \quad (11.12)$$

$$W_{k+1}^- = (A_k^- + \xi_k)W_k^-(1 + g_k) \circ r_1 + (A_k^- - (1 + \lambda)\xi_k)W_k^- \circ r_2 \quad (11.13)$$

If he decides to do nothing then  $\xi_k = 0$ .

In general the control  $\xi_k$  must obey realistic leverage constraints. The risky growth  $g_k$  over the interval is comes from a jump diffusion model and solution methodology has already been discussed by us in Chapter 5 on *portfolio deformation schemes*. Given the transaction costs, current value of exchange rate and amount of wealth in a particular asset our dynamic investor can now decide how much wealth to dynamically transfer from one asset to another over the time horizon. It is possible to model exchange rate as stochastic volatility jump diffusion in which case  $g_k = g_k(E_k)$ . For the special case of CARA, CRRA and log-utility for example the optimal policy is independent of the level of wealth and depends upon the fraction/amount of wealth held in a particular currency with one currency being the *numeraire*. Clearly it can be seen that many transfer of wealth models have a similar structure to our original formulation in terms of risky and non-risky assets.

The purpose had been to show the effectiveness of our modeling framework to a wide variety of situations.

Consider the case of options for example. Their primary role is to hedge risks in a portfolio. But it will be interesting to examine the stochastic option value evolution from a portfolio stand point. The risky growth vector construction is the key. The thesis modeled risky assets. Accordingly, the risky growth vector of option is given by  $g^* = \frac{V(S_k(1+g_k),k)}{V(S_k,k)}$  as in a standard Black-Scholes framework. Introduction of the options would only increase the dimensionality of state space by introducing  $S_k$ .

Consider for instance a renewable energy company trying to position solar plants over a wide geographical region. Each solar plant is essentially a risky asset with a value. Depending upon risk factors which vary geographically but which do have some correlation structure we could again model our situation in context of dynamic portfolio theory and examine mean-variance optimality of our geographical positioning.

$$V_k^A = \phi_k(f_k^1, f_k^2, \dots, f_k^N) \quad (11.14)$$

$$V_{k+1}^A = \phi_k((1 + g_k^1)f_k^1, (1 + g_k^2)f_k^2, \dots, (1 + g_k^N)f_k^N) \quad (11.15)$$

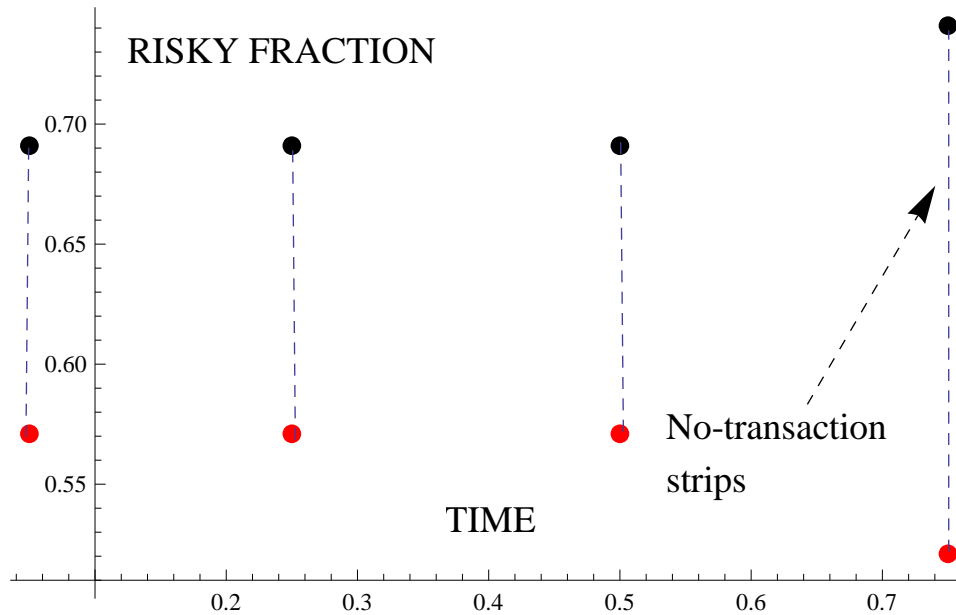


Figure 11.5: No-transaction region variation with time for exchange rate model under a simple jump diffusion model with growth rate maximization for exchange rate portfolio. In the discrete time re-balancing we have no-transaction strips at  $t = 0, 0.25, 0.5, 0.75$ . Parameter choice is :  $T = 1, N = 4, \lambda = \mu = 0.01, r_1 = e^{0.05\Delta T}, r_2 = e^{0.07\Delta T}, m = 0.14, \sigma = 0.6, \theta = 0.1, \delta = 0.05$ .

### 11.3 Analyze theoretical economic problems

It will be interesting to apply the methods of the thesis to more theoretical economic problems in portfolio choice. A notable example is the habit formation literature [68].

It would be interesting to explore formulations like these in markets with frictions i.e. transaction costs, liquidity constraints etc.

### 11.4 Incorporating parameter uncertainty into our decision making methodology

The thesis also wishes the reader to think about prescriptions to deal with *estimation error* and *parameter uncertainty* over the investment horizon. Estimation errors are mainly statistical in nature. Assume we do not have a model of how the parameters evolve dynamically. The true parameter values only become visible with time. Can we incorporate this feature in to our dynamic programming modeling framework ? Should the tools of dynamic programming not be applied at all because this make the problem time inconsistent. But the central question should be: are their approximate heuristics that could deal with such problems ?

We believe such heuristics could be constructed:

**I-** How about we apply standard dynamic programming in a non-commitment situation ? The dynamic investor estimates the parameter vector  $\mu_k$  and as soon as

$$\|\mu_{k'} - \mu_k\| \geq \delta$$

the investor resets the controls for the remaining horizon.

**II-** We had earlier seen that some investment objectives allow nice decomposability structures. Now consider there are two investors each with a growth rate maximization objective over the horizon  $T$ . One investor maximizes  $E[\text{Log}(W_T)]$  over the horizon  $T$ . Parameter uncertainty does not allow this investor to allow time consistent controls under transaction costs<sup>3</sup>. However, the other investor decomposes his objective so that he maximizes:

$$E[\text{Log}(W_{T/N})], E[\text{Log}(W_{2T/N})], \dots, E[\text{Log}(W_T)]$$

for successive intervals. This allows the investor to apply standard dynamic programming in a time consistent manner.

Consider the dynamic investor trying to minimize the variability of his terminal wealth about a target level  $\gamma$ . We had earlier seen in Chapter 6 that varying  $\gamma$  quite essentially traces out an efficient frontier and could help maximize his Sharpe ratio over the given horizon. There are  $N$  re-balancing periods to choose controls for and as new parameters become visible with time we could re-write the optimal controls.

A possible algorithm could be:

**Step 1:** Estimate the model parameters for risky growth using an optimal look back determined historically

**Step 2:** Need to find  $\gamma_i$  at the period that maximizes Sharpe ratio over the remaining horizon

**Step 3:** Find the optimal controls for the remaining horizon

**Step 4:** Once you move forward in time your forward horizon length shortens and we start from step 1 again.

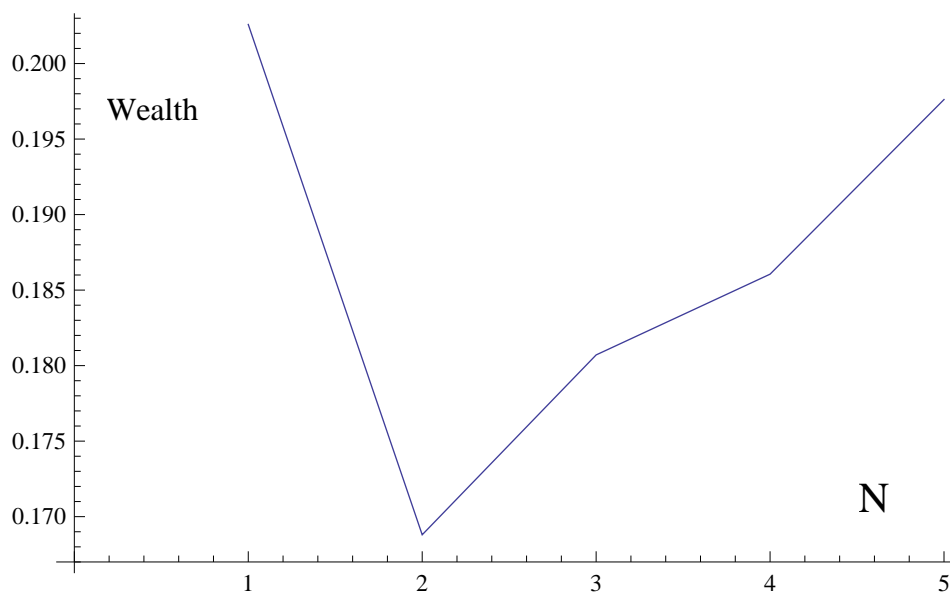


Figure 11.6: Realization of wealth for an investor trying to maximize Sharpe ratio by investing in SP500 and GS starting (2010,1,1) for one year with initial wealth =0.5 and initial fraction in SP500=0.5. Also Lookback =40 days. Parameter choice  $T = 1, N = 5, \lambda = 0.005, r = 0.05$

<sup>3</sup>Under no-transaction costs provided his utility function allows separability in wealth then it is easy to see that even under parameter uncertainty we could have time consistent controls. This is because value function only depends on time and is separable in wealth.

## 11.5 Incorporating macro-economic factors in to our decision making methodology

It will be interesting to make our models more comprehensive by bringing macro-economic and financial variables as factors in the dynamics of risky assets. The forecast of these variables could go as an input in to our dynamic decision making methodology. That is:

$$\frac{dS_t}{S_t} = (\mu + \alpha_t)dt + \sigma dW_t \quad (11.16)$$

with  $\alpha_t = Bf_t$  where  $f_t$  is a *factor*.

Analyzing more complex capital gain tax models would be very interesting.

## 11.6 A rigorous analysis of different dynamic trading strategies

The thesis analyzed one particular of algorithmic trading strategy using the available tools. It will be interesting to analyze different kinds of trading strategies based on this pattern. For example, what are the risk-return characteristics of buying relative to various moving averages compared other dynamic trading strategies? There are several novel ways we could introduce transaction costs in to our model.

The valuation of target date funds could be made more rigorous by including transaction costs and making trading frequency to be less than observation points in a discrete time framework.

---

# Bibliography

- [1] Akian, M., and Sulem, A. (1996). Dynamic Optimization of Long-Term Growth Rate for a portfolio with transaction costs and logarithmic utility. *Mathematical Finance*, Vol.11 No. 2, 153-188.
- [2] Alexander, G.J., and Baptista, A.M. (2006). Portfolio selection with a draw-down constraint. *Journal of Banking and Finance*, 30(11), 3171-3189.
- [3] Atkinson, C., Pliska, S., and Wilmott, P. (1997). Portfolio Management with transaction costs. *Proceedings: Mathematical, Physical and Engineering Sciences*, Vol. 453, No. 1958, pp 551-562.
- [4] Atkinson, C., and Quek, G. (2012). Dynamic Portfolio Optimization in Discrete-Time with Transaction Costs. *Applied Mathematical Finance*, 1-34.
- [5] Atkinson, C., and Storey, E. (2010). Building an optimal portfolio in discrete time in the presence of transaction costs. *Applied Mathematical Finance*, 17(4), 323-357.
- [6] Atkinson, C., and Wilmott, P. (1995). Portfolio Management under transaction costs: an asymptotic analysis of Merton and Pliska model. *Mathematical Finance*, 5:357-367.
- [7] Basak, S., and Chabakauri, G. (2010). Dynamic mean-variance asset allocation. *Review of Financial Studies*, 23:2970.
- [8] Bertram, W.K. (2010). Analytic solutions for optimal statistical arbitrage trading. *Physica A: Statistical Mechanics and its Applications*, 389(11), 2234-2243.
- [9] Bertsimas, D., Lauprete, G.J., and Samarov, A. (2004). Shortfall as a risk measure: properties, optimization and applications. *Journal of Economic Dynamics and Control*, 28(7), 1353-1381.
- [10] Bielecki, T.R., and Pliska, S.R. (2000). Risk sensitive asset management with transaction costs. *Finance and Stochastics*, 4(1), 1-33.
- [11] Black, F., and Perold, A. F. (1992). Theory of constant proportion portfolio insurance. *Journal of Economic Dynamics and Control*, 16(3), 403-426.
- [12] Black, F., and Jones, R.C. (1987). Simplifying portfolio insurance. *The Journal of Portfolio Management*, 14(1), 48-51.

- [13] Black, F., and Scholes, M. (1973). The pricing of options and corporate liabilities. *The Journal of Political Economy*, 637-654.
- [14] Bollerslev, T., and Melvin, M. (1994). Bidask spreads and volatility in the foreign exchange market: An empirical analysis. *Journal of International Economics*, 36(3), 355-372.
- [15] Boyle, P.P. (1988). A lattice framework for option pricing with two state variables. *Journal of Financial and Quantitative Analysis*, 23(1), 1-12.
- [16] Brandt, M.W., Goyal, A., Santa-Clara, P., and Stroud, J.R. (2005). A simulation approach to dynamic portfolio choice with an application to learning about return predictability. *Review of Financial Studies*, 18(3), 831-873.
- [17] Broadie, Mark, and Paul Glasserman. "A stochastic mesh method for pricing high-dimensional American options." *Journal of Computational Finance* 7 (2004): 35-72.
- [18] Butt, N. Portfolio Management under Transaction costs. MSc thesis. The University of Western Ontario.
- [19] Chen, J.S., Chang, C.L., Hou, J.L., and Lin, Y.T. (2008). Dynamic proportion portfolio insurance using genetic programming with principal component analysis. *Expert systems with applications*, 35(1), 273-278.
- [20] Constantinides, G.M. (1986). Capital market equilibrium with transaction costs. *The Journal of Political Economy*, 842-862.
- [21] Cox, J.C., Ross, S.A., and Rubinstein, M. (1979). Option pricing: A simplified approach. *Journal of financial Economics*, 7(3), 229-263.
- [22] Cvitanic, J., Lazrak, A., and Wang, T. (2008). Implications of the Sharpe ratio as a performance measure in multi-period settings. *Journal of Economic Dynamics and Control*, 32(5), 1622-1649.
- [23] Chen, Y., Dai, M., and Zhao, K. Finite Horizon Optimal Investment and Consumption with CARA Utility and Proportional Transaction costs, Working Paper.
- [24] Dai, M., and Zhong, F.H. (2010). Penalty methods for continuous-time portfolio selection under transaction cost. *Journal of Computational Finance*, 13(3), 1-31.
- [25] Dai, M., Jiang, L., Li, P.F, and Yi, F.H. (2009). Finite horizon optimal consumption and investment with transaction cost. *SIAM Journal on Control and Optimization*, 48(2), 1134-1154.
- [26] Dai, M., Xu, Z., and Zhou, X.Y. (2010). Continuous-time mean-variance portfolio selection with proportional transaction costs. *SIAM Journal on Financial Mathematics*, 1(1), 96-125.
- [27] Dammon, R.M., Spatt, C.S., and Zhang, H.H. (2001). Optimal consumption and investment with capital gains taxes. *Review of Financial Studies*, 14(3), 583-616.

- [28] Davis, M.H.A., and Norman, A.R. (1990). Portfolio selection with transaction costs. *Mathematics of Operations Research*, 676-713.
- [29] Brigo, D. and Mercurio, F. (2001). *Interest rate models : theory and practice*. Springer-Verlag, Berlin, Heidelberg.
- [30] Kuhn, D. and Luenberger, D.G. (2010). Analysis of the re-balancing frequency in log-optimal portfolio selection. *Quantitative Finance*, 10(2), 221-234.
- [31] Duffie, D. and Sun, T. (1990). Transactions costs and portfolio choice in a discrete-continuous-time setting. *Journal of Economic Dynamics and Control*, 14(1), 35-51.
- [32] Elliott, R.J., Van Der Hoek, J., and Malcolm, W.P. (2005). Pairs trading. *Quantitative Finance*, 5(3), 271-276.
- [33] Fleming W., and Soner H. (1993). *Controlled Markov Processes and Viscosity Solutions*. Springer Ver-lag, 1993.
- [34] Forsyth, P., Vetzal, K., and Zvan, R. (2002). Convergence of numerical methods for valuing path-dependent options using interpolation. *Review of Derivatives Research*, 5(3), 273-314.
- [35] Garlappi, L., and Skoulakis, G. (2010). Solving Consumption and Portfolio Choice Problems: The State Variable Decomposition Method. *Review of Financial Studies*, 23(9), 3346-3400.
- [36] Gatev, E. (2006). Pairs Trading: Performance of a Relative-Value Arbitrage Rule. *Review of Financial Studies*, 19(3), 797-827.
- [37] Gray, L. (2003). A mathematician looks at Wolfram's new kind of science. *Notices-American Mathematical Society*, 50(2), 200-211.
- [38] Grossman, S.J., and Zhou, Z. (1993). Optimal investment strategies for controlling draw-downs. *Mathematical Finance*, 3(3), 241-276.
- [39] Hamelink, F., and Hoesli, M. (2004). Maximum draw-down and the allocation to real estate. *Journal of Property Research*, 21(1), 5-29.
- [40] Hasbrouk, J. (1991). The summary informativeness of stock trades: an econometric analysis. *Review of Financial Studies*, Volume 4, Issue 3, pp. 571-595.
- [41] Hausman, J.A., and Lo, A.W. (1992). An ordered probit analysis of transaction stock prices. *Journal of Financial Economics*, Volume 31, Issue 3, 319-379
- [42] Huck, N. (2009). Pairs selection and outranking: An application to the SP 100 index. *European Journal of Operational Research*, 196(2), 819-825, 2009
- [43] Ishii, H., and Pierre-Luis L. (1990). Viscosity solutions of Fully Nonlinear Second Order Elliptic Partial Differential Equations. *Journal of Differential Equations*, 83 : 26-78.

- [44] Jiang, L., and Dai, M. (2005). Convergence of binomial tree methods for European/American path-dependent options. *SIAM Journal on Numerical Analysis*, 1094-1109.
- [45] Kamrad, B., and Ritchken, P. (1991). Multinomial Approximating Models for Options with k State Variables. *Management Science*, Vol. 37, No. 12, 1640-1652.
- [46] Keefe, D.L. and Bodily, S.E. (1983) Three-point approximations for continuous random variables. *Management Science*, 29(5), 595-609.
- [47] Keefe, D.L. (1994). Certainty Equivalents distribution for Approximations. *Management Science*, 40(6), 760-773.
- [48] Kim, H.Y., and Viens, F.G. (2010). Portfolio optimization in discrete time with proportional transaction costs under stochastic volatility. *Annals of Finance*, 1-21.
- [49] Korn, R. (1998). Portfolio optimization with strictly positive transaction costs and impulse control. *Finance and Stochastics*, 2(2), 85-114.
- [50] Kuhn, D., and Luenberger, D.G. (2010). Analysis of the re-balancing frequency in log-optimal portfolio selection. *Quantitative Finance*, Volume 10, Issue 2, pp 221-234.
- [51] Kumar, S., and Mutharaman, K. (2004). A Numerical Method for Solving Singular Stochastic Control Problems. *Operations Research*, Vol. 52, pp. 563-582.
- [52] Lee, H.I., Hsu, H., and Chiang, M.H. (2010). Portfolio insurance with a dynamic floor. *Journal of Derivatives Hedge Funds*, 16(3), 219-230.
- [53] Leland, H. (2000). Optimal portfolio implementation with transactions costs and capital gains taxes. Unpublished manuscript, Haas School of Business, University of California, Berkeley.
- [54] Leland, H.E., and Rubinstein, M. (1976). The evolution of portfolio insurance, in: D.L. Luskin, ed., *Portfolio insurance: a guide to dynamic hedging*, Wiley.
- [55] Liu, H. (2004). Optimal consumption and investment with transaction costs and multiple risky assets. *The Journal of Finance*, 59(1), 289-338.
- [56] Liu, H., and Loewenstein, M. (2002). Optimal portfolio selection with transaction costs and finite horizons. *Review of Financial Studies*, 15, 805-835.
- [57] Longstaff, Francis A., and Eduardo S. Schwartz. "Valuing American options by simulation: A simple least-squares approach." *Review of Financial studies* 14.1 (2001): 113-147.
- [58] Lorenz, J. (2008). Optimal trading algorithms: Portfolio transactions, multi-period portfolio selection, and competitive online search. PhD Thesis, ETH Zurich.
- [59] Lynch, A., and Tan, S. (2002). Multiple risky assets, transaction costs and return predictability: Implications for portfolio choice. NYU Working Paper No. SC-AM-02-13.



- [60] Magill, M.J.P. and Constantinides, G.M. (1976). Portfolio selection with transaction costs. *Journal of Economic Theory*, 13(2), 245-263.
- [61] Markowitz, H.M. (1952). Portfolio selection. *The Journal of Finance*, 7(1), 77-91.
- [62] Markowitz, H.M. (1979). Approximating Expected Utility by a Function of Mean and Variance. *The American Economic Review*, 69(3), 308-317.
- [63] McInish, T.H., and Wood, R.A. (1992). An analysis of intra-day patterns in bid/ask spreads for NYSE stocks. *Journal of Finance*, 753-764.
- [64] Merton, R.C. (1969). Lifetime portfolio selection under uncertainty: The continuous-time case. *The review of Economics and Statistics*, 51(3), 247-257.
- [65] Miller, A.C. and Rice, T.R. (1983). Discrete Approximations to probability distributions. *Management Science*, 29(3), 352-362.
- [66] Mookhavesa, S., and Atkinson, C. (2002). Perturbation Solution of optimal portfolio theory with transaction costs for any utility function. *IMA Journal of Management Mathematics*, 13 : 131-151.
- [67] Morgenstern, O., and Neumann, J.V. (1944). *Theory of Games and Economic Behavior*, Princeton University Press, Princeton
- [68] Naryshkin, R., and Davison, M. (2008). Portfolio Optimization under Habit Formation. Arxiv preprint arXiv:0810.0678.
- [69] Morton, A., and Pliska S. (1995). Optimal portfolio management with fixed transaction costs. *Mathematical Finance*, 5:337-356.
- [70] Mudchanatongsuk, S., Primbs, J.A., and Wong, W. (2008). Optimal Pairs Trading: A Stochastic Control Approach 2008 American Control Conference, Seattle, Washington, USA, June 11-13.
- [71] Mutharaman, K, and Kumar, S. (2006). Multidimensional portfolio optimization with proportional transaction costs. *Mathematical Finance*, Vol.16, No.2, 301-335.
- [72] Mutharaman, K, and Zha, H. (2008). Simulation-based portfolio optimization for large portfolios with transaction costs. *Mathematical Finance*, Vol. 18, No. 1, 115-134.
- [73] Mutharaman, K. (2007). A computational scheme for optimal investment -consumption with proportional transaction costs. *Journal of Economic Dynamics and Control*, 31 :1132-1159, 2007.
- [74] O'Hara, M., and Oldfield, G.S. (1986). The Microeconomics of Market Making. *Journal of Financial and Quantitative Analysis*, 21 :pp. 361-376
- [75] Pawula, R.F. (1987). Approximating Distributions from moments, *Physical Review*, 36(10).

- [76] Pflug, G.H. (2001). Scenario tree generation for multi-period financial optimization by optimal discretization. *Math Programming*, 271, 251-271.
- [77] Plerou, V., Gopikrishnan, P., and Stanley, H. (2005). Quantifying fluctuations in market liquidity: Analysis of the bid-ask spread., 1-20. *Physical Review E*, 71(4), 1-8.
- [78] Shreve, S.E., and Soner, H.M. (1994). Optimal investment and consumption with transaction costs. *The Annals of Applied Probability*, 609-692.
- [79] Smith, J. E. (1993). Moment Methods for Decision Analysis. *Decision Analysis*, 39(3), 340-358.
- [80] Stoll, H.R. (1978). The Supply of Dealer Services in Securities Markets. *The Journal of Finance*, Vol. 33, No. 4, pp. 1133-1151
- [81] Taksar, M., Klass, M. J., and Assaf, D. (1988). A diffusion model for optimal portfolio selection in the presence of brokerage fees. *Mathematics of Operations Research*, 277-294.
- [82] Thomas, H.T., and Stoll, H.R. (1980). On Dealer Markets Under Competition. *The Journal of Finance*, Vol. 35, No. 2, Papers and Proceedings Thirty-Eighth Annual Meeting American Finance Association, Atlanta, Georgia, December 28-30, pp. 259-267
- [83] Thompson, M., and Davison, M. High Dimensional Stochastic Dynamic Portfolio Optimization with Transaction Costs. Working Paper.
- [84] Tourin, A., and Zariphopoulou, T. (1994). Numerical schemes for investment models with singular transactions. *Computational Economics*, 7(4), 287-307.
- [85] Wallace, K.H.S.W. (2001). Generating Scenario Decision Trees for Multistage Problems. *Management Science*, 47(2), 295-307.
- [86] Weiner, S.M. (2000). The effect of stochastic volatility on portfolio optimization with transaction costs. University of Oxford PhD Thesis.
- [87] Zhou, X. (2003). Markowitz's World in Continuous Time, and Beyond. *Stochastic Modeling and Optimization with Applications in Queues, Finance, and Supply Chains*, pp.279-310.
- [88] Zumbach, G. (2004). How the trading activity scales with the company sizes in the FTSE 100. Arxiv preprint cond-mat/0407769, arxiv.org

# Appendix A

## Mathematica code for chapter 4

### A.1 Tree construction code:

#### A.1.1 Tree construction in 2-D

```
pvals = {p, q, r, 1 - p - q - r};
rvals = {(1 + g1) * (1 + g2),  $\frac{1 + g1}{1 + g2}$ ,  $\frac{1 + g2}{1 + g1}$ ,  $\frac{1}{(1 + g1) * (1 + g2)}$ };

rvals1 = {1 + g1,  $\frac{1}{1 + g1}$ };
rvals2 = {1 + g2,  $\frac{1}{1 + g2}$ };
pvals1 = {p + q, 1 - p - q};
pvals2 = {p + r, 1 - p - r};
exp = {
  rvals1.pvals1 == 1 + m1 * ΔT,
  (rvals1^2).pvals1 - (rvals1.pvals1)^2 == σ1^2 * ΔT,
  rvals2.pvals2 == 1 + m2 * ΔT,
  (rvals2^2).pvals2 - (rvals2.pvals2)^2 == σ2^2 * ΔT,
  rvals.pvals - (1 + m1 * ΔT) * (1 + m2 * ΔT) == ρ * σ1 * σ2 * ΔT};

sol = {pvals, rvals} /. (ss = NSolve[exp, {g1, g2, p, q, r}]);

dist = {{{(1 + g1), (1 + g2)}, p}, {{(1 + g1),  $\frac{1}{(1 + g2)}$ }, q},
  {{{ $\frac{1}{(1 + g1)}$ , (1 + g2)}, r}, {{ $\frac{1}{1 + g1}$ ,  $\frac{1}{1 + g2}$ }, 1 - p - q - r}} /. ss[[2]]
```

## A.1.2 Tree construction in 3-D

```
pvals = {p, q, r, ss, t, u, v, 1 - p - q - r - ss - t - u - v};
rvals = {u1 * u2 * d3, u1 * u2 * u3, u1 * d2 * d3,
  u1 * d2 * u3, d1 * u2 * d3, d1 * u2 * u3, d1 * d2 * u3, d1 * d2 * d3};
```

```
rvals1 = {u1, d1};
rvals2 = {u2, d2};
rvals3 = {u3, d3};
pvals1 = {p + q + r + ss, 1 - p - q - r - ss};
pvals2 = {p + q + t + u, 1 - p - q - t - u};
pvals3 = {q + ss + u + v, 1 - q - ss - u - v};
```

```
rvals12 = {u1 * u2, u1 * d2, d1 * u2, d1 * d2};
pvals12 = {p + q, r + ss, t + u, 1 - p - q - r - ss - t - u};
rvals13 = {u1 * u3, u1 * d3, d1 * u3, d1 * d3};
pvals13 = {q + ss, p + r, u + v, 1 - q - ss - p - r - u - v};
rvals23 = {u2 * u3, u2 * d3, d2 * u3, d2 * d3};
pvals23 = {q + u, p + t, ss + v, 1 - q - u - p - t - ss - v};
```

```
exp = {
  rvals1.pvals1 == 1 + m1 * ΔT,
  (rvals1^2).pvals1 - (rvals1.pvals1)^2 == σ1^2 * ΔT,
  ((rvals1 - (1 + m1 * ΔT))^3).pvals1 == 0,
  rvals2.pvals2 == 1 + m2 * ΔT,
  (rvals2^2).pvals2 - (rvals2.pvals2)^2 == σ2^2 * ΔT,
  ((rvals2 - (1 + m2 * ΔT))^3).pvals2 == 0,
  rvals3.pvals3 == 1 + m3 * ΔT,
  (rvals3^2).pvals3 - (rvals3.pvals3)^2 == σ3^2 * ΔT,
  ((rvals3 - (1 + m3 * ΔT))^3).pvals3 == 0,
  rvals12.pvals12 - (1 + m1 * ΔT) * (1 + m2 * ΔT) == ρ12 * σ1 * σ2 * ΔT,
  rvals13.pvals13 - (1 + m1 * ΔT) * (1 + m3 * ΔT) == ρ13 * σ1 * σ3 * ΔT,
  rvals23.pvals23 - (1 + m2 * ΔT) * (1 + m3 * ΔT) == ρ23 * σ2 * σ3 * ΔT,
  p == 0.1
};
(*dist={{u1,u2},p},{{u1,d2},q},{{d1,u2},r},{{d1,d2},1-p-q-r}}/.
  NSolve[exp,{u1,d1,u2,d2,p,q,r}][[2]]*)
```

```
dist = {{u1, u2, d3}, p}, {{u1, u2, u3}, q},
  {{u1, d2, d3}, r}, {{u1, d2, u3}, ss}, {{d1, u2, d3}, t}, {{d1, u2, u3}, u},
  {{d1, d2, u3}, v}, {{d1, d2, d3}, 1 - p - q - r - ss - t - u - v}};
dist = dist /. NSolve[exp, {u1, d1, u2, d2, u3, d3, p, q, r, ss, t, u, v}][[2]]
```

## A.2 Trees via more general probability deformation code:

### A.2.1 SQID scheme in 1-D

```

rk1 = 0.001;
rku = rmean + 5 * Sqrt[rvar];
pu = f2[rku];
pl = f2[rk1];
dp = (pu - pl) / Num;
g1[p_] := InverseCDF[LogNormalDistribution[mean, Sqrt[var]], p];

dist = Table[{NIntegrate[x * (f1[x] / dp), {x, g1[i], g1[i + dp]}, dp], {i, pl, pu - dp, dp}}];
rvals = Transpose[dist][[1]];
pvals = Transpose[dist][[2]];

```

### A.2.2 SQID scheme in 2-D

```

fx1[r_] := PDF[LogNormalDistribution[mean1, Sqrt[var1]], r];
fx2[r_] := CDF[LogNormalDistribution[mean1, Sqrt[var1]], r];
pu = 1;
pl = 0;
dp = (pu - pl) / Num;
gx1[p_] := InverseCDF[LogNormalDistribution[mean1, Sqrt[var1]], p];
xvals = Flatten[{rk1l, Table[gx1[i + dp], {i, pl, pu - 2 * dp, dp}], rk1u}];

fy1[r_] := PDF[LogNormalDistribution[mean2, Sqrt[var2]], r];
fy2[r_] := CDF[LogNormalDistribution[mean2, Sqrt[var2]], r];
pu = 1;
pl = 0;
dp = (pu - pl) / Num;
gy1[p_] := InverseCDF[LogNormalDistribution[mean2, Sqrt[var2]], p];
yvals = Flatten[{rk2l, Table[gy1[i + dp], {i, pl, pu - 2 * dp, dp}], rk2u}];

f[l_, k_] := Evaluate[PDF[D, {l, k}]];

dist =
  Flatten[Table[{prob = (NIntegrate[f[A, B], {A, Log[xvals[[i]], Log[xvals[[i + 1]]}],
    {B, Log[yvals[[j]], Log[yvals[[j + 1]]}]}); (NIntegrate[(Exp[A] * f[A, B]) / prob
, {A, Log[xvals[[i]], Log[xvals[[i + 1]]}],
    {B, Log[yvals[[j]], Log[yvals[[j + 1]]}]}),
    NIntegrate[(Exp[B] * f[A, B]) / (prob), {A, Log[xvals[[i]], Log[xvals[[i + 1]]}],
    {B, Log[yvals[[j]], Log[yvals[[j + 1]]}]}],
    prob}, {i, 1, Num}, {j, 1, Num}], 1];

```

## A.3 Recursion via dynamic programming code

### A.3.1 Initial recursion

```
(soll = FindMaximum[{Total[(dist /. {r1_Real, r2_Real}, p_Real) ->
(Log[(ξ1 * r1 + ξ2 * r2 + (1 - ξ1 - ξ2) * s) * (1 - λ)] * p)]},
ξ1 ≥ 0 && ξ2 ≥ 0 && (ξ1 + ξ2) ≤ 1}, {{ξ1, 0.25}, {ξ2, 0.25}}, AccuracyGoal -> 5]
tlist1 = Parallelize[ParallelEvaluate[
Off[FindMinimum::reged]]; ParallelEvaluate[Off[FindMaximum::lstol]]; Table[{{a, b},
{l = Max[templist = {soll[[1]], If[a + b > 1, 0, Total[dist /.
{r1_Real, r2_Real}, p_Real] -> Log[a * r1 + b * r2 + (1 - a - b) * s] * p]}]},
If[templist[[2]] == 1, 2, Flatten[Position[templist, 1]][[1]]], Piecewise[
{{a, b}, templist[[2]] == 1}, {{ξ1, ξ2} /. soll[[2]], templist[[1]] == 1}}]],
{a, amin, amax, da}, {b, bmin, bmax, db}]; // Timing

points = Select[Flatten[tlist1, 1], #[[2, 2]] == 2 &] /. {{a_, b_}, {J_, I_, Δ_}} -> {a, b};
Graphics[Point[points], Axes -> True]
JN = Interpolation[Flatten[tlist1, 1] /. {{a_, b_}, {J_, I_, Δ_}} -> {{a, b}, J}];
```

### A.3.2 Subsequent recursion

```
soll1 = FindMaximum[{{Total[dist /.
{r1_Real, r2_Real}, p_Real] -> ((Log[(ξ1 * r1 + ξ2 * r2 + (1 - ξ1 - ξ2) * s) * (1 - λ)] +
JN[
$$\frac{\xi_1 * r_1}{\xi_1 * r_1 + \xi_2 * r_2 + (1 - \xi_1 - \xi_2) * s}, \frac{\xi_2 * r_2}{\xi_1 * r_1 + \xi_2 * r_2 + (1 - \xi_1 - \xi_2) * s}$$
]) * p)},
ξ1 ≥ 0 && ξ2 ≥ 0 && (ξ1 + ξ2) ≤ 1}, {{ξ1, 0.25}, {ξ2, 0.25}}, AccuracyGoal -> 6]

some1 = NestList[{{tlist = Parallelize[ParallelEvaluate[
Off[FindMinimum::reged]]; ParallelEvaluate[Off[FindMaximum::lstol]];
ParallelEvaluate[Off[InterpolatingFunction::dmval]];
ParallelEvaluate[Off[Interpolation::udeg]];
Table[(*nlist = (#[[1]] /. {x_, {z_, w_, y_} -> y})*) {a, b},
{l = Max[templist = {#[[3]][[1]], If[a + b > 1, 0,
Total[dist /. {r1_Real, r2_Real}, p_Real] ->
((Log[a * r1 + b * r2 + (1 - a - b) * s] + #[[2]] [
$$\frac{a * r_1}{a * r_1 + b * r_2 + (1 - a - b) * s}, \frac{b * r_2}{a * r_1 + b * r_2 + (1 - a - b) * s}$$
]) * p]}]}]},
If[templist[[2]] == 1, 2, Flatten[Position[templist, 1]][[1]]],
Piecewise[{{0, 0}, templist[[2]] == 1},
{{ξ1, ξ2} /. #[[3]][[2]], templist[[1]] == 1}}]],
{a, amin, amax, da}, {b, bmin, bmax, db}], intepo = Interpolation[
Flatten[tlist, 1] /. {{a_, b_}, {J_, I_, Δ_}} -> {{a, b}, J}],
tempsol = FindMaximum[{{Total[dist /. {r1_Real, r2_Real}, p_Real] ->
((Log[(ξ1 * r1 + ξ2 * r2 + (1 - ξ1 - ξ2) * s) * (1 - λ)] + intepo[

$$\frac{\xi_1 * r_1}{\xi_1 * r_1 + \xi_2 * r_2 + (1 - \xi_1 - \xi_2) * s}, \frac{\xi_2 * r_2}{\xi_1 * r_1 + \xi_2 * r_2 + (1 - \xi_1 - \xi_2) * s}$$
]) * p)},
ξ1 ≥ 0 && ξ2 ≥ 0 && (ξ1 + ξ2) ≤ 1}, {{ξ1, 0.25}, {ξ2, 0.25}},
AccuracyGoal -> 6]}] &, {tlist1, JN, soll1}, nn - 1]; // Timing
```

### A.3.3 Analysis of optimal controls obtained - say constructing the boundaries of no-transaction regions using ConvexHull[]

```
data2D = Select[Flatten[some1[[nn, 1]], 1], #[[2, 2]] == 2 && (Total[#[[1]]] < 1) &] /.
  {{a_, w_}, {J_, I_, Δ_}} -> {a, w};
g1 = Graphics[BSplineCurve[data2D[[ConvexHull[data2D]]], SplineClosed -> True],
  Axes -> True]
```

### A.3.4 Code that uses creation of small ‘Balls’ to create the no-transaction region in chapter 6

```
points =
  Select[Flatten[some[[nn, 1]], 1], #[[2, 2]] == 3 &] /. {{a_, w_}, {J_, I_, Δ_}} -> {a, w};
nf = Nearest[points];
inRegion[pt : {_Real, _Real}, eps_Real] := TrueQ[Norm[nf[pt, 1][[1]] - pt] < eps];
reg1 = RegionPlot[inRegion[N[{a, w}], N[.01]], {a, 0, 1}, {w, 0, 0.6},
  Mesh -> False, BoundaryStyle -> Directive[Black, Dashed], PlotStyle -> White]
points = Select[Flatten[some[[2, 1]], 1], #[[2, 2]] == 3 &] /.
  {{a_, w_}, {J_, I_, Δ_}} -> {a, w};
nf = Nearest[points];
inRegion[pt : {_Real, _Real}, eps_Real] := TrueQ[Norm[nf[pt, 1][[1]] - pt] < eps];
reg2 = RegionPlot[inRegion[N[{a, w}], N[.01]], {a, 0, 1}, {w, 0, 0.6},
  Mesh -> False, BoundaryStyle -> Directive[Blue, Dashed], PlotStyle -> White]
Show[
  reg2,
  reg1]
```

## A.4 Analysis of the optimal control law

### A.4.1 Code snippet showing control storage

```
K1 = Map[Interpolation[Flatten[#[[1]], 1] /. {{a_, w_}, {J_, II_, Δ_}} -> {{a, w}, II}] &,
  some[[2 ;; nn]]];
K2 = Map[Interpolation[Flatten[#[[1]], 1] /. {{a_, w_}, {J_, II_, Δ_}} -> {{a, w}, Δ}] &,
  some[[2 ;; nn]]];
```

## A.4.2 Code snippet showing use of stored controls for further analysis to generate efficient frontier for benchmark problem in section 3.4.

```

some = NestList[{templist = Parallelize[
  ParallelEvaluate[
    Off[FindMinimum::fmgz]]; ParallelEvaluate[Off[FindMinimum::reged]];
  ParallelEvaluate[Off[FindMinimum::lstol]];
  ParallelEvaluate[Off[InterpolatingFunction::dmval]];
  ParallelEvaluate[Off[FindMinimum::sdprec]];
  count = count + 1;
  Table[{a, w},
    Piecewise[{{
      sol1 =
      Total[
        dist /. {r_Real, p_Real} -> (((#[2][1](ξ * r) / (s + ξ (r - s) + μ (ξ - a) s),
          w * (s + ξ (r - s) + μ (ξ - a) s))) /. ξ → K2[[count]][a, w]) * p]

      , K1[[count]][a, w] == 1}, {sol2 =
      Total[dist /. {r_Real, p_Real} -> (((#[2][1](ξ * r) / (s + ξ (r - s) - λ (ξ - a) s),
          w * ((s + ξ (r - s) - λ (ξ - a) s))) /. ξ → K2[[count]][a, w]) * p]

      , K1[[count]][a, w] == 2}, {
      Total[dist /. {r_Real, p_Real} -> (#[2][1](a * r) / (a * r + (1 - a) s),
          w * ((s + a (r - s)))) /. ξ → K2[[count]][a, w]) * p]

      , K1[[count]][a, w] == 3}}], {a, amin, amax, da}, {w, wmin, wmax, dw}]],
Interpolation[Flatten[templist, 1]] &, {0, JN}, nn - 1];

```



# Appendix B

## Pair Trading Models

### B.1 Alternate Pair trading models in section 1 of chapter 11

#### B.1.1 Model using $Log(\mathcal{Z}_k) = A_k - \phi_1 - \phi_2 B_k$ signal

Here long one unit of spread is long one unit of wealth in stock A and short  $-\phi_2$  units of wealth in stock B. Here  $\mathcal{Z}_k$  denotes the spread process and  $(\phi_1, \phi_2)$  are estimated from the historical data. Here  $A_k^1$  denotes the price of stock A at the beginning of the cycle and  $A_k^2$  denotes the price of the stock at the end of the cycle. Also  $(\lambda, \mu)$  are the transaction cost factors in the buy and sell side direction respectively.

A cycle from going long to short in spread results in:

$$\delta_k = \left( \frac{A_k^2}{A_k^1} - 1 \right) + \left( -\phi_2 \frac{B_k^2}{B_k^1} + \phi_2 \right) \quad (\text{B.1})$$

$$\approx \text{Log} \left( \frac{A_k^2}{A_k^1} \right) - \phi_2 \text{Log} \left( \frac{B_k^2}{B_k^1} \right) \quad (\text{B.2})$$

$$= (\text{Log}(A_k^2) - \phi_2 \text{Log}(B_k^2)) - (\text{Log}(A_k^1) - \phi_2 \text{Log}(B_k^1)) \quad (\text{B.3})$$

Assuming  $\mathcal{Z}_k$  is constructed using the mid-point of bid-ask spread we could factor in transaction costs and have a new formula for profit  $\delta_k$  in a cycle:

$$\delta_k = (\text{Log}((1 - \mu)A_k^2) - \phi_2 \text{Log}((1 + \lambda)B_k^2)) - (\text{Log}((1 - \mu)A_k^1) - \phi_2 \text{Log}((1 + \lambda)B_k^1)) \quad (\text{B.4})$$

So we have:

$$\delta_k^{\text{realized}} = \text{Log} \left( \frac{1 - \mu}{1 + \lambda} \right) + \phi_2 \text{Log} \left( \frac{1 - \mu}{1 + \lambda} \right) + \delta_k^{\text{gross}} \quad (\text{B.5})$$

where  $\delta_k^{\text{gross}} = \mathcal{Z}_k^2 - \mathcal{Z}_k^1$

## B.2 Dynamic Pair Trading Model in section 2 of chapter 11

**B.2.1 Position 2:**  $\mathcal{A}_{1,k}^- > 0$ ,  $\mathcal{A}_{2,k}^- < 0$  with  $\mathcal{A}_{1,k}^- < |\mathcal{A}_{2,k}^-|$ :

A-L-S:

$$a_{i,k}^+ = \mathcal{A}_{1,k}^- \mathcal{W}_k^- + \Delta_k^1 = h \mathcal{W}_k^- \quad (\text{B.6})$$

$$b_{i,k}^+ = \mathcal{A}_{2,k}^- \mathcal{W}_k^- - \Delta_k^2 = -h \mathcal{W}_k^- \quad (\text{B.7})$$

$$c_{i,k}^+ = (1 - \mathcal{A}_{1,k}^- - \mathcal{A}_{2,k}^-) \mathcal{W}_k^- - (1 + \lambda_k) \Delta_k^1 + (1 - \mu_k) \Delta_k^2 \quad (\text{B.8})$$

This implies that  $0 \leq \xi_k^1 \leq \alpha^* - \mathcal{A}_{1,k}^-$ . The second control can be expressed in terms of the first control via  $\xi_k^2 = \mathcal{A}_{2,k}^- + \mathcal{A}_{1,k}^- + \xi_k^1$ .

The state processes now evolve as:

$$\mathcal{A}_{k+1}^{1,-} = \frac{(\mathcal{A}_{1,k}^- + \xi_k^1) r_1}{\beta_{1,k}} \quad (\text{B.9})$$

$$\begin{aligned} \beta_{1,k} &= (\mathcal{A}_{1,k}^- + \xi_k^1) r_1 - (\mathcal{A}_{1,k}^- + \xi_k^1) r_2 \\ &\quad + ((1 - \mathcal{A}_{1,k}^- - \mathcal{A}_{2,k}^-) - (1 + \lambda_k) \xi_k^1 + (1 - \mu_k) (\mathcal{A}_{2,k}^- + \mathcal{A}_{1,k}^- + \xi_k^1)) s \end{aligned} \quad (\text{B.10})$$

$$\mathcal{A}_{k+1}^{2,-} = \frac{-(\mathcal{A}_{1,k}^- + \xi_k^1) r_2}{\beta_{2,k}} \quad (\text{B.11})$$

$$\begin{aligned} \beta_{2,k} &= ((\mathcal{A}_{1,k}^- + \xi_k^1) r_1 - (\mathcal{A}_{1,k}^- + \xi_k^1) r_2 \\ &\quad + ((1 - \mathcal{A}_{1,k}^- - \mathcal{A}_{2,k}^-) - (1 + \lambda_k) \xi_k^1 + (1 - \mu_k) (\mathcal{A}_{2,k}^- + \mathcal{A}_{1,k}^- + \xi_k^1)) s \end{aligned} \quad (\text{B.12})$$

B-L-L:

$$a_{i,k}^+ = \mathcal{A}_{1,k}^- \mathcal{W}_k^- + \Delta_k^1 = h \mathcal{W}_k^- \quad (\text{B.13})$$

$$b_{i,k}^+ = \mathcal{A}_{2,k}^- \mathcal{W}_k^- + \Delta_k^2 = -h \mathcal{W}_k^- \quad (\text{B.14})$$

$$c_{i,k}^+ = (1 - \mathcal{A}_{1,k}^- - \mathcal{A}_{2,k}^-) \mathcal{W}_k^- - (1 + \lambda_k) \Delta_k^1 - (1 + \lambda_k) \Delta_k^2 \quad (\text{B.15})$$

This implies that  $0 \leq \xi_k^1 \leq \alpha^* - \mathcal{A}_{1,k}^-$ . Also the second control can be expressed in terms of the first control via  $\xi_k^2 = -\mathcal{A}_{2,k}^- - (\mathcal{A}_{1,k}^- + \xi_k^1)$ .

The state particles now evolve as:

$$\mathcal{A}_{k+1}^{1,-} = \frac{(\mathcal{A}_{1,k}^- + \xi_k^1) r_1}{\beta_{1,k}} \quad (\text{B.16})$$

$$\begin{aligned} \beta_{1,k} &= (\mathcal{A}_{1,k}^- + \xi_k^1) r_1 - (\mathcal{A}_{1,k}^- + \xi_k^1) r_2 \\ &\quad + ((1 - \mathcal{A}_{1,k}^- - \mathcal{A}_{2,k}^-) - (1 - \lambda_k) \xi_k^1 - (1 + \lambda_k) (-\mathcal{A}_{2,k}^- - (\mathcal{A}_{1,k}^- + \xi_k^1))) s \end{aligned} \quad (\text{B.17})$$

$$\mathcal{A}_{k+1}^{1,-} = \frac{-(\mathcal{A}_{1,k}^- + \xi_k^1)r_2}{\beta_{2,k}} \quad (\text{B.18})$$

$$\begin{aligned} \beta_{2,k} &= (\mathcal{A}_{1,k}^- + \xi_k^1)r_1 - (\mathcal{A}_{1,k}^- + \xi_k^1)r_2 \\ &\quad ((1 - \mathcal{A}_{1,k}^- - \mathcal{A}_{2,k}^-) - (1 - \lambda_k)\xi_k^1 - (1 + \lambda_k)(-\mathcal{A}_{2,k}^- - (\mathcal{A}_{1,k}^- + \xi_k^1)))s \end{aligned} \quad (\text{B.19})$$

**C- S - L:**

$$a_{i,k}^+ = \mathcal{A}_{1,k}^- \mathcal{W}_k^- - \Delta_k^1 = h\mathcal{W}_k^- \quad (\text{B.20})$$

$$b_{i,k}^+ = \mathcal{A}_{2,k}^- \mathcal{W}_k^- + \Delta_k^2 = -h\mathcal{W}_k^- \quad (\text{B.21})$$

$$c_{i,k}^+ = (1 - \mathcal{A}_{1,k}^- - \mathcal{A}_{2,k}^-)\mathcal{W}_k^- + (1 - \mu_k)\Delta_k^1 - (1 + \lambda_k)\Delta_k^2 \quad (\text{B.22})$$

This implies that  $0 \leq \xi_k^1 \leq \mathcal{A}^* + \mathcal{A}_{1,k}^-$ . Also the second control can be expressed in terms of the first control via  $\xi_k^2 = -\mathcal{A}_{2,k}^- - \mathcal{A}_{1,k}^- + \xi_k^1$ .

The state processes now evolve as:

$$\mathcal{A}_{k+1}^{1,-} = \frac{(\mathcal{A}_{1,k}^- - \xi_k^1)r_1}{\beta_{1,k}} \quad (\text{B.23})$$

$$\begin{aligned} \beta_{1,k} &= (\mathcal{A}_{1,k}^- - \xi_k^1)r_1 - (\mathcal{A}_{1,k}^- - \xi_k^1)r_2 \\ &\quad + ((1 - \mathcal{A}_{1,k}^- - \mathcal{A}_{2,k}^-) + (1 - \mu_k)\xi_k^1 - (1 + \lambda_k)(-\mathcal{A}_{2,k}^- - \mathcal{A}_{1,k}^- + \xi_k^1))s \end{aligned} \quad (\text{B.24})$$

$$\mathcal{A}_{k+1}^{2,-} = \frac{-(\mathcal{A}_{1,k}^- - \xi_k^1)r_2}{\beta_{2,k}} \quad (\text{B.25})$$

$$\begin{aligned} \beta_{2,k} &= (\mathcal{A}_{1,k}^- - \xi_k^1)r_1 - (\mathcal{A}_{1,k}^- - \xi_k^1)r_2 \\ &\quad + ((1 - \mathcal{A}_{1,k}^- - \mathcal{A}_{2,k}^-) + (1 - \mu_k)\xi_k^1 - (1 + \lambda_k)(-\mathcal{A}_{2,k}^- - \mathcal{A}_{1,k}^- + \xi_k^1))s \end{aligned} \quad (\text{B.26})$$

**D- N - N:**

$$a_{i,k}^+ = \mathcal{A}_{1,k}^- \mathcal{W}_k^- \quad (\text{B.27})$$

$$b_{i,k}^+ = \mathcal{A}_{2,k}^- \mathcal{W}_k^- \quad (\text{B.28})$$

$$c_{i,k}^+ = (1 - \mathcal{A}_{1,k}^- - \mathcal{A}_{2,k}^-)\mathcal{W}_k^- \quad (\text{B.29})$$

State control constraints are absent here as state particles evolve with *complete freedom*.

The state processes now evolve as:

$$\mathcal{A}_{k+1}^{1,-} = \frac{\mathcal{A}_{1,k}^- r_1}{\mathcal{A}_{1,k}^- r_1 + \mathcal{A}_{2,k}^- r_2 + (1 - \mathcal{A}_{1,k}^- - \mathcal{A}_{2,k}^-)s} \quad (\text{B.30})$$

$$\mathcal{A}_{k+1}^{2,-} = \frac{\mathcal{A}_{2,k}^- r_2}{\mathcal{A}_{1,k}^- r_1 + \mathcal{A}_{2,k}^- r_2 + (1 - \mathcal{A}_{1,k}^- - \mathcal{A}_{2,k}^-)s} \quad (\text{B.31})$$

**B.2.2 Position 3:**  $\mathcal{A}_{1,k}^- < 0$ ,  $\mathcal{A}_{2,k}^- > 0$  with  $|\mathcal{A}_{1,k}^-| < \mathcal{A}_{2,k}^-$  :

A- L - S:

$$a_{i,k}^+ = \mathcal{A}_{1,k}^- \mathcal{W}_k^- + \Delta_k^1 = h \mathcal{W}_k^- \quad (\text{B.32})$$

$$b_{i,k}^+ = \mathcal{A}_{2,k}^- \mathcal{W}_k^- - \Delta_k^2 = -h \mathcal{W}_k^- \quad (\text{B.33})$$

$$c_{i,k}^+ = (1 - \mathcal{A}_{1,k}^- - \mathcal{A}_{2,k}^-) \mathcal{W}_k^- - (1 + \lambda_k) \Delta_k^1 + (1 - \mu_k) \Delta_k^2 \quad (\text{B.34})$$

This implies that  $0 \leq \xi_k^1 \leq \alpha^* - \mathcal{A}_{1,k}^-$ . The second control can be expressed in terms of the first control via  $\xi_k^2 = \mathcal{A}_{2,k}^- + \mathcal{A}_{1,k}^- + \xi_k^1$ .

The state processes now evolve as:

$$\mathcal{A}_{k+1}^{1,-} = \frac{(\mathcal{A}_{1,k}^- + \xi_k^1) r_1}{\beta_{1,k}} \quad (\text{B.35})$$

$$\begin{aligned} \beta_{1,k} = & (\mathcal{A}_{1,k}^- + \xi_k^1) r_1 - (\mathcal{A}_{1,k}^- + \xi_k^1) r_2 \\ & + ((1 - \mathcal{A}_{1,k}^- - \mathcal{A}_{2,k}^-) - (1 + \lambda_k) \xi_k^1 + (1 - \mu_k) (\mathcal{A}_{2,k}^- + \mathcal{A}_{1,k}^- + \xi_k^1)) s \end{aligned} \quad (\text{B.36})$$

$$\mathcal{A}_{k+1}^{2,-} = \frac{-(\mathcal{A}_{1,k}^- + \xi_k^1) r_2}{\beta_{2,k}} \quad (\text{B.37})$$

$$\begin{aligned} \beta_{2,k} = & ((\mathcal{A}_{1,k}^- + \xi_k^1) r_1 - (\mathcal{A}_{1,k}^- + \xi_k^1) r_2 \\ & + ((1 - \mathcal{A}_{1,k}^- - \mathcal{A}_{2,k}^-) - (1 + \lambda_k) \xi_k^1 + (1 - \mu_k) (\mathcal{A}_{2,k}^- + \mathcal{A}_{1,k}^- + \xi_k^1)) s \end{aligned} \quad (\text{B.38})$$

B- S - S:

$$a_{i,k}^+ = \mathcal{A}_{1,k}^- \mathcal{W}_k^- - \Delta_k^1 = h \mathcal{W}_k^- \quad (\text{B.39})$$

$$b_{i,k}^+ = \mathcal{A}_{2,k}^- \mathcal{W}_k^- - \Delta_k^2 = -h \mathcal{W}_k^- \quad (\text{B.40})$$

$$c_{i,k}^+ = (1 - \mathcal{A}_{1,k}^- - \mathcal{A}_{2,k}^-) \mathcal{W}_k^- + (1 - \mu_k) \Delta_k^1 + (1 - \mu_k) \Delta_k^2 \quad (\text{B.41})$$

This implies that  $0 \leq \xi_k^1 \leq \mathcal{A}^* + \mathcal{A}_k^1$ . Also the second control can be expressed in terms of the first control via  $\xi_k^2 = \mathcal{A}_k^2 + \mathcal{A}_k^1 - \xi_k^1$ .

The state processes now evolve as:

$$\mathcal{A}_{k+1}^{1,-} = \frac{(\mathcal{A}_{1,k}^- - \xi_k^1) r_1}{\beta_{1,k}} \quad (\text{B.42})$$

$$\begin{aligned} \beta_{1,k} = & (\mathcal{A}_{1,k}^- - \xi_k^1) r_1 - (\mathcal{A}_{1,k}^- - \xi_k^1) r_2 \\ & + ((1 - \mathcal{A}_{1,k}^- - \mathcal{A}_{2,k}^-) + (1 - \mu_k) \xi_k^1 + (1 - \mu_k) (\mathcal{A}_{2,k}^- + \mathcal{A}_{1,k}^- - \xi_k^1)) s \end{aligned} \quad (\text{B.43})$$

$$\mathcal{A}_{k+1}^{2,-} = \frac{-(\mathcal{A}_{1,k}^- - \xi_k^1)r_2}{\beta_{2,k}} \quad (\text{B.44})$$

$$\begin{aligned} \beta_{2,k} &= (\mathcal{A}_{1,k}^- - \xi_k^1)r_1 - (\mathcal{A}_{1,k}^- - \xi_k^1)r_2 \\ &\quad + ((1 - \mathcal{A}_{1,k}^- - \mathcal{A}_{2,k}^-) + (1 - \mu_k)\xi_k^1 + (1 - \mu_k)(\mathcal{A}_{2,k}^- + \mathcal{A}_{1,k}^- - \xi_k^1))s \end{aligned} \quad (\text{B.45})$$

**C- S - L:**

$$a_{i,k}^+ = \mathcal{A}_{1,k}^- \mathcal{W}_k^- - \Delta_k^1 = h\mathcal{W}_k^- \quad (\text{B.46})$$

$$b_{i,k}^+ = \mathcal{A}_{2,k}^- \mathcal{W}_k^- + \Delta_k^2 = -h\mathcal{W}_k^- \quad (\text{B.47})$$

$$c_{i,k}^+ = (1 - \mathcal{A}_{1,k}^- - \mathcal{A}_{2,k}^-)\mathcal{W}_k^- + (1 - \mu_k)\Delta_k^1 - (1 + \lambda_k)\Delta_k^2 \quad (\text{B.48})$$

This implies that  $0 \leq \xi_k^1 \leq \mathcal{A}^* + \mathcal{A}_{1,k}^-$ . Also the second control can be expressed in terms of the first control via  $\xi_k^2 = -\mathcal{A}_{2,k}^- - \mathcal{A}_{1,k}^- + \xi_k^1$ .

The state processes now evolve as:

$$\mathcal{A}_{k+1}^{1,-} = \frac{(\mathcal{A}_{1,k}^- - \xi_k^1)r_1}{\beta_{1,k}} \quad (\text{B.49})$$

$$\begin{aligned} \beta_{1,k} &= (\mathcal{A}_{1,k}^- - \xi_k^1)r_1 - (\mathcal{A}_{1,k}^- - \xi_k^1)r_2 \\ &\quad + ((1 - \mathcal{A}_{1,k}^- - \mathcal{A}_{2,k}^-) + (1 - \mu_k)\xi_k^1 - (1 + \lambda_k)(-\mathcal{A}_{2,k}^- - \mathcal{A}_{1,k}^- + \xi_k^1))s \end{aligned} \quad (\text{B.50})$$

$$\mathcal{A}_{k+1}^{2,-} = \frac{-(\mathcal{A}_{1,k}^- - \xi_k^1)r_2}{\beta_{2,k}} \quad (\text{B.51})$$

$$\begin{aligned} \beta_{2,k} &= (\mathcal{A}_{1,k}^- + \xi_k^1)r_1 - (\mathcal{A}_{1,k}^- - \xi_k^1)r_2 \\ &\quad + ((1 - \mathcal{A}_{1,k}^- - \mathcal{A}_{2,k}^-) + (1 - \mu_k)\xi_k^1 - (1 + \lambda_k)(-\mathcal{A}_{2,k}^- - \mathcal{A}_{1,k}^- + \xi_k^1))s \end{aligned} \quad (\text{B.52})$$

**D- N - N:**

$$a_{i,k}^+ = \mathcal{A}_{1,k}^- \mathcal{W}_k^- \quad (\text{B.53})$$

$$b_{i,k}^+ = \mathcal{A}_{2,k}^- \mathcal{W}_k^- \quad (\text{B.54})$$

$$c_{i,k}^+ = (1 - \mathcal{A}_{1,k}^- - \mathcal{A}_{2,k}^-)\mathcal{W}_k^- \quad (\text{B.55})$$

State control constraints are absent here as state particles evolve with *complete freedom*.

The state processes now evolve as:

$$\mathcal{A}_{k+1}^{1,-} = \frac{\mathcal{A}_{1,k}^- r_1}{\mathcal{A}_{1,k}^- r_1 + \mathcal{A}_{2,k}^- r_2 + (1 - \mathcal{A}_{1,k}^- - \mathcal{A}_{2,k}^-)s} \quad (\text{B.56})$$

$$\mathcal{A}_{k+1}^{2,-} = \frac{\mathcal{A}_{2,k}^- r_2}{\mathcal{A}_{1,k}^- r_1 + \mathcal{A}_{2,k}^- r_2 + (1 - \mathcal{A}_{1,k}^- - \mathcal{A}_{2,k}^-)s} \quad (\text{B.57})$$

**B.2.3 Position 4:**  $\mathcal{A}_{1,k}^- < 0$ ,  $\mathcal{A}_{2,k}^- > 0$  with  $|\mathcal{A}_{1,k}^-| > \mathcal{A}_{2,k}^-$ :

A-L-S:

$$a_{i,k}^+ = \mathcal{A}_{1,k}^- \mathcal{W}_k^- + \Delta_k^1 = h \mathcal{W}_k^- \quad (\text{B.58})$$

$$b_{i,k}^+ = \mathcal{A}_{2,k}^- \mathcal{W}_k^- - \Delta_k^2 = -h \mathcal{W}_k^- \quad (\text{B.59})$$

$$c_{i,k}^+ = (1 - \mathcal{A}_{1,k}^- - \mathcal{A}_{2,k}^-) \mathcal{W}_k^- - (1 + \lambda_k) \Delta_k^1 + (1 - \mu_k) \Delta_k^2 \quad (\text{B.60})$$

This implies that  $0 \leq \xi_k^1 \leq \alpha^* - \mathcal{A}_{1,k}^-$ . The second control can be expressed in terms of the first control via  $\xi_k^2 = \mathcal{A}_{2,k}^- + \mathcal{A}_{1,k}^- + \xi_k^1$ .

The state processes now evolve as:

$$\mathcal{A}_{k+1}^{1,-} = \frac{(\mathcal{A}_{1,k}^- + \xi_k^1) r_1}{\beta_{1,k}} \quad (\text{B.61})$$

$$\begin{aligned} \beta_{1,k} = & (\mathcal{A}_{1,k}^- + \xi_k^1) r_1 - (\mathcal{A}_{1,k}^- + \xi_k^1) r_2 \\ & + ((1 - \mathcal{A}_{1,k}^- - \mathcal{A}_{2,k}^-) - (1 + \lambda_k) \xi_k^1 + (1 - \mu_k) (\mathcal{A}_{2,k}^- + \mathcal{A}_{1,k}^- + \xi_k^1)) s \end{aligned} \quad (\text{B.62})$$

$$\mathcal{A}_{k+1}^{2,-} = \frac{-(\mathcal{A}_{1,k}^- + \xi_k^1) r_2}{\beta_{2,k}} \quad (\text{B.63})$$

$$\begin{aligned} \beta_{2,k} = & ((\mathcal{A}_{1,k}^- + \xi_k^1) r_1 - (\mathcal{A}_{1,k}^- + \xi_k^1) r_2 \\ & + ((1 - \mathcal{A}_{1,k}^- - \mathcal{A}_{2,k}^-) - (1 + \lambda_k) \xi_k^1 + (1 - \mu_k) (\mathcal{A}_{2,k}^- + \mathcal{A}_{1,k}^- + \xi_k^1)) s \end{aligned} \quad (\text{B.64})$$

B-L-L:

$$a_{i,k}^+ = \mathcal{A}_{1,k}^- \mathcal{W}_k^- + \Delta_k^1 = h \mathcal{W}_k^- \quad (\text{B.65})$$

$$b_{i,k}^+ = \mathcal{A}_{2,k}^- \mathcal{W}_k^- + \Delta_k^2 = -h \mathcal{W}_k^- \quad (\text{B.66})$$

$$c_{i,k}^+ = (1 - \mathcal{A}_{1,k}^- - \mathcal{A}_{2,k}^-) \mathcal{W}_k^- - (1 + \lambda_k) \Delta_k^1 - (1 + \lambda_k) \Delta_k^2 \quad (\text{B.67})$$

This implies that  $0 \leq \xi_k^1 \leq \alpha^* - \mathcal{A}_{1,k}^-$ . Also the second control can be expressed in terms of the first control via  $\xi_k^2 = -\mathcal{A}_{2,k}^- - (\mathcal{A}_{1,k}^- + \xi_k^1)$ .

The state particles now evolve as:

$$\mathcal{A}_{k+1}^{1,-} = \frac{(\mathcal{A}_{1,k}^- + \xi_k^1) r_1}{\beta_{1,k}} \quad (\text{B.68})$$

$$\begin{aligned} \beta_{1,k} = & (\mathcal{A}_{1,k}^- + \xi_k^1) r_1 - (\mathcal{A}_{1,k}^- + \xi_k^1) r_2 \\ & + ((1 - \mathcal{A}_{1,k}^- - \mathcal{A}_{2,k}^-) - (1 - \lambda_k) \xi_k^1 - (1 + \lambda_k) (-\mathcal{A}_{2,k}^- - (\mathcal{A}_{1,k}^- + \xi_k^1))) s \end{aligned} \quad (\text{B.69})$$

$$\mathcal{A}_{k+1}^{1,-} = \frac{-(\mathcal{A}_{1,k}^- + \xi_k^1)r_2}{\beta_{2,k}} \quad (\text{B.70})$$

$$\begin{aligned} \beta_{2,k} &= (\mathcal{A}_{1,k}^- + \xi_k^1)r_1 - (\mathcal{A}_{1,k}^- + \xi_k^1)r_2 \\ &\quad ((1 - \mathcal{A}_{1,k}^- - \mathcal{A}_{2,k}^-) - (1 - \lambda_k)\xi_k^1 - (1 + \lambda_k)(-\mathcal{A}_{2,k}^- - (\mathcal{A}_{1,k}^- + \xi_k^1)))s \end{aligned} \quad (\text{B.71})$$

**C- S - L:**

$$a_{i,k}^+ = \mathcal{A}_{1,k}^- \mathcal{W}_k^- - \Delta_k^1 = h\mathcal{W}_k^- \quad (\text{B.72})$$

$$b_{i,k}^+ = \mathcal{A}_{2,k}^- \mathcal{W}_k^- + \Delta_k^2 = -h\mathcal{W}_k^- \quad (\text{B.73})$$

$$c_{i,k}^+ = (1 - \mathcal{A}_{1,k}^- - \mathcal{A}_{2,k}^-)\mathcal{W}_k^- + (1 - \mu_k)\Delta_k^1 - (1 + \lambda_k)\Delta_k^2 \quad (\text{B.74})$$

This implies that  $0 \leq \xi_k^1 \leq \mathcal{A}^* + \mathcal{A}_{1,k}^-$ . Also the second control can be expressed in terms of the first control via  $\xi_k^2 = -\mathcal{A}_{2,k}^- - \mathcal{A}_{1,k}^- + \xi_k^1$ .

The state processes now evolve as:

$$\mathcal{A}_{k+1}^{1,-} = \frac{(\mathcal{A}_{1,k}^- - \xi_k^1)r_1}{\beta_{1,k}} \quad (\text{B.75})$$

$$\begin{aligned} \beta_{1,k} &= (\mathcal{A}_{1,k}^- - \xi_k^1)r_1 - (\mathcal{A}_{1,k}^- - \xi_k^1)r_2 \\ &\quad + ((1 - \mathcal{A}_{1,k}^- - \mathcal{A}_{2,k}^-) + (1 - \mu_k)\xi_k^1 - (1 + \lambda_k)(-\mathcal{A}_{2,k}^- - \mathcal{A}_{1,k}^- + \xi_k^1))s \end{aligned} \quad (\text{B.76})$$

$$\mathcal{A}_{k+1}^{2,-} = \frac{-(\mathcal{A}_{1,k}^- - \xi_k^1)r_2}{\beta_{2,k}} \quad (\text{B.77})$$

$$\begin{aligned} \beta_{2,k} &= (\mathcal{A}_{1,k}^- - \xi_k^1)r_1 - (\mathcal{A}_{1,k}^- - \xi_k^1)r_2 \\ &\quad + ((1 - \mathcal{A}_{1,k}^- - \mathcal{A}_{2,k}^-) + (1 - \mu_k)\xi_k^1 - (1 + \lambda_k)(-\mathcal{A}_{2,k}^- - \mathcal{A}_{1,k}^- + \xi_k^1))s \end{aligned} \quad (\text{B.78})$$

**D- N - N:**

$$a_{i,k}^+ = \mathcal{A}_{1,k}^- \mathcal{W}_k^- \quad (\text{B.79})$$

$$b_{i,k}^+ = \mathcal{A}_{2,k}^- \mathcal{W}_k^- \quad (\text{B.80})$$

$$c_{i,k}^+ = (1 - \mathcal{A}_{1,k}^- - \mathcal{A}_{2,k}^-)\mathcal{W}_k^- \quad (\text{B.81})$$

State control constraints are absent here as state particles evolve with *complete freedom*.

The state processes now evolve as:

$$\mathcal{A}_{k+1}^{1,-} = \frac{\mathcal{A}_{1,k}^- r_1}{\mathcal{A}_{1,k}^- r_1 + \mathcal{A}_{2,k}^- r_2 + (1 - \mathcal{A}_{1,k}^- - \mathcal{A}_{2,k}^-)s} \quad (\text{B.82})$$

$$\mathcal{A}_{k+1}^{2,-} = \frac{\mathcal{A}_{2,k}^- r_2}{\mathcal{A}_{1,k}^- r_2 + \mathcal{A}_{2,k}^- r_2 + (1 - \mathcal{A}_{1,k}^- - \mathcal{A}_{2,k}^-)s} \quad (\text{B.83})$$

For the sake of completeness we also give the equations of particle evolution along the line of perfect hedge  $\ell$ :

**A-L-S:**

$$a_{i,k}^+ = \mathcal{A}_{1,k}^- \mathcal{W}_k^- + \Delta_k^1 = h \mathcal{W}_k^- \quad (\text{B.84})$$

$$b_{i,k}^+ = \mathcal{A}_{2,k}^- \mathcal{W}_k^- - \Delta_k^2 = -h \mathcal{W}_k^- \quad (\text{B.85})$$

$$c_{i,k}^+ = (1 - \mathcal{A}_{1,k}^- - \mathcal{A}_{2,k}^-) \mathcal{W}_k^- - (1 + \lambda_k) \Delta_k^1 + (1 - \mu_k) \Delta_k^2 \quad (\text{B.86})$$

This implies that  $0 \leq \xi_k^1 \leq \alpha^* - \mathcal{A}_{1,k}^-$ . The second control can be expressed in terms of the first control via  $\xi_k^2 = \mathcal{A}_{2,k}^- + \mathcal{A}_{1,k}^- + \xi_k^1$ .

The state processes now evolve as:

$$\mathcal{A}_{k+1}^{1,-} = \frac{(\mathcal{A}_{1,k}^- + \xi_k^1) r_1}{\beta_{1,k}} \quad (\text{B.87})$$

$$\begin{aligned} \beta_{1,k} &= (\mathcal{A}_{1,k}^- + \xi_k^1) r_1 - (\mathcal{A}_{1,k}^- + \xi_k^1) r_2 \\ &\quad + ((1 - \mathcal{A}_{1,k}^- - \mathcal{A}_{2,k}^-) - (1 + \lambda_k) \xi_k^1 + (1 - \mu_k) (\mathcal{A}_{2,k}^- + \mathcal{A}_{1,k}^- + \xi_k^1)) s \end{aligned} \quad (\text{B.88})$$

$$\mathcal{A}_{k+1}^{2,-} = \frac{-(\mathcal{A}_{1,k}^- + \xi_k^1) r_2}{\beta_{2,k}} \quad (\text{B.89})$$

$$\begin{aligned} \beta_{2,k} &= ((\mathcal{A}_{1,k}^- + \xi_k^1) r_1 - (\mathcal{A}_{1,k}^- + \xi_k^1) r_2 \\ &\quad + ((1 - \mathcal{A}_{1,k}^- - \mathcal{A}_{2,k}^-) - (1 + \lambda_k) \xi_k^1 + (1 - \mu_k) (\mathcal{A}_{2,k}^- + \mathcal{A}_{1,k}^- + \xi_k^1)) s \end{aligned} \quad (\text{B.90})$$

**B-S-L:**

$$a_{i,k}^+ = \mathcal{A}_{1,k}^- \mathcal{W}_k^- - \Delta_k^1 = h \mathcal{W}_k^- \quad (\text{B.91})$$

$$b_{i,k}^+ = \mathcal{A}_{2,k}^- \mathcal{W}_k^- + \Delta_k^2 = -h \mathcal{W}_k^- \quad (\text{B.92})$$

$$c_{i,k}^+ = (1 - \mathcal{A}_{1,k}^- - \mathcal{A}_{2,k}^-) \mathcal{W}_k^- + (1 - \mu_k) \Delta_k^1 - (1 + \lambda_k) \Delta_k^2 \quad (\text{B.93})$$

This implies that  $0 \leq \xi_k^1 \leq \mathcal{A}^* + \mathcal{A}_{1,k}^-$ . Also the second control can be expressed in terms of the first control via  $\xi_k^2 = -\mathcal{A}_{2,k}^- - \mathcal{A}_{1,k}^- + \xi_k^1$ .

The state processes now evolve as:

$$\mathcal{A}_{k+1}^{1,-} = \frac{(\mathcal{A}_{1,k}^- - \xi_k^1) r_1}{\beta_{1,k}} \quad (\text{B.94})$$



$$\begin{aligned} \beta_{1,k} = & (\mathcal{A}_{1,k}^- - \xi_k^1)r_1 - (\mathcal{A}_{1,k}^- - \xi_k^1)r_2 \\ & + ((1 - \mathcal{A}_{1,k}^- - \mathcal{A}_{2,k}^-) + (1 - \mu_k)\xi_k^1 - (1 + \lambda_k)(-\mathcal{A}_{2,k}^- - \mathcal{A}_{1,k}^- + \xi_k^1))s \end{aligned} \quad (\text{B.95})$$

$$\mathcal{A}_{k+1}^{2,-} = \frac{-(\mathcal{A}_{1,k}^- - \xi_k^1)r_2}{\beta_{2,k}} \quad (\text{B.96})$$

$$\begin{aligned} \beta_{2,k} = & (\mathcal{A}_{1,k}^- - \xi_k^1)r_1 - (\mathcal{A}_{1,k}^- - \xi_k^1)r_2 \\ & + ((1 - \mathcal{A}_{1,k}^- - \mathcal{A}_{2,k}^-) + (1 - \mu_k)\xi_k^1 - (1 + \lambda_k)(-\mathcal{A}_{2,k}^- - \mathcal{A}_{1,k}^- + \xi_k^1))s \end{aligned} \quad (\text{B.97})$$

**D- N - N:**

$$a_{i,k}^+ = \mathcal{A}_{1,k}^- \mathcal{W}_k^- \quad (\text{B.98})$$

$$b_{i,k}^+ = \mathcal{A}_{2,k}^- \mathcal{W}_k^- \quad (\text{B.99})$$

$$c_{i,k}^+ = (1 - \mathcal{A}_{1,k}^- - \mathcal{A}_{2,k}^-) \mathcal{W}_k^- \quad (\text{B.100})$$

State control constraints are absent here as state particles evolve with *complete freedom*.

The state processes now evolve as:

$$\mathcal{A}_{k+1}^{1,-} = \frac{\mathcal{A}_{1,k}^- r_1}{\mathcal{A}_{1,k}^- r_1 + \mathcal{A}_{2,k}^- r_2 + (1 - \mathcal{A}_{1,k}^- - \mathcal{A}_{2,k}^-)s} \quad (\text{B.101})$$

$$\mathcal{A}_{k+1}^{2,-} = \frac{\mathcal{A}_{2,k}^- r_2}{\mathcal{A}_{1,k}^- r_2 + \mathcal{A}_{2,k}^- r_2 + (1 - \mathcal{A}_{1,k}^- - \mathcal{A}_{2,k}^-)s} \quad (\text{B.102})$$

### B.3 General trading model

**B- LL:**

$$a_{i,k}^+ = \mathcal{A}_{1,k}^- \mathcal{W}_k^- + \Delta_k^1 = h_k^{1,+} \mathcal{W}_k^- \quad (\text{B.103})$$

$$b_{i,k}^+ = \mathcal{A}_{2,k}^- \mathcal{W}_k^- + \Delta_k^2 = h_k^{2,+} \mathcal{W}_k^- \quad (\text{B.104})$$

$$c_{i,k}^+ = (1 - \mathcal{A}_{1,k}^- - \mathcal{A}_{2,k}^-) \mathcal{W}_k^- - (1 + \lambda_k) \Delta_k^1 - (1 + \lambda_k) \Delta_k^2 \quad (\text{B.105})$$

$$(\text{B.106})$$

The state particles now evolve as:

$$\mathcal{A}_{k+1}^{1,-} = \frac{h_k^{1,+} r_1}{\beta_{1,k}} \quad (\text{B.107})$$

$$\begin{aligned} \beta_{1,k} &= h_k^{1,+} r_1 + h_k^{2,+} r_2 \\ &\quad ((1 - \mathcal{A}_{1,k}^- - \mathcal{A}_{2,k}^-) - (1 + \lambda_k)(h_k^{1,+} - \mathcal{A}_{1,k}^-) - (1 + \lambda_k)(h_k^{2,+} - \mathcal{A}_{2,k}^-))s \end{aligned} \quad (\text{B.108})$$

$$\mathcal{A}_{k+1}^{2,-} = \frac{h_k^{2,+} r_2}{\beta_{2,k}} \quad (\text{B.109})$$

$$\begin{aligned} \beta_{2,k} &= h_k^{1,+} r_1 + h_k^{2,+} r_2 \\ &\quad + ((1 - \mathcal{A}_{1,k}^- - \mathcal{A}_{2,k}^-) - (1 + \lambda_k)(h_k^{1,+} - \mathcal{A}_{1,k}^-) - (1 + \lambda_k)(h_k^{2,+} - \mathcal{A}_{2,k}^-))s \end{aligned} \quad (\text{B.110})$$

**C-SL:**

$$a_{i,k}^+ = \mathcal{A}_{1,k}^- \mathcal{W}_k^- - \Delta_k^1 = h_k^{1,+} \mathcal{W}_k^- \quad (\text{2.111})$$

$$b_{i,k}^+ = \mathcal{A}_{2,k}^- \mathcal{W}_k^- + \Delta_k^2 = h_k^{2,+} \mathcal{W}_k^- \quad (\text{2.112})$$

$$c_{i,k}^+ = (1 - \mathcal{A}_{1,k}^- - \mathcal{A}_{2,k}^-) \mathcal{W}_k^- + (1 - \mu_k) \Delta_k^1 - (1 + \lambda_k) \Delta_k^2 \quad (\text{2.113})$$

$$(2.114)$$

The state particles now evolve as:

$$\mathcal{A}_{k+1}^{1,-} = \frac{h_k^{1,+} r_1}{\beta_{1,k}} \quad (\text{2.115})$$

$$\begin{aligned} \beta_{1,k} &= h_k^{1,+} r_1 + h_k^{2,+} r_2 \\ &\quad + ((1 - \mathcal{A}_{1,k}^- - \mathcal{A}_{2,k}^-) + (1 - \mu_k)(\mathcal{A}_{1,k}^- - h_k^{1,+}) - (1 - \lambda_k)(h_k^{2,+} - \mathcal{A}_{2,k}^-))s \end{aligned} \quad (\text{2.116})$$

$$\mathcal{A}_{k+1}^{2,-} = \frac{h_k^{2,+} r_2}{\beta_{2,k}} \quad (\text{2.117})$$

$$\begin{aligned} \beta_{2,k} &= h_k^{1,+} r_1 + h_k^{2,+} r_2 \\ &\quad ((1 - \mathcal{A}_{1,k}^- - \mathcal{A}_{2,k}^-) + (1 - \mu_k)(\mathcal{A}_{1,k}^- - h_k^{1,+}) - (1 + \lambda_k)(h_k^{2,+} - \mathcal{A}_{2,k}^-))s \end{aligned} \quad (\text{2.118})$$

**D-SS:**

$$a_{i,k}^+ = \mathcal{A}_{1,k}^- \mathcal{W}_k^- - \Delta_k^1 = h_k^{1,+} \mathcal{W}_k^- \quad (\text{2.119})$$

$$b_{i,k}^+ = \mathcal{A}_{2,k}^- \mathcal{W}_k^- - \Delta_k^2 = h_k^{2,+} \mathcal{W}_k^- \quad (\text{2.120})$$

$$c_{i,k}^+ = (1 - \mathcal{A}_{1,k}^- - \mathcal{A}_{2,k}^-) \mathcal{W}_k^- + (1 - \mu_k) \Delta_k^1 + (1 - \mu_k) \Delta_k^2 \quad (\text{2.121})$$

The state particles now evolve as:

$$\mathcal{A}_{k+1}^{1,-} = \frac{h_k^{1,+} r_1}{\beta_{1,k}} \quad (2.122)$$

$$\beta_{1,k} = h_k^{1,+} r_1 h_k^{1,+} r_2 + h_k^{2,+} r_2 + ((1 - \mathcal{A}_{1,k}^- - \mathcal{A}_{2,k}^-) + (1 - \mu_k)(\mathcal{A}_{1,k}^- - h_k^{1,+}) + (1 - \mu_k)(\mathcal{A}_{2,k}^- - h_k^{2,+}))s \quad (2.123)$$

$$\mathcal{A}_{k+1}^{2,-} = \frac{h_k^{2,+} r_2}{\beta_{2,k}} \quad (2.124)$$

$$\beta_{2,k} = h_k^{1,+} r_1 + h_k^{2,+} r_2 + (1 - \mathcal{A}_{1,k}^- - \mathcal{A}_{2,k}^-) + (1 - \mu_k)(\mathcal{A}_{1,k}^- - h_k^{1,+}) + (1 - \mu_k)(\mathcal{A}_{2,k}^- - h_k^{2,+}))s \quad (2.125)$$

**E- N - N:**

$$a_{i,k}^+ = \mathcal{A}_{1,k}^- \mathcal{W}_k^- \quad (2.126)$$

$$b_{i,k}^+ = \mathcal{A}_{2,k}^- \mathcal{W}_k^- \quad (2.127)$$

$$c_{i,k}^+ = (1 - \mathcal{A}_{1,k}^- - \mathcal{A}_{2,k}^-) \mathcal{W}_k^- \quad (2.128)$$

State control constraints are absent in this stencil as state particles evolve with *complete freedom*.

The state particles now evolve as:

$$\mathcal{A}_{k+1}^{1,-} = \frac{\mathcal{A}_{1,k}^- r_1}{\mathcal{A}_{1,k}^- r_2 + \mathcal{A}_{2,k}^- r_2 + (1 - \mathcal{A}_{1,k}^- - \mathcal{A}_{2,k}^-)s} \quad (2.129)$$

$$\mathcal{A}_{k+1}^{2,-} = \frac{\mathcal{A}_{2,k}^- r_2}{\mathcal{A}_{1,k}^- r_2 + \mathcal{A}_{2,k}^- r_2 + (1 - \mathcal{A}_{1,k}^- - \mathcal{A}_{2,k}^-)s} \quad (2.130)$$

# Curriculum Vitae

**Name:** Nabeel Butt

**Post-Secondary Education and Degrees:** Beacon House Public School  
Lahore, Pakistan  
2000 - 2002 University of Cambridge GCE A Levels

Lahore University of Management Sciences  
Lahore, Pakistan  
2002 - 2006 B.Sc.

University of Western Ontario  
London, ON  
2007 - 2008 M.Sc.

University of Western Ontario  
London, ON  
2008 - 2012 Ph.D.

**Honours and Awards:** Western Graduate Student Research Award  
2008-2009

Western Graduate Research Scholarship  
2007-2012

**Related Work Experience:** Pre-doctoral fellow  
CASM, LUMS, Pakistan  
2006 - 2007  
Teaching Assistant  
The University of Western Ontario  
2008 - 2012

**Publications:**

1- I. Beg and N. Butt, (2010). (Im)Possibility Theorems in Fuzzy Framework, Critical Review, vol. 4, Society for Mathematics of Uncertainty.

2- Beg, I., Butt, N. (2012). Belief Merging and Judgment Aggregation in Fuzzy Setting. Advances in Fuzzy Systems.

3- Novel temperature index for energy risky management ( To be submitted to Energy Economics).

4- Homotopy method to find roots of analytic functions (To be submitted to Numerical Algorithms).

5- Novel tree approximation methods for dynamic portfolio theory under transaction costs. (To be submitted to Mathematics and Computer Modeling )

6- Towards novel probability deformation schemes in dynamic portfolio theory under transaction costs (To be submitted).

7- Dynamic portfolio theory under stochastic transaction costs (To be submitted).

8- Dynamic portfolio theory under realistic portfolio constraints (To be submitted).

9- Towards a novel lattice based framework for dynamic pairs trading (To be submitted).

10- A framework for dynamic pairs trading under transaction costs (To be submitted).

11- Novel convergent lattice methods for risk-neutral option pricing (To be submitted).

12- Towards a novel framework for robust and efficient algorithmic trading (In preparation).